CHARACTERIZATION OF ELEVATED HUMAN CYTOMEGALOVIRUS-SPECIFIC $CD4^+$ T CELLS IN HIV-INFECTED SUBJECTS

By

Chike Osita Abana

Dissertation

Submitted to the Faculty of the

Graduate School of Vanderbilt University

in partial fulfillment of the requirements

for the degree of

DOCTOR OF PHILOSOPHY

in

Microbiology and Immunology

October 31, 2017

Nashville, Tennessee

Approved:

Wonder P. Drake, M.D.

James E. Crowe, Jr., M.D.

Matthew J. Lang, Ph.D.

Mia A. Levy, M.D., Ph.D.

Spyros A. Kalams, M.D.

Simon A. Mallal, MB.BS.

To God Almighty,

for strength and perseverance,

and

to my beloved wife and the love of my life,

Dr. Courtney A. Mitchell Abana, Ph.D.,

for unwavering support.

ACKNOWLEDGMENTS

…my soul will rejoice in the Lord, exulting His salvation.

—Psalm 35:9 ESV

Even though I never saw Him, I knew and felt God Almighty has always been there with me from the inception to the end of my journey to obtain my Ph.D. He has been my recourse through moments of uncertainty, episodes of seemingly infeasible or daunting experiments, and days and nights of writing this dissertation. I am ever grateful to and always rejoice in and exult the good Lord who has truly blessed me with the strength and wisdom to complete this challenging journey.

My success as a Ph.D. candidate would have been impossible without the contributions of so many people at Vanderbilt University. Importantly, I am extremely thankful to the members of the labs of Simon Mallal, Spyros Kalams, and Elizabeth Phillips. I am especially grateful for my mentors, Dr. Simon Mallal, MB.BS. and Dr. Spyros Kalams, M.D., for teaching me how to think critically as a scientist, to ask and thoroughly address important scientific questions. In no particular order, I am grateful for the invaluable assistance provided by Dr. Elizabeth Phillips, M.D., Dr. Abha Chopra, Ph.D., Dr. Mark Pilkinton, M.D., Ph.D., Dr. Silvana Gaudieri, Ph.D., Dr. Katie White, M.D., Ph.D., Dr. Celestine Wanjalla, M.D., Ph.D., Louise Barnett, Rama Gangula, Cindy Hager, Dr. Katie Nicholas, Ph.D., Rita Smith, Katherine Konvinse, Wyatt McDonnell, Dr. Alec Redwood, Ph.D., Dr. Ian James, Ph.D., Dr. Mark Watson, Ph.D., Dr. Kaija Strautins, Ph.D., Shay Leary, Dr. Ramesh Ram, Ph.D., Dr. Matthew Scholz, Ph.D., Dr. Paul Klenerman, M.D., Ph.D., Dr. David Koelle, M.D., Dr. Madan Jagasia, M.D., Dr. Brian Engelhardt, M.D., Dae Jung, Dr. David Haas, M.D., Dr. John Koethe, M.D., Dr. Heather Long, Ph.D., Dr. Jessica Thomas, M.D., Ph.D., Wannakuwatte Fernando, and Kristina Williams in helping with my project in various ways including developing and optimizing assays; designing and conducting experiments; troubleshooting various equipment or experiment problems; collecting, analyzing and interpreting data; as well as editing manuscripts. I am also grateful to the members of my dissertation committee, including the Chair, Dr. Wonder Drake, M.D., Dr. James Crowe, M.D., Dr. Matthew Lang, Ph.D., and Dr. Mia Levy, M.D., Ph.D., as well as the former member, Dr. Terence Dermody, M.D., for their guidance throughout my training.

I am highly appreciative for the individuals who donated their blood samples for all the studies I discuss in this dissertation, the Vanderbilt Comprehensive Care Clinic (VCCC), the Vanderbilt-Ingram Cancer Center (VICC), the Vanderbilt Flow Cytometry Core, the Vanderbilt Oxford House staff, the Vanderbilt Stem-Cell Clinic, the Vanderbilt Technologies for Advanced Genomics (VANTAGE) and the Institute for Immunology and Infectious Diseases (IIID).

An education is a visa that can take you to anywhere.

—Mrs. Chinwe Christiana Abana

A delay is not a denial.

—Mrs. Chinwe Christiana Abana

What an adult foresees while sitting on the ground, a child can never foresee while standing on the tallest building in the world.

—Mr. Osita Patrick Abana

Obtaining my Ph.D. has not been my aspiration alone, but also the dream of my parents, Mr. Osita Abana and Mrs. Chinwe Abana; my siblings, Mrs. Chinelo Chukwudinka, Ms. Ifeyinwa Abana, Ms. Uzoamaka Abana, and Mr. Okechukwu Abana; and my wife, Dr. Courtney A. Mitchell Abana, Ph.D. Despite never having the opportunity to attend college, my parents laid and continue to build upon the best educational foundation any child could have asked for. Their foresight to realize that my education could never be denied from me will forever inspire me. From growing up in Lagos, Nigeria, to embarking on this endeavor to obtain my Ph.D. at Vanderbilt University School of Medicine, my family has made incredible sacrifices to ensure my success through prayers, encouragement and financial support.

There are very few persons in the world who truly understand, empathize and provide relentless support that one needs during the challenging pursuit of obtaining a Ph.D. I found that person in my beloved wife, Dr. Courtney A. Mitchell Abana. Whether in the middle of work in the daytime, or in the middle of a much-deserved sleep at nighttime, Courtney has always and continues to always demonstrate the selflessness to be a good listener, a thinker, a comforter, and a fountain of knowledge. I am forever indebted to her support throughout this training.

In addition to my immediate family, my extended family and relatives have also played a significant role in this pursuit. Starting with my aunts and uncles, Mrs. Anulika Rita Ikeji; Mr. Isaac and Mrs. Sika Abana; Mr. Vitus Amah; Mr. Okwudili Amah; Dr. Hyacinth Ezeani, D.D.S. and Dr. Ifeoma Ezeani, O.D.; and Mr. Chukwuma Oguejiofor who have always assisted with advancing my education however they could. I am very thankful for the support from my grandmothers, Mrs. Kutanya Caroline Amaefuna (Ekwulo), and Mrs. Mgbeke Eunice Abana (Agu-mma), as well as my adopted great-grandmother in London, Mrs. Phyllis Wanderpuye (Maa). I am also grateful for the understanding, support and prayers from Mr. Curtis Mitchell, Ms. Keya Mitchell, Mr. Henry Lee, Mrs. Malissia Lee, Ms. Kelly Mitchell, Mrs. Cayla Wood, Ms. Kiara Mitchell, and Mr. John Mitchell. Finally, I thank the families of Mr. Kajetan and Mrs. Ogochukwu

Obi; the families of Dr. Afam and Mrs. Amaka Okoye; the families of Mr. Bernard and Mrs. Amy Nnoli; and the families of Mrs. Azuka Uchefuna.

There are so many people who have played academic roles in ensuring that I obtain the best possible education available to me. I would love to thank my pre-nursery schoolteacher, Mrs. Amaka Oreffo for her very important foundational work and patience; my high school Chemistry and Physics teachers, Mrs. C. A. Vowa and Mrs. Jane Nwannah, respectively, for helping me believe in myself during my introductory years to the sciences; Management Education and Training (M.E.T.) Limited in Nigeria for preparing me for the Scholastic Assessment Test; Dr. Johnny Evans and Mr. Phil Cook from Lee University; and the members of Dr. Louis J. Picker's scientific laboratory, especially Dr. Louis Picker, M.D., Dr. Afam Okoye, Ph.D., Dr. Andrew Sylwester, Ph.D., and Dr. Yoshinori Fukazawa, Ph.D. I am also highly indebted to Dr. Charles R. Thomas, Jr., M.D., and Dr. Donn Spight, M.D., for patiently and successfully mentoring me through the process of getting accepted to the Vanderbilt University School of Medicine Medical Scientist Training Program (MSTP) for my M.D. and Ph.D. training.

I am grateful for the strong and supportive network of friends who also helped see me through my Ph.D. training. I would love to thank in a special way, Dr. Valentine Uche Chukwuma, Ph.D., a colleague and friend of the last twelve years who has provided immense support and guidance on navigating the path to success in my Ph.D. training, as well as his wife, Mrs. Kenechi Chukwuma. I would also love to thank other very supportive friends including Mr. Vincent Ossai, Mr. Gideon Olatuyi, Mr. Tunde Animashaun, Mr. Paul Olopade, Ms. Amarachukwu Unigwe, Ms. Temple Ofikulu Ms. Amaka Oghenekaro, Mr. Chijioke Onyia and Mr. Chukwuma Onyia.

I am also thankful for the guidance, emotional and financial support provided for my education by Vanderbilt University School of Medicine and the Vanderbilt Medical Scientist Training Program current leadership especially the director, Dr. Christopher Williams, M.D., Ph.D., and the Assistant Director for Student Affairs, Mrs. Melissa Krasnove, M.Ed., as well as the previous leadership of Dr. Terence Dermody, M.D., Dr. Michelle Grundy, Ph.D., Mr. Jim Bills, and Dr. Larry Swift, Ph.D. Additionally, I appreciate the support from Dr. Nancy Brown, M.D., the Chair of the Department of Medicine, and Dr. Anuradha Bapsi Chakravarthy, M.D., both at Vanderbilt University Medical Center.

Finally, I would like to thank my sources of funding: the National Institute of Health grants P30 AI110527 to Simon Mallal; T32 AI007474 to Spyros Kalams; P50 GM115305 to Elizabeth Phillips; P01 AI030731 and R01 AI094019 to David Koelle; the National Institute of General Medical Sciences grant T32 GM007347 for the Medical Scientist Training Program to Chike Abana; and the National Institute of Allergy and Infectious Diseases grant HHSN272201300006C to the National Institute of Health Tetramer Core Facility for making the tetramers.

TABLE OF CONTENTS

LIST OF TABLES

LIST OF FIGURES

LIST OF EQUATIONS

Equation **Page**

LIST OF ABBREVIATIONS

AIDS	Acquired Immune Deficiency Syndrome
ART	antiretroviral therapy
ATAC-seq	Assay for Transposase-Accessible Chromatin using Sequencing
CLIP	human class II-associated invariant chain peptide
CDR3	complementarity determining region 3
cDNA	complementary DNA
DC	dendritic cell
ddPCR	droplet digital polymerase chain reaction
DR7	HLA-DRB1*07:01
$DR7^{+}$	HLA-DRB1*07:01 carrier
$DR7^{-}$	HLA-DRB1*07:01 non-carrier
DYS	DYSNTHSTRYV
ELISpot	enzyme-linked immunospot
EOMES	eomesodermin
EPD	EPDVYYTSAFVFPTK
FACS	fluorescence-activated cell sorting
fDC	follicular dendritic cell
FRD	FRDYVDRFYKTLRAEQASQE
gB	glycoprotein B
h	hour
HCMV	human cytomegalovirus

$HCMV^-$	human cytomegalovirus-seronegative
$HCMV^+$	human cytomegalovirus-seropositive
HIV	human immunodeficiency virus
HIV^-	human immunodeficiency virus-seronegative
HIV^+	human immunodeficiency virus-seropositive
HSCT	hematopoietic stem cell transplantation
IE1, *ie1*	immediate early gene type 1
IE2, *ie2*	immediate early gene type 2
IFN-γ	interferon-gamma
IL-	interleukin-
LCLs	lymphoblastoid cell lines
LIN	LINSTKIYSYFPSVISKVNQ
LN	lymph node
m	minute
MCMV	murine cytomegalovirus
MFI	median fluorescence intensity
MIEP	major immediate early promoter
pp65	phosphoprotein-65
PRS	PRSPTVFYNIPPMPLPPSQL
RhCMV	rhesus cytomegalovirus
RNA-seq	RNA sequencing
rpm	revolutions per minute
s	second

scRNA-seq	single-cell RNA sequencing
SOT	solid-organ transplantation
T_{CM}	central memory T cells
TCR	T cell receptor
TCRα	T cell receptor-alpha
TCRβ	T cell receptor-beta
TCRβJ	T cell receptor-beta-joining
TCRβV	T cell receptor-beta-variable
T_{EM}	effector memory T cells
T_{EMRA}	effector memory-RA^+ T cells
T_{Int}	intermediate T cells
T_{Nai}	naïve T cells
TNF-α	tumor necrosis factor-alpha
tp1	time-point 1
tp2	time-point 2
TT	tetanus toxoid
T_{TM}	transitional memory T cells
VECs	vascular endothelial cells
V(D)J	variable-diversity-joining
VOA	viral outgrowth assay

DISSERTATION OVERVIEW

This dissertation describes my scientific contribution to our understanding of the interactions between cytomegalovirus (CMV) and $CD4^+$ T cell immunity. CMV-specific T cell responses uniquely undergo unusual expansion, and this phenomenon is known as memory inflation. Memory inflation is a lifelong observation of unusually elevated magnitudes of MHC- or HLA-restricted CMV epitope-specific T cells in immunocompetent CMV-seropositive (CMV^+) hosts such as humans, rhesus macaques and mice with chronic, latent CMV infection. Memory-inflated CMV-specific T cell responses are different from conventional (or classical, i.e. non-inflated) CMV-specific T cell responses because the latter contract to lower magnitudes after primary CMV infection. This feature is unique to CMV for reasons that are yet to be elucidated. There have been more studies on memory inflation of $CD8^+$ T cells than of $CD4^+$ T cells. Furthermore, most of the studies have been conducted only on immunocompetent hosts despite CMV's burden on immunodeficient subjects. The overarching objective of this dissertation is to characterize conventional and memory-inflated human CMV (HCMV) epitope-specific $CD4^+$ T cell responses in HIV-seropositive (HIV^+) and HIV-seronegative (HIV^-) individuals.

In **Chapter I**, I start with an overview of CMV disease and virology. I describe the lytic and latent infection caused by CMV, an important pathogen that over 70% of Americans are exposed to by 60 years of age, which typically causes asymptomatic infection in immunocompetent hosts. Next, I discuss the adaptive immune response to CMV, beginning with the ontogeny of $CD4^+$ T cells and their protective response against

CMV. I then describe the characteristics of and proposed mechanisms that cause memory-inflated CMV-specific T cell responses. I include a comprehensive list of major histocompatibility complex class II HCMV epitopes that display conventional- or inflationary-like phenotypes based on published literature and the level of evidence supporting each epitope. A similar list for class I HCMV epitopes is also included for comparison because memory inflation is well-documented for $CD8^+$ T cells. I wrap up this chapter with a brief overview of the pathway of HIV infection, how that intersects with the formation of memory-inflated HCMV-specific $CD4^+$ T cell response in HIV^+ individuals, and why inflated responses with a $CD28^-$ and a $CD38^+$HLA-DR^+ activation profile might be important mediators of emerging non-Acquired Immune Deficiency Syndrome-related cardiovascular comorbidities in HIV^+ subjects since the advent effective antiretroviral therapy.

In **Chapter II**, I show evidence of the presence, functional properties, as well as provide potential mechanistic explanations for and clinical implications of memory-inflated HCMV-specific $CD4^+$ T cells in HIV^+ and HIV^- individuals who were HCMV-seropositive ($HCMV^+$) with undetectable HCMV plasma viremia. For these HCMV studies and the remaining work in this dissertation, I focus primarily on $CD4^+$ T cells specific for the HLA-DRB1*07:01 (DR7)-restricted DYSNTHSTRYV (DYS) epitope of HCMV glycoprotein B because of the robust immune response induced by this epitope. I used HLA-DR7 tetramers loaded with the DYS epitope to facilitate *ex vivo* analysis. DYS-specific $CD4^+$ T cells were inflated among the HIV^+ subjects compared to those from a HIV^- $HCMV^+$ HLA-$DR7^+$ cohort, or to HLA-DR7-restricted $CD4^+$ T cells from an HIV and HCMV co-infected cohort that were specific for epitopes of HCMV

phosphoprotein-65 (EPDVYYTSAFVFPTK [EPD] epitope), tetanus toxoid precursor, Epstein-Barr virus nuclear antigen 2 or HIV gag protein. Inflated DYS-specific $CD4^+$ T cells comprised effector memory or effector memory-RA^+ subsets. These cells possessed restricted T cell receptor beta chain and nearly monoclonal complementarity-determining region 3 (CDR3) that contained novel conserved amino acids. Inflated DYS^+ $CD4^+$ T cells were polyfunctional, not senescent, and displayed high *ex vivo* levels of granzyme-B, CX_3CR1, CD38 or HLA-DR, but were less often $CD38^+HLA\text{-}DR^+$ co-expressing. The inflation mechanism did not involve apoptotic suppression, increased proliferation or HIV gag cross-reactivity. Instead, these findings suggest that intermittent or chronic expression of epitopes such as DYS might drive inflation of activated $CD4^+$ T cells that traffic to endothelial cells that express the fractalkine ligand for CX_3CR1, serve as possible latent HCMV reservoirs, and have the potential to mediate cytotoxicity and vascular disease.

In **Chapter III**, I describe the contributions of the inflated DYS^+ $CD4^+$ T cells to latent HIV reservoirs. This determination was made by quantitating the HIV DNA content using droplet digital polymerase chain reaction (ddPCR). The hypothesis is that DYS^+ $CD4^+$ T cells are enriched latent HIV reservoirs due to their high magnitude and near monoclonality, while the alternate hypothesis is that inflated DYS^+ $CD4^+$ T cells do not serve as enriched reservoirs of latent HIV DNA. The frequency of $CD4^+$ T cell latent HIV reservoirs among total CD4 populations in a given, chronically infected subject on antiretroviral therapy is less than 1-in-1,000,000. Therefore, a very sensitive technique is needed to accurately quantify and compare low frequency reservoirs. ddPCR sensitivity for detecting this reservoir was optimized by comparing EvaGreen primers to

TaqMan assays. The results showed that TaqMan assays were much better at sensitively and specifically detecting very low frequency targets. With this assay, I detected HIV DNA in whole $CD4^+$ T cells from a HIV^+ cohort. Using a subject who had an adequately high DYS^+ tetramer response for bulk cell sorting, I demonstrated that memory-inflated DYS^+ $CD4^+$ T cells might not be enriched HIV latent reservoirs. This finding refutes the initial hypothesis and confirmed the alternate hypothesis instead. Nevertheless, this finding should be confirmed using samples from additional subjects. If confirmed, a possible explanation is that CMV-specific T cell memory inflation occurs in cellular and anatomical locations that do not intersect with the sites where HIV infection is established. Additional explanation of this possibility is discussed in **Chapter I** (Introduction) of this dissertation. One drawback of ddPCR's application in studying HIV latent reservoir is that it is currently unable to determine whether detected latent HIV DNA is replication-competent or defective. In summary, my findings in this chapter show that ddPCR is a powerful yet limited tool in characterizing latent HIV reservoirs and that memory-inflated $CD4^+$ T cells might not be enriched in HIV reservoirs despite the oligoclonal nature of these cells.

In **Chapter IV**, I investigate the use of single-cell RNA sequencing (scRNA-seq) to determine the transcriptomic profile of the inflated DYS^+ $CD4^+$ T cells in order to identify a potential mechanism of inflation that is intrinsic to inflated DYS^+ $CD4^+$ T cells. The primary hypothesis is that inflated DYS^+ $CD4^+$ T cells contain upregulated mRNA transcripts of genes such as *CX_3CR1* that mediate interaction with endothelial cells, and *CD38*, *CD74* (HLA-DR), *granzyme B*, *IFN-γ*, and *TNF-α* that are produced upon T cell activation compared to conventional EPD^+ $CD4^+$ T cells based on observed protein

expression in **Chapter II**. The method involved single-cell sorting, RNA sequencing and comparison of transcriptomic profiles of $CD4^+$ T cells specific to both of these epitopes. Although the results were derived from only one subject and thus requires validation to determine whether they refute the primary hypothesis, they seem to suggest that genes of other relevant but undetected proteins in **Chapter II** that mediate endothelial cell interaction and T cell activation might be upregulated within inflated DYS^+ $CD4^+$ T cells compared to conventional EPD^+ $CD4^+$ T cells. The findings show a fundamental difference in the consensus transcriptome of inflated DYS^+ T cells compared to that of the non-inflated control. At the individual gene expression level, the upregulation of *SELL* and *PSTK* is observed among the inflated DYS^+ $CD4^+$ T cells; the protein products of these genes facilitate both the interaction of lymphocytes with endothelial cells and the activation of T cells via stimulation of the T cell receptors. In addition, higher levels of *VPS13D* and *EXOC4* transcripts are detected; VPS13D and EXOC4 proteins mediate the trafficking of secretory vesicles to cell membranes, a finding that complements the polyfunctionality and cytotoxicity documented in **Chapter II**. A host of other proteins that are involved in cell proliferation were also detected. In summary, this chapter identifies additional potential phenotypic characteristics of inflated DYS^+ $CD4^+$ T cells that, when validated, would suggest that the mechanism of their inflation might involve the activation and subsequent proliferation after stimulation of their TCR.

In **Chapter V**, I summarize my findings and discuss the future directions of the integrated body of work from **Chapters II**, **III** and **IV**. I highlight the major observations and discuss the implications, possible teleological reasons and potential mechanistic explanations based on current literature. It is important to separately evaluate inflated

and non-inflated CMV-specific T cell responses in future studies. Overall, memory inflation is a phenomenon that depends on multifactorial elements that are all necessary but not individually sufficient in order for it to occur. The critical elements documented in this dissertation include CMV seropositivity, specific TCR CDR3 repertoire with conserved amino acid residues, and a unique transcriptome and protein expression profile. Based on the collective findings outlined in this dissertation and current literature on memory inflation, I describe a multi-omic criterion that improves the resolution of identifying memory-inflated T cells. The identification criterion of memory-inflated T cells is defined by the following:

1. Upregulated mRNA transcripts for the following genes: *TBX21* (T-bet), *EOMES*, *PRDM1* (Blimp-1), *ADRB2* (beta-2 adrenergic receptor), *FGFBP2* (fibroblast growth factor binding protein 2) and *GPR56* (G protein-coupled receptor 56); and after validation of the scRNA-seq findings, *SELL* (CD62L protein), *PSTK* (phosphoseryl-TRNA kinase), *VPS13D* (vacuolar protein sorting-associated protein 13D), *EXOC4* (exocyst complex component 4 protein), and *IL12RB1* (IL-12 receptor beta 1 subunit);
2. Downregulated *MAF1* gene transcript (repressor of RNA polymerase III transcription MAF1 homolog protein) after validation of the scRNA-seq findings;
3. Upregulated expression of the following proteins: CX_3CR1, granzymes A, B and H, perforin, IFN-γ and TNF-α; and
4. Downregulated expression of the following proteins: CD28, CD27, CD127 (IL-7R), TIGIT, and for most of the cells, and CCR7.

The future directions of this work include determining the mechanisms governing memory inflation from virological and immunological viewpoints; defining the contributions of memory-inflated T cell responses, especially T_{EMRA} subsets to the increased T cell activation that is believed to mediate cardiovascular comorbidities in HIV^+ subjects as the findings could raise safety implications for CMV vaccines in trials being planned in both HIV^+ and HIV^- subjects; and finally, determining the mechanism of latent HIV persistence in epitope-specific $CD4^+$ T cell reservoirs.

In **Chapter VI**, I describe all materials and methods for the experiments presented in my dissertation. I also highlight the contributions of various members of the laboratories of Simon Mallal, Spyros Kalams and Elizabeth Phillips in assay development, experiment execution and data analysis.

(this page was intentionally left blank)

CHAPTER I

INTRODUCTION

Human Cytomegalovirus (HCMV) Discovery and Transmission

The characteristic intranuclear inclusion pathology (**Figure I.1**) with an owl's eye that is induced by human cytomegalovirus (HCMV) was initially observed in sectioned tissues from patients by three German scientists (Ribbert H., Jesionek A., and Kiolemenoglou B.) around 1881 (Ho, 2008). This clinical finding earned it the initial name, "cytomegalic inclusion disease," until the causative viral agent was discovered and named "cytomegalovirus" by Dr. Thomas Weller in the 1950s (Craig et al., 1957; Ho, 2008). Drs. Margaret Smith and Wallace Rowe independently discovered CMV around the same time as Dr. Weller (Rowe et al., 1956; Smith, 1956).

HCMV, also known as human herpesvirus-5 (HHV-5) is a member of the *betaherpesvirinae* subfamily, with other host-specific species besides humans that include mice (murine CMV, MCMV), monkeys, rats (RCMV) and pigs (Davison et al., 2013). Antigenic variability exists within subfamilies, as HCMV strains propagated during natural infection have been shown to possess highly heterogeneous genomes (Gorzer et al., 2010; Renzette et al., 2011). HCMV is commonly transmitted via bodily fluids including saliva, urine, semen, tears, stool, blood, and breast milk; breast milk is one of the methods of maternal vertical transmission to a newborn (Sia and Patel, 2000). The virus can also be transmitted to the fetus during pregnancy across the

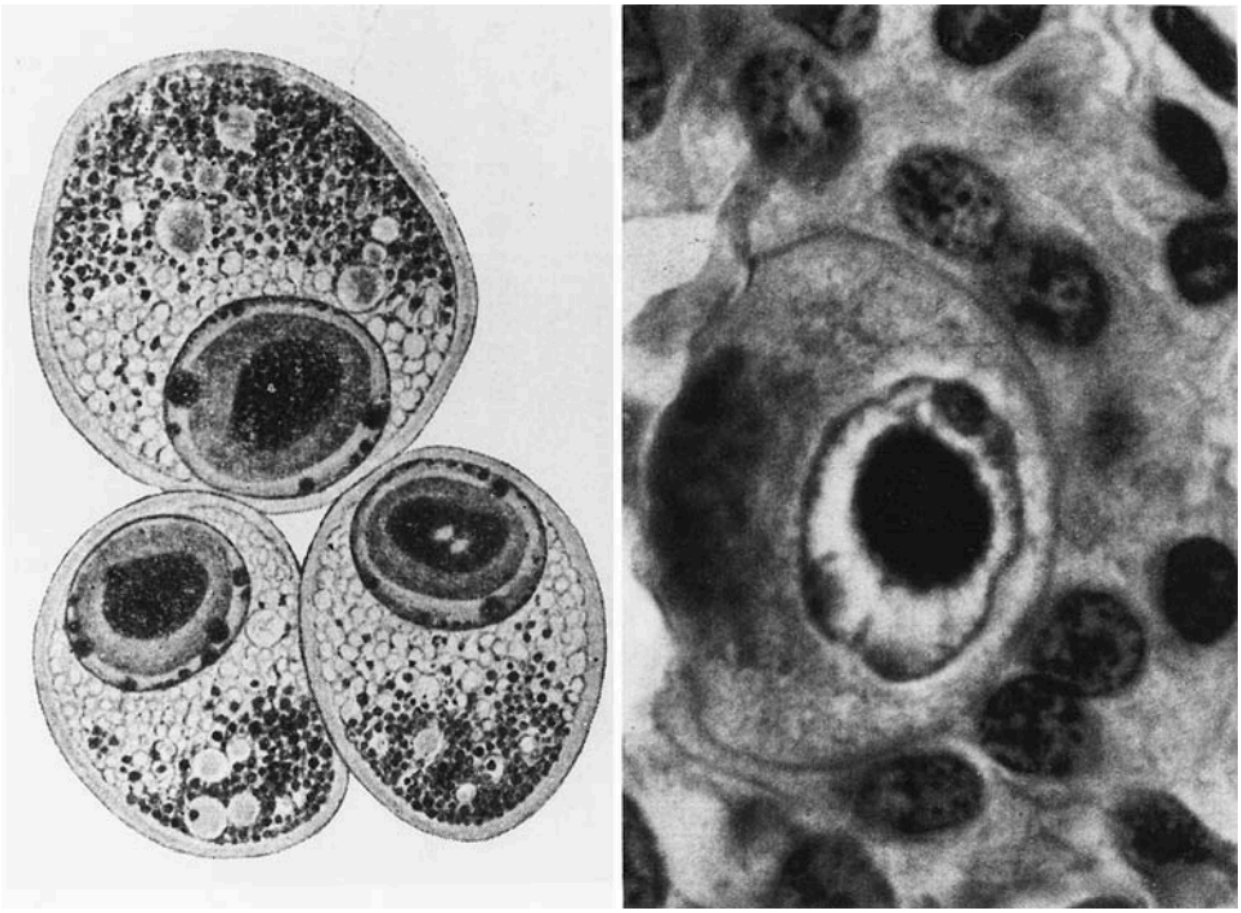

Figure I.1 First documented evidence of HCMV inclusion bodies. *Left* Cells with intranuclear inclusions with halo thought by Jesionek and Kiolemenoglou to represent parasites. *Right* CMV infected cytomegalic cell with intranuclear inclusion with halo. Note also cytoplasmic inclusion on the *left side* of the cell. This figure and its caption were obtained from Ho, 2008 and used upon approval by Springer under license number 4175030518734.

placenta. HCMV is also transmitted via either solid-organ transplantation (SOT) or hematopoietic stem cell transplantation (HSCT) (Sia and Patel, 2000). The seroincidence of HCMV infection increases with age from 6 years to over 75 years (**Figure I.2**). In developed countries, seroprevalence ranges from 30% to 90%, depending on age and other demographic factors (Staras et al., 2006), and is influenced by living conditions, as subjects living in less hygienic conditions suffer higher and earlier rates of transmission (Mocarski et al., 2013).

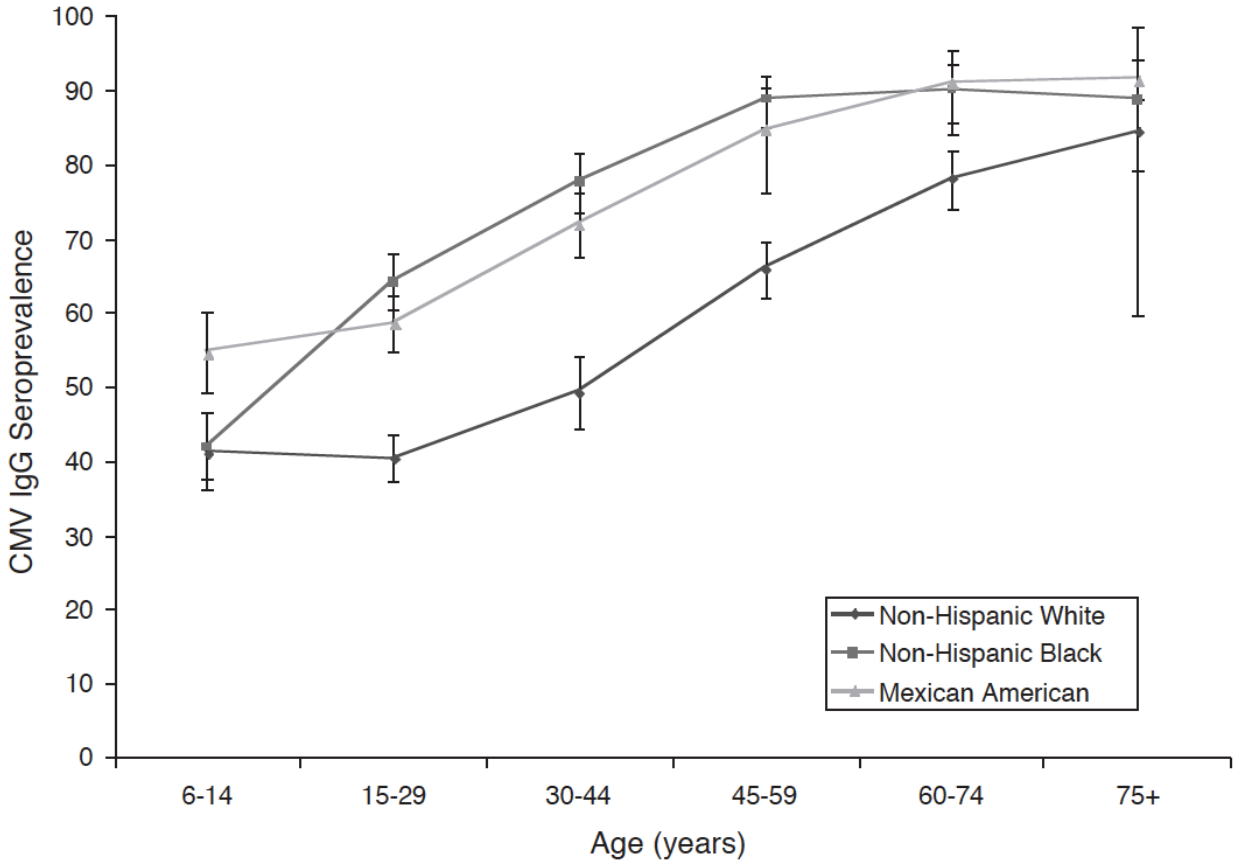

Figure I.2. HCMV seroprevalence increases with age. Data from the Third National Health and Nutrition Examination Survey, 1988–1994, showing results of testing for seroprevalence of cytomegalovirus (CMV), by age and race. Data were adjusted for sex, household income level, education, marital status, area of residence, census region, family size, country of birth, and type of medical insurance. This figure and its caption were obtained from Staras et al., 2016 and used upon approval by Lin Liu and Oxford University Press under license number 4175040990043.

HCMV Disease

HCMV infection of immunocompetent individuals usually results in asymptomatic infection (Rowe et al., 1958), including over 90% of pregnant mothers who suffer primary infection during pregnancy (Stagno et al., 1986). Some patients develop mononucleosis that is accompanied by fever, fatigue, headache and muscle ache, elevated liver enzymes (alanine aminotransferase, ALT, and aspartate

aminotransferase, AST), lymphocytosis, atypical lymphocytes, and in rare instances, adenopathy, hepatomegaly and splenomegaly (Mocarski et al., 2013).

Overt clinical manifestations of HCMV infection are observed in immunosuppressed subjects including transplant recipients and patients with Acquired Immunodeficiency Syndrome (AIDS) with CMV-induced retinitis, and gastrointestinal and other complications (Andersen and Spencer, 1969; Gertler et al., 1983; Knapp et al., 1983). These complications of CMV are comprised of either “end-organ disease” or CMV syndrome (Ljungman et al., 2017). Diagnosis of HCMV-associated end-organ disease requires observation of HCMV clinical signs and symptoms and detection of HCMV in the tissue (Ljungman et al., 2017). These include HCMV retinitis, HCMV hepatitis, HCMV gastrointestinal disease, central nervous system (CNS) disease, HCMV pneumonia, nephritis, cystitis, myocarditis and pancreatitis (Ljungman et al., 2017). The ability of HCMV to cause severe complications in immunosuppressed subjects led to the early observation that it caused opportunistic infection among HIV subjects during the early years of HIV’s first incidence (Drew et al., 1981). Before the development and administration of antiretroviral therapy (ART) to human immunodeficiency virus (HIV)-infected subjects, about 40% of patients with advanced HIV infection eventually suffered from HCMV-related opportunistic infections (Bowen et al., 1996). This typically occurred in subjects with $CD4^+$ T cell counts of <100 per µl of blood (Palella et al., 1998; Salmon-Ceron et al., 2000). The most common HCMV disease in HIV^+ subjects is retinitis (**Figure I.3**) (Keunen and Rothova, 1995). Esophagitis, colitis, gastritis, hepatitis and encephalitis have also been reported

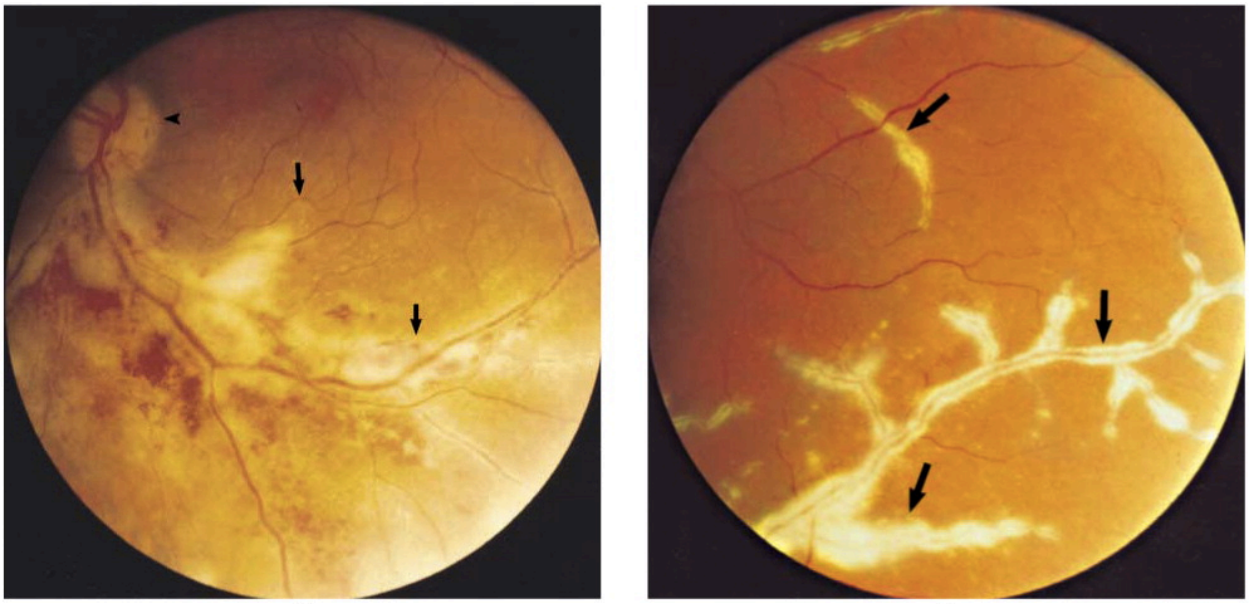

Figure I.3 Cytomegalovirus retinitis in AIDS. A 35-year-old man with the [sic] acquired immunodeficiency syndrome presented with floaters and blurred vision in both eyes. In the left eye (Panel A), the white wedge-shaped areas with accompanying hemorrhage along the inferior vascular arcade (arrows) represent necrosis of the retina. The arrowhead points to the optic disk. In the right eye (Panel B), the peripheral retina shows white sheathing along the blood vessels, so-called frosted-branch sheathing (arrows), a finding characteristic of vasculitis but not pathognomonic for cytomegalovirus retinitis. This figure and its caption were obtained from Keunen and Rothova, 1995 and reproduced with permission from The New England Journal of Medicine, Copyright Massachusetts Medical Society.

(Gallant et al., 1992; Steininger et al., 2006). Furthermore, the rate of HIV disease progression to AIDS or death is more rapid in HCMV co-infected individuals; homosexual men with AIDS have higher HCMV titer compared to subjects without AIDS (Fiala et al., 1986). In another group of HIV^+ homosexual men, 100% of them had CMV IgG antibody and CMV was detected in the semen of 45% of them (Leach et al., 1993).

Among solid-organ transplantation (SOT) recipients, HCMV seronegative recipients (R^-) receiving organs from seropositive donors (D^+) on immunosuppressive therapy have the greatest risk of developing HCMV disease. Among a cohort of 320 D^+R^- renal transplant recipients, about 56% were infected with HCMV after SOT, which caused the death of 25% of recipients and graft rejection in 20% of the recipients (Marker et al., 1981). The definition of CMV syndrome encompasses prolonged fever,

malaise, leukopenia, elevated atypical lymphocytes, thrombocytopenia, neutropenia, and elevated ALT and AST liver enzymes (Ljungman et al., 2017; Mocarski et al., 2013). Other CMV complications in SOT patients include pneumonitis (Neiman et al., 1977), enterocolitis (Veroux et al., 2007), esophagitis (Harada et al., 2005), gastritis (Llado et al., 2008), and pancreatitis (Klassen et al., 2000). These manifestations occur at different times in different types of SOT. The type of organ being transplanted (Sia and Patel, 2000), quality and extent of suppressive immunotherapy regimen (Best et al., 1995; Portela et al., 1995), and co-infection with human herpesvirus-6 (Dockrell et al., 1997), all determine whether a solid-organ recipient develops CMV-related complications. While early administration of ganciclovir or valganciclovir prophylactic anti-CMV treatment reduces the incidence of CMV disease in SOT recipients, about 26–29% of the kidney transplant recipients (Arthurs et al., 2008; Boudreault et al., 2011) or 7% of liver transplant recipients (Limaye et al., 2004) still suffer from delayed disease onset after treatment is discontinued post-transplantation. HCMV is associated with the rejection of both cardiac allografts in about 30% of transplant recipients (Grattan et al., 1989) and renal allografts in about 61% of transplant recipients (Sagedal et al., 2002). Furthermore, it is associated with stenosis of coronary arteries in heart transplant patients (Koskinen et al., 1993; McDonald et al., 1989) and renal arteries in kidney transplant patients (Audard et al., 2006; Pouria et al., 1998).

Hematopoietic stem cell transplantation (HSCT) patients undergo extended immune suppression, especially after allogeneic transplant. In addition to D^+/R^- recipients, D^+/R^+ and D^-/R^+ asymptomatic HCMV-seropositive recipients have high risks of developing HCMV disease (Broers et al., 2000). The risk of CMV disease occurrence

in D^-/R^+ HSCT recipients is most likely due to treatment related mortality (Broers et al., 2000). HCMV-seropositive leukemia patients receiving T cell-depleted bone marrow transplantation from matched unrelated donors are more likely to have increased transplant-related mortality and reduced overall survival compared to HCMV-seronegative subjects receiving similar tissues (Meijer et al., 2002). The age of the recipient, the level of mismatch in the human leukocyte antigen (HLA) between the donor and recipient, the source and use of T cell-depleted hematopoietic stem cells and the amount and quality of post-transplant immunosuppression all determine whether or not an HSCT recipient experiences HCMV reactivation (Boeckh et al., 2003; Hebart and Einsele, 2004). An important complication in SOT and HSCT recipients receiving allogeneic tissues with mismatched HLA alleles is graft-versus-host-disease (GVHD). GVHD in renal allograft recipients is believed to be partly mediated by a variety of alloreactive virus-specific $CD4^+$ and $CD8^+$ memory T cells, including CMV-specific T cells, that can be induced by vaccination, and likely cross-react with allogeneic HLA class II and I molecules from donors, respectively (Amir et al., 2010; D'Orsogna et al., 2011).

HCMV is the leading infectious cause of deafness (Fowler and Boppana, 2006) and neurodevelopmental deficits in newborns (Ross and Boppana, 2005). Most congenital HCMV infections are asymptomatic. However, up to 27% and 40% of congenital HCMV-infected newborns develop hearing loss and neurological deficits, respectively (Boppana et al., 1992). Other complications from congenital HCMV infection include petechiae, jaundice, hepatosplenomegaly, microcephaly, hepatitis, thrombocytopenia, and elevated cerebrospinal fluid proteins (Boppana et al., 1992)

Infection of seronegative pregnant women during the first trimester poses the greatest risk of severe HCMV disease (Pass et al., 2006). The combined prevalence of congenital infection either by neo-infection of or latent reactivation within pregnant mothers from a world-wide collection of studies is about 0.64% (Kenneson and Cannon, 2007). Compared to primary HCMV infection of pregnant women, recurrent HCMV infection from latent reactivation during pregnancy poses lesser risk of symptomatic congenital HCMV disease probably due to protective maternal HCMV antibodies (Fowler et al., 1992; Stagno et al., 1982). Also, congenital infection from primary infection is more likely to occur among high-income pregnant women (Fowler et al., 1992; Stagno et al., 1982). Overall, the fetal gestational age when the mother acquires infection, whether the mother has primary infection or latent reactivation, viral load, and clinical features of the neonate all determine the risks and consequences of congenital HCMV infection (Mocarski et al., 2013).

HCMV Virology

HCMV is a double-stranded DNA herpesvirus (Roizmann et al., 1992). The HCMV virion consists of a human cell membrane-derived outer, lipid bilayer envelope that is embedded with structural transmembrane glycoproteins (Mach et al., 2007). The envelope encloses the phosphoprotein-rich tegument, which surrounds an icosahedral, 162-capsomere nucleocapsid that houses the genome (Caposio et al., 2013). The genome is comprised of a linear, 235 kilobase-pair double-stranded DNA that is the

largest of all human herpes viruses (LaFemina, 1980) and encodes between 165 and 181 genes (Dolan et al., 2004; Scalzo et al., 2009).

HCMV's genome consists of unique-long (U_L) and unique-short (U_s) sequence segments that are each flanked by inverted repeats, a feature unique to HCMV among cytomegaloviruses of the primates and not shared by murine cytomegaloviruses. U_L is flanked by terminal-repeat-long (TR_L) and internal-repeat-long (IR_L) and they are all adjacent to the terminal-repeat-short (TR_S) and internal-repeat-short (IR_S) (Davison et al., 2003; Weststrate et al., 1980) (**Figure I.4**).

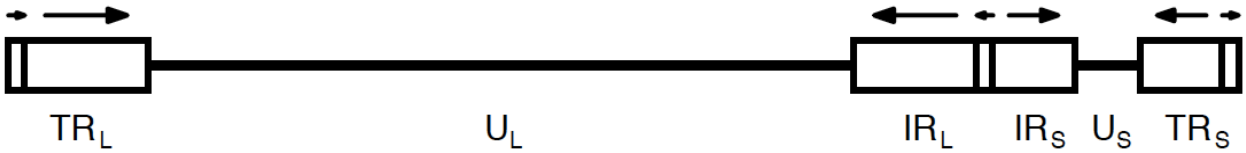

Figure I.4 CMV genome structure (not to scale). Unique and repeated regions are shown as horizontal lines and rectangles, respectively, with the orientations of the latter shown by arrows. This figure and its caption were obtained from Davison et al., 2013 and used upon approval by Caister Academic Press under written permission granted by Dr. Andrew Davison.

There are identical direct terminal repeat sequences that flank both ends of the entire genome, including an inverted repeat of the sequence in-between the IR_L and the IR_s sequences (Davison et al., 2013). A list of all proteins and their respective open reading frames (ORFs) contained within a mature HCMV virion—as determined by liquid chromatography and Fourier Transform Ion Cyclotron Resonance mass spectrometry—are shown in (**Table I.1**) (Caposio et al., 2013). HCMV DNA replication during its lytic cycle (discussed below) begins at the *cis*-acting, origin of replication site—*ori*Lyt—a three kilobase-long nucleotide sequence that is embedded between UL57 and UL69 ORFs (Zhu et al., 1998) and that is strongly conserved between human herpesviruses.

Group	HCMV ORF	Comments
Capsid	UL46	Minor capsid binding protein
	UL48–49	Smallest capsid protein
	UL80	Assembly precursor
	UL85	Minor capsid protein
	UL86	Major capsid protein
Tegument	UL24	Tegument protein
	UL25	Tegument protein; UL25 family
	UL26	Tegument protein, US22 family
	UL32	Tegument protein, pp150
	UL35	Tegument phosphoprotein, UL25 family
	UL43	Tegument protein, US22 family
	UL47	Tegument protein
	UL48	Large tegument protein
	UL71[a]	Tegument protein
	UL82	Upper matrix phosphoprotein, pp71
	UL83	Lower matrix phosphoprotein, pp65
	UL88	Tegument protein
	UL94	Tegument protein
	UL96	Tegument protein
	UL99	Tegument protein, pp28
	UL103[a]	Tegument protein
	US22	Tegument protein; US22 family
	US23[a]	Tegument protein, US22 family
	US24[a]	Tegument protein, US22 family
Glycoproteins	RL10	
	TRL14[a]	
	UL5[a]	RL11 family
	UL22A	Secreted glycoprotein
	UL33	G-protein coupled receptor
	UL38[a]	
	UL41A	
	UL50	Membrane protein involved in nuclear capsid egress
	UL55	gB
	UL73	gN
	UL74	gO
	UL75	gH
	UL77	Pyruvoyl decarboxylase; DNA packaging protein
	UL93	
	UL100	gM
	UL115	gL
	UL119	IgG Fc-binding glycoprotein
	UL132[a]	
	US27	G-protein coupled receptor
Transcription/ replication machinery	IRS1	Transcriptional transactivator; US22 family
	TRS1	Viral gene transactivator
	UL44	DNA processivity factor
	UL45	Ribonucleotide reductase homologue (enzymatically inactive)
	UL51	Terminase component
	UL54	DNA polymerase
	UL57	ssDNA-binding protein
	UL69	Posttranscriptional regulator of gene expression
	UL72	Deoxyuridine triphosphatase homologue (enzymatically inactive)
	UL79*	DNA replication
	UL84	Transdominant inhibitor of IE2-mediated transactivation
	UL89	Terminase component
	UL97	Phosphotransferase
	UL104	DNA packaging protein; capsid portal protein
	UL112	DNA replication
	UL122	Viral and cellular gene transactivator, IE2

Table I.1 HCMV proteins found in virions. HCMV proteins isolated from virions that were identified by liquid chromatography-mass spectrometry/mass spectrometry and Fourier Transform Ion Cyclotron Resonance. This table and its caption were obtained from Caposio et al., 2013 and used upon approval by Caister Academic Press under written permission granted by Dr. Patrizia Caposio.

[a]Denotes proteins newly identified associated [sic] with HCMV virions.

The glycoproteins of the HCMV envelope include glycoprotein B (gB from UL55 ORF), H (gH from UL75 ORF), L (gL from UL115 ORF), M (gM from UL100 ORF), N (gN from UL73 ORF) and O (gO from UL74 ORF) (**Figure I.5**) (Caposio et al., 2013; Feire, 2013; Varnum et al., 2004). Neutralizing antibodies have been identified that recognize gB (Britt et al., 1990), gH (Cranage et al., 1988), gH/gL (Macagno et al., 2010) and gM/gN (Shimamura et al., 2006) as primary targets. The primary role of these proteins is to facilitate entry into host cells. Specifically, gB, gH and gL help attach HCMV to the cell surface for entry, while gM and gN are important for the maturation of newly synthesized HCMV virions. During attachment, HCMV uses gB to bind the heparan sulfate proteoglycan on the surface of the host cell from where gB undergoes cell entry into the plasma membrane or endocytic vesicles via a pH-independent mechanism (Compton et al., 1993). The Endoplasmic Reticulum-Golgi Intermediate Compartment (ERGIC) of HCMV-infected cells produces cytoplasmic vacuoles that are proximal to the Golgi apparatus and facilitate the formation of the HCMV envelope membrane for new virions (Homman-Loudiyi et al., 2003).

The envelope membrane surrounds the tegument that is comprised of phosphoproteins, with the lower matrix phosphoprotein-65 (pp65; also known as unique long 83, UL83) being the most abundant. pp65 is the most dominant protein in dense bodies, comprising up to 60% of the total protein (Baldick and Shenk, 1996; Irmiere and Gibson, 1983). pp65 is commonly used to determine the size and quality of CMV-specific T cell responses in subjects being screened for immunity against CMV (van der Bij et al., 1988) based on its extremely high immunogenicity (Jahn et al., 1987). One of

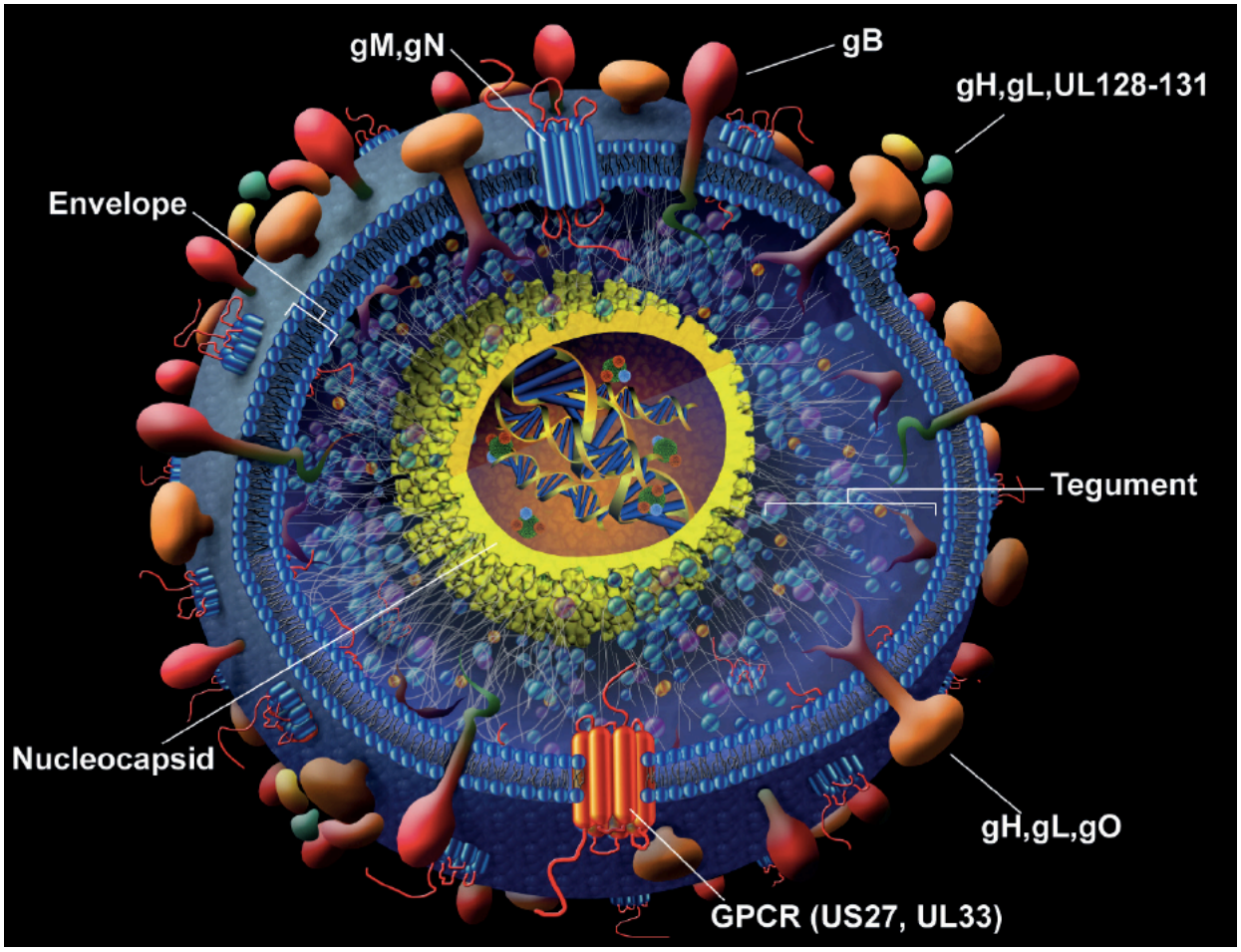

Figure I.5 HCMV structure. HCMV virions are comprised of three major layers. The first layer is the nucleocapsid containing the linear double-stranded viral DNA genome, which is surrounded by a proteinaceous tegument layer. The tegumented capsids are enveloped by a host-derived lipid bi-layer that is studded with viral glycoproteins. This figure and its caption were obtained from Caposio et al., 2013 and used upon approval by Caister Academic Press under written permission granted by Dr. Patrizia Caposio.

the major actions of pp65 is to suppress the immediate type 1 interferon response that occurs after HCMV binds and infects a new cell (Abate et al., 2004). This enables the newly infected cell to evade immune recognition, as the virus is able to prevent it from inducing an early anti-viral immune response. Some of the other proteins that make up the tegument include upper matrix pp71, which enhances HCMV infectivity (encoded by UL82) (Baldick et al., 1997; Ruger et al., 1987); large matrix pp150 (encoded by UL32) (Jahn et al., 1987); pp28 (encoded by UL99) (Meyer et al., 1988); and the largest

tegument protein (encoded by UL48) (Yu et al., 2011). In all, there are 32 proteins within the tegument that are expressed by HCMV genes (Silva et al., 2003). These proteins have a wide range of functions including the facilitation of nucleocapsid trafficking to nuclear pores along microtubules during initial infection, from where HCMV enters the nucleus (Ogawa-Goto et al., 2003). In all, the tegument contains a majority of HCMV's protein (Varnum et al., 2004), and most of them likely help with virion assembly, disassembly and regulation of host cellular response (Kalejta, 2008).

The nucleocapsid is made up of four herpesvirus proteins: (i) the major capsid protein from UL86 gene, (ii) the minor capsid protein from UL46 gene, (iii) the minor capsid protein binding protein from UL85, and (iv) the smallest capsid protein from UL48A (Mocarski et al., 2013). Additionally, present within the nucleocapsid are (i) a 500-base-pair-long virus associated-RNA (vRNA-1), and (ii) a 300-base-pair-long vRNA-2 that forms a RNA-DNA hybrid with HCMV's genome at the origin of lytic replication (Prichard et al., 1998).

HCMV Infection

Lytic or productive infection

HCMV infects a wide range of cells and tissues. The major cells within the gastrointestinal tract, placenta, lungs, nasal mucosa, trachea, thyroid, bone marrow, spleen, urinary bladder, and urethra that are infected by HCMV include epithelial cells; systemic endothelial cells, especially those in the vasculature; fibroblasts; and smooth muscle cells (Chen and Hudnall, 2006; Gordon et al., 2017; Muhlemann et al., 1992;

Ng-Bautista and Sedmak, 1995; Roberts et al., 1989; Sinzger et al., 1993). Other cells/tissues infected by HCMV include monocytes and/or macrophages, brain glial/neuronal cells, neutrophils, stromal cells, cardiac myocytes, reticular cells in the spleen and lymph nodes, hepatocytes, endometrial stromal and glandular cells, breast myometrium, fallopian tube submucosa and the kidney (Ibanez et al., 1991; Myerson et al., 1984; Sinzger et al., 2000).

HCMV can infect both undifferentiated and differentiated cells, but viral replication can only occur in differentiated cells (Sissons et al., 2002). The process of HCMV replication depends on eight important proteins from the following ORFs: UL54 (polymerase), UL57 (single-stranded DNA-binding protein), UL102 (helicase), UL105 (primase), UL44 (polymerase-associated factor), UL70 (primase-associated factor) (Iskenderian et al., 1996; Kagele et al., 2012; Pari and Anders, 1993), IE2 (encoded by UL-123), and UL84 (Pari et al., 1993). An important promoter in the replication cycle of HCMV is the major immediate early promoter (MIEP). This promoter plays a significant role in the initiation of transcription of immediate early 1 (IE1) and IE2 genes after cell infection (Puchtler and Stamminger, 1991; Stenberg et al., 1989), suppression of HCMV genes during latency and the re-expression of viral genes during reactivation (Mocarski et al., 2013). The replication cycle of HCMV in a human cell is depicted in (**Figure I.6**).

There are three sequential stages of HCMV transcription, which correspond to five classes of genes: immediate early (IE), early (E), delayed early, late (L) and true late gene transcriptions (Spaete and Mocarski, 1985). CMV IE genes are defined as genes expressed within the first two hours of cell infection, while early genes are expressed in the first twenty-four hours, and late genes are expressed after the first

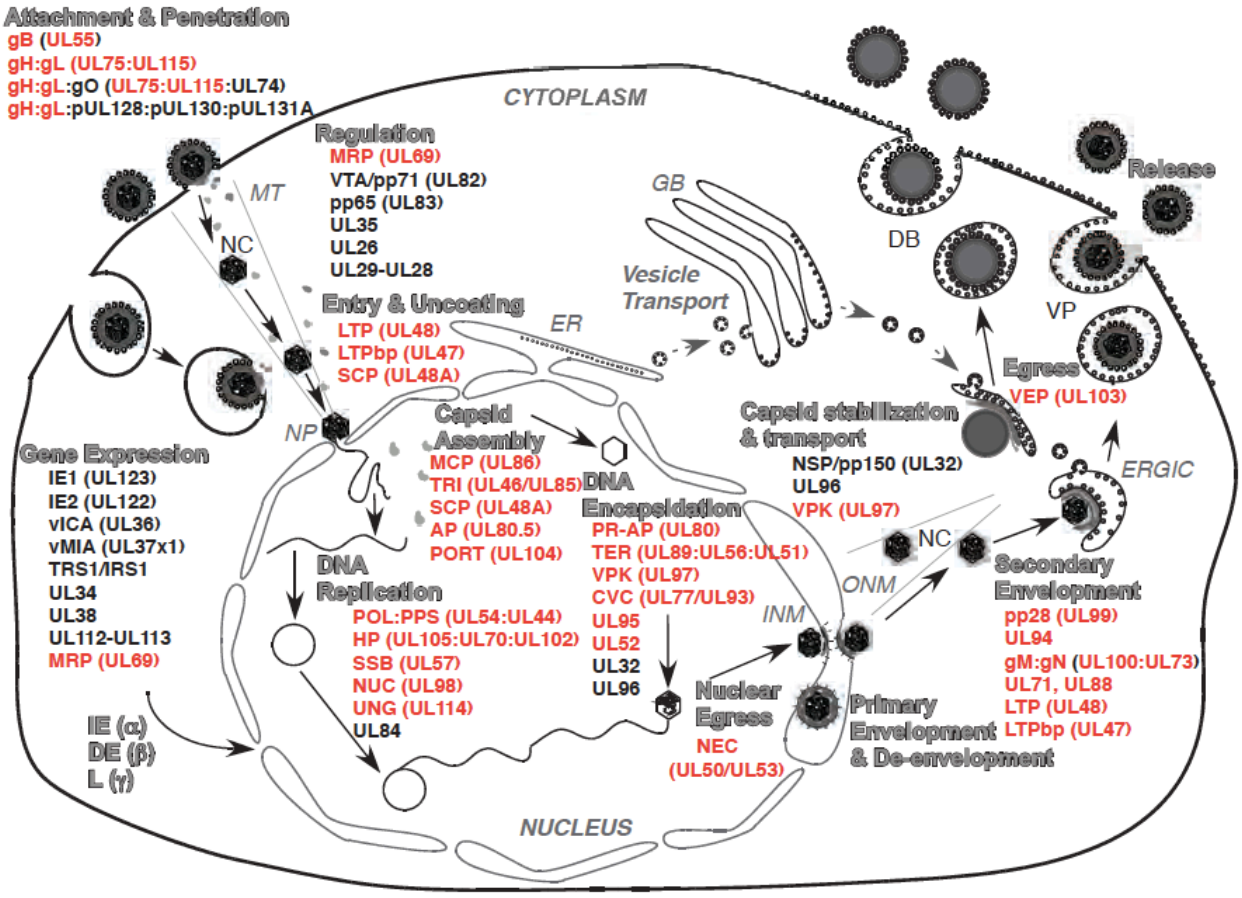

Figure I.6 Summary of the human cytomegalovirus (HCMV) replication pathway. Major steps in productive replication are indicated in *large gray font with outline, black arrows* indicate the progression of steps and viral functions. Individual gene products listed under each step are identified by provisional abbreviated names as either herpesvirus core (*red text*) or beta herpesvirus conserved (*black text*). Viral attachment and penetration occur either via direct fusion at the cell surface (fibroblasts), dependent on gB, gH:gL and gH:gL:gO, or via endocytosis into other cell types (endothelial and epithelial cells) where the pentameric complex, gH:gL:p128:p130:p131A, also facilitates entry (see text). In addition to the interferon (IFN)–like activation of cells by the process of attachment and penetration, input virion tegument proteins (UL69/MRP, pp71/VTA, pp65, UL35, UL26, and UL29-UL28) regulate cellular pathways. NC-associated UL47, UL48, and smallest capsid protein (SCP) are predicted to facilitate the final steps in entry and uncoating that deliver input nucleocapsid (NC) via microtubules (*MT*) to nuclear pore (*NP*) complexes where the viral genome is released into the nucleus. Transcriptional regulation of viral and host cell gene expression is mediated by IE genes (IE1, IE2) or DE genes (UL34, UL35, UL112-UL113, and UL69); cell death suppression is mediated by IE gene products vICA and vMIA, and other regulatory processes are facilitated by UL34, UL38, and UL112-UL113 proteins. DNA replication depends on core proteins (POL:PPS, HP, SSB, NUC, and UNG) as well as one beta herpesvirus-specific protein (UL84 gene product) that facilitates initiation of DNA synthesis. Capsids assemble from MCP, TRI, SCP, PORT, and AP. Preformed capsids process PR-AP (UL80) and AP as viral DNA is encapsidated by the TER complex (UL89, UL56, UL51) through a PORT (UL104) pentamer, followed by predicted addition of the CVC complex (UL77, UL93) onto NC pentamers, with UL95, UL52, UL32, and UL96 added for NC stabilization. Nuclear egress of the NC is mediated by the NEC (UL50, UL53). Following primary envelopment at the inner nuclear membrane (*INM*), and de-envelopment at the outer nuclear membrane (*OMN*), capsid stabilization is ensured by the function of NSP/pp150 (UL32) and UL96, with nuclear egress and transport facilitated by VPK (UL97). Glycoproteins incorporated into the envelope are synthesized in the endoplasmic reticulum (*ER*), glycosylated in the Golgi body (*GB*), and delivered by vesicle transport (*dashed gray arrow*) to join NC at sights of secondary envelopment on ER Golgi intermediate compartment (*ERGIC*). Secondary envelopment requires UL99, UL94, gM/UL100:gN/UL73, UL71, UL88, UL47, and UL48, acting together with VPK. Following the acquisition of an envelope, virus particle (VP) as well as capsidless dense body (DB) egress is facilitated by VEP/UL103 for release into the extracellular space. This figure and its caption were obtained from Mocarski et al., 2013 and used upon approval by Lin Liu and Oxford University Press under license number 4175060572987.

twenty-four hours (Stinski, 1978). Host and viral factors play significant roles in the initiation and regulation of viral genome transcription. Transcription of IE1 genes occurs without initial protein synthesis. MIEP enhances the gene transcription and expression of IE1 and IE2 transactivators (Ghazal et al., 2013). IE2 regulates- and IE1 enhances the transactivation of CMV's E1.7 early promoter that induces CMV gene expression (Chang et al., 1989; Malone et al., 1990). Additionally, IE1 and IE2 both induce host gene promoters including c-fos and c-myc proto-oncogenes as well as the heat shock protein 70 (Hagemeier et al., 1992). Other studies have proposed that IE1 proteins control MIEP to enhance IE2 gene expression (Hermiston et al., 1990; Malone et al., 1990). The early and late phases of CMV gene expression are completely dependent on the availability of IE proteins that modulate gene expression (Ghazal et al., 2013).

An important characteristic of CMV immune response is that proteins of genes expressed during the same phase of lytic infection can elicit different magnitudes of T cell response. One of the main observations I discuss in **Chapter II** is that an epitope of CMV glycoprotein B, whose UL55 ORF is expressed as one of the late genes, elicits a higher magnitude of $CD4^+$ T cell response than another epitope of CMV pp65, whose UL83 ORF is also expressed as a late gene. The exact reason for this and other immune response magnitudes between different CMV proteins or different epitopes within the same CMV protein is not fully understood. As I will show in **Chapter II**, one of the possible explanations for the observation is the presence of specific T cell receptors with conserved amino acid residues that might facilitate avid binding by the HLA-epitope ligand to induce a response of higher magnitude.

Latent infection

HCMV establishes latency in a variety of cells and while there is strong evidence that this occurs in cells of the myeloid lineage, it has been proposed to be established in hematopoietic cells of myeloid origin (Sinclair and Sissons, 2006); monocytes/macrophages (Soderberg et al., 1993; Taylor-Wiedeman et al., 1991); lymphocytes (Schrier et al., 1985); $CD34^+$ bone marrow progenitors (Mendelson et al., 1996); immature dendritic cells (Senechal et al., 2004); non-hematopoietic cells such as endothelial cells (Grefte et al., 1993; Sinzger et al., 1995), liver sinusoidal endothelial cells for mCMV (Dag et al., 2014; Seckert et al., 2009), and LN endothelial cells (Fiorentini et al., 2011). Using PCR *in situ* hybridization, latent HCMV genome has been detected in 0.004 – 0.01% of peripheral blood- and bone marrow- mononuclear cells that are induced by granulocyte colony-stimulating factor (Slobedman and Mocarski, 1999). In order to establish latency, heterochromatin protein 1 suppresses MIEP (Reeves et al., 2005), while HCMV's pp71 suppresses IE gene expression (Kalejta, 2013).

Latent HCMV reactivation

Although the exact mechanism is unclear, it has been demonstrated that the expression of certain HCMV genes during reactivation from latency determines the magnitude of T cell response to the epitopes of those genes (Dekhtiarenko et al., 2013). Therefore, it is important to understand the steps known to be involved in HCMV reactivation. The reactivation of HCMV from latency is induced by inflammation and/or infection (sepsis), immunosuppression, or stress (Kutza et al., 1998; Mutimer et al., 1997; Prosch et al.,

2000). Although the precise mechanism by which reactivation is induced is unknown, it is believed to be mediated by tumor necrosis factor-alpha (TNFα) (Fietze et al., 1994) which activates protein kinase C and nuclear factor kappa-B (NF-κB) to initiate IE gene transcription in a fashion analogous to HIV reactivation (Prosch et al., 1995; Stein et al., 1993). Prostaglandins (Kline et al., 1998) and stress-induced catecholamines such as epinephrine and norepinephrine (Prosch et al., 2000) cause increased cyclic-AMP (cAMP) levels that result in the binding of CREB-1/aTF-1 to cAMP-responsive elements within MIEP or the IE gene enhancer. When latency is not reactivated, it is maintained by the suppression of major IE gene transcription that facilitates new virion formation (Sissons et al., 2002). pp65 facilitates the re-expression of suppressed IE genes by recruiting a cellular protein (IFI16) to bind and induce MIEP via an unknown mechanism (Cristea et al., 2010). It is important to note that CMV reactivation does not always result in productive virion formation (Kurz et al., 1999).

Immunity Against CMV

Acute CMV infection elicits innate and adaptive immune responses including potent $CD4^+$ and $CD8^+$ T cell responses that prevent the host from being overwhelmed by acute dissemination of CMV. However, these responses do not prevent CMV from establishing latency (Balthesen et al., 1994). These cells are presumed to be protective as subjects with impaired T cell responses experience various CMV-related complications such as retinitis in AIDS (Keunen and Rothova, 1995) or reduced overall survival in HSCT recipients (Meijer et al., 2002), etc. There is a correlation between

restoration of cytotoxic T cell activity of allogeneic bone marrow transplant recipients and control of HCMV disease (Quinnan et al., 1982; Reusser et al., 1991). The latent virus and its intermittent reactivations can induce $CD4^+$ and $CD8^+$ T cell responses in most subjects (Sylwester et al., 2005). While pp65 is often recognized, there are many individuals that preferentially recognize other CMV proteins (Sylwester et al., 2005). It is important to note that the size of the response varies among different subjects (Jackson et al., 2014). A balance exists between T cells and latent HCMV in immunocompetent subjects as T cell responses control HCMV reactivation, while the virus itself expresses certain genes including US2, US3, US6 and US11 that interrupt efficient HLA-I and HLA-II antigen processing and expression on the cell surface (Hegde et al., 2002; Jones et al., 1995; Llano et al., 2003; Tomazin et al., 1999), as well as NK-mediated cytotoxicity (Falk et al., 2002) in the setting of lytic infection. This balance is less effective in immunocompromised individuals such as SOT or HSCT recipients and subjects with AIDS during either productive or latent infection (Falk et al., 2002).

Overview of $CD4^+$ T cell ontogeny, TCR rearrangement and HLA class II epitope presentation

As with any $CD4^+$ T cell, the development of a $CD4^+$ T cell immune response against HCMV involves the formation of activated effector $CD4^+$ T cells that differentiate from progenitor cells, which are derived from pluripotent hematopoietic stem cells of the bone marrow (**Figure I.7**) (Murphy and Weaver, 2017). The progenitor cells from the bone marrow migrate to and mature in the thymus. Mature $CD4^+$ T cells then travel from the

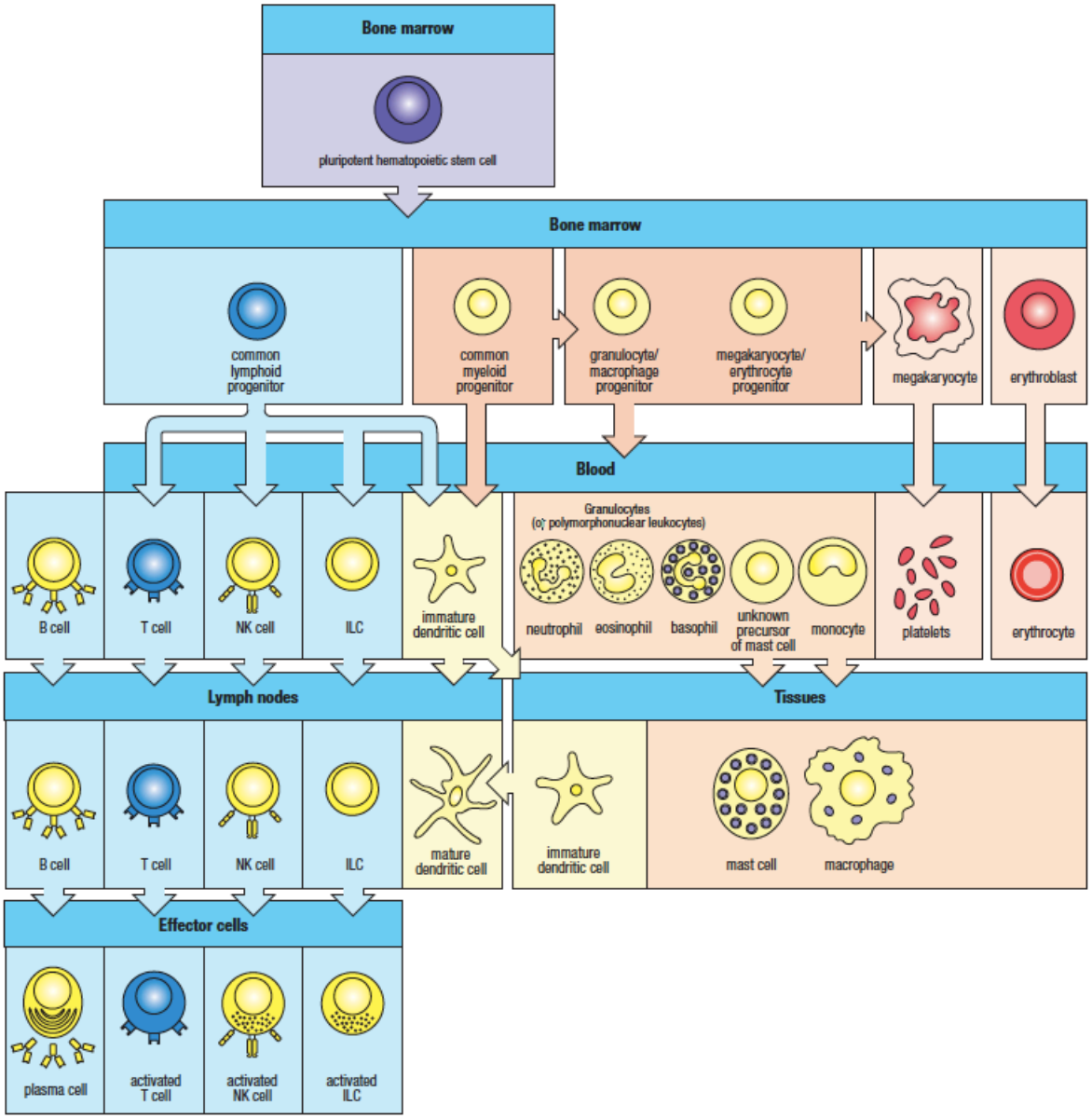

Figure I.7 All the cellular elements of the blood, including the cells of the immune system, arise from pluripotent hematopoietic stem cells in the bone marrow. These pluripotent cells divide to produce two types of stem cells. A common lymphoid progenitor gives rise to the lymphoid lineage (blue background) of white blood cells or leukocytes—the innate lymphoid cells (ILCs) and natural killer (NK) cells and the T and B lymphocytes. A common myeloid progenitor gives rise to the myeloid lineage (pink and yellow backgrounds), which comprises the rest of the leukocytes, the erythrocytes (red blood cells), and the megakaryocytes that produce platelets important in blood clotting. T and B lymphocytes are distinguished from the other leukocytes by having antigen receptors and from each other by their sites of differentiation—the thymus and bone marrow, respectively. After encounter with antigen, B cells differentiate into antibody-secreting plasma cells, while T cells differentiate into effector T cells with a variety of functions. Unlike T and B cells, ILCs and NK cells lack antigen specificity. The remaining leukocytes are the monocytes, the dendritic cells, and the neutrophils, eosinophils, and basophils. The last three of these circulate in the blood and are termed granulocytes, because of the cytoplasmic granules whose staining gives these cells a distinctive appearance in blood smears, or polymorphonuclear leukocytes, because of their irregularly shaped nuclei. Immature dendritic cells (yellow background) are phagocytic cells that enter the tissues; they mature after they have encountered a potential pathogen. The majority of dendritic cells are derived from the common myeloid progenitor cells, but some may also arise from the common lymphoid progenitor. Monocytes enter tissues, where they differentiate into phagocytic macrophages or dendritic cells. Mast cells also enter tissues and complete their maturation there. This figure and its caption were obtained from Murphy and Weaver, 2017 and used upon approval by Garland Science, Taylor & Francis Group under license number 4180800875858.

thymus to the peripheral and secondary lymphoid organs where they encounter novel antigens that are typically presented by professional antigen presenting cells including dendritic cells, macrophages, and B cells using HLA class II molecules. Thymic epithelial cells induce progenitor cells via Notch1 receptor to commit to the T cell lineage and this process is accompanied by the upregulation of T-cell factor-1 (TCF1) and GATA3 (Hattori et al., 1996; Ting et al., 1996). These transcription factors permit the expressions of important genes that are critical and unique to T cells, including the members of the CD3 complex and *Rag1*. The complex stages of T cell maturation in the lymph node begin with the differentiation of double-negative (DN) thymocytes from DN1 to DN2 to DN3 to DN4 (characterized by downregulation of CD44 and upregulation and downregulation of CD25), which mature into either $CD4^-$ $CD8^-$ γ:δ T cells or $CD4^+$ $CD8^+$ (double-positive) α:β T cells. The latter eventually differentiate into $CD4^+$ or $CD8^+$ single-positive T cells upon expression of ThPOK or Runx3 transcription factors, respectively, via the process of positive selection and the presentation of self peptides by self HLA class II or I molecules, respectively. T cells with extremely strong affinity for self-antigens undergo apoptosis via negative selection, and are phagocytosed by macrophages. HLA molecules inducing positive selection determine whether a cell expresses a CD4 or CD8 receptor as HLA class II molecules restrict epitopes recognized by CD4s, while HLA class I molecules restrict epitopes recognized by CD8s. These single-positive T cells then travel from the thymus to peripheral sites where they encounter foreign antigens (Murphy and Weaver, 2017). It is important to note that there are also cases where $CD8^+$ T cells can be restricted by HLA class II (Ranasinghe et al., 2016).

α:β T cell receptor gene recombination occurs during the differentiation of DN1 cells to $CD4^+$ $CD8^+$ α:β T cells, after abortive recombination of the gamma and delta T cell receptor gene segment. The variable (V_β), diverse (D_β) and joining (J_β) segments of the beta chain gene of the α:β T cell receptor recombine first during differentiation from DN1 through DN4. On the other hand, the transition from DN4 to $CD4^+$ $CD8^+$ α:β T cells is characterized by the surface expression of the rearranged beta chain and the nuclear rearrangement of the V_α and J_α of the alpha chain gene. The remarkable diversity exhibited by the α:β T cell receptor that mediates the recognition of the milieu of pathogen epitopes that exist, is achieved by the multiple different combinations of the 52 V_β, 2 D_β, and 13 J_β segments to form the beta-chain of the TCR, as well as those of the 70 V_α and 61 J_α segments to form the alpha chain of the TCR. This results in a highly diverse recombination repertoire (Bassing et al., 2000). Despite all of these possibilities, the TCR of a $CD4^+$ (and $CD8^+$) T cell focuses much of its diversity within the third complementarity-determining region (CDR3). The CDR3 is formed by the end of the V segment, all of the D segment and the beginning of the J segment for the beta chain, and by the end of the V and start of the J segments for the alpha chain (Murphy and Weaver, 2017). The rearrangements of the TCRα and TCRβ genes are depicted in (**Figure I.8**).

HLA class II molecules include HLA-DP, HLA-DQ and HLA-DR. These molecules are typically expressed by professional antigen presenting cells, which include dendritic cells, macrophages and B cells. They are formed by the dimerization of two nearly identical transmembrane glycoproteins, one α and one β protein. The α_1 and β_1 subunits of each monomer come together to form the binding groove where epitopes dock and

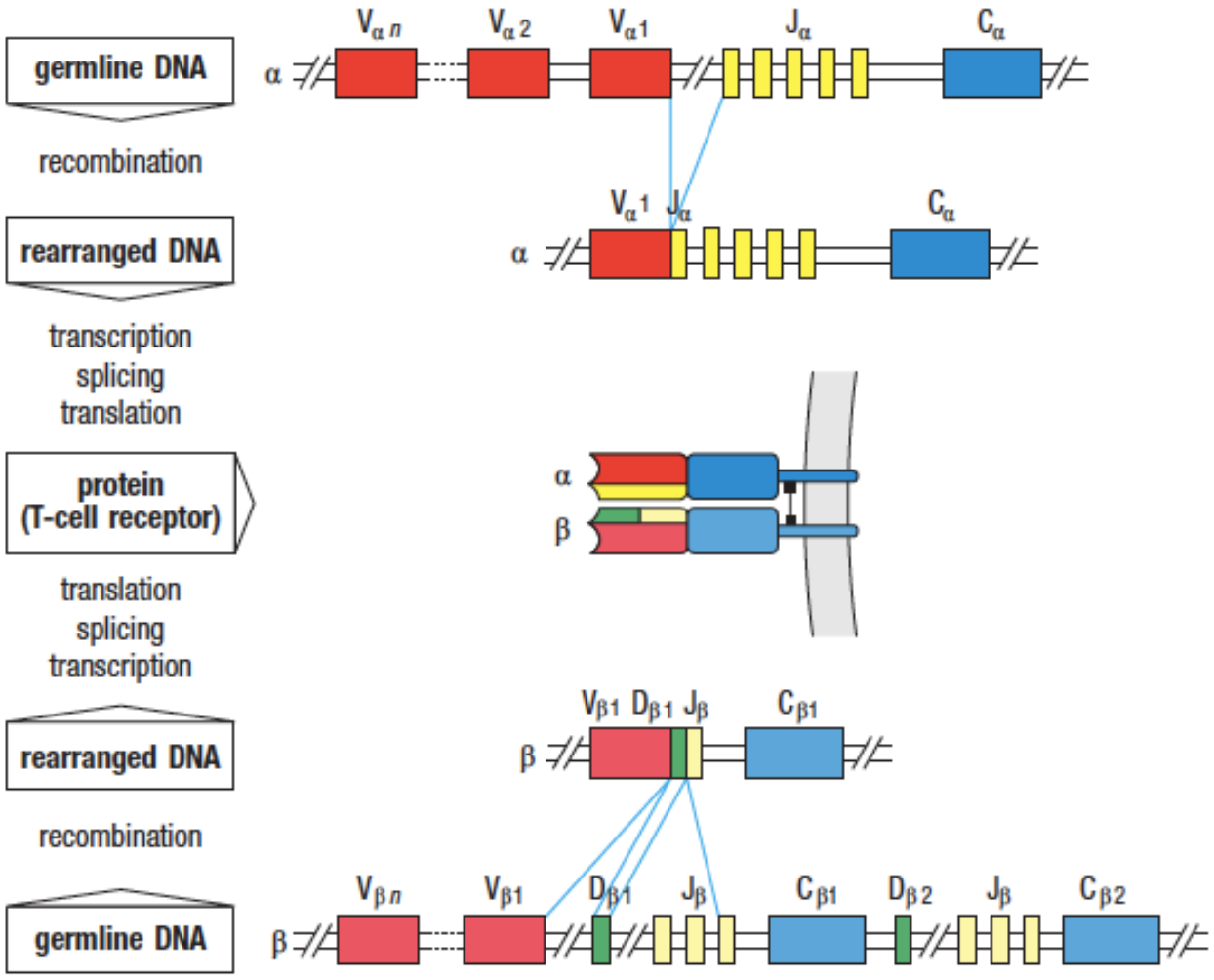

Figure I.8 T-cell receptor α- and β-chain gene rearrangement and expression. The TCRα- and β-chain genes are composed of discrete segments that are joined by somatic recombination during development of the T cell. Functional α- and β-chain genes are generated in the same way that complete immunoglobulin genes are created. For the α chain (upper part of figure), a Vα gene segment rearranges to a Jα gene segment to create a functional V-region exon. Transcription and splicing of the VJα exon to Cα generates the mRNA that is translated to yield the T-cell receptor α-chain protein. For the β chain (lower part of figure), like the immunoglobulin heavy chain, the variable domain is encoded in three gene segments, Vβ, Dβ, and Jβ. Rearrangement of these gene segments generates a functional VDJβ V-region exon that is transcribed and spliced to join to Cβ; the resulting mRNA is translated to yield the T-cell receptor β chain. The α and β chains pair soon after their synthesis to yield the α:β T-cell receptor heterodimer. Not all J gene segments are shown, and the leader sequences preceding each V gene segment are omitted for simplicity. This figure and its caption were obtained from Murphy and Weaver, 2017 and used upon approval by Garland Science, Taylor & Francis Group under license number 4180800875858.

bind using their side-chains to anchor residues on the HLA molecule for presentation to TCR. HLA class II molecules typically present epitopes of extracellular proteins that are endocytosed into endosomes. Acidification of these endosomes initiates proteosomal processing of the proteins into epitopes. The endosomes fuse with vesicles containing

new HLA class II molecules that are still bound to the human class II-associated invariant chain peptide (CLIP). Before the fused vesicles reach the cell surface, an HLA-DM molecule interacts with the CLIP-bound class II molecule, resulting in the release of CLIP and making room for newly processed epitopes of extracellular protein to bind for surface presentation. Unlike HLA class I, HLA class II molecules are able to present epitopes that are up to 20 amino-acids long. This is due to the open ends of the grooves, which are different from the closed ends of HLA class I molecules (Murphy and Weaver, 2017). A representative binding of an epitope to an HLA class II molecule with the epitope's terminal sticking out of the open end is shown in (**Figure I.9**).

HLA class II presentation of epitopes to $CD4^+$ T cells results in their activation and proliferation. There are various pathways by which an activated T cell transitions into a memory T cell. Some studies have indicated that interleukin-7 (IL-7) facilitates this process based on the association of IL-7 receptor expression on T cells with their survival (Kondrack et al., 2003; Li et al., 2003). Other studies suggest a critical role for the avidity of TCRs for their cognate HLA-epitope ligand (Williams et al., 2008).

$CD4^+$ T cell adaptive immunity to HCMV

$CD4^+$ T cells play a significant role in the control of CMV infection. In immunocompetent children, poor CD4 responses (reduced interferon-gamma, IFN-γ, production) are associated with prolonged detection of HCMV in saliva and urine after acute HCMV infection (Tu et al., 2004). In addition to HCMV viral load, the extent of the HCMV-

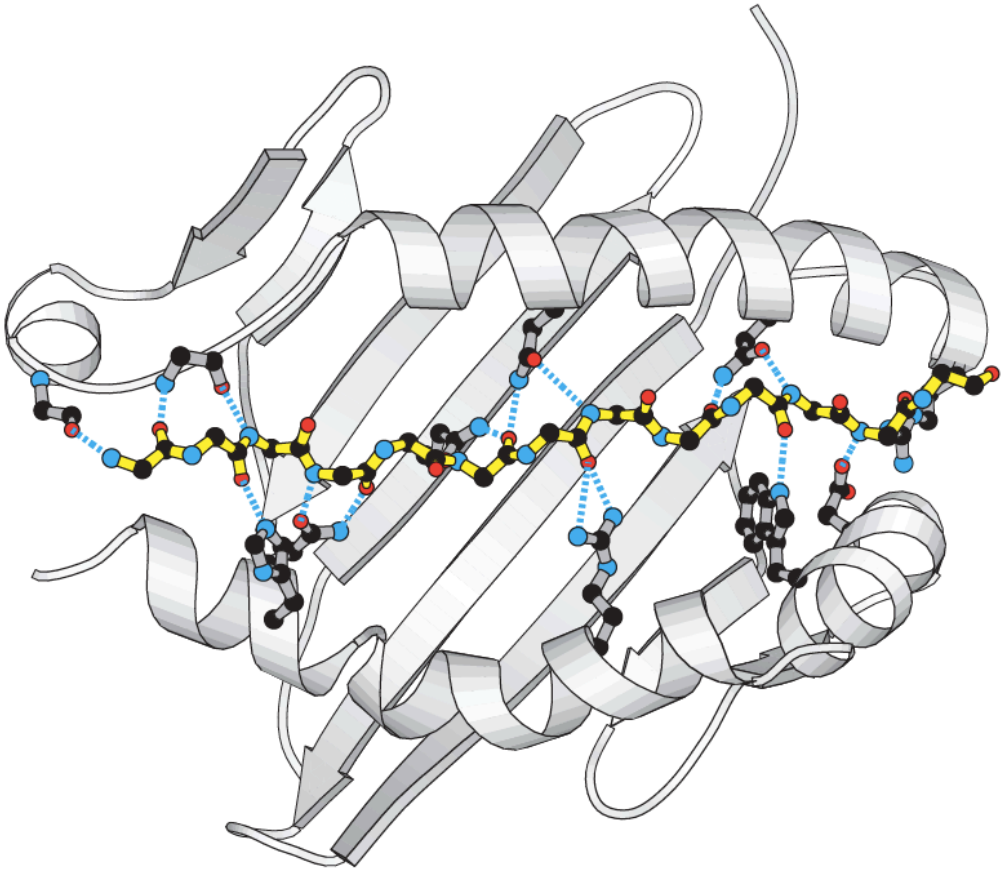

Figure I.9 Peptides bind to MHC class II molecules by interactions along the length of the binding groove. A peptide (yellow; shown as the peptide backbone only, with the amino terminus to the left and the carboxy terminus to the right) is bound by an MHC class II molecule through a series of hydrogen bonds (dotted blue lines) that are distributed along the length of the peptide. The hydrogen bonds toward the amino terminus of the peptide are made with the backbone of the MHC class II polypeptide chain, whereas throughout the peptide's length bonds are made with residues that are highly conserved in MHC class II molecules. The side chains of these residues are shown in gray on the ribbon diagram of the MHC class II groove. This figure and its caption were obtained from Murphy and Weaver, 2017 and used upon approval by Garland Science, Taylor & Francis Group under license number 4180800875858.

specific $CD4^+$ T cell response serves as a prognostic disease indicator in renal transplant patients (Sester et al., 2001). HCMV-specific $CD4^+$ T cells are also important in the suppression of HCMV viral load and maintenance of HCMV-specific $CD8^+$ T cells in allo-HSCT patients (Einsele et al., 2002).

The nature of HCMV-specific $CD4^+$ T cell response during acute, natural infection of immunocompetent subjects is not known. However, most of the current knowledge is based on data obtained from HCMV-seronegative persons who received renal

transplants from HCMV-seropositive donors (D^+/R^-) without gangiclovir administration. The quality of response might be dampened by the anti-rejection immunosuppressants that are usually administered to transplant recipients (Gamadia et al., 2003; Rentenaar et al., 2000).

pp65 and IE1-specific $CD4^+$ T cells are detected in about 60% of chronically infected HCMV-seropositive patients (Beninga et al., 1995; Davignon et al., 1995; Fuhrmann et al., 2008; Kern et al., 2002). Most peripheral blood HCMV-specific $CD4^+$ T cells secrete IFN-γ, but only a subset of them secrete TNF-α or IL-2, indicating a T_h1 phenotype with very few T_h2 phenotypic $CD4^+$ T cells present (Rentenaar et al., 2000). More recent evidence suggests that $CD4^+$ T cells stimulated with a pool of peptides spanning UL138 protein of CMV secrete IL-10, which indicates a Th2 phenotype (Mason et al., 2013). Renal transplant recipients with a higher proportion of HCMV-specific $CD4^+$ T cells that secrete more IFN-γ *ex vivo* better control viral replication, eliminate infection faster, and are typically less symptomatic (Gamadia et al., 2003; Sester et al., 2001). Polyfunctional $CD4^+$ T cells in peripheral blood mononuclear cells (PBMCs) obtained from circulating blood of liver transplant recipients that secrete IFN-γ and IL-2 are associated with lower HCMV DNAemia (Nebbia et al., 2008). In addition to the characteristic Th1 functions, these cells can also serve the cytotoxic function of effector cells when they encounter HCMV-infected cells (Appay et al., 2002b; Gamadia et al., 2004; Rentenaar et al., 2000). Epitopes from gB, pp65, IE1 and gH have been reported to expand cytotoxic HCMV-specific $CD4^+$ T cells *in vitro* (Elkington et al., 2004; Hegde et al., 2005). HCMV-specific $CD4^+$ T cells that were obtained from three HCMV-seropositive subjects and expanded *in vitro* by CMV pp65 peptide pools display

oligoclonal TCR repertoires (Weekes et al., 2004). However, it is not known whether this TCR focusing is the result of selection by culture conditions or whether it occurs *in vivo* during the course of natural infection (Weekes et al., 2004).

Memory inflation against HCMV epitopes

Conventional (or classical) HLA-restricted CMV epitope-specific $CD4^+$ and $CD8^+$ T cell responses typically display elevated magnitudes during acute infection before contracting to very low levels during latent CMV infection. For instance, conventional $CD4^+$ T cell responses (0.03 – 1.4%) were detected against HCMV's UL86 protein epitopes in HCMV chronically infected subjects (Fuhrmann et al., 2008). However, certain CMV epitopes induce $CD4^+$ or $CD8^+$ T cell responses that expand during acute CMV infection and remain unusually elevated during CMV latency, and this phenomenon is known as "memory inflation." CMV-specific T cell memory inflation is a lifelong event, and is characteristic of natural CMV infection in an immune-competent host. This phenomenon was first described to occur in the $CD8^+$ T cell compartment some time after resolution of the acute phase of CMV infection (Karrer et al., 2003), but has not been thoroughly investigated among $CD4^+$ T cells. The primary goals of this dissertation are to determine whether HLA-restricted epitope-specific $CD4^+$ T cells undergo memory inflation and to characterize these memory-inflated responses.

A list of identified class II-restricted CMV epitopes and their potential classifications as either conventional or inflationary is shown in (**Table I.2**) (Wills et al., 2013). Memory inflation of MCMV epitope-specific $CD4^+$ T cell responses is uncommon as most $CD4^+$ T cells undergo conventional T cell expansion (peaking at day 8 post-

Gene	Pro-duct	Peptide	MHC class II restriction	C	I	Reference
UL55	gB	DYSNTHSTRYV	DR7	?	f,g,h,j	(Crompton et al., 2008; Elkington et al., 2004; Pachnio et al., 2016)
UL75	gH	HELLVLVKKAQL	DR11	a	?	(Elkington et al., 2004)
UL123	IE1	91-VRVDMVRHRIKEHMLKKYTQ-110	DR3	?	?	(Davignon et al., 1996)
		96-VRHRIKEHMLKKYTQTTEEKF-115	DR13	?	?	(Davignon et al., 1996)
		162-DKREMWMACIKELH-175	DR8	a	?	(Gautier et al., 1996)
UL83	pp65	41-LLQTGIHVRVSQPSLILVSQ-60	DQ6	?	f,g,j	(Pachnio et al., 2016; Weekes et al., 2004)
	pp65	117-PLKMLNIPSINVHHY-131	DR1 DR3	?	?	(Li Pira et al., 2004)
	pp65	169-TRQQNQWKEPDVYYT-183	DR1	?	?	(Li Pira et al., 2004)
	pp65	177-EPDVYYTSAFVFPTK-191	DR7	?	?	(Li Pira et al., 2004)
	pp65	225-KVYLESFCEDVPSGK-239	DR15	?	?	(Li Pira et al., 2004)
	pp65	245-TLGSDVEEDLTMTRN-259	DR3	?	?	(Li Pira et al., 2004)
	pp65	261-QPFMRPHERNGFTVL-275	DR13	?	f,g,h,i	(Li Pira et al., 2004; Weekes et al., 2004)
	pp65	281-IIKPGKISHIMLDVA-295	DR4 DR7 DR53	?	?	(Kern et al., 2002; Li Pira et al., 2004)
	pp65	365-EHPTFTSQYRIQGKL-379	DR11	?	?	(Kern et al., 2002; Li Pira et al., 2004)
	pp65	373-YRIQGKLEYRHTWDR-387	DR3	?	?	(Li Pira et al., 2004)
	pp65	413-TERKTPRVTGGGAMA-427	DR14	?	?	(Li Pira et al., 2004)
	pp65	429-ASTSAGRKRKSASSA-443	DR11	?	?	(Li Pira et al., 2004)
	pp65	445-ACTSGVMTRGRLKAE-459	DR1	?	?	(Li Pira et al., 2004)
	pp65	489-AGILARNLVPMVATV-503	DR11 DR3	?	f,g	(Kern et al., 2002; Li Pira et al., 2004; Pachnio et al.. 2016)
	pp65	509-KYQEFFWDANDIYRI-523	DR1 DR3	?	f,h	(Bitmansour et al., 2002; Li Pira et al.,
	pp65	513-FFWDANDIYRI-523	DR1	?	?	(Trivedi et al., 2005)
	pp65	166-LAWTRQQNQWKEPDV-180	DR1	?	?	(Kern et al., 2002; Li Pira et al., 2004)
	pp65	510-YQEFFWDANDIYRIF-524	DR1DR3	?	?	(Kern et al., 2002; Li Pira et al., 2004)
	pp65	512-EFFWDANDIYRIF-524	DR1 DR3	?	?	(Kern et al., 2002; Li Pira et al., 2004)
	pp65	250-VEEDLTMTRNPQPFM-264	DR3	?	?	(Li Pira et al., 2004)
	pp65	283-KPGKISHIMLDVAFTSH-299	DR4 DR7	?	?	(Kern et al., 2002; Li Pira et al., 2004)
	pp65	370-TSQYRIQGKLEYRHT-384	DR4 DR13	?	?	(Li Pira et al., 2004)
	pp65	180-VYYTSAFVFPTKDVA-194	DR7	?	?	(Li Pira et al., 2004)
	pp65	360-GPQYSEHPTFTSQYRI-375	DR11	?	?	(Kern et al., 2002; Li Pira et al., 2004)
	pp65	366-HPTFTSQYRIQGKLE-380	DR11	?	?	(Kern et al., 2002; Li Pira et al., 2004)
	pp65	39-TRLLQTGIHVRVSQP-53	DR15	?	?	(Kern et al., 2002; Li Pira et al., 2004)
	pp65	109-MSIYVYALPLKMLNI-123	DR7	?	?	(Nastke et al., 2005)
	pp65	339-LRQYDPVAALFFFDI-353	DR7	?	?	(Nastke et al., 2005)

Table I.2 MHC-II peptide epitopes recognized by human CD4$^+$ T-cells from a number of HCMV ORFs. This table shows all class II CMV epitopes with their classification as either conventional (C), inflationary (I), or both, based on reported evidence in the references.

C; Conventional column key:

a: low magnitude response (<1% of CD4$^+$ T cells) during latent (chronic) CMV infection
b: conventional CD4$^+$ T cell phenotype
c: diverse TCR repertoire
d: longitudinal confirmation of low magnitude response
e: transcriptome profile of conventional CD4$^+$ T cell responses

I; Inflationary column key:

f: high magnitude response (≥1% of CD4$^+$ T cells) during latent (chronic) CMV infection
g: inflationary CD4$^+$ T cell phenotype
h: oligoclonal or monoclonal TCR repertoire
i: longitudinal confirmation of high magnitude response
j: transcriptome profile of inflated CD4$^+$ T cell responses

"?": unknown because none of the property was determined in the reference

This table was obtained and modified from Wills et al., 2013 and used upon approval by Caister Academic Press under written permission granted by Dr. Mark Wills. It has been modified by the addition of the conventional and inflationary columns as well as the addition of this caption.

infection) and contraction after MCMV infection of C57BL/6 mice except for an epitope within the m09 protein that induces delayed inflation after 15 days of infection (Arens et al., 2008).

Understanding CMV-specific $CD4^+$ T cell memory inflation requires an appreciation of CMV-specific $CD8^+$ T cells because most of the knowledge on memory inflation has been determined from studies involving the latter. Therefore, I will discuss important features of memory-inflated T cell responses in the next couple of paragraphs using observations from CMV-specific $CD8^+$ T cells. HLA-A2 or HLA-B7-restricted $CD8^+$ T cell response to pp65 or IE1 proteins range from <1–35% of total blood $CD8^+$ T cells in chronically infected subjects (Sylwester et al., 2005). However, the size of these responses differ widely between different persons (Jackson et al., 2014), and they do not always expand linearly with age as illustrated in (**Figure I.10**) and (**Figure I.11**) (Komatsu et al., 2006; Komatsu et al., 2003).

Conventional and inflated CMV-specific T cells comprise of mainly T_{EM} and/or T_{EMRA} phenotypes in humans (Pachnio et al., 2016), although T_{EMRA} subsets are absent in mice (Marvel et al., 1991). Inflated $CD8^+$ T cells do not have any specific surface markers but most of them express CX_3CR1 (fractalkine receptor), perforin, granzymes, CD57 and high levels of T-bet (O'Hara et al., 2012). CX_3CR1 is elevated in expanded CMV-specific T cells and it interacts with fractalkine (CX_3CL1) on vascular endothelial cells (VECs), some of which might be latently infected with HCMV (Hertoghs et al., 2010). These infected cells are capable of processing and presenting class I or class II

CMV proteins including gB (Hegde et al., 2005; Pachnio et al., 2015) and IE1 (Seckert et al., 2011) using HLA class I or IFN-γ-induced HLA class II (Kambayashi and Laufer, 2014).

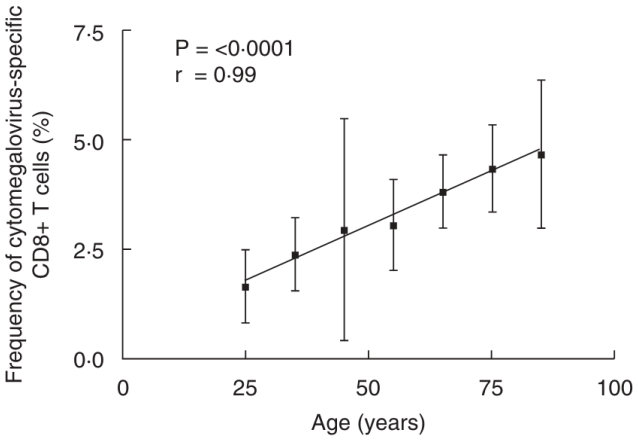

Figure I.10 CMV-specific T cell populations as a function of age. Mean frequencies of tetramer positive cells as a fraction of total $CD8^+$ cells in individuals of different ages. Of 581 individuals screened, 275 were HLA-A2-positive. Only tetramer positive samples are included in the analysis (mean ± s.e.m. displayed in 10-year age groups). Staining using matched controls established a threshold of detection of 0·05%. Frequencies of those HLA-A2-positive individuals scoring tetramer-positive in each 10-year age group are shown in Table 1 [of the primary article] − the highest and lowest 10-year age groups are not included due to lack of positive samples. The correlations shown are for the 10-year age groups included. Values for breakdown by individual year age groups showed P= 0·0014, r= 0·32. This figure and its caption were obtained from Komatsu *et al.*, 2003 and used upon approval by John Wiley and Sons under license number 4180240963982.

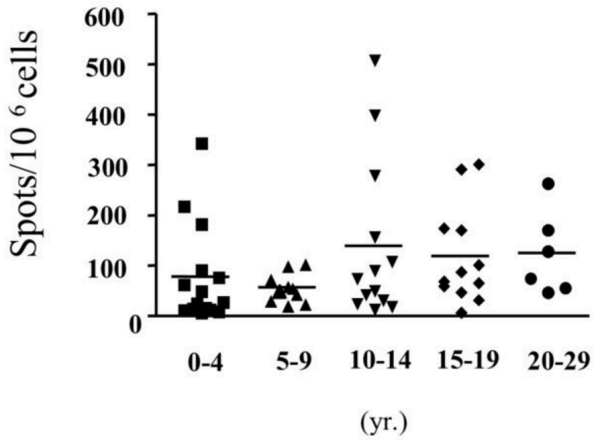

Figure I.11 IFN-γ ELISPOT assay of HLA-A2 individuals by age-group. Individuals from different age groups as indicated were analyzed for HLA-A2 peptide specific responses using ELISPOT as previously. The differences shown were not significant. This figure and its caption were obtained from Komatsu *et al.*, 2006 and used under the Creative Commons public license permission of BioMed Central.

The magnitude of inflation of $CD8^+$ T cell responses depends on various factors including the inoculum of infection in mouse model (Redeker et al., 2014), duration of infection or the specific HLA molecule (Jackson et al., 2014). MCMV models have suggested that HCMV latently-infected non-hematopoietic cells from bone marrow (Seckert et al., 2011), lymph node (Torti et al., 2011), and VECs (Smith et al., 2014) drive memory inflation. These studies also confirm that memory inflation requires MHC molecules because inflation is inhibited when MHC genes are depleted by specific mutation in embryonic stem cells in mouse models (Bolinger et al., 2013). Another study highlights that full MCMV reactivation or productive virion formation is not required for memory inflation to occur as evidenced by CD8 memory inflation observed during infection with a spread-incompetent modified MCMV strain (Redeker et al., 2014). A proposed model for memory inflation is that latently infected non-hematopoietic stromal cells in LNs initially prime naïve T cells (T_{Nai}) into central memory T cells (T_{CM}) via MHC-restricted MCMV antigen presentation. These infected LN stromal cells would later re-stimulate T_{CM}, causing their proliferation or inflation and differentiation to T effector memory cells (T_{EM}). Inflated T_{EM} then migrate from the LN to peripheral sites via circulation where they are re-stimulated by VECs latently infected with CMV and where memory inflation is more easily detected in humans (Klenerman and Oxenius, 2016; Torti et al., 2011). This is depicted in (**Figure I.12**). The only evidence for a potential T_{CM} precursor of clonal T_{EM} populations is the report of a slight overlap between clonal TCRs of CMV-specific $CD8^+$ T cells that were obtained from both peripheral blood (which would predominantly be T_{EM}) and LN (which would predominantly be T_{CM}) of renal transplant recipients post-transplantation (Remmerswaal et al., 2015). The caveat of

this study is that they did not confirm using any type of analysis that the LN T cells possessed a T_{CM} phenotype ($CCR7^{+}CD45RO^{+}CD27^{+}$); this is critical because T_{EM} are also present in LNs, albeit at lower magnitudes (Masopust et al., 2001; Sallusto et al., 1999).

Gene expression patterns might also affect the ability of certain epitopes to induce inflation. This has been demonstrated in a mouse model (Dekhtiarenko et al., 2013) where a memory-inflated T cell response was detected for an HSV-1 peptide reconstructed into MCMV *ie2* gene (whose normal product induces memory inflation (Karrer et al., 2004)), while a non-inflated T cell response was detected when the same HSV-1 peptide was reconstructed into MCMV *m45* gene (whose normal product induces a conventional response (Munks et al., 2006)). However, this fails to explain differential memory inflation to different epitopes from the same protein (Munks et al., 2006). The ability of CMV latently infected cells to present antigen directly without the need for antigen presenting cells also plays a significant role; MCMV studies demonstrate that M45 protein epitope-specific conventional T cell responses require immunoproteasome unlike M38 epitope-specific inflated T cell responses that depend on proteasomes (Hutchinson et al., 2011). It is also possible that epitope competition plays a role in memory inflation; genes of inflation-inducing epitopes might be more efficiently transcribed and expressed, and therefore stimulate more T cell responses compared to genes of conventional response-inducing epitopes (Dekhtiarenko et al., 2013; Farrington et al., 2013).

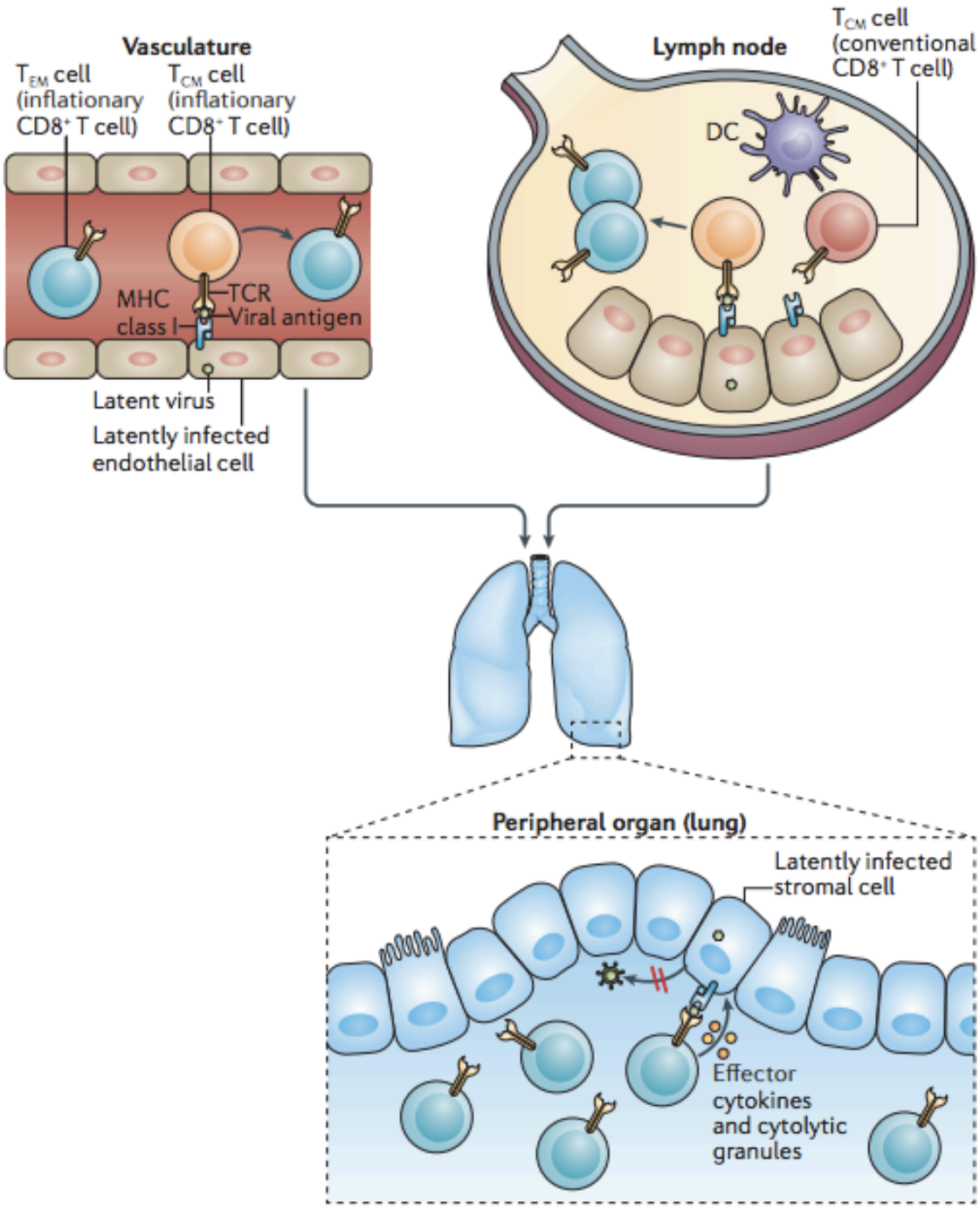

Figure I.12 Dynamic features of memory inflation. This figure shows a model for how cytomegalovirus (CMV)-specific inflationary CD8+ T cell responses could be maintained at high levels over long-term periods. Antigens are central to this process, in which viral antigen in latency is presented by non-professional non-haematopoietic-derived antigen-presenting cells in lymph nodes or the vasculature (for example, by stromal cells or endothelial cells). Such antigens can drive the differentiation of specific (inflationary) central memory T (TCM) cells into effector memory T (TEM) cells, which recirculate into tissues where they can exert antiviral effector functions and maintain long-term control of viral replication. DC, dendritic cell; TCR, T cell receptor. This figure and its caption were obtained from Klenerman and Oxenius, 2016 and used upon approval by Nature Publishing group under license number 4180331275727.

Inflationary anti-CMV memory T cell responses might potentially be exploited with some vaccines. Simian immunodeficiency virus (SIV) vaccines are now being designed using replication-incompetent CMV vectors that have demonstrated some success in inducing strong MHC I-and II-restricted T cell responses in rhesus macaques (Hansen et al., 2011; Hansen et al., 2013a; Hansen et al., 2013b). It should be noted however, that the safety implications of vaccines that contain inflation-inducing epitope need to be carefully considered. This caution is necessary because of potential roles of inflated T cell responses in mediating the immunopathogenesis of cardiovascular morbidities as discussed in the section below on cardiovascular comorbidities in $HCMV^+$ and HIV^+ subjects.

$CD8^+$ T cell adaptive immunity to CMV

$CD8^+$ T cells play a significant role in the control of CMV infection. In mouse models, depletion of CMV-specific $CD8^+$ T cells leads to the loss of CMV control and development of CMV-related multi-organ complications involving the liver and spleen (Podlech et al., 1998). HCMV-specific $CD8^+$ T cells in AIDS subjects positively correlate with the control of CMV retinitis (Jacobson et al., 2004). These cells also play a critical role in protecting against CMV disease in both allogeneic bone marrow transplant recipients (Li et al., 1994) and kidney SOT recipients (Reusser et al., 1999). The frequency of $CD8^+$ T cells specific or reactive to CMV epitopes can be unusually high (Crough et al., 2005; Dunn et al., 2002). In general, CMV-specific CD8 responses are directed to a wide range of ORFs within the CMV genome; IE1, IE2 and pp65 are the proteins most frequently recognized by these cells (Sylwester et al., 2005). A list of

characterized MHC class I-restricted CMV epitopes is presented in (**Table I.3**). These cells mainly display an effector memory, T_{EM} ($CD45RA^-$ $CD45RO^+$ $CD27^-$ $CD28^-$ $CCR7^-$) or effector memory-RA^+, T_{EMRA} phenotype ($CD45RA^+$ $CD45RO^-$ $CD27^-$ $CD28^-$ $CCR7^-$) (Appay et al., 2002a), especially during chronic infection with very few CMV-specific naïve or central memory T cells. The clonotypes of CMV-specific CD8 TCRs are mostly oligoclonal with high antigen avidity (Price et al., 2005). The HLA molecule and epitope both determine the degree of TCR clonality of these cells (Wynn et al., 2008). $CD8^+$ T cells in humans can sometimes display high response magnitudes with highly restricted TCR repertoires as seen in HLA-A2 restricted NLV-specific $CD8^+$ T cells from one subject that had a 7% response magnitude with 98% of the cells using the same TCR (Khan et al., 2002b). However, the phenotypes or longitudinal magnitudes of these responses over a period of time were not determined, and therefore, these cells cannot be considered to be memory inflated.

Intersection Between HCMV, HIV, and CMV-Related Cardiovascular Comorbidities in $HCMV^+$ HIV^+ Subjects

Overview of HIV infection

HIV requires CD4 receptor and CCR5 or CXCR4 chemokine co-receptor to infect a human cell (Deng et al., 1996). CCR5 and CXCR4 are expressed by T cells, dendritic cells (DCs), tissue macrophages, monocytes (Zaitseva et al., 1997), and all of these cells can be infected by HIV (Cameron et al., 1992; Zhu et al., 1993). Expression of CCR5 or CXCR4 co-receptor determines the tropism of the HIV strain: R5-tropic HIV

ORF	Protein	Peptide	MHC class I molecule	Conventional	Inflationary	Reference
UL32	pp150	945-TTVYPPSSTAK-955	HLA-A3	?	?	(Longmate et al., 2001)
		792-QTVTSTPVQGR-802	HLA-A68	?	?	(Longmate et al., 2001)
UL44	pp50	245-VTEHDTLLY-253	HLA-A1	a	?	(Elkington et al., 2003)
UL55	gB	618-(F)IAGNSAYEYV-628	HLA-A2	?	?	(Utz et al., 1992)
		731-AVGGAVASV-739	HLA-A2	a	?	(Elkington et al., 2003)
UL83	pp65	363-YSEHPTFTSQY-373	HLA-A1	?	?	(Longmate et al., 2001)
		14-VLGPISGHV-22	HLA-A2	?	?	(Solache et al., 1999)
		120-MLNIPSINV-128	HLA-A2	a	?	(Solache et al., 1999)
		490-ILARNLVPM-498	HLA-A2	a	?	(Elkington et al., 2003)
		495-NLVPMVATV-503	HLA-A2	a	f,h	(Khan et al., 2002b; Wills et al., 1996)
		522-RIFAELEGV-530	HLA-A0207	a	?	(Kondo et al., 2004)
		16-GPISGHVLK-24	HLA-A11	?	?	(Longmate et al., 2001)
		501-ATVQGQNLK-509	HLA-A11	a	?	(Kondo et al., 2004)
		248-AYAQKIFKIL-257	HLA-A23/24	?	?	(Elkington et al., 2003)
		113-VYALPLKML-121	HLA-A24	a	?	(Masuoka et al., 2001)
		341-QYDPVAALF-349	HLA-A24	a	?	(Kuzushima et al., 2001)
		369-FTSQYRIQGKL-37	HLA-A24	?	?	(Longmate et al., 2001)
		186-FVFPTKDVALR-196	HLA-A68	?	?	(Longmate et al., 2001)
		265-RPHERNGFTV-274	HLA-B7	?	h	(Weekes et al., 1999)
		417-(T)PRVTGGGAM-426	HLA-B7	?	f,h	(Khan et al., 2002b; Weekes et al.,
		215-KMQVIGDQY-223	HLA-B15	a	?	(Kondo et al., 2004)
		103-CPSQEPMSIYVY-114	HLA-B35	a	?	(Burrows et al., 2008)
		123-IPSINVHHY-131	HLA-B35	a	?	(Hassan-Walker et al., 2001)
		187-VFPTKDVAL-195	HLA-B35	?	?	(Wills et al., 1996)
		174-NQWKEPDVY-182	HLA-B35	?	?	(Kern et al., 2002)
		283-KPGKISHIMLDVA-295	HLA-B35	?	?	(Elkington et al., 2003)
		367-PTFTSQYRIQGKL-379	HLA-B38	?	?	(Longmate et al., 2001)
		232-CEDVPSGKL-240	HLA-B40	a	?	(Kondo et al., 2004)
		267-HERNGFTVL-275	HLA-B40	a	?	(Kondo et al., 2004)
		525-AELEGVWQPA-534	HLA-B40	a	?	(Kondo et al., 2004)
		364-SEHPTFTSQY-373	HLA-B44	a	?	(Kondo et al., 2004)
		512-EFFWDANDIY-521	HLA-B44	?	?	(Wills et al., 1996)
		545-DALPGPCI-552	HLA-B51	a	?	(Kondo et al., 2004)
		155-QMWQARLTV-163	HLA-B52	?	?	(Kern et al., 2002)
		211-TRATKMQVI-219	HLA-B57/58	?	?	(Elkington et al., 2003)
		7-RCPEMISVL-15	HLA-CW1	a	?	(Kondo et al., 2004)
		341-QYDPVAALF-349	HLA-CW4	a	?	(Kondo et al., 2004)
		198-VVCAHELVC-206	HLA-CW8	?	?	(Kern et al., 2002; Kondo et al., 2004)
		294-VAFTSHEHF-302	HLA-CW12	?	?	(Kondo et al., 2004)
		198-VVCAHELVC-206	HLA-CW15	?	?	(Kondo et al., 2004)
UL98		277-ARVYEIKCR-285	HLA-B27	a	?	(Elkington et al., 2003)
UL123,	IE1,	81-VLAELVKQI-89	HLA-A2	a	?	(Elkington et al., 2003)
UL122	pp72,	315-Y(V/I)LEETSVM-323	HLA-A2	?	f,g,h	(Khan et al., 2002a)
	IE2	316-VLEETSVML-324	HLA-A2	?	f,g,h	(Khan et al., 2002a)
		354-YILGADPLRV-363	HLA-A2	?	?	(Frankenberg et al., 2002)
		184-KLGGALQAK-192	HLA-A3	?	?	(Jackson et al., 2014)
		309-CRVLCCYVL-317	HLA-B7	a,b	?	(Kern et al., 1999; Wills et al., 2002)
		88-QIKVRVDMV-96	HLA-B8	a	?	(Elkington et al., 2003)
		198-(D)ELRRKMMYM-207	HLA-B8	a,b	?	(Kern et al., 1999; Wills et al., 2002)
		199-ELKRKMIYM-207	HLA-B18	?	?	(Retiere et al., 2000)
		279-CVETMCNEY-287	HLA-B18	?	?	(Retiere et al., 2000)
		379-DEEDAIAAY-387	HLA-B18	?	?	(Retiere et al., 2000)
		381-FEQPTETPP-389	HLA-B41	a	?	(Rist et al., 2005)
US2		190-SMMWMRFFV-198	HLA-A2	a	?	(Elkington et al., 2003)

Table I.3 Class I MHC peptide epitopes recognized by human CD8+ T-cells derived from HCMV proteins. This table shows all class I CMV epitopes with their classification as either conventional, inflationary, or both, based on reported evidence in the references.

Conventional column key:

a: low magnitude response (<1%) during latent (chronic) CMV infection
b: conventional $CD8^+$ T cell phenotype
c: diverse TCR repertoire
d: longitudinal confirmation of low magnitude response
e: transcriptome profile of conventional $CD8^+$ T cell responses

Inflationary column key:

f: high magnitude response (≥1%) during latent (chronic) CMV infection
g: inflationary $CD8^+$ T cell phenotype
h: oligoclonal or monoclonal TCR repertoire
i: longitudinal confirmation of high magnitude response
j: transcriptome profile of inflated $CD8^+$ T cell responses

"?": unknown because none of the property was determined in the reference

This table was obtained and modified from Wills et al., 2013 and used upon approval by Caister Academic Press under written permission granted by Dr. Mark Wills. It has been modified by the addition of the conventional and inflationary columns as well as the addition of this caption.

infects CCR5 co-expressing cells and are typically present early during infection; while X4-tropic HIV infects CXCR4 co-expressing cells and are typically present during advanced infection (Li et al., 1999). Of the myriad of HIV variants in the inoculum, only one or a few strains usually establish infection, and they are known as the "founder virus" (Keele et al., 2008). The founder virus is usually R5-tropic; R4-tropic virus appears later in natural infection and is associated with CD4 decline (Kaleebu et al., 2007). Upon breaching the epithelial barrier of a human at the foreskin, vaginal, anal or ectocervical mucosa, HIV founder virus (Keele et al., 2008) predominantly infects Langerhan cells (Spira et al., 1996), which are specialized DCs located in the mucosa and involved in initial encounter with, and transportation of, HIV to the draining lymph node via afferent lymphatic vessels (Edwards and Morris, 1985; Miller et al., 1992). Langerhan cells transfer and coat HIV onto the surfaces of follicular DCs (fDCs) that are situated in germinal centers of secondary lymphoid follicles in LNs (Biberfeld et al., 1988; Cameron et al., 1996; Heath et al., 1995). Therefore, germinal centers are important sites of latent HIV reservoirs that are poorly permeated by $CD8^+$ T cells

(Fukazawa et al., 2015). fDCs transmit their trapped HIV to naïve $CD4^+$ T cells as the latter passes through the germinal center to paracortical areas that is dominated by T cells before leaving the LN for systemic infection (Cameron et al., 1996; Embretson et al., 1993). After dissemination, HIV establishes latency predominantly in resting $CD4^+$ T cells that persist even during effective ART (Finzi et al., 1999; Finzi et al., 1997; Ho et al., 1995). Other less studied reservoirs for HIV include peripheral monocytes/tissue macrophages (Gartner et al., 1986; Igarashi et al., 2001; Koenig et al., 1986; Lambotte et al., 2000), $CD4^+$ memory stem cells (T_{SCM}; (Buzon et al., 2014)), $CD34^+$ hematopoetic progenitor cells (Carter et al., 2011; Carter et al., 2010), astrocytes and microglia (Gorry et al., 1999; Price et al., 1988; Tornatore et al., 1994), semen (Quayle et al., 1997; Zhang et al., 1998) and other cells within the urogenital tract (Zhu et al., 1996).

In order to study CMV-specific $CD4^+$ T cell memory inflation in $HCMV^+$ HIV^+ subjects, it is important to understand the process involved in the priming of these cells in the LN. As described above, HIV-infected/specific $CD4^+$ naïve T cells are primed by HIV-coated fDCs. On the other hand, non-hematopoietic LN stromal cells that have been proposed as potential CMV latent reservoirs (Seckert et al., 2009), and unlike fDCs, have been hypothesized to present CMV antigens to T cells that eventually undergo memory inflation (Klenerman and Oxenius, 2016). Therefore, this would indicate that memory inflated CMV-specific $CD4^+$ T cells are less likely to be enriched with HIV DNA. As I discuss in **Chapter III**, this observation was made after measuring the frequency of latent HIV DNA in inflated DYS^+ $CD4^+$ T cells of CMV gB protein from an HIV^+ subject, even though it was initially thought that inflated cells might be enriched with HIV DNA simply based on the magnitude of response.

CMV-related cardiovascular comorbidities

Since its discovery more than thirty years ago, HIV remains an incurable disease that has claimed over thirty million lives by causing AIDS-related opportunistic infections (UNAIDS, 2017). The main obstacle to curing HIV is the persistent, latently integrated and replication-competent HIV provirus in resting $CD4^+$ T cells that causes rebound plasma viremia typically within two months of cessation of ART in aviremic individuals (Davey et al., 1999; Finzi et al., 1999; Fischer et al., 2003; Harrigan et al., 1999; Pierson et al., 2000; Ruiz et al., 2000). These reservoirs have a long half-life of about forty-four months, and therefore, persist over the lifetime of an infected individual (Finzi et al., 1999). The emergence of ART as an efficacious management transformed HIV infection from a lethal disease to a chronically manageable condition by suppressing plasma viral loads to clinically undetectable levels and preventing the depletion of its $CD4^+$ T cell primary target (Gulick et al., 1997; Klatzmann et al., 1984).

However, since the advent of suppressive ART that reduces the risk of developing AIDS, more HIV^+ subjects are being diagnosed with CMV-related non-AIDS cardiovascular comorbidities (Barbaro et al., 2001; Cheng et al., 2009; Hsue et al., 2004; Lichtner et al., 2015; Slot et al., 2017; Wall et al., 2013). Over 90% of HIV^+ subjects are co-infected with HCMV (Rabenau et al., 2010; Robain et al., 1998). HIV^+ subjects also have a higher CMV disease burden compared to HIV^- individuals (Maidji et al., 2017). Subjects who are both HIV^+ and $HCMV^+$ and also have high magnitudes of activated $CD4^+$ or $CD8^+$ T cells that each co-express CD38 and HLA-DR activation proteins are at an increased risk of developing carotid artery lesions (Kaplan et al., 2011). Analysis of the antigen specificity of $CD4^+$ $CD38^+HLA\text{-}DR^+$ T cells from HIV^+

HCMV$^+$ co-infected subjects revealed that a majority of these cells are specific for HCMV (Smith et al., 2013). Increased frequencies of CD4$^+$CD28$^-$ T cells that express high levels of CX_3CR1 are associated with stiffer arterial walls, which is one of the cardiovascular comorbidities observed (Chanouzas et al., 2015), and these cells decrease in frequency after administration of valacyclovir to HCMV$^+$ subjects with antineutrophil cytoplasmic antibody (ANCA)-associated vasculitis (AAV) in a randomized controlled clinical trial (Chanouzas et al., 2017). Furthermore, CD4$^+$ CX_3CR1^+ T cells that are reactive to CMV have been suggested to mediate cardiovascular morbidities including atherosclerosis due to their strong correlation with CMV seropositivity (Broadley et al., 2017; Sacre et al., 2012; van de Berg et al., 2012). As discussed above, CMV-specific CD4 and CD8 T cell responses are categorized as either conventional or inflated responses. Inflated CMV-specific T cell responses express low levels of CD28 (O'Hara et al., 2012). Another group has shown that expanded CD4$^+$ CD28$^-$ T cell populations in rheumatoid arthritis patients is associated with thicker carotid intima-media and more endothelial dysfunction, although the mechanism was not defined (Gerli et al., 2004). Therefore, inflated CD4$^+$ CD28$^-$ T cells might play a role in the immunopathogenesis of these cardiovascular comorbidities in HIV$^+$ subjects. Within inflated CD4$^+$ T cells, the T_{EMRA} subset likely play a significant role in this pathogenesis because CD4$^+$ T cells with identical phenotype to T_{EMRA} from HIV$^+$ subjects have been shown to contain less HIV DNA (Casazza et al., 2009; Oswald-Richter et al., 2007). This finding was speculated to be caused either by macrophage inflammatory protein 1 alpha (MIP-1α)- and MIP-1β-induced CCR5 downregulation that would make the cells less permissive to HIV infection (Casazza et al., 2009) or by a

cellular-intrinsic factor such as APOBEC3G that restricts HIV replication (Oswald-Richter et al., 2007; Pido-Lopez et al., 2009). An additional aim of this dissertation is to determine whether the magnitudes of CD38 and HLA-DR expression or co-expression on inflated CMV-specific $CD4^+$ T cells from HIV^+ $HCMV^+$ subjects are elevated compared to those of conventional T cells.

CHAPTER II

CYTOMEGALOVIRUS EPITOPE-SPECIFIC $CD4^+$ T CELLS ARE INFLATED IN HIV^+ $HCMV^+$ SUBJECTS

Introduction

In this chapter, I describe the investigation of the phenomenon of memory inflation among HLA-DR7-restricted $CD4^+$ T cells specific for HCMV proteins and proteins of other pathogens or antigens in HIV and HCMV co-infected subjects. This work led to the discovery that DYS^+ $CD4^+$ T cells are inflated compared to a different CMV epitope as well as to other pathogen or antigen epitopes in the co-infected cohort or to similar DYS^+ $CD4^+$ T cells in HCMV-only-infected subjects. Remarkably, these inflated DYS^+ $CD4^+$ T cells display nearly monoclonal CDR3 repertoire with previously unidentified conserved amino acid residues. This work confirms that memory inflation occurs among $CD4^+$ T cells and the mechanism of inflation likely involves clonal expansion.

Conventional $CD4^+$ and $CD8^+$ memory T cell responses against viruses expand during primary infection and contract to low magnitudes during post-infection resolution (Klenerman and Oxenius, 2016). However, $CD8^+$ T cell responses to select epitopes of human (HCMV) (Klarenbeek et al., 2012; Waller et al., 2008), rhesus (Cicin-Sain et al., 2011), and murine cytomegalovirus (MCMV) (Bolinger et al., 2015; Dekhtiarenko et al., 2016; Karrer et al., 2003; Munks et al., 2006; Sierro et al., 2005) persist for decades at very high magnitudes after primary infection or during latency. This phenomenon is

termed “memory inflation” and has been best characterized among CMV-specific $CD8^+$ T cells that consist of mainly $CD45RO^+$ $CCR7^-$ $CD27^-$ T cells (effector memory/T_{EM}) and their $CD45RA^+$ revertants, $CD45RO^-$ $CCR7^-$ $CD27^-$ T cells (effector memory-RA^+/T_{EMRA}) (Burgers et al., 2009; Munks et al., 2006; Pachnio et al., 2016; Sierro et al., 2005; Snyder et al., 2008). CMV-specific $CD8^+$ T cells express high levels of CX_3CR1 that bind CX_3CL1 (fractalkine), which is expressed on vascular endothelial cells (VECs), a major target of CMV latent infection (Klenerman and Oxenius, 2016).

Conventional CMV-specific $CD8^+$ T cells display an IL-7-receptor-alpha/$CD127^+$, programmed cell death protein-1^-, PD-1^- phenotype (capable of homeostatic proliferation controlled by IL-7 and other cytokines), while inflated CMV-specific $CD8^+$ T cells are $CD127^-$, PD-1^-, T cell immunoglobulin and ITIM domain/$TIGIT^-$, Granzyme B^+, CX_3CR1^+ with evidence suggesting they are maintained by low-level exposure to persistent antigen from stochastic CMV reactivation (Conrad et al., 2011; Johnston et al., 2014; Klenerman and Oxenius, 2016; O'Hara et al., 2012; Okoye et al., 2015). These data suggest inflated responses are maintained through recurrent stimulation by peptide-MHC (Gamadia et al., 2004; Klenerman and Hill, 2005; Lang et al., 2009) produced by persistent, stochastic expression of specific CMV transcripts (Holtappels et al., 2000; Seckert et al., 2012; Simon et al., 2006). These epitopes are presented to CMV-specific T cells by latent HCMV-infected, non-hematopoietic reservoirs, including VECs, lymph node (LN) stroma cells, and cells in the bone marrow and lungs (Gordon et al., 2017; Klenerman and Oxenius, 2016; Seckert et al., 2011; Torti et al., 2011). Maintenance of inflated CMV-specific T cell responses might also depend on their longer telomeres that positively correlate with persistence (O'Bryan et al., 2013), or on

epitope cleavage by constitutive proteasomes (Dekhtiarenko et al., 2016; Hutchinson et al., 2011).

CMV-specific $CD4^+$ T cells suppress HCMV lytic replication (Hegde et al., 2005) and maintain $CD8^+$ T cell inflation (Walton et al., 2011). HCMV lysate-specific $CD4^+$ T cells persist at high magnitudes in HIV^+ $HCMV^+$ co-infection (Komanduri et al., 2001), which might be due to higher HCMV disease burden (Lichtner et al., 2015; Maidji et al., 2017). However, it is not known whether $CD4^+$ T cells specific to individual HCMV epitopes undergo memory inflation in co-infected subjects. Glycoprotein B/gB has the highest population prevalence of CD4 responses of any HCMV protein (Sylwester et al., 2005). The gB polyprotein colocalizes to endosomes that process and present its class II epitopes directly from infected endothelial cells upon IFN-γ-induced HLA class II expression (Hegde et al., 2005; Kambayashi and Laufer, 2014; Pachnio et al., 2015) without needing professional APCs. gB-loaded endosomes are also secreted as immunogenic exosomes that stimulate $CD4^+$ memory T cells (Broadley et al., 2017; Walker et al., 2009). In HLA-DRB1*07:01 ($DR7^+$) persons, the most immunogenic gB epitope is the extremely conserved DYSNTHSTRYV (DYS) epitope that is recognized by cytotoxic, CX_3CR1^+ $CD4^+$ T cells (Elkington et al., 2004; Pachnio et al., 2016).

HIV^+ $HCMV^+$ co-infection is implicated in the emerging higher incidence of HCMV-related, non-AIDS comorbidities of cardiovascular diseases including hypertension, coronary artery disease, and stroke despite suppressive antiretroviral therapy (ART) (Barbaro et al., 2001; Cheng et al., 2009; Hsue et al., 2004; Lichtner et al., 2015; Slot et al., 2017; Wall et al., 2013). These disease risks are further increased in co-infected subjects with elevated $CD4^+$ T cell activation ($CD38^+HLA\text{-}DR^+$) (Kaplan et

al., 2011), which are mostly CMV-reactive (Smith et al., 2013) and are reduced by anti-CMV therapy (Hunt et al., 2011). Indeed, CMV-reactive $CD4^+$ CX_3CR1^+ T cells have been proposed as potential mediators of these comorbidities (Broadley et al., 2017; Sacre et al., 2012; van de Berg et al., 2012). Increased magnitudes of $CD4^+$ CX_3CR1^+ T cells positively correlate with arterial stiffness (Chanouzas et al., 2015), and these populations significantly decrease in magnitude after anti-CMV therapy (Chanouzas et al., 2017). However, the specific epitopes and activation phenotype of these identified CMV-reactive $CD4^+$ CX_3CR1^+ T cells (Sacre et al., 2012) remain unknown.

In this dissertation, a model has been proposed where HIV^+ $HCMV^+$ co-infection increases stochastic, nonproductive HCMV reactivation that drives CD4 memory inflation. We hypothesized that HLA-DR7-restricted DYS-specific (DYS^+) $CD4^+$ T cells from HIV^+ $HCMV^+$ $DR7^+$ subjects undergo increased memory inflation compared to similar cells from HIV^- $HCMV^+$ $DR7^+$ subjects, and these cells upregulate CX_3CR1, CD38 and HLA-DR. To test this hypothesis, we studied the *ex vivo* response magnitudes, frequencies and properties of DYS^+ $CD4^+$ T cells both in HIV^+ $HCMV^+$ long-term non-progressors (to avoid confounding effects of HIV-induced subclinical HCMV expression) and in HIV^- $HCMV^+$ individuals using DR7-restricted DYS (DR7:DYS) tetramer. Tetramers were used because cytokine-based assays can underestimate actual T cell response magnitudes and the expression of phenotypic markers can change after re-stimulation (Klenerman et al., 2002). The threshold for inflation was arbitrarily set at 1% of circulating $CD4^+$ T cells as there is no standard minimum in the literature.

Results

HLA-DR7-restricted DYS$^+$ CD4$^+$ T cells are inflated in HIV$^+$ HCMV$^+$ DR7$^+$ compared to HIV$^-$ HCMV$^+$ DR7$^+$ subjects

Following the gating hierarchy in (**Figure II.1**), tetramer specificity was verified using DR7:CLIP tetramer stain of CD4-enriched PBMCs from time-point 1 (tp1; no ART) of 8 HIV$^+$ HCMV$^+$ DR7$^+$ subjects (**Table II.1**, and **Figure II.2A**). The HLA-DR7 restriction of the response was also confirmed by staining CD4-enriched PBMCs from 7 co-infected subjects lacking HLA-DR7 allele i.e. DR7$^-$ (**Table II.2** and **Figure II.3A**). To determine the HLA-DR7$^+$ DYS$^+$ CD4$^+$ T cell response magnitude in the HIV$^+$ HCMV$^+$ DR7$^+$ subjects, the tp1 CD4-enriched or untouched PBMCs were stained with DR7:DYS tetramer. DYS$^+$ CD4$^+$ T cell response (0.43–17.91%) was high in 7 subjects, with 6 of them displaying inflated responses (**Figure II.2A**). To determine whether DYS$^+$ CD4$^+$ T cell inflation was abrogated after ART-induced HIV suppression, aviremic PBMCs from later time-points (9.5 years median time lapse) of 4 co-infected individuals (time-point 2, tp2, in **Table II.1**) were stained with the tetramer and values ranging from 0.11–26.34% (**Figure II.2B**) were detected. Inflation frequency did not correlate with age (possibly due to small sample size, which could be increased in future studies), HIV infection duration, time-point CD4 count, nadir CD4 count or HIV load (**Figure II.4**).

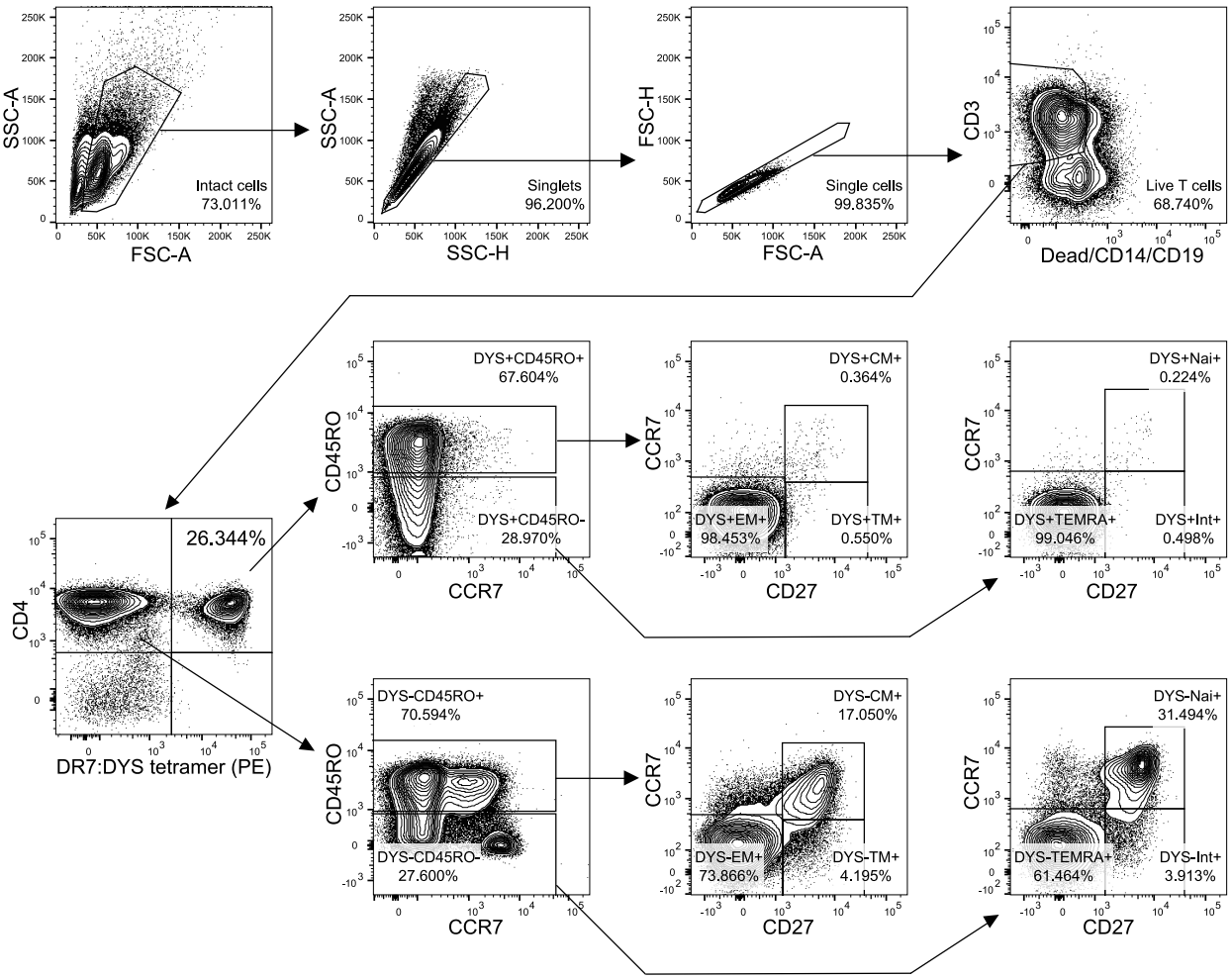

Figure II.1 Representative gating hierarchy for CD4+ T cell tetramer staining. FlowJo plots were obtained from CD4-enriched PBMCs of subject 10027's tp2 using PE-conjugated DR7:DYS tetramer. DYS- and DYS+: DYS- and DYS+ CD4+ T cells, respectively; CM+, TM+, and EM+: central, transitional and effector memory T cells, respectively; Nai+, Int+ and TEMRA+: naïve, intermediate and T-effector memory-RA+ T cells, respectively. Data represent ten biological replicates.

Importantly, significantly lower magnitudes of DYS^+ $CD4^+$ T cells (0.01–1.32%) were detected in 10 HIV^- $HCMV^+$ $DR7^+$ subjects (**Table II.3** and **Figure II.2C**) compared to those of the HIV^+ $HCMV^+$ $DR7^+$ individuals (median 0.06% vs. 4.76%, P=0.004; **Figure II.2D**). Samples from tp1 of Subject 10013, and tp2 of Subjects 10004, 10027 and 10032 (**Table II.1**) were used in this and all future experiments unless otherwise indicated.

Subject ID	HLA-DRB1 alleles	Time-point	Age (years)	Years of HIV infection	CD4 T cell count/µl blood	HIV load (RNA copies/ml plasma)	Time on ART (years)
10004	07:01, 03:01	1	58	22	203	<50	-
		2	62	26	181	<50	2.17
10013	07:01, 04:08	1	47	22	420	5,354	-
		2	60	35	380	<50	5.0
10027	07:01, 03:01	1	66	14	378	7,340	-
		2	75	23	977	<50	7.17
10032	07:01, 03:01	1	46	5	543	2,837	-
		2	56	15	886	<50	4.42
10040	07:01, 13:01	1	47	14	1,161	<50	-
10030	07:01, 09:01	1	60	13	856	<50	-
10066	07:01, 07:01	1	52	14	1,063	<50	-
10069	07:01, 08:04	1	46	6	903	2,470	-

Table II.1 Characteristics of HIV$^+$ HCMV$^+$ DR7$^+$ subjects.

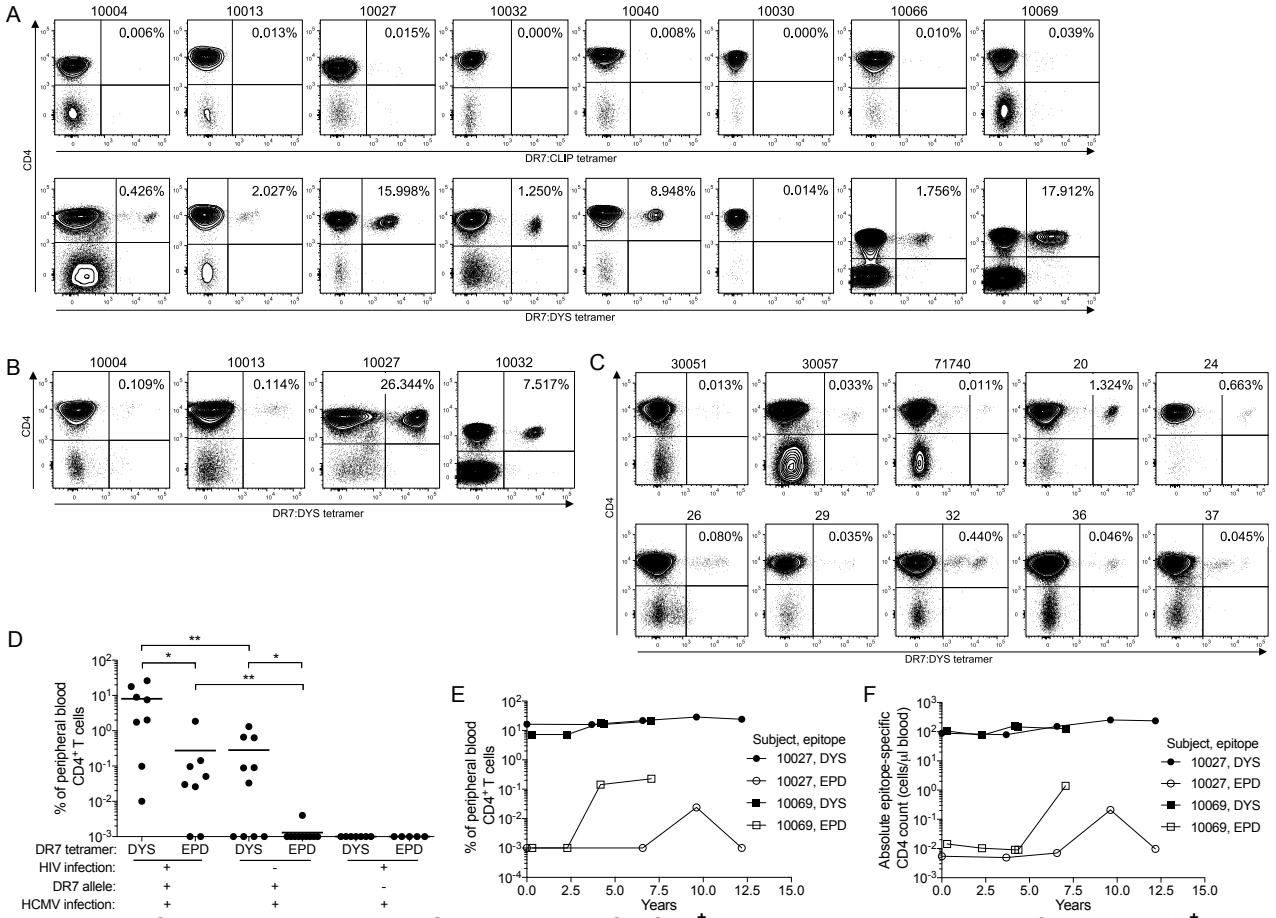

Figure II.2 HLA-DR7-restricted HCMV glycoprotein B DYS-epitope specific CD4$^+$ T cells undergo memory inflation in HIV$^+$ HLA-DR7$^+$ subjects. A–B: CD4-enriched or untouched peripheral blood mononuclear cells (PBMCs) from HIV$^+$ DR7$^+$ subjects were stained with DR7:CLIP or DR7:DYS tetramer for their (**A**) tp1 (no ART) (*n*=8), and (**B**) tp2 (on ART) samples (*n*=4). (**C**) DR7:DYS tetramer staining of HIV$^-$ DR7$^+$ subjects' PBMCs (*n*=10). (**D**) Response magnitude comparisons of DYS$^+$ and EPD$^+$ CD4$^+$ T cells from HIV$^+$ HCMV$^+$ DR7$^+$ (*n*=8; tp1 of Subject 10013, and tp2 of Subjects 10004, 10027 and 10032), HIV$^-$ HCMV$^+$ DR7$^+$ (*n*=10) and HIV$^+$ HCMV$^+$ DR7$^-$ (*n*=5-7) subjects determined simultaneously from the same samples per subject. **E–F**: Longitudinal (**E**) response magnitudes and (**F**) absolute counts of DYS$^+$ and EPD$^+$ CD4$^+$ T cells from Subjects 10027 and 10069. Values in (**D**) represent ≥3 biological replicates with means, except for the HIV$^+$ HCMV$^+$ DR7$^-$ cohort with no replicates.

Subject ID	HLA-DRB1 alleles	Age (years)	Years of HIV infection	CD4 T cell count/µl blood	HIV load (RNA copies/ml plasma)	Time on ART (years)
10031	11:01, 15:03	37	8	612	<50	-
10042	01:01, 13:02	45	24	599	<50	2.75
10071	13:01, 15:03	46	16	881	<50	-
10074	03:01, 04:04	43	6	210	<50	1.5
20011	03:01, 03:01	37	<1	512	2,655	-
20018	03:01, 16:02	22	2	1,374	1,886	-
20049	01:01, 11:01	29	1	740	50,696	-

Table II.2 Characteristics of HIV^+ $HCMV^+$ $DR7^-$ subjects.

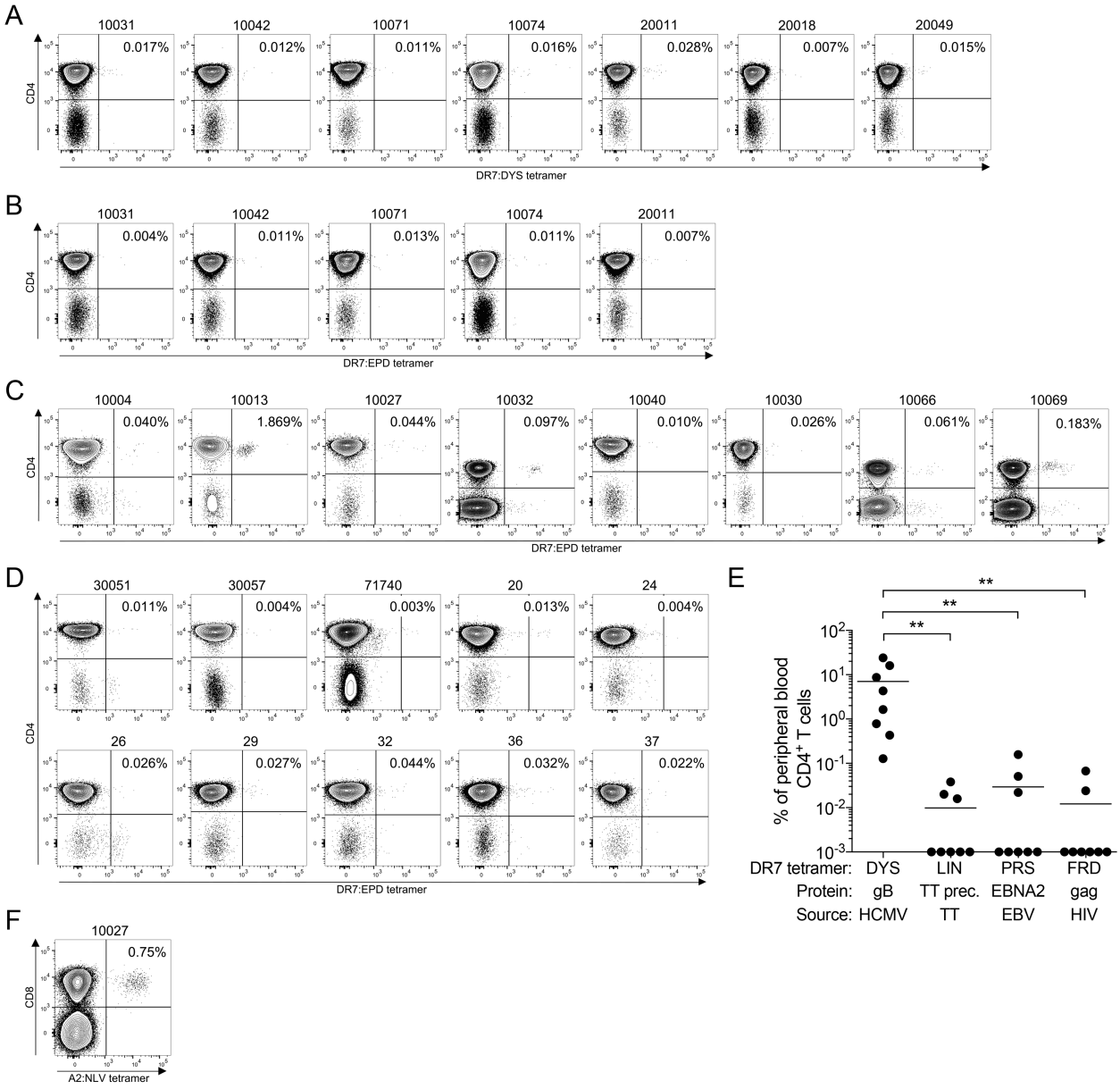

Figure II.3 DYS$^+$ CD4$^+$ T cell responses are dependent on HLA-DR7 allele, and other DR7$^+$ epitope-specific CD4$^+$ T cells are present at low frequencies in HIV$^+$ DR7$^+$ subjects. (**A**) DYS (*n*=7) and (**B**) EPD (*n*=5) tetramer stains of HIV$^+$ DR7$^-$ subjects representing single experiments. EPD tetramer stain of PBMCs from (**C**) HIV$^+$ DR7$^+$ (*n*=8) and (**D**) HIV$^-$ DR7$^+$ (*n*=10) subjects. (**E**) Frequency comparisons of DR7-restricted CD4$^+$ T cells from the HIV$^+$ HCMV$^+$ DR7$^+$ cohort that are specific for DYS, tetanus toxoid precursor LIN, EBV EBNA2 PRS or HIV gag FRD epitopes (n=8; tp1 of Subject 10004, and tp2 of Subjects 10013, 10027 and 10032). (**F**) CD8 A2:NLV tetramer stain of Subject 10027's tp2 PBMCs. Data represent at least two biological replicates except Subject 10032's EPD tetramer stain due to insufficient cells and panel (**E**). PBMCs were CD4-enriched or left untouched.

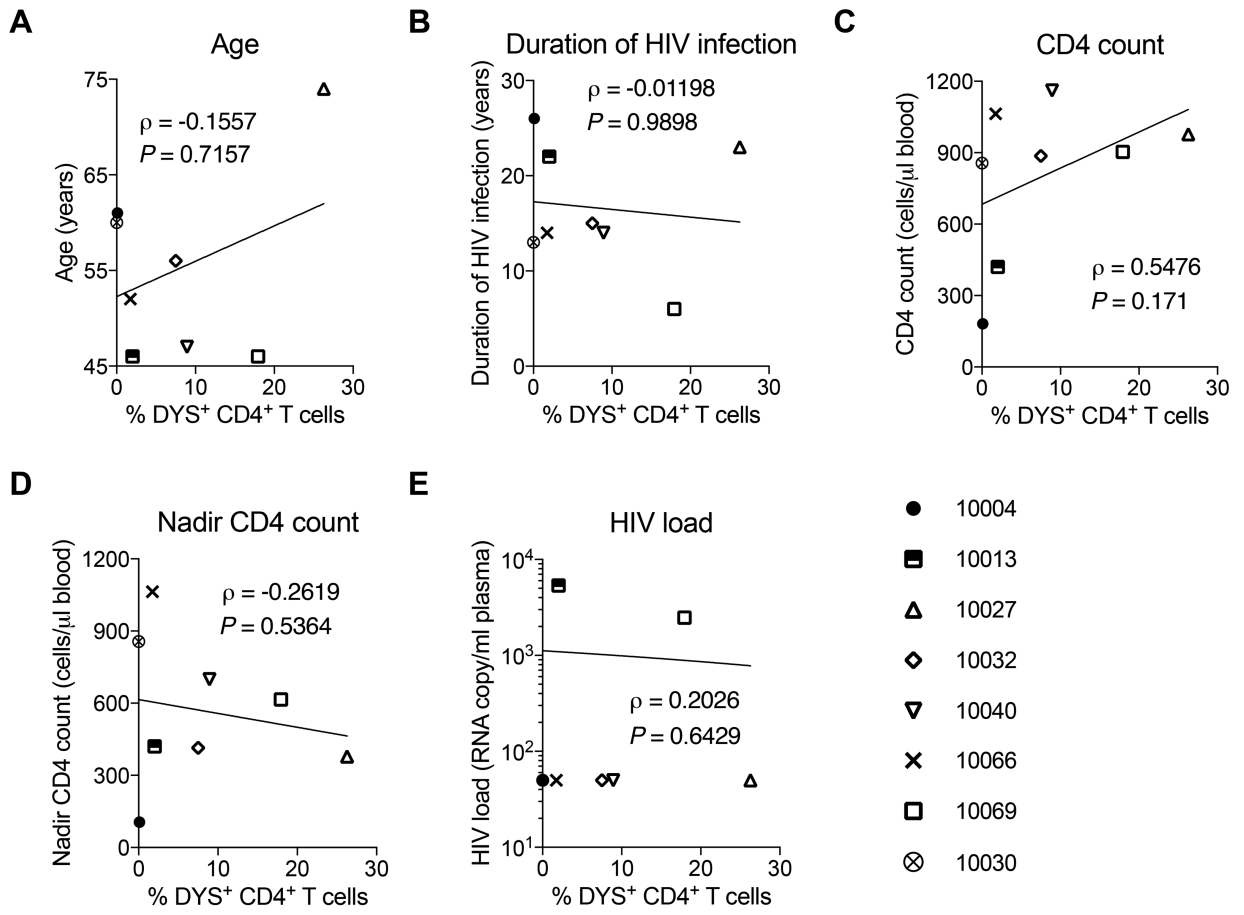

Figure II.4 DYS$^+$ CD4$^+$ T cell inflations do not correlate with clinical parameters. HIV$^+$ HCMV$^+$: *n*=8 (time-point 1 of Subject 10013, and time-point 2 of Subjects 10004, 10027 and 10032). Data represent single experiments. ρ: *Spearman correlation*.

CD4 counts of the HIV$^-$ cohort were unavailable for absolute DYS$^+$ CD4 count comparison. To confirm that these cells were undergoing memory inflation, DYS$^+$ CD4$^+$ T cells from five time-points of two HIV$^+$ DR7$^+$ subjects spanning a period of up to twelve years were analyzed and stable magnitudes and absolute counts (**Figure II.2E** and **Figure II.2F**, respectively) were detected. Together, these findings identify inflated CD4$^+$ T cells against the HLA-DR7-restricted DYS epitope of HCMV gB in HIV$^+$ HCMV$^+$ co-infected subjects.

Subject ID	HLA-DRB1 alleles	Age (years)
30051	07:01, 04:04	47
30057	07:01, 03:01	27
71740	07:01, 11:01	Unknown
20	07:01, 15:01	66
24	07:01, 01:01	45
26	07:01,04:01	55
29	07:01, 01:02	42
32	07:01, 01:01	52
36	07:01, 04:08	49
37	07:01, 04:07	50

Table II.3 Characteristics of HIV$^-$ HCMV$^+$ DR7$^+$ subjects.

HLA-DR7-restricted CD4$^+$ T cells responses to other persistent and non-persistent epitopes are low in HIV$^+$ HCMV$^+$ DR7$^+$ subjects

Tetramer stains of CD4$^+$ T cells specific for a DR7-restricted, highly conserved HCMV pp65 EPD epitope, which were absent in HIV$^+$ HCMV$^+$ DR7$^-$ subjects (**Figure II.3B**), revealed a significantly lower range of frequencies in the HIV$^+$ HCMV$^+$ DR7$^+$ cohort (0.01–1.87%, **Figure II.3C**) compared to inflated DYS$^+$ CD4$^+$ T cells in this cohort (median 0.04% vs. 4.76%, *P*=0.02; **Figure II.2D**). Memory inflation of these EPD$^+$ CD4$^+$ T cells was not detected in four longitudinal samples obtained from the two subjects with the highest DYS-specific inflation over a twelve-year or less period (**Figure II.2E** and **Figure II.2F**). A similar trend was observed in the HIV$^-$ HCMV$^+$ DR7$^+$ cohort between EPD$^+$ (0.003–0.04%, **Figure II.3D**) and DYS$^+$ CD4$^+$ T cells (median 0.001% vs.

0.06%, *P*=0.03; **Figure II.2D**). As observed for DYS^+ $CD4^+$ T cells, EPD^+ CD4 response magnitudes were also significantly higher in HIV^+ $HCMV^+$ $DR7^+$ than in HIV^- $HCMV^+$ $DR7^+$ cohort (*P*=0.002; **Figure II.2D**), confirming a recent report using pp65 peptide pools instead (Garg et al., 2017). To determine whether the inflation could be due to generalized HIV-induced inflammation, the magnitudes of $CD4^+$ T cells specific for DR7-restricted TT, EBV or HIV epitopes from the HIV^+ $DR7^+$ subjects were compared to their DYS^+ $CD4^+$ T cell counterparts. It was observed that the magnitudes of responses to these other epitopes were undetectable or very low compared to the inflated DYS-specific response (*P*=0.0078 for each comparison; **Figure II.3E**). To evaluate potential $CD8^+$ T cell inflation, PBMCs from Subject 10027, who had the highest DYS^+ CD4 inflation (26.34%) and carried a HLA-A2:01 allele, was stained with A2:NLV tetramer, but detected an NLV-specific $CD8^+$ T cell response magnitude of only 0.75% (**Figure II.3F**). Collectively, these results indicate that other $DR7^+$ epitope-specific $CD4^+$ T cells in most co-infected subjects are present at lower magnitudes than DYS^+ $CD4^+$ T cells.

DYS^+ $CD4^+$ T cells consist of T_{EM} and/or T_{EMRA} subsets

The memory phenotype of DYS^+ $CD4^+$ T cells was determined by measuring surface expression of memory markers CD45RO, CCR7 and CD27 to define T_{EM}, T_{EMRA}, central (T_{CM}; $CD45RO^+$ $CCR7^+$ $CD27^+$), transitional (T_{TM}; $CD45RO^+$ $CCR7^-$ $CD27^+$), naïve (T_{Nai}; $CD45RO^-$ $CCR7^+$ $CD27^+$), and intermediate (T_{Int}; $CD45RO^-$ $CCR7^-$ $CD27^+$) subsets (**Figure II.1**) (Burgers et al., 2009). Compared to the non-DYS^+ (DYS^-) $CD4^+$ T cells, DYS^+ $CD4^+$ T cells from HIV^+ $HCMV^+$ $DR7^+$ subjects were biased toward T_{EM} (46.6–97.97% vs. 6.1–51.9%, *P*=0.016) and T_{EMRA} (0.03–48.1% vs. 0.4–16.7%, *P*=0.078)

(**Figure II.5A**), and similar observations were made in the HIV$^-$ HCMV$^+$ DR7$^+$ cohort (**Figure II.5B**). Most CD45RO$^-$ DYS$^+$ and DYS$^-$ CD4$^+$ T cells were CD45RA$^+$ as shown in Subject 10027 (**Figure II.5C**).

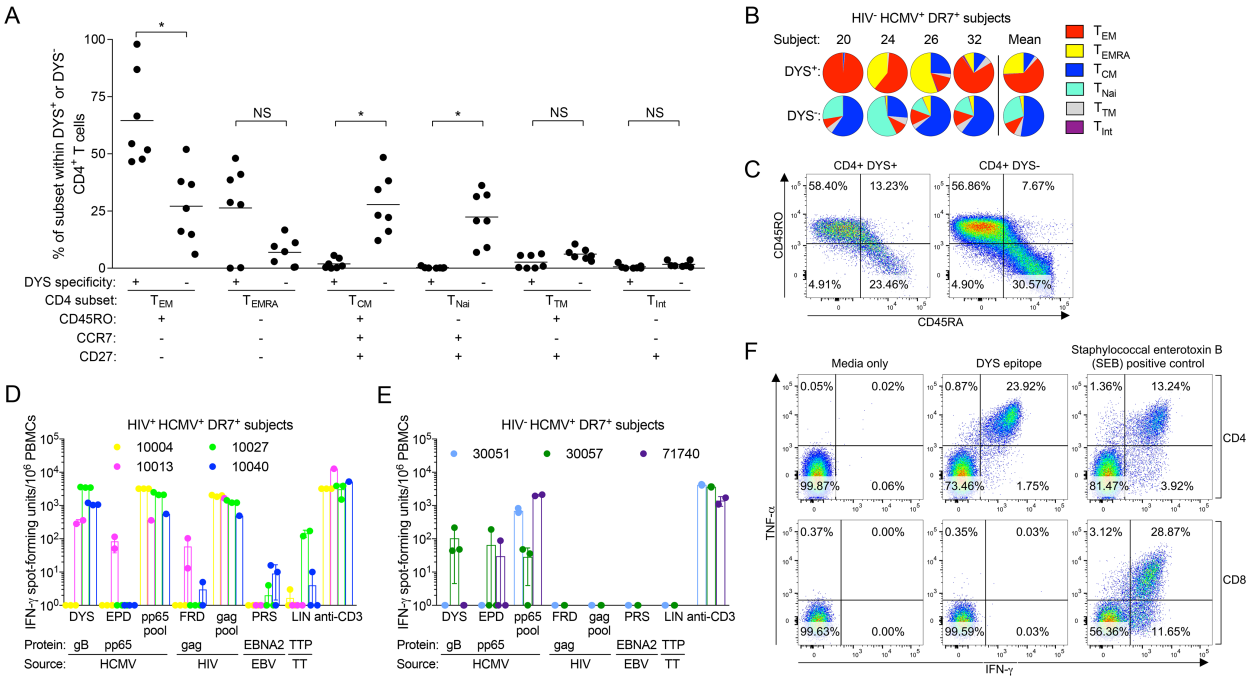

Figure II.5 CD4$^+$ T cells specific for DYS epitope consist of T_{EM} and T_{EMRA} subsets, and secrete cytokines upon DYS stimulation. (**A**) Response magnitude comparisons of DYS$^+$ and DYS$^-$ CD4$^+$ T cell subsets from HIV$^+$ HCMV$^+$ DR7$^+$ subjects (*n*=7). PBMCs were stained with the tetramer and memory markers to identify the subsets. Plots show grand means and represent at least two biological replicates. (**B**) Normalized magnitudes of CD4 subsets within DYS$^+$ or DYS$^-$ CD4$^+$ T cells from HIV$^-$ HCMV$^+$ DR7$^+$ subjects with sufficient tetramer$^+$ response for analyses. (**C**) CD45RO and CD45RA staining of Subject 10027's PBMCs. **D–E**: Background-corrected IFN-γ ELISpot responses of PBMCs from (**D**) HIV$^+$ HCMV$^+$ DR7$^+$ (*n*=4; tp1) and (**E**) HIV$^-$ HCMV$^+$ DR7$^+$ (*n*=3) subjects upon stimulation with 0.001 μg/ml of DYS, EPD, FRD, PRS, LIN epitopes, and of the following controls: HCMV pp65 overlapping 15-mer peptide pool, HIV's gag overlapping 15-mer peptide pool and anti-human CD3. Data represent technical triplicates except in conditions without mean±SD. (**F**) Intracellular cytokine staining of Subject 10027's PBMCs after DYS or SEB stimulation.

DYS-stimulated CD4$^+$ T cells secrete IFN-γ and TNF-α

Most HIV$^+$ HCMV$^+$ DR7$^+$ PBMC samples stimulated with DYS produced IFN-γ in high-throughput ELISpot, and only Subject 10013 responded to EPD (**Figure II.5D**), indicating that tetramer staining was more sensitive or that the cells were dysfunctional.

Subject 10004 did not respond to either epitope on the IFN-γ ELISpot, possibly as the result of dysfunction or absence of epitope-specific TCR among the $CD4^+$ T cells. 1 of 3 screened HIV^- $HCMV^+$ $DR7^+$ subjects responded to DYS stimulation (**Figure II.5E**). Responses to HIV FRD epitope, EBV PRS epitope or TT LIN epitope were relatively diminished in HIV^+ $DR7^+$ subjects compared to DYS-induced responses and not detected in HIV^- $DR7^+$ subjects (**Figure II.5D** and **Figure II.5E**, respectively). Dual IFN-γ and TNF-α intracellular cytokine staining of Subject 10027's PBMCs, which produced the largest IFN-γ ELISpot response to DYS, confirmed that the ELISpot responses originated from CD4s and not CD8s, and suggested that these inflated cells were likely polyfunctional (**Figure II.5F**), as previously reported (Pachnio et al., 2016; Pachnio et al., 2015).

Inflated $DR7^+$ DYS^+ $CD4^+$ T cells have highly restricted TCRβ repertoires

TCR analyses were conducted only on subjects with adequate DYS^+ CD4 magnitudes of response for bulk cell sorting and sequencing: HIV^+ Subjects 10027, 10040, 10069 and 10032 (26.34%, 8.95%, 17.91% and 7.52%, respectively) and HIV^- Subject 20 (1.32%) as a control. Highly restricted TCR-beta-variable (TCRβV) and -joining (TCRβJ) gene pairing was observed in bulk-sorted T_{EM} and T_{EMRA} subsets of DYS^+ $CD4^+$ T cells compared to the more diverse DYS^- counterparts in all subjects (**Figure II.6**, **A** - **E**). The dominant TCRβV and TCRβJ gene families of each individual's DYS^+ $CD4^+$ T cells comprised 69.5% to 99.7% of the DYS^+ $CD4^+$ T cell repertoire, and were identical between their T_{EM} and T_{EMRA} subsets (**Figure II.7, A** - **E**).

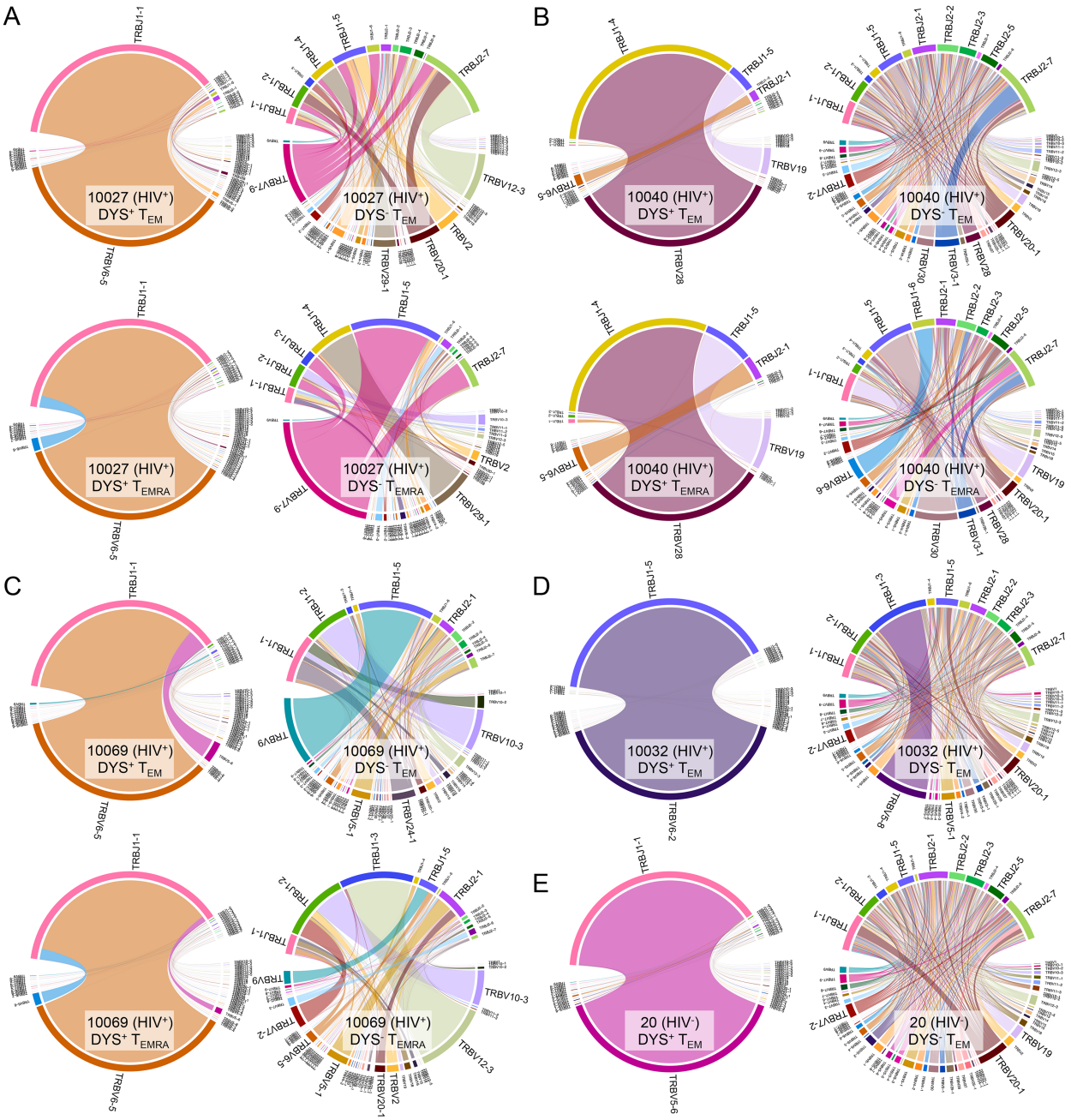

Figure II.6 Productive TCRβ V and J gene pairs of bulk-sorted, inflated DYS$^+$ CD4$^+$ T cells are highly restricted. TCRβV and TCRβJ gene family pairings of T_{EM} and/or T_{EMRA} subsets of productive DYS$^+$ and DYS$^-$ CD4 TCRs from Subjects (**A**) 10027, (**B**) 10040, (**C**) 10069, (**D**) 10032, and (**E**) 20. Data shown represent single experiments. V and J gene pairs are connected by stems between their arcs. Arc lengths reflect gene family proportions within the sample's repertoire. High magnitude V and J gene families are emphasized.

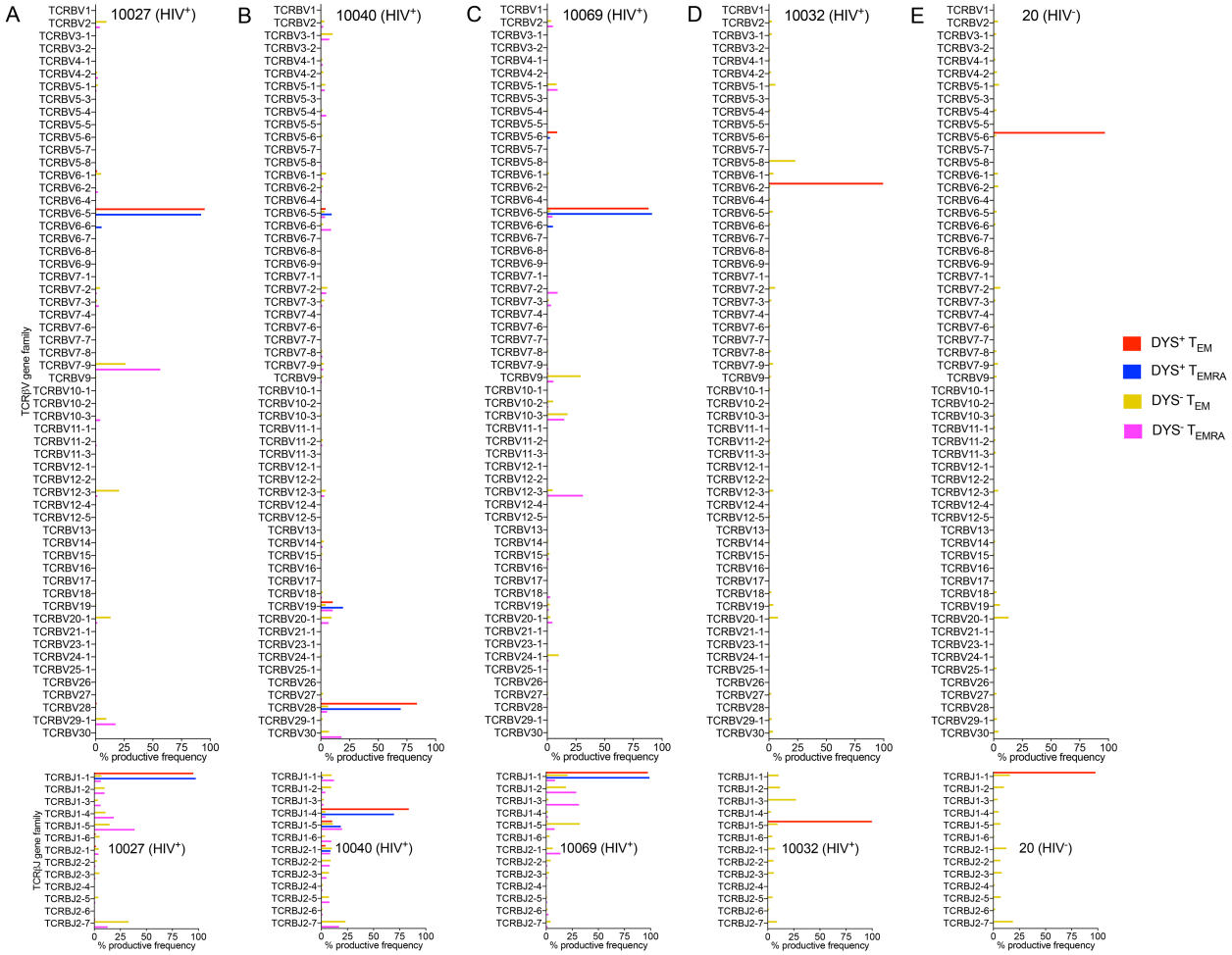

Figure II.7 Magnitudes of the highly restricted TCRβV and TCRβJ gene families of bulk-sorted, inflated DYS$^+$ CD4$^+$ T cells. Data represent single experiments for Subjects (**A**) 10027, (**B**) 10040, (**C**) 10069, (**D**) 10032, and (**E**) 20, which complement figure II.6. Top row: TCRβV; bottom row: TCRβJ.

However, the dominant TCRβV and TCRβJ gene families of DYS$^-$ CD4$^+$ T cells were lower (10.42–56.46%) and different between T_{EM} and T_{EMRA} subsets (**Figure II.7**, **A** - **E**). These findings indicate a strong TCRβ conservation among inflated DYS$^+$ CD4$^+$ T cells.

Inflated, DR7$^+$ DYS$^+$ CD4$^+$ T cells utilize nearly monoclonal CDR3s

The CDR3 repertoires of productive V(D)J rearrangements (in-frame and without stop codons) of the bulk-sorted DYS$^+$ CD4$^+$ T cells were analyzed, and it was observed that

they were dominated by specific clones with unique V(D)J rearrangements (69.41–99.64%, median=91.37%) (**Figure II.8**, **A** - **E**). Interestingly, we observed that 97.29% and 7.6% of the productive DYS^+ $CD4^+$ T_{EM} CDR3 repertoires of Subjects 20 (HIV^-) and 10069 (HIV^+), respectively, were comprised of public clonotypes shared between the two individuals. T_{EM} CDR3 analysis of an HIV^- $HCMV^-$ subject showed no clonal expansion (**Figure II.9**), suggesting that clonal expansion among DYS^- T_{EM} CDR3s might be tied to $HCMV^+$ status. The DYS^+ and DYS^- CDR3 clonal dominance reflected their respective TCRβ gene-family distributions. DYS^+ T_{EM} and T_{EMRA} dominant clones within each subject were identical, and this is likely a reflection of the reversible T cell differentiation from T_{EM} ($CD45RO^+$ $CD45RA^-$) to T_{EMRA} ($CD45RO^-$ $CD45RA^+$) (Pachnio et al., 2016).

In vivo stimulation of inflated cells involves NFAT-mediated cellular activation and proliferation upon TCR ligation by peptide-MHC. To confirm this activity and the accuracy of the clonal CDR3 sequence, the antigen presentation conditions for Subject 10027 was simulated using autologous B cell-derived LCLs and the DYS epitope to stimulate autologous DYS^+ α:β TCR expressed on Jurkat cells with an NFAT-mediated luciferase reporter. Using single-cell sorting and TCR sequencing, we first determined the paired α:β TCR CDR3 sequences of autologous DYS^+ $CD4^+$ T cells to be TCRα CAGRSSNTGKLIF CDR3 (TCRαV25 and TCRαJ37), and TCRβ CASIHQGSTEAFF CDR3 (TCRβV6-5 and TCRβJ1-1) that matched Subject 10027's nearly monoclonal CDR3 sequence (**Figure II.10A**).

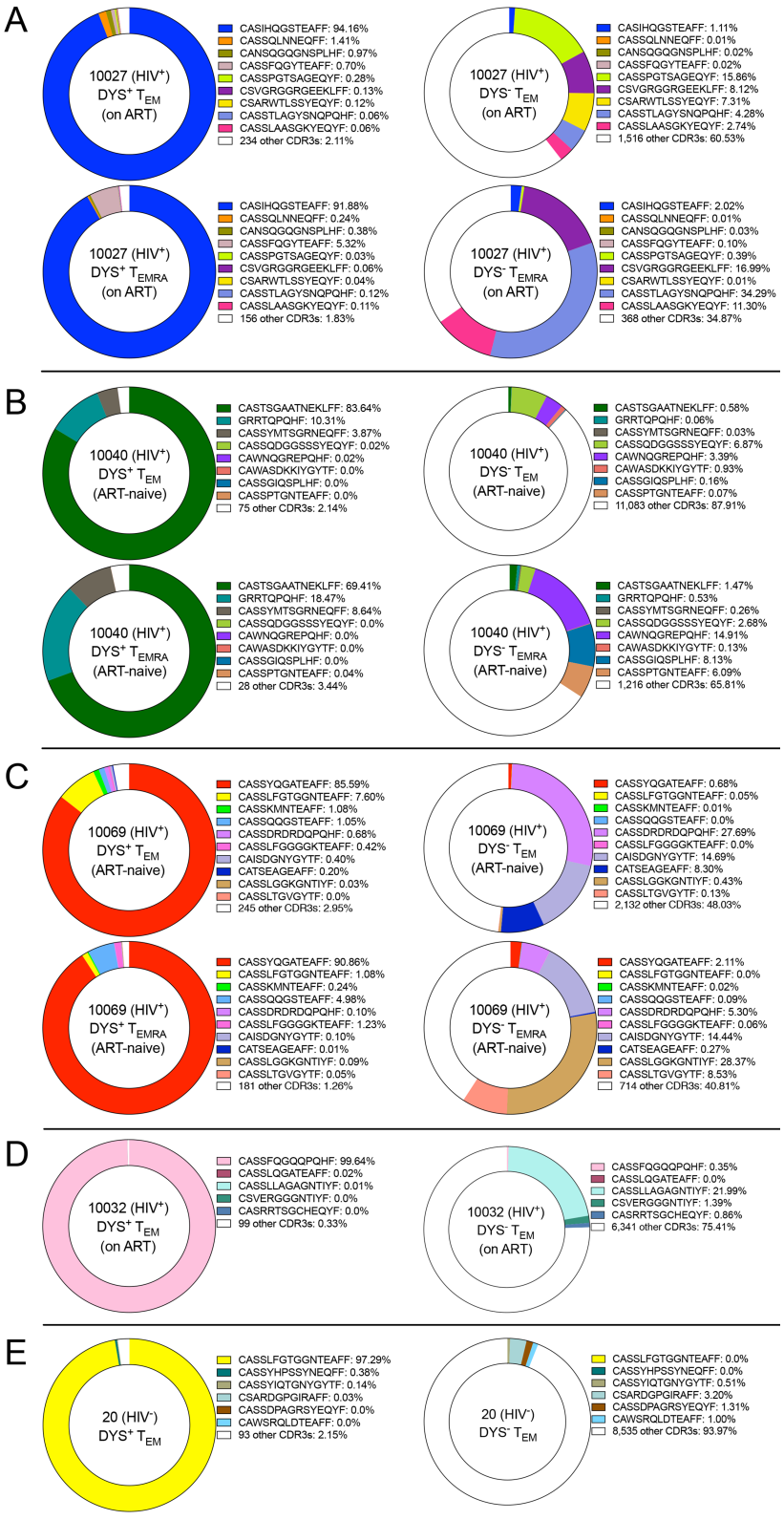

Figure II.8 Inflated DYS$^+$ CD4$^+$ T cells have nearly monoclonal productive CDR3s. Productive and unique TCRβ CDR3 clones of DYS$^+$ and DYS$^-$ T_{EM} and/or T_{EMRA} subsets from Subjects (**A**) 10027, (**B**) 10040, (**C**) 10069, (**D**) 10032 and (**E**) 20. Data represent single experiments.

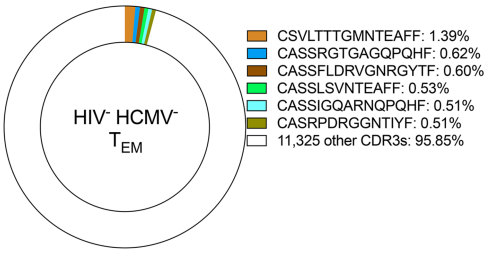

Figure II.9 Highest-frequency CDR3 sequences of T_{EM} from a HIV$^-$ HCMV$^-$ subject. Data represents a single experiment.

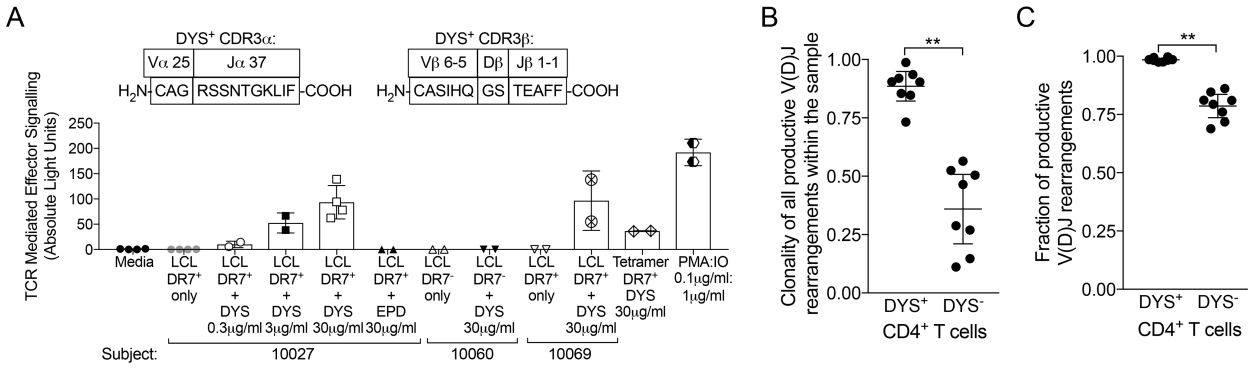

Figure II.10 Expressed clonal TCR of inflated DYS$^+$ CD4$^+$ T cells recognize DR7-restricted DYS epitope. (**A**) Subject 10027's DYS$^+$ single cell α:β TCR CDR3 sequences, and NFAT-mediated luciferase luminescence response of DR7$^+$ LCL-presented, serially diluted DYS epitope stimulation of DYS$^+$ TCR. Subject 10027's DYS$^+$ α:β TCR gene sequences were determined from single cell sorting and expressed using plasmids in an NFAT-luciferase reporter Jurkat cell line for stimulation. Graph shows mean±SD: conditions with two data-points represent technical replicates, while those with four represent two biological replicates of two technical replicates. (**B**) Clonality comparison of productive CDR3s of DYS$^+$ to DYS$^-$ CD4$^+$ T_{EM} and T_{EMRA} subsets from Subjects 10027, 10040, 10069, 10032 and 20. Clonality fractions were bioinformatically determined after productive entropy normalization. Values near 1: more clonal. (**C**) Fractional comparison of productive V(D)J rearrangements of DYS$^+$ to DYS$^-$ CD4$^+$ T_{EM} and T_{EMRA} subsets from all five subjects. Values near 1: fewer out-of-frame sequences or stop codons. **B–C**: Data represent single experiments for each subject with mean±95% CI.

After TCR expression and stimulation with autologous, DYS-pulsed DR7$^+$ LCLs, we detected a dose-dependent luminescence that was not observed without epitope, with a different epitope (EPD) or using a DR7$^-$ LCL (**Figure II.10A**). Subject 10069's LCL (DR7, DR8) confirmed that DYS was presented by DR7 and not DR3, which was the other DRB1 allele of Subject 10027 (**Figure II.10A**). Clonality analysis revealed that DYS$^+$ CD4$^+$ T_{EM} and T_{EMRA} cells were significantly more clonal than their DYS$^-$

counterparts, and were almost monoclonal in Subject 10032 (*P*=0.0078; **Figure II.10B**). The expectation of more productive V(D)J rearrangements within DYS^+ compared to DYS^- $CD4^+$ T cells since the former were sorted based on specific HLA-restricted epitope recognition was verified (*P*=0.0078; **Figure II.10C**). These results suggest that DYS^+ $CD4^+$ T cells are inflated via a highly clonal mechanism that likely involves DYS stimulation.

Different DYS^+ CDR3 clones share conserved amino acids

An assessment was made of whether potential amino acid conservation among the different, dominant DYS^+ CDR3s of all subjects could explain their common recognition of DYS. Remarkably, the V(D)J alignments revealed two new conserved amino acids (serine (S), and threonine (T)) within the D-segments in addition to the published glutamine (Q) (Crompton et al., 2008), all of which have polar, neutral side chains (**Table II.4**). Such conservation was not seen among DYS^- CDR3 clones (**Table II.5**). These findings indicate that amino acids with polar and neutral side chains might be critical in DYS recognition.

Inflated $DR7^+$ DYS^+ $CD4^+$ T cells are $CD127^-$ $TIGIT^-$ and Granzyme B^+

Plasma HCMV DNA loads of all subjects were measured, but no viral DNA was detected despite the HCMV-seropositive status of the subjects, suggesting that inflation of these circulating cells was not due to ongoing HCMV replication in the blood. It is possible that persistent CMV epitopes from non-productive reactivation occurring in HCMV latently-infected vascular endothelial cells are driving inflation.

Subject ID	CDR3 freq.	TCRβV family	V segment (start of CDR3)	N1	D segment	N2	J segment	TCRβJ family
10027	94%	6-5	C A S tgtgccagc	I H Q atccatcaa	G S gggagc		T E A F F act gaa gct ttc ttt	1-1
10040	84%	28	C A S tgtgccagc	T act	S G tcaggg	A A T N E K L F F gcggca act aatgaaaaa ctg ttt ttt		1-4
10069	91%	6-5	C A S S Y tgtgccagc agt tat		Q G cagggc	A gcc	T E A F F act gaa gct ttc ttt	1-1
10032	99%	6-2	C A S S tgtgccagc agt	F ttc	Q G cagggg	Q caa	Q P Q H F cag ccc cagcatttt	1-5
20	96%	5-6	C A S S L tgtgccagcagcttg	F ttc	G T G G gggacaggggggg	N T aac act	E A F F gaa gct ttc ttt	1-1

Table II.4 Dominant CDR3-β of inflated DYS^+ $CD4^+$ T cells share conserved polar, neutral amino acids. Conserved glutamine (Q), serine (S) and threonine (T) within the D-segment are underlined. The dominant CDR3s were identical for DYS^+ $CD4^+$ T_{EM} and T_{EMRA} in all subjects.

Subject	CD4 subset	CDR3 Freq.	TCRβV family	V gene start of CDR3	N1	D gene	N2	J gene	TCRβJ family
10027	T_{EM}	16%	12-3	C A S S	P	G T S	A G	E Q Y F	2-7
				tgt gcc agc agt	ccg	ggg act agc	gcc ggc	gag cag tac ttc	
	T_{EMRA}	34%	7-9	C A S S	T L A G	Y	S N Q P Q H F		1-5
				tgt gcc agc agc	acg ttg gcg gga	tat	agc aat cag ccc cag cat ttt		
10040	T_{EM}	7%	3-1	C A S S Q D	G G S	S	S Y E Q Y F		2-7
				tgt gcc agc agc caa gac	ggc ggg agt	agc	tcc tac gag cag tac ttc		
	T_{EMRA}	15%	30	C A W	N Q G	R	E P Q H F		1-5
				tgt gcc tgg	aat cagggg	cgc	gag ccc cag cat ttt		
10069	T_{EM}	28%	9	C A S S	D R D R		D Q P Q H F		1-5
				tgt gcc agc agc	gac cgggacagg		gat cag ccc cag cat ttt		
	T_{EMRA}	28%	12-3	C A S S	L G G	K	G N T I Y F		1-3
				tgt gcc agc agc	ctg gggggg	aaa	ggaaac acc ata tat ttt		
10032	T_{EM}	22%	5-8	C A S S L	L A G		A G N T I Y F		1-3
				tgt gcc agc agc tta	cta gcaggg		gct ggaaac acc ata tat ttt		
20	T_{EM}	3%	20-1	C S A R D	G P G	I R	A F F		1-1
				tgc agt gct aga gat	ggt cca ggg	att cga	gct ttc ttt		

Table II.5 Dominant CDR3-β of DYS^{-} $CD4^{+}$ T cells do not share conserved polar, neutral amino acids. Glutamine (Q) within the D-segment is underlined.

Other samples such as saliva and semen in which active HCMV replication has been reported were unavailable for testing. Next, we determined whether these cells displayed similar CD127$^-$ PD-1$^-$ TIGIT$^-$ granzyme B$^+$ phenotype of inflated CMV-specific CD8$^+$ T cells (Johnston et al., 2014; Klenerman and Oxenius, 2016; O'Hara et al., 2012). For all onward comparison experiments of inflated DYS$^+$ CD4$^+$ T cells (*n*=7), I used HIV$^-$ HCMV$^-$ controls (*n*=10) to provide contrast with conventional T_{EM} cells and avoid other potential inflationary HCMV epitope-specific responses, and also because HIV$^+$ HCMV$^-$ subjects are extremely rare. Only T_{EM} was focused on because DYS$^+$ T_{EMRA} was present in only 5 HIV$^+$ HCMV$^+$ DR7$^+$ subjects. CD127, PD-1, and TIGIT expressions on DYS$^+$ CD4$^+$ T_{EM} were compared to those on CD4$^+$ T_{EM} from HIV$^-$ HCMV$^-$ controls, and we detected significantly lower CD127 (*P*=0.025), no difference in PD-1 (*P*=0.36), and significantly lower TIGIT (*P*=0.0001) among the inflated cells (**Figure II.11**, **A** - **C**). The dual IFN-γ and TNF-α secretions in **Figure II.5F** also suggest these cells are not exhausted. To further examine polyfunctionality, *ex vivo* intracellular granzyme B levels of DYS$^+$ CD4$^+$ T_{EM} from the HIV$^+$ HCMV$^+$ DR7$^+$ subjects were compared to controls, and significantly higher levels on cells with DYS specificity were detected (*P*=0.0001; **Figure II.11D**), confirming previous cytotoxicity (Crompton et al., 2008; Elkington et al., 2004; Hegde et al., 2005; Pachnio et al., 2016; Pachnio et al., 2015) and polyfunctionality (Pachnio et al., 2016; Pachnio et al., 2015) reports for DYS$^+$ CD4$^+$ T cells. B-cell lymphoma-2 (Bcl-2) protein MFI of inflated DYS$^+$ CD4$^+$ T cells were not different compared to controls (*P*=0.54; **Figure II.11E**). None of these protein levels correlated with the magnitude of DYS$^+$ CD4 inflation (**Figure II.12**). These findings reveal that inflated DYS$^+$ CD4$^+$ T cells are CD127$^-$ PD-1$^{+/-}$ TIGIT$^-$ and Granzyme B$^+$.

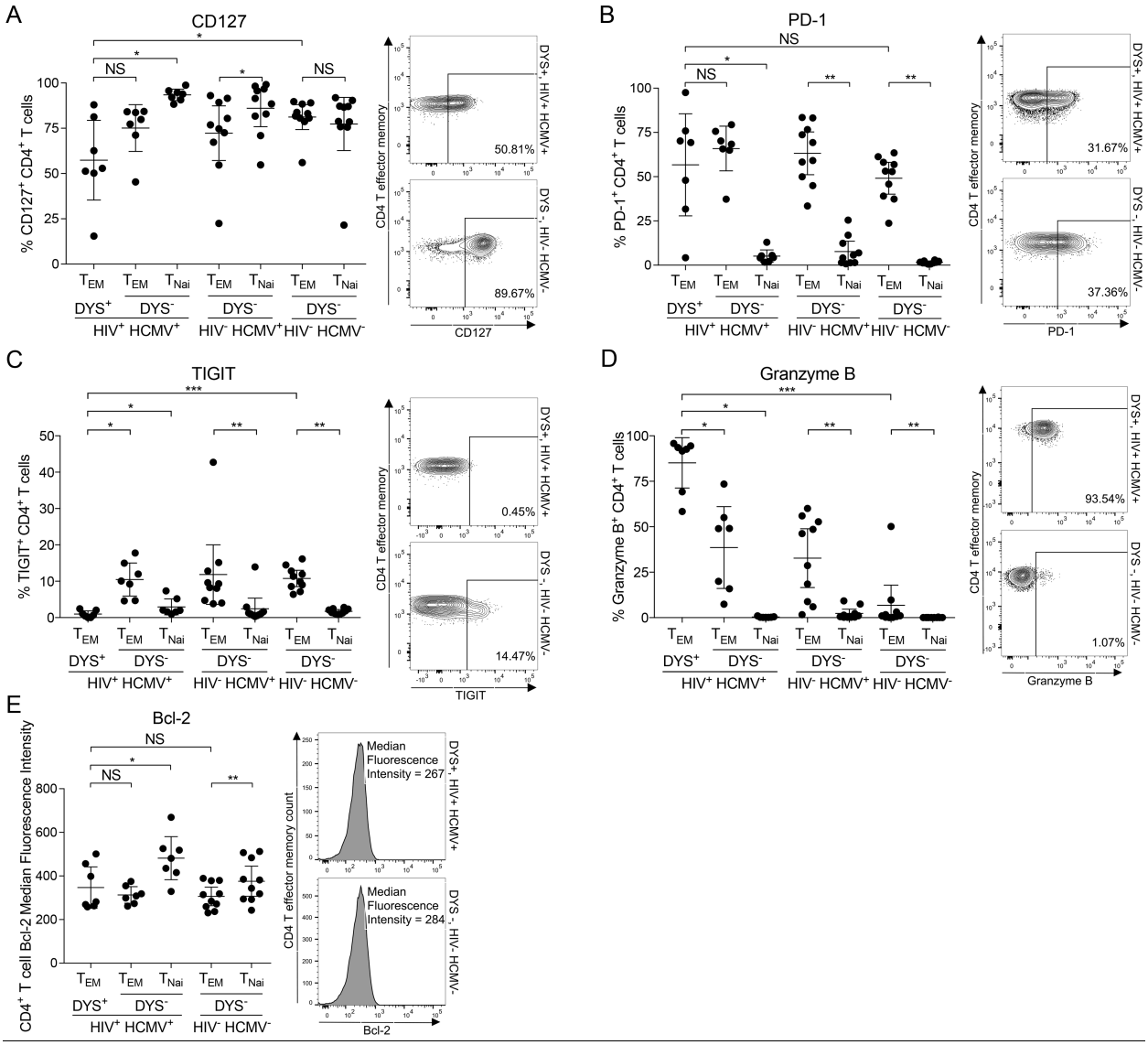

Figure II.11 Inflated DYS$^+$ CD4$^+$ T cells have a CD127$^-$ TIGIT$^-$ Granzyme B$^+$ phenotype. *Ex vivo* comparisons of (**A**) CD127, (**B**) PD-1, (**C**) TIGIT, (**D**) Granzyme B expressions or (**E**) Bcl-2 median fluorescence intensity (MFI) of DYS$^+$ CD4$^+$ T_{EM} of HIV$^+$ HCMV$^+$ subjects to DYS$^-$ CD4$^+$ T_{EM} of HIV$^-$ HCMV$^-$ controls. PBMCs were stained with tetramer and mAbs for either surface PD-1, CD127 and TIGIT or intracellular granzyme B and Bcl-2 proteins. HIV$^+$ HCMV$^+$: *n*=7, HIV$^-$ HCMV$^+$: *n*=10 and HIV$^-$ HCMV$^-$: *n*=10. Graphs represent single experiments for each subject, with mean±95% CI for all subjects.

Inflated DR7$^+$ DYS$^+$ CD4$^+$ T cells are CX$_3$CR1^{high} and are not undergoing higher proliferation

Latent HCMV reservoirs present endogenous DYS epitopes to DYS$^+$ CD4$^+$ T cells (Hegde et al., 2005; Pachnio et al., 2015; Ventura et al., 2012). Therefore, it was

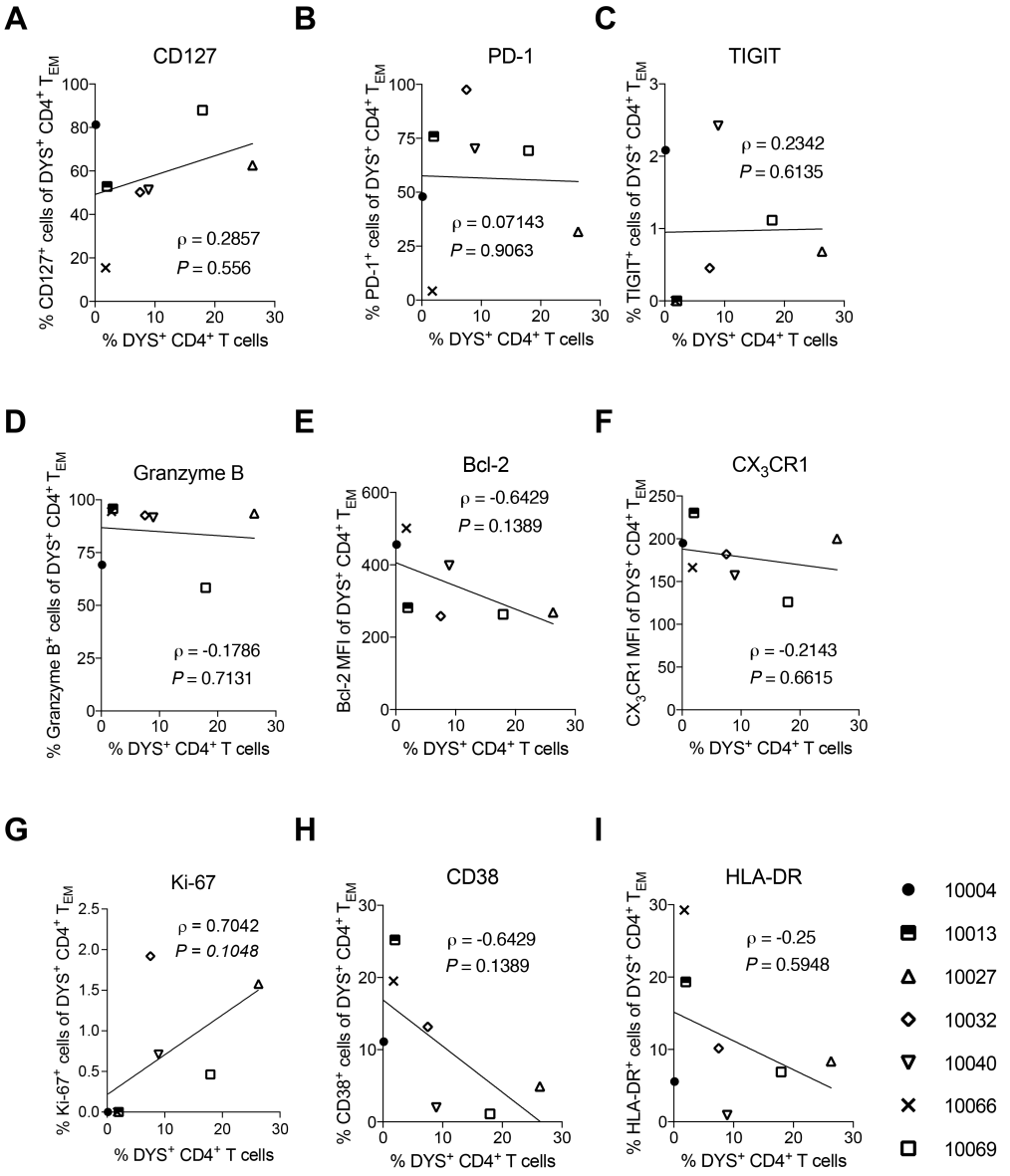

Figure II.12 DYS$^+$ CD4$^+$ T cell inflation does not correlate with frequencies of their T_{EM} intracellular or surface proteins. HIV$^+$ HCMV$^+$: *n*=7 (tp1 of Subject 10013, and tp2 of Subjects 10004, 10027 and 10032). Data represent single experiments. ρ: *Spearman correlation*.

hypothesized that such reservoirs expand with HIV co-infection to cause memory inflation due to potential depletion of CMV-specific CD4$^+$ T cells that occurred during acute HIV infection. While HCMV reservoir size could not be directly measured, it was further hypothesized that expanded HCMV latent reservoirs, including VECs, would express more CX_3CL1 and consequently correlate with higher expression of CX_3CR1 on

inflated DYS^+ $CD4^+$ T cells. Indeed, these cells had significantly higher CX_3CR1 MFI compared to controls (*P*=0.0007; **Figure II.13A**), confirming previous reports (Pachnio et al., 2016). To determine whether effective TCR stimulation by DYS-presenting latent reservoirs caused ongoing proliferation *in vivo* and by extension memory inflation, *ex vivo* Ki-67^+ levels within inflated DYS^+ CD4 T_{EM} were measured and a slightly wider range of, but not significantly higher, magnitudes were detected in these cells compared to controls (*P*=0.47; **Figure II.13B**), in keeping with studies on MCMV epitope-specific $CD8^+$ T cell inflation (Bolinger et al., 2015; Sierro et al., 2005). Using CD57 and CD28 dual staining of Subject 10027's tp2 PBMCs, it was observed that <2% of $CD4^+$ DYS^+ T cells displayed the $CD57^+$ $CD28^{+/-}$ phenotype for replicative senescence (**Figure II.13C**) (Brenchley et al., 2003). CX_3CR1 and Ki-67 levels did not correlate with DYS^+ CD4 inflation magnitudes (**Figure II.12**). These findings suggest that inflated DYS^+ CD4 T cells might interact with HCMV reservoirs that express CX_3CL1 and their inflation is not linked to increased ongoing proliferation.

Inflation is not caused by DR7-restricted HIV gag epitope cross-reactivity

TCR cross-reactivity is ubiquitous and can occur between unrelated pathogens including HIV (gag) and influenza A virus (Acierno et al., 2003). To assess cross-reactive TCR role in inflation, the HLA-epitope-TCR simulation experiment was repeated using high-affinity DR-7-restricted HIV gag epitopes instead, but detected no response (**Figure II.13D**). Also, HIV viremia was not associated with a significant increase in inflation compared to aviremia (*P*=0.63; **Figure II.13E**). These findings suggest that the inflation is not likely caused by cross-reactive HIV gag epitopes.

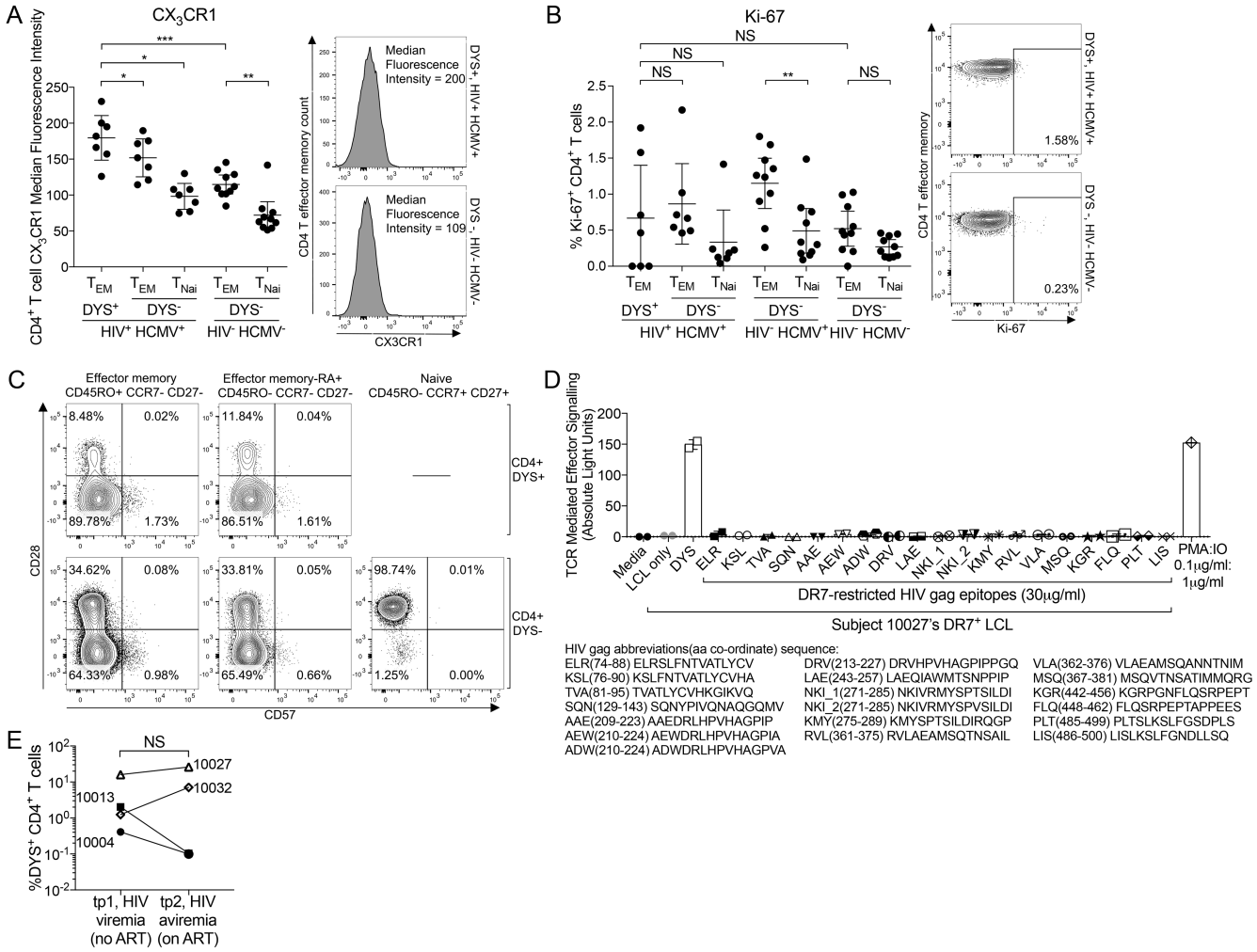

Figure II.13 Inflated DYS$^+$ CD4 T cells are CX$_3$CR1^{high}, not replicatively senescent and do not cross-react with HIV gag proteins. A–B: *Ex vivo* comparisons of (**A**) CX$_3$CR1 MFI and (**B**) Ki-67 response magnitude of DYS$^+$ CD4$^+$ T$_{EM}$ of HIV$^+$ HCMV$^+$ subjects to DYS$^-$ CD4$^+$ T$_{EM}$ of HIV$^-$ HCMV$^-$ controls. HIV$^+$ HCMV$^+$: *n*=7, HIV$^-$ HCMV$^+$: *n*=10 and HIV$^-$ HCMV$^-$: *n*=10. (**C**) CD57 and CD28 expressions of Subject 10027 DYS$^+$ and DYS$^-$ CD4$^+$ T cells. (**D**) Luciferase luminescence response of 19 DR7-presented HIV gag epitopes stimulation of Subject 10027's DYS$^+$ TCR expressed in the Jurkat cell line. (**E**) DYS$^+$ CD4 magnitude change from tp1 (HIV viremia) to tp2 (HIV aviremia). **A–B**, **E**: graphs show mean±95% CI for all subjects and represent single experiments with no replicates except (**E**) showing technical replicates. **D**: data shows mean±SD of technical duplicates.

Whether HCMV might latently infect the inflated CMV-specific memory $CD4^+$ T cells it induces was also investigated. ddPCR quantitation of HCMV DNA was optimized using HCMV AD169 strain, but HCMV DNA was not detected in DYS^+ $CD4^+$ T cells (**Figure II.14A** and **Figure II.14B**).

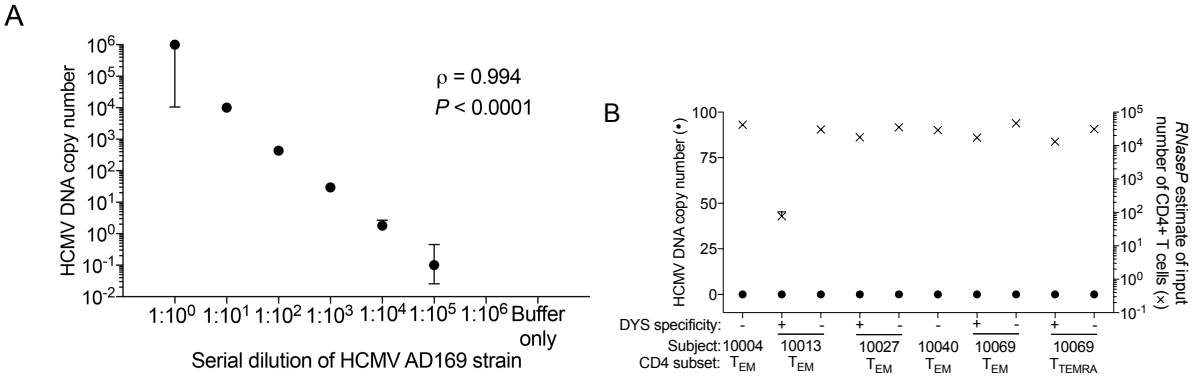

Figure II.14 Inflated DYS^+ $CD4^+$ T cells do not serve as HCMV reservoirs. A–B: Droplet digital PCR (ddPCR) HCMV DNA quantitation in single experiments of (**A**) HCMV AD169 strain serial dilutions, and (**B**) DYS^+ and DYS^- $CD4^+$ T cells from HIV^+ $HCMV^+$ $DR7^+$ subjects (n=6). Data points at 10^{-1} indicate undetected HCMV DNA. (**B**) Left y-axis: HCMV genome copy number after normalization with *RNaseP* housekeeping gene. Right y-axis: input number of cells, which was determined by dividing the *RNaseP* concentration (in g/µl) in the PCR volume by 2 (because there are two copies of *RNaseP* per cell) and multiplying by the total ddPCR volume (20 µl). This product is divided by the standard number of DNA per cell (6 pg/cell) to determine the input number of cells in the reaction. Graph shows 95% CI determined from the ratio of the concentration of HCMV *IE1+IE2* to *RNaseP*.± 1.96 times the standard error ratio of HCMV *IE1+IE2* to *RNaseP* as described in more details in the materials and methods in **Equation VI.1**.

Inflated DYS^+ $CD4^+$ T cells display elevated levels of CD38 or HLA-DR, but less often co-express CD38 and HLA-DR

CD38 and HLA-DR dual and individual expression was also measured on inflated DYS^+ $CD4^+$ T cells. Although no significant difference was observed in their $CD38^+HLA\text{-}DR^+$ co-expression magnitude compared with HIV^- $HCMV^-$ DYS^- T_{EM} controls (P=0.091; **Figure II.15A**), significantly higher levels of $CD38^+HLA\text{-}DR^+$ co-expression were observed on their DYS^- T_{EM} counterparts within the HIV^+ $HCMV^+$ cohort compared to the same controls (P=0.0001; **Figure II.15A**). Additionally, individual protein analyses

revealed significantly higher levels of CD38 and HLA-DR (*P*=0.03 and *P*=0.03; **Figure II.15B** and **Figure II.15C**, respectively). There was a stepwise increase in the mean expressions from DYS^- T_{EM} of HIV^- $HCMV^-$ to DYS^- T_{EM} of HIV^- $HCMV^+$ to DYS^- and DYS^+ T_{EM} of HIV^+ $HCMV^+$ subjects. These protein levels on DYS^+ $CD4^+$ T cells did not correlate with the magnitudes of DYS^+ CD4 inflation (**Figure II.12**). CD38 was elevated on naïve T cells as expected (Chattopadhyay and Roederer, 2010). Overall, these findings indicate that inflated DYS^+ $CD4^+$ T cells do contribute to the increased T cell activation associated with higher risk of HCMV-related non-AIDS comorbidities in HIV^+ $HCMV^+$ subjects, but further studies are required to define the specific subsets of activated cells that correlate most closely with these adverse outcomes.

Discussion

In this chapter, I described the memory inflation of HLA-DR7 restricted, HCMV epitope-specific $CD4^+$ T cells in $HCMV^+$ long-term non-progressor HIV subjects that could potentially contribute to the higher T cell activation associated with elevated risks of HCMV-related non-AIDS cardiovascular comorbidities in such co-infected patients. *Ex vivo* DR7:DYS tetramer stains revealed persistent, inflated percentages of HCMV's DYS^+ $CD4^+$ T cells in the HIV^+ $HCMV^+$ $DR7^+$ subjects that consisted of mostly T_{EM} and T_{EMRA} subsets, and secreted IFN-γ and TNF-α upon *in vitro* DYS stimulation of their nearly monoclonal TCR repertoires. The 28.8% DYS^+ CD4 response magnitude of Subject 10027 measured in the fourth time-point of the longitudinal analyses is the largest reported CD4 response magnitude against DYS epitope to our knowledge, and

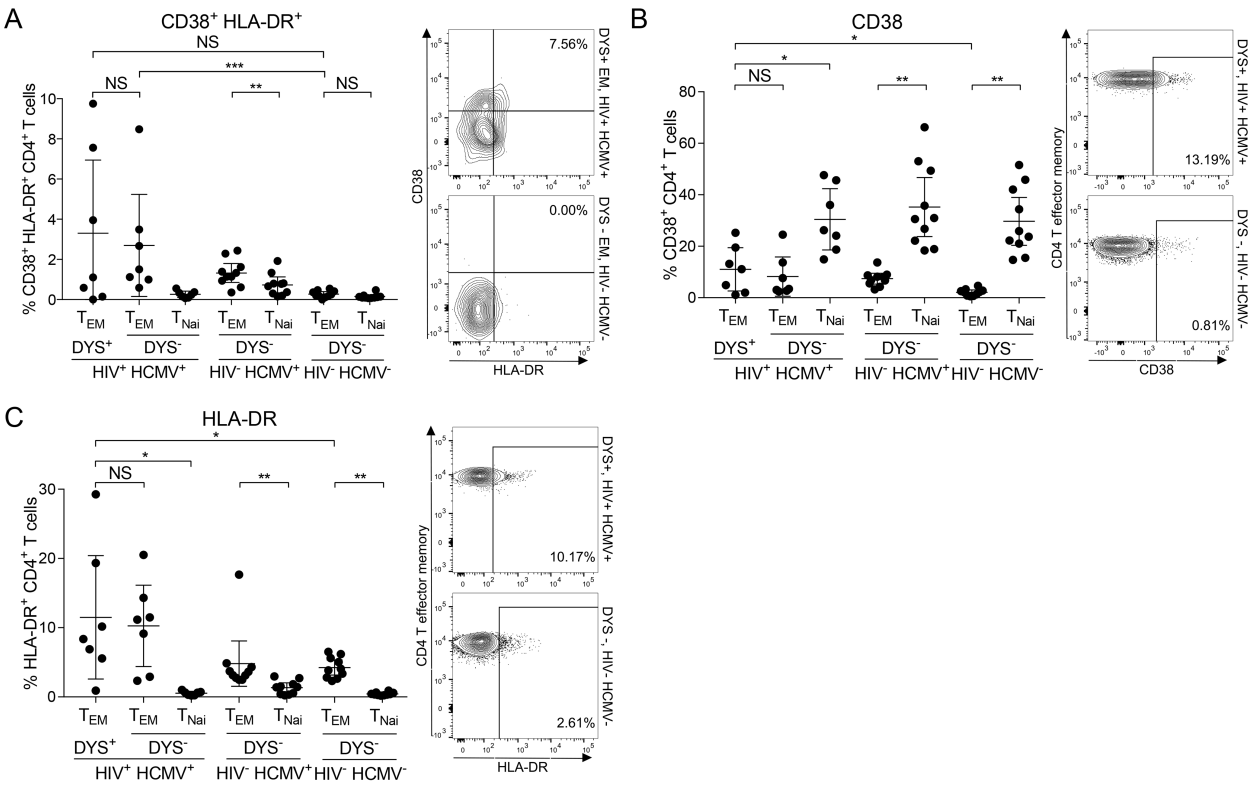

Figure II.15 Inflated DYS$^+$ CD4$^+$ T cells have a wide distribution of CD38$^+$HLA-DR$^+$ co-expression. *Ex vivo* comparisons of (**A**) CD38$^+$HLA-DR$^+$ (**B**) CD38 and (**C**) HLA-DR magnitudes on DYS$^+$ CD4$^+$ T_{EM} of HIV$^+$ HCMV$^+$ subjects to DYS$^-$ CD4$^+$ T_{EM} of HIV$^-$ HCMV$^-$ controls. HIV$^+$ HCMV$^+$: *n*=7, HIV$^-$ HCMV$^+$: *n*=10 and HIV$^-$ HCMV$^-$: *n*=10. Graphs represent single experiments for each subject and mean±95% CI for all subjects.

is similar to the 24% magnitude of a DQ6-restricted pp65$_{41\text{-}55}$ LLQTGIHVRVSQPSL-specific CD4 response (Pachnio et al., 2016), although the HIV status of the subject was not specified. It is not clear why Subject 10030 had an extremely low DYS$^+$ CD4$^+$ T cell magnitude. We doubt this was due to CMV sequence variation because the DYS epitope and adjacent residues involved in proteosomal cleavage are highly conserved. It is possible that the TCR of these cells lack glutamine, threonine or serine amino acid residues that are conserved among inflated DYS$^+$ T cells, and this warrants investigation.

These findings represent the first *ex vivo* and tetramer-based evidence for CD4 memory inflation in HIV$^+$ subjects and it is striking in frequency and magnitude for the

DYS epitope. It is quite remarkable that $DR7^+$ CD4 responses to other HCMV, TT, EBV or HIV epitopes analyzed in the same cohort were significantly lower. The reduced magnitude of IFN-γ responses to stimulations by these additional epitopes was reflected in the lower absolute counts among the stimulated cells in the ICS assay. Therefore, I believe that the inflation of DYS-specific $CD4^+$ T cells is more likely due to specific HLA-epitope-TCR interactions, and unlikely to be due to HIV-induced inflammation. This is also supported by the finding of a highly enriched CDR3 clonotype in HIV^- Subject 20. Also, it does not appear that this is an intrinsic feature of persistent viruses, as EBV epitope-specific responses were of low magnitude or absent within the same individuals. Although I was unable to measure these responses among the HIV^- $DR7^+$ cohort due to IRB restrictions on re-inviting the subjects, I believe their magnitudes will similarly be low or undetectable. The EPD^+ $CD4^+$ T cell response was of unusually high magnitude in the HIV^+ Subject 10013 at both tp1 (1.87%) and tp2 (1.4%). This individual was also the only subject in whom secreted IFN-γ was detected upon EPD stimulation. These findings suggest that the EPD epitope may drive a memory-inflated response in HIV, and the possibility that EPD might not also drive an inflated rarely response in HIV^- individuals cannot be excluded. Interestingly, low-level DYS^+ $CD4^+$ T cell responses were detected in all HIV^- $HCMV^+$ $DR7^+$ subjects with the exception of one subject with 1.32% magnitude of response. The observation that one HIV^- subject had DYS^+ $CD4^+$ T cell, which were predominantly of the T_{EM} phenotype, illustrates that memory inflation with this epitope can occur in HIV^- subjects. However, the prevalence and magnitude of memory inflation was substantially higher with HIV co-infection. Taken together these

findings suggest that $CD4^+$ memory inflation can occur in HIV negative individuals but HIV acts to increase the prevalence and magnitude.

It is not fully understood how CMV, and why only CMV, induces chronic memory inflation and why this property has been conserved in mice (Bolinger et al., 2015; Dekhtiarenko et al., 2016; Karrer et al., 2003; Munks et al., 2006; Sierro et al., 2005), rhesus macaques (Cicin-Sain et al., 2011) and man (Klarenbeek et al., 2012; Waller et al., 2008). The inflated DYS and comparatively lower EPD responses in five HIV co-infected subjects parallel recent reports of different epitopes from the same protein inducing both high- and low-magnitude responses (Bolinger et al., 2015; Munks et al., 2006). Potential explanations for DYS-specific inflation include the translation of gB mRNA without HCMV replication (Smuda et al., 1997), gB colocalization to endosomes and endogenous presentation (Hegde et al., 2005; Pachnio et al., 2015), and the secretion of such gB epitope-loaded endosomes as immunogenic exosomes (Broadley et al., 2017; Walker et al., 2009). Endogenous epitope processing and presentation has been demonstrated recently to drive CD8 memory inflation (Dekhtiarenko et al., 2016; Hutchinson et al., 2011). However, the low pp65 EPD-specific responses might be due to pp65 polyprotein absence in immunogenic exosomes (Walker et al., 2009). Yet, this mechanism does not explain the published DQ6-restricted $pp65_{41\text{-}55}$ LLQTGIHVRVSQPSL epitope-induced inflation (Pachnio et al., 2016), suggesting that multiple factors underlie inflation. Differential gene expression patterns (Dekhtiarenko et al., 2013), and the presence of higher avidity TCRs specific for DYS might also play some role. It is important to note that cytotoxic $CD4^+$ T cells in general are elevated in HIV infection (Appay et al., 2002b). This may be due to low CCR5 expression,

especially by CMV-specific $CD4^+$ T cells (Casazza et al., 2009), which protects such cells from HIV infection and might explain the lack of HIV DNA enrichment in the results or APOBEC3G-mediated inhibition of HIV replication (Oswald-Richter et al., 2007; Pido-Lopez et al., 2009).

Few studies have described the TCR repertoire of HLA class II-restricted epitope-specific CD4 responses based on tetramer sorted cells, and most were conducted *in vitro* or without TCR sequencing (Ertelt et al., 2011; Falta et al., 2005; Kim et al., 2013; Kimata et al., 2012; Koehne et al., 2015; Lanzer et al., 2014; Legoux et al., 2013; Nose et al., 2007; Petersen et al., 2015; Poli et al., 2013; Sabatino et al., 2011; Vingert et al., 2010). Notably, some of the repertoires of these single epitope-specific T cells are diverse with over six unique, dominant TCR gene families (Ertelt et al., 2011; Nose et al., 2007; Sabatino et al., 2011; Vingert et al., 2010). Therefore, to our knowledge, this work represents the first combination of *ex vivo*, class II tetramer-derived and deep sequencing-based identification of a nearly monoclonal TCR repertoire of inflated HLA-restricted epitope-specific $CD4^+$ T cells at the resolution of the CDR3. Three new DYS-specific TCRβV gene families were discovered: TCRβV6-2, TCRβV5-6 and TCRβV28 in addition to the published TCRβV6-5 (Crompton et al., 2008). CDR3 sequencing confirmed that the inflations were driven by nearly monoclonal expansions, especially in Subject 10032 where 99.4% of all DYS^+ T_{EM} were a single clonotype. HIV^- Subject 20's DYS^+ $CD4^+$ T cell clonality indicates that clonal expansion to DYS was not unique to HIV^+ subjects, a finding that again suggests that HIV co-infection is not necessary for, but rather increases the likelihood of, and amplifies DYS^+ $CD4^+$ T cell inflation. To determine if the inflation was unique to DYS, a comparison

between bulk DYS$^+$ CDR3s and those of EPD, LIN, PRS, or FRD epitope would have been sufficient; however, magnitudes of cells specific to these additional epitopes were too low for that analysis. CDR3 sequences within DYS$^-$ CD4 samples were generally polyclonal with a few exceptions. These noteworthy exceptions (Fig. 4, right column) might be driven by clonal expansions induced by epitopes that overlap with DYS as observed in HCMV IE1 epitopes (Braendstrup et al., 2014), or to other inflation-inducing epitopes of HCMV or other pathogens. The presence of the dominant DYS$^+$ CDR3s within the DYS$^-$ repertoire at relatively lower magnitudes reflected potential loss of tetramer binding, while the reverse could reflect non-specific binding to the DYS tetramer. The *in vitro* HLA-DR7-presented DYS stimulation of the inflated DYS$^+$ CD4 TCR in our Jurkat cell transfection system confirmed the specificity of the tetramer stain and accuracy of our bulk-cell and single-cell TCRα and TCRβ sequencing. The dominant DYS$^+$ CDR3 sequences were analyzed from different subjects for amino acid conservation as: (i) there are no reports of such conservation within inflationary CD4$^+$ T cell CDR3s, and (ii) even dominant clones of well-characterized, non-inflated HLA-A2:NLV CD8 responses from different individuals do not always contain conserved motifs (Glanville et al., 2017). In addition to the published glutamine (Crompton et al., 2008), it was also discovered that novel conservations of serine and threonine that preceded the germline glycine within the D-segment of the different, dominant DYS$^+$ CD4 CDR3 clones. These amino acids are polar with neutral side chains that might serve as TCR binding residue sites for hydrogen bond formation with DYS and HLA-DR7. Further verification by crystallographic reconstruction of the DR7-DYS-TCR complex is required.

Inflation may be due to intermittent, subclinical CMV reactivation or expression of specific transcripts. HCMV DNA was not detected in plasma samples from this cohort. Future studies could investigate this reactivation through monitoring of other specimens such as saliva, semen, etc. Although the exact mechanism by which HCMV stimulates inflated responses in our human subjects was unable to be determined, *ex vivo* protein expressions of DYS^+ $CD4^+$ T cells and observed similarities ($CD127^-$ $PD\text{-}1^{+/-}$ $TIGIT^-$ Granzyme B^+) were analyzed and compared to those on inflated CMV-specific $CD8^+$ T cells reported to be maintained by low-level exposure to antigens from stochastic HCMV reactivation (Johnston et al., 2014; Klenerman and Oxenius, 2016; Pachnio et al., 2016; Pachnio et al., 2015). PD-1 might not be an appropriate co-inhibitory protein to evaluate on DYS^+ $CD4^+$ T cells due to their low levels of CD28 (Crompton et al., 2008), which has been recently shown to mediate PD-1 suppression of T cells (Hui et al., 2017; Kamphorst et al., 2017). The normal expression levels of anti-apoptotic Bcl-2 suggest that DYS^+ $CD4^+$ T cell inflation is not due to apoptotic suppression, but might be due to other maintenance mechanisms such as longer telomeres (O'Bryan et al., 2013) that could offset the normal rate of apoptosis. The persistence of inflated DYS^+ T_{EM} and T_{EMRA} subsets, despite the lack of $CCR7^+$ DYS^+ T cell thymic emigrants, is explained by reports that thymectomy does not affect memory T cell inflation or homeostasis (Okoye et al., 2012).

Ki-67 data suggests that the DYS^+ $CD4^+$ T cell inflations were not driven to significantly higher proliferation. While this observation might be due to cross-sectional sampling limitations, it does confirm findings in chronic MCMV models of inflation (Bolinger et al., 2015; Sierro et al., 2005). CD28 and CD57 analyses confirm that only a

very limited number of the inflated cells are too senescent to replicate (Brenchley et al., 2003). The cause of inflation does not appear to involve DYS^+ $CD4^+$ TCR cross-reactivity with the $DR7^+$ HIV gag epitopes either. But, cross-reactivity with other $DR7^+$ HIV epitopes cannot be excluded. Increased inflation was observed in two subjects when HIV replication was suppressed to undetectable levels with ART, suggesting that HIV replication is not required for maintenance of inflation.

The sites of HCMV latency are important (Klenerman and Oxenius, 2016) and HIV could alter the environment to help HCMV persist in long-lived non-hematopoietic cells in HCMV reservoir sites such as LNs and vascular endothelial cells (VECs). VECs can serve as latent HCMV reservoirs and also express the CX_3CR1 ligand—fractalkine. Vascular homing might bring CX_3CR1^{high} DYS^+ $CD4^+$ T cells in close contact with these potential HCMV reservoirs, resulting in re-stimulation and inflation. Although HCMV DNA was not detected in the inflated cells, it is possible that they passively disseminate HCMV from LNs to vascular endothelium without getting infected, as LN DCs do for HIV. Herpes viruses such as CMV are species-specific and cause life-long infection. Therefore, it is also possible that the inflated responses provide a degree of protective immunity against other infections, making them mutually beneficial to CMV and its host.

Although $CD38^+$HLA-DR^+ co-expression on the inflated cells was not significantly elevated compared with HIV^- $HCMV^-$ DYS^- T_{EM} controls, a wider distribution was observed with inflation. Remarkably, a similar comparison of $CD38^+$HLA-DR^+ co-expression on the DYS^- T_{EM} counterpart of the inflated cells with the same controls produced a significant difference. These DYS^- T_{EM}s consist of clonal CDR3 expansions (**Figure II.8**) that are potentially induced by other inflationary epitopes. Consequently, it

is plausible that analyses of CD4 responses against a collection of inflationary epitopes or in a larger number of subjects might yield a difference. Both statistical trends are not due to generalized, HIV-induced activation because other pathogen/antigen specific $CD4^+$ T cells, including TT, are not necessarily more activated with HIV infection (Smith et al., 2013). This observation implies that inflated $CD4^+$ T cells in these subjects could potentially contribute to the increased T cell activation associated with greater risks of HCMV-related non-AIDS cardiovascular comorbidities that continue to plague HIV^+ subjects despite effective ART. The capacity of DYS^+ $CD4^+$ T cells to secrete granzyme B, IFN-γ and TNF-α might facilitate the development of these comorbidities (Broadley et al., 2017; Sacre et al., 2012; van de Berg et al., 2012). A larger cohort of HIV^+ $HCMV^+$ $DR7^+$ subjects with varying magnitudes of DYS^+ $CD4^+$ T cells is needed to directly evaluate the correlation of their activation with disease outcomes. The stepwise increments in $CD38^+HLA\text{-}DR^+$ levels indicate that HCMV infection without HIV co-infection increases $CD4^+$ T_{EM} activation in general, and HIV co-infection further synergizes such activation. This elevated activation might be tied to an HIV-induced latent HCMV reservoir expansion, presenting potential unintended negative consequences of HCMV vaccine candidates that contain inflation-inducing epitopes for all individuals, especially HIV^+ $DR7^+$ subjects. Although HIV long-term non-progressors were studied in this work, a previous study found that CMV lysate induces high levels of CMV-specific $CD4^+$ T cells in HIV^+ subjects with ART-induced HIV aviremia (Komanduri et al., 2001), suggesting that the findings may generalize to a broader range of HIV-infected patients.

In conclusion, I have shown that HIV^+ $HCMV^+$ co-infection boosts CD4 responses to HCMV gB's DYS and pp65's EPD epitopes, resulting in mostly memory-inflated DYS^+ $CD4^+$ T cells. To our knowledge, this is the first *ex vivo* evidence of both $CD4^+$ T cell memory inflation against the DYSNTHSTRYV epitope in HIV^+ subjects and nearly monoclonal CDR3 repertoire of inflated $CD4^+$ T cells that contain novel conserved motifs. Although the underlying mechanism may be multifactorial, I hypothesize that increased low-level exposure and subsequent clonal expansion targeting the DYS epitope from stochastic HCMV reactivation or expression largely contributes to the observation. The findings suggest that "memory inflation"-inducing epitopes might contribute to the immunopathogenesis of non-AIDS comorbidities and raise safety implications for CMV vaccines that contain inflation-inducing epitopes that should be considered in trials being planned in both HIV and non-HIV infected subjects. This work also suggests that the relative contributions of conventional and inflated CMV-specific T cell responses to protection of the host from infection or malignancy, vaccine responsiveness or co-morbidities of aging such as vascular disease should be considered separately.

Contributions

HIV^+ subjects were recruited by Dr. Spyros Kalams and Dr. Simon Mallal. HIV^- subjects were recruited by Dr. Kalams, Dr. Mallal, Dr. Madan Jagasia, Dr. Brian Engelhardt and me. PBMCs from HIV^+ and HIV^- subjects were processed into lymphocytes and frozen by Ms. Rita Smith, Ms. Cindy Hager, Ms. Louise Barnett, Mrs. Rama Gangula, and Dae Jung. I performed all DNA extractions that were based on standard protocols following manufacturers instructions, and all modified DNA extraction procedures after assay development by Ms. Gangula. HLA-typing was coordinated by Dr. Mallal, Dr. Kalams, Dr. David Haas and me, and done by Dr. Mark Watson and Dr. Abha Chopra. I optimized the tetramer staining protocol using a published technique by-, and advice from-, Dr. Heather Long (Long et al., 2013). I performed all tetramer and monoclonal antibody stains for flow cytometry, data collection and analysis after an initial orientation on flow cytometry principles including set-up, compensation and gating by Ms. Barnett. Ms. Barnett also assisted with all fluorescence-activated cell sorting in this dissertation. High throughput IFN-γ ELISpot was developed by Dr. Watson and Dr. Chopra following a published protocol (Almeida et al., 2009), and optimized by Dr. Mark Pilkinton and me. I conducted all IFN-γ ELISpots. Intracellular cytokine staining was performed by Dr. Silvana Gaudieri. TCR amplification with Adaptive Biotechnologies TCR sequencing kit was optimized by Dr. Pilkinton, Dr. Chopra and Ms. Gangula. Ms. Gangula assisted with the PCR amplification of bulk-sorted samples after I extracted and diluted the genomic DNA, while Dr. Chopra sequenced the amplicons and transmitted the data to Adaptive Biotechnologies for quality control checks and bioinformatic analysis. Mr. Wyatt

McDonnell analyzed the TCRs to generate the circos plots showing TCRβV and TCRβJ pairs. I analyzed the TCR and CDR3 quantitation. The Jurkat cell transfection system was optimized by Dr. Chopra and Dr. Gaudieri, both of who reconstructed the TCRs for cloning into plasmids, and Ms. Gangula who expressed the plasmids in Jurkat cells and conducted the rest of the optimization experiments. Dr. Gaudieri conducted and analyzed the main experiments with DYS-specific TCRs and peptide-pulsed lymphoblastoid cell lines. I optimized the droplet digital PCR (ddPCR) assay following a protocol developed by Dr. Chopra. Dr. Jessica Thomas optimized CMV DNA detection by ddPCR, while I performed the experiments.

Most of the introduction, results, and discussion in this chapter as well as the relevant methods (in **Chapter VI**) have been published in the *Journal of Immunology* as a manuscript titled: “Cytomegalovirus (CMV) Epitope-Specific $CD4^+$ T Cells Are Inflated in HIV^+ CMV^+ Subjects.” The publication can be found on this webpage: http://www.jimmunol.org/content/early/2017/09/29/jimmunol.1700851.

CHAPTER III

DETECTION OF HIV DNA IN HLA-RESTRICTED EPITOPE-SPECIFIC $CD4^+$ T CELLS

Introduction

In the previous chapter, I described $CD4^+$ T cell memory inflation of HLA-DR7 $CD4^+$ T cells, which are specific for DYS epitope of HCMV's gB protein in HIV^+ $HCMV^+$ $DR7^+$ subjects. The presence of these $CD4^+$ T cells in subjects infected with HIV at high magnitudes raises the question whether these cells serve as enriched latent HIV reservoirs. The initial hypothesis was that DYS^+ $CD4^+$ T cells are enriched with HIV DNA. Instead, the result validates the alternate hypothesis that inflated DYS^+ $CD4^+$ T cells are not enriched with HIV DNA compared to DYS^- $CD4^+$ T_{EM} cells. This observation warrants validation with more subjects because it was made from a single subject. If confirmed, it would fit with the proposition that inflated $CD4^+$ T cell responses are more likely to be stimulated by latent HCMV infected stroma cells in lymph nodes and less likely by HIV-coated follicular dendritic cells.

HIV infection occurs primarily in active $CD4^+$ T cells that revert to resting states (Pierson et al., 2000) and produce oligoclonal HIV variants during viral reactivation and rebound after ART interruption (Bailey et al., 2006; Evering et al., 2012; Kearney et al., 2014; Kieffer et al., 2004; Mens et al., 2007; Persaud et al., 2007; Persaud et al., 2004; Ruff et al., 2002). These oligoclonal virions may be due, at least in part, to HIV's integration in genes associated with clonal expansion (Cohn et al., 2015; Maldarelli et al., 2014; Wagner et al., 2014). The resting $CD4^+$ T cells recirculate between peripheral

blood and lymph nodes (Chun et al., 1997) and become latent HIV reservoirs that are neither depleted by ART nor eliminated by host immune responses (Archin et al., 2014). The frequency of latently infected $CD4^+$ T cells is less than 1 cell per 1 x 10^6 resting $CD4^+$ T cells in patients on ART (Chun et al., 1997; Finzi et al., 1997; Wong et al., 1997). Daily lifelong consumption of the ART cocktail is required to prevent viral rebound (Chun et al., 1997; Chun et al., 1998; Chun et al., 1995; Davey et al., 1999; Finzi et al., 1999; Fischer et al., 2003; Harrigan et al., 1999; Ruiz et al., 2000). Though critical genomic deletions or mutations render most of the integrated viruses in the $CD4^+$ T cell reservoir defective, a small proportion remain replication-competent and are responsible for the rebound viremia (Ho et al., 2013; Wong et al., 1997). Lifelong ART remedy is not sustainable for many patients for reasons such as cost, toxicity, accessibility or stigma, and therefore a concerted research effort exists to identify strategies to completely eliminate the latent $CD4^+$ T cell reservoirs. Attaining a cure will require characterization and elimination of this persistent, replication-competent resting $CD4^+$ T cell latent reservoir. However, the specific epitopes recognized by the $CD4^+$ T cells that comprise these reservoirs, and the HIV persistence mechanism within these cells is not completely understood.

Some groups have argued that the persistence mechanism is due to continuous low-level HIV replication (Lorenzo-Redondo et al., 2016). However, the current consensus view is that this is unlikely because of the lack of genetic evolution in isolated plasma viruses that would have been expected given the low-fidelity HIV reverse transcriptase (Bailey et al., 2006; Evering et al., 2012; Kearney et al., 2014; Kieffer et al., 2004; Mens et al., 2007; Persaud et al., 2007; Persaud et al., 2004; Ruff et

al., 2002). From a host standpoint, IL-7-induced homeostatic- and TCR stimulation-induced cellular proliferations have been shown to maintain latently infected $CD4^+$ transitional and central memory T cell reservoirs, respectively (Chomont et al., 2009). Additionally, HIV integration into genes including MKL2 and BACH2 that are associated with cell proliferation might directly contribute to the persistence of the HIV latent reservoir (Maldarelli et al., 2014; Wagner et al., 2014). Another potential persistence mechanism is the possible establishment of HIV reservoirs in T follicular cells within the germinal center of LNs, which are not accessible by $CD8^+$ T cells that could otherwise help eliminate the reservoir (Fukazawa et al., 2015).

Antigen-specific $CD4^+$ T cells harboring potentially replication-competent, latent HIV could therefore be activated and stimulated to trigger productive HIV replication after cessation of ART by various chronic or ubiquitous pathogens. $CD4^+$ memory T cells recognize pathogens such as the herpesviruses CMV and EBV, *Mycobacterium tuberculosis* (MTB) (Geldmacher et al., 2010), *Helicobacter pylori* (Monack et al., 2004), or antigens such as TT or influenza. HIV can potentially infect any CCR5- or CXCR4-expressing activated $CD4^+$ T cell with immunological memory against any pathogen or antigen. This infectivity has been demonstrated *in vivo* using pools of proteins or lysates from HIV (Douek et al., 2002), CMV (Brenchley et al., 2006; Douek et al., 2002; Geldmacher et al., 2010), *Mycobacterium tuberculosis* (MTB) (Geldmacher et al., 2010), influenza (Jones et al., 2012) and TT (Jones et al., 2012). What have yet to be determined are the contributions of various latent $CD4^+$ memory T cell reservoirs that recognize specific epitopes from persistent pathogens, and whether HIV persistence in such cells is tied to clonal proliferation upon TCR stimulation.

The median frequencies of $CD4^+$ memory T cells reactive to CMV lysate/protein pools are greater than both those against HIV (2 - 3% vs. 0.3%; (Brenchley et al., 2006)) or MTB (3.32% vs. undetectable levels; (Geldmacher et al., 2010)) in chronic HIV-infected subjects, and those against tetanus-toxoid proteins (9.1% vs. <0.15%; (Sylwester et al., 2005) vs. (Cellerai et al., 2007)) in HIV-uninfected subjects. These CMV-reactive $CD4^+$ memory T cells possess oligoclonal TCRVβ (Sester et al., 2002), expand with age (Vescovini et al., 2007) and persist during long-term ART (Naeger et al., 2010). As shown in **Chapter II**, inflated HLA-restricted HCMV epitope-specific $CD4^+$ T cells possess nearly monoclonal CDR3s. I hypothesized that these cells contribute significantly as HIV latent reservoirs and they facilitate HIV persistence via a clonal expansion mechanism.

As part of the foundational work towards elimination of HIV latent reservoir, measuring the amount of latent HIV DNA within inflated DYS^+ $CD4^+$ T cells will help identify a specific epitope of $CD4^+$ T cells that might significantly contribute to the latent reservoir, and help elucidate the mechanisms of HIV persistence within them. This knowledge will enable clinicians to specifically target and shrink significant portions of latent HIV reservoir that may rebound upon ART cessation by driving HIV out of latency. It will also identify opportunities to interrupt HIV's persistence mechanism to shorten the half-life of the latent reservoir.

To address these questions, epitope-specific $CD4^+$ T cells against CMV's DYS epitope of gB protein were analyzed. Based on the high magnitudes of responses of these cells, I proposed that they might contribute significantly to the HIV latent reservoir in seropositive subjects. First, the most common HLA-DR alleles among HIV^+ subjects

were determined by undertaking full high-resolution allelic HLA typing on nearly 1000 HIV^+ subjects being actively followed in the Vanderbilt Comprehensive Care Clinic. The highest carriage rates were for DRB1*07:01 (26.36%), DRB1*03:01 (18.96%) and DRB1*15:01 (18.84%). Based on the $CD4^+$ T cell frequency associated with functional HLA class II tetramers needed to test the hypotheses, the analyses were focused only on DR7-restricted DYS epitope of gB. The relatively novel droplet digital polymerase chain reaction (ddPCR) assay was optimized to measure total HIV DNA in $CD4^+$ T cells. ddPCR is a highly sensitive and specific PCR technique compared to real-time quantitative PCR that uses end-point reaction to determine absolute concentrations of target template. The sensitivity of this assay relies on its unique partitioning of the PCR polymerase, primers and probe and DNA target into picoliter-size oil droplets that facilitates effective amplification of the sequence target even in extremely diluted circumstances. In order to maximize the signal-to-noise ratio, the PBMC samples from the subjects were enriched either by positive selection with anti-CD4 beads when analyzing $CD4^+$ T cells as a whole, or negative selection with beads against all cells except $CD4^+$ T cells when analyzing $tetramer^+$ $CD4^+$ T cells. HIV DNA was measured using primers targeting *gag* or *LTR*, while *RNaseP RPP30* primers were used to detect this housekeeping gene to provide a denominator of the number of cells that had been assayed. Due to ddPCR's inability to determine the replication-competence of latent HIV genome, a viral outgrowth assay (VOA) was also optimized, which was used to confirm the replicative ability of HIV genomes in $CD4^+$ T cells from aviremic subjects.

Results

26% of HIV$^+$ Subjects carry HLA-DR7 allele

To identify subjects who possessed the DR7 allele that restrict the class II tetramers of the CMV, EBV, TT and HIV immunodominant epitopes, the high resolution (six-digit) HLA haplotype of 865 HIV$^+$ subjects and 40 HIV$^-$ volunteers were determined. 228 (26.36%) of the HIV-infected subjects (**Figure III.1**) and 3 (7.5%) of the HIV$^-$ volunteers (**Figure III.2**) were DR7$^+$ (i.e. HLA-DRB1*07:01:01G). The patient demographics, information and four-digit class II DRB1 alleles of some of these HIV$^+$ and HIV$^-$ subjects are shown in (**Table II.1**) and (**Table II.3**).

ddPCR TaqMan Assay yields better separation than EvaGreen primers between positive droplets of rare targets and negative droplets of high amounts of background DNA

After identifying the HLA allele of interest, the amount of HIV DNA in DR7-restricted CD4$^+$ T cells needed to be measured using droplet digital PCR. To optimize the ddPCR, quantitative and qualitative abilities between EvaGreen and TaqMan ddPCR kits were compared by measuring HIV DNA in serially diluted, latent HIV-infected ACH-2 cell line. To more accurately simulate the rarity of HIV-infected cells in HIV subjects, serial dilutions of ACH-2 were performed with healthy PBMCs before DNA extraction, instead of already extracted DNA. *RNase P* housekeeping gene confirmed the presence of DNA in each dilution using both EvaGreen and TaqMan assays (**Figure III.3**).

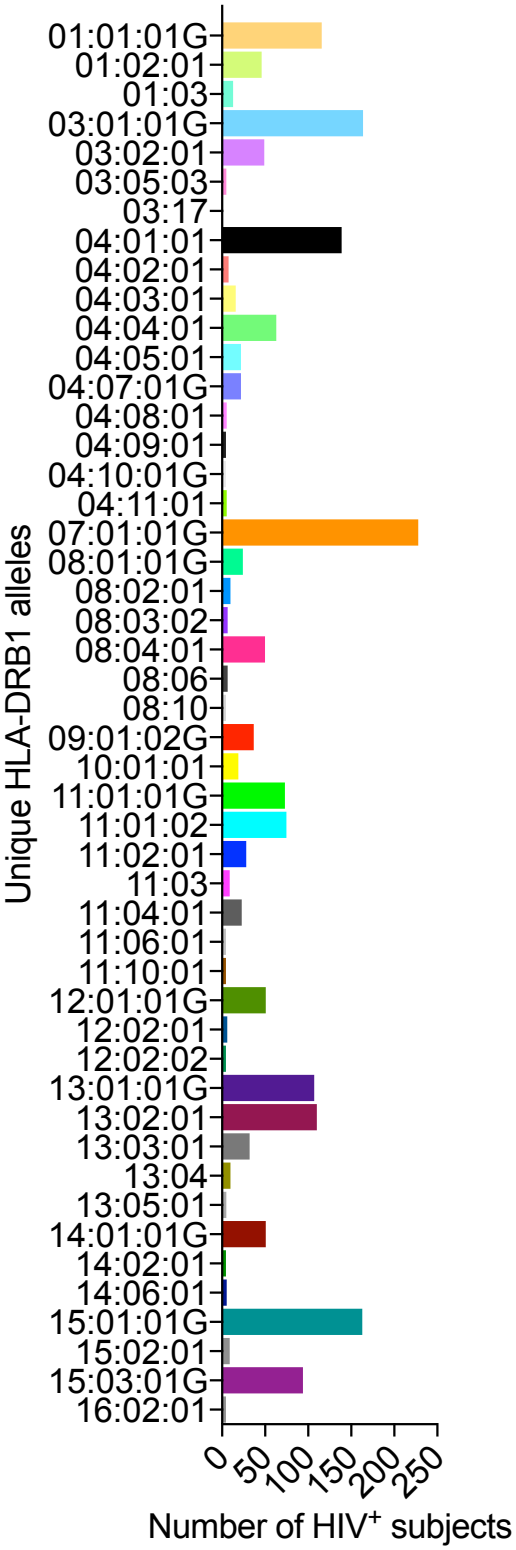

Figure III.1 HLA-DR allele frequency distribution in HIV$^+$ subjects.

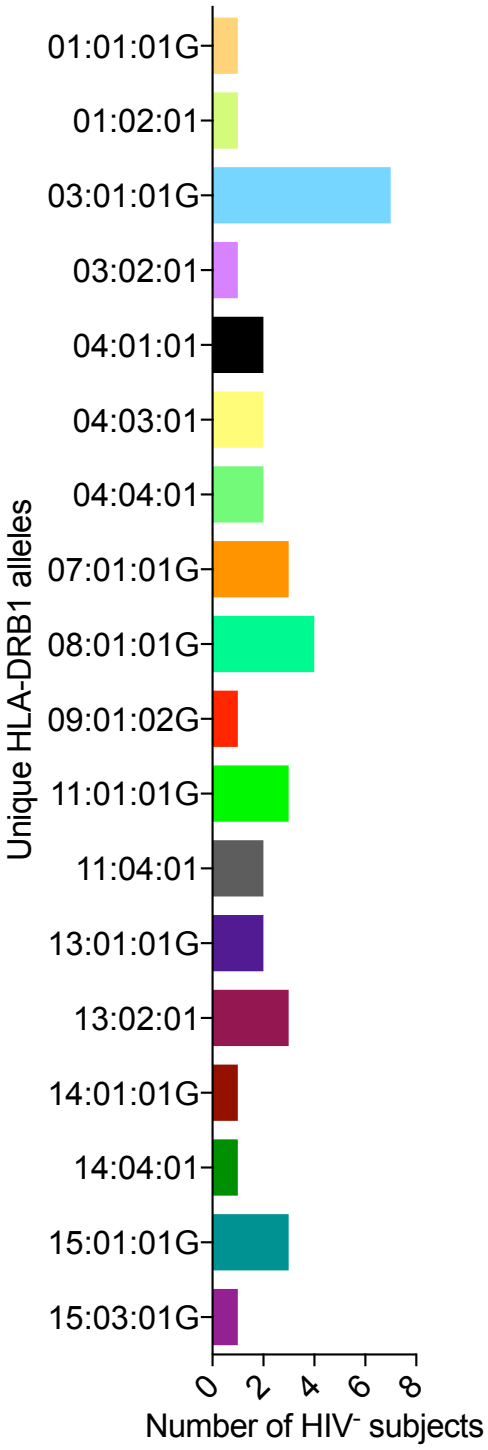

Figure III.2 HLA-DR allele frequency distribution in HIV$^-$ subjects.

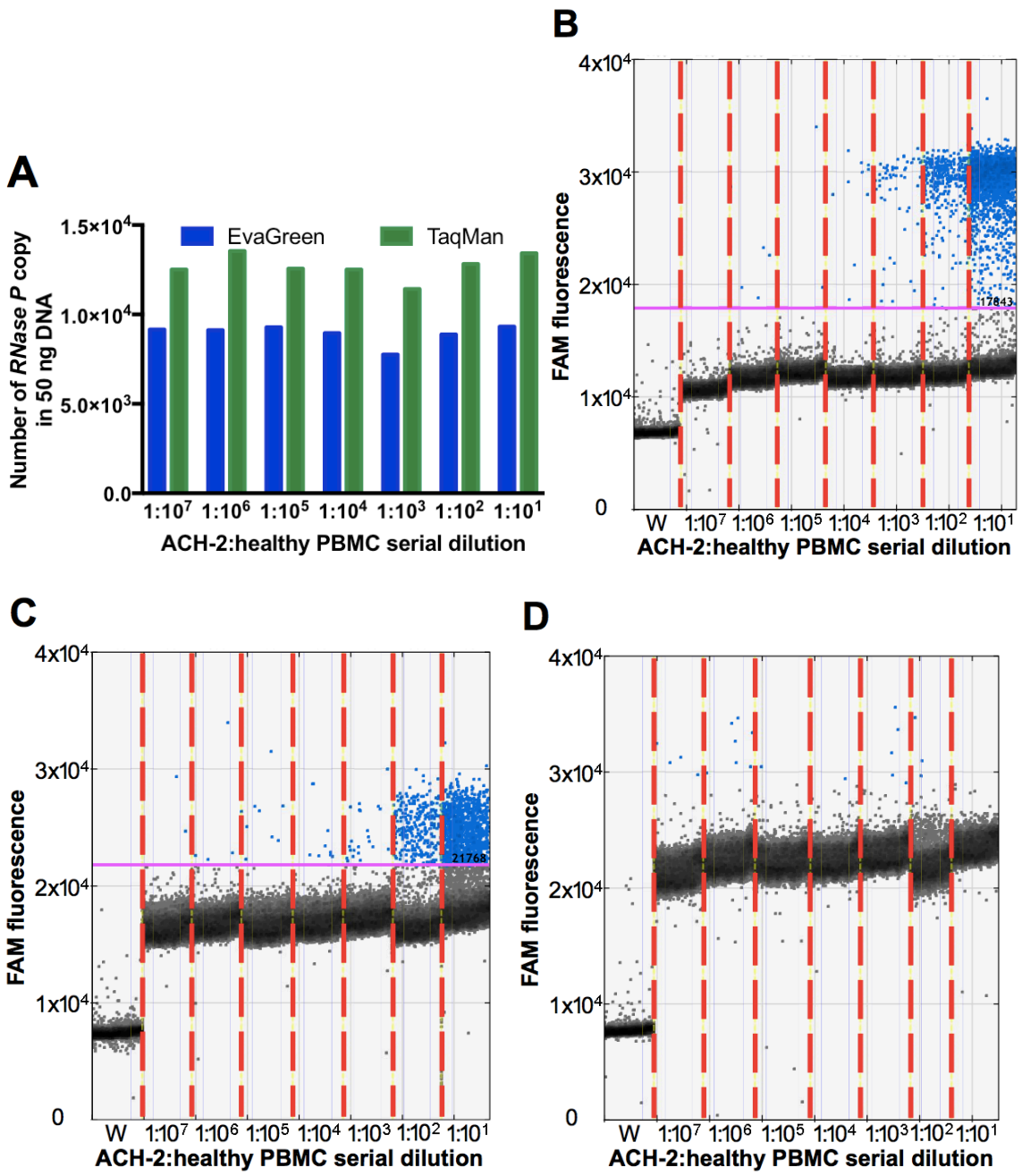

Figure III.3 Housekeeping and HIV genes detection in ACH-2:healthy PBMC serial dilution using ddPCR EvaGreen or TaqMan assay. (**A**) Quantitation of housekeeping *RNase P* in 50 ng of DNA using EvaGreen primers (blue bars) and TaqMan probes (green bars). **B** – **D**: EvaGreen ddPCR detection of HIV *env-V3* in (**B**) 125 ng, (**C**) 250 ng, and (**D**) 500 ng of DNA. Blue or dark gray dots: droplets containing (positive) or lacking (negative) amplified HIV *env-V3* gene segment, respectively. Vertical red dash lines separate individual ddPCR wells. Horizontal purple lines mark threshold separating positive droplets from negative droplets. FAM, 6-carboxyfluorescein; W, Water.

A good separation between the positive and negative droplet amplitudes were observed when 125 ng of the mixture was quantified with HIV *gag* EvaGreen forward and reverse

primers (**Figure III.4A**). However, this separation reduced progressively as the DNA input was increased to 250 ng and 500 ng (**Figure III.4B** and **Figure III.4C**, respectively). The poor separation was due to progressive increments in the amplitudes of the negative droplets, which may be explained by the expected fluorescing of EvaGreen dye when it binds to increasing amounts of double-stranded DNA loaded in the ddPCR reactions.

To ensure that these observations were independent of the *gag* primers, the EvaGreen experiments with *env* primers that target the V_3 loop were repeated, and similar results were obtained (**Figure III.3, B-D**). Of note, when 500 ng was used with the V_3 EvaGreen primers, the negative droplet amplitudes were high enough that they merged with the positive droplets because EvaGreen intercalates with dsDNA, it also intercalates and fluoresces with the template (**Figure III.3**).

To compare these findings to TaqMan ddPCR, the experiments were repeated using a *gag* TaqMan assay that was made by mixing the same *gag* EvaGreen primers with a probe. *RNase P* TaqMan probe was used to confirm the presence of DNA in each dilution (**Figure III.3**). Compared EvaGreen, *gag* TaqMan assay yielded a good separation between the positive and negative droplets using both 250 ng (**Figure III.4B** vs. **Figure III.4D**) and 500 ng (**Figure III.4C** vs. **Figure III.4E**) of DNA. Collectively, these findings suggest that the TaqMan probe assay yields better positive droplet separation compared to EvaGreen when loading large amounts of DNA into ddPCR.

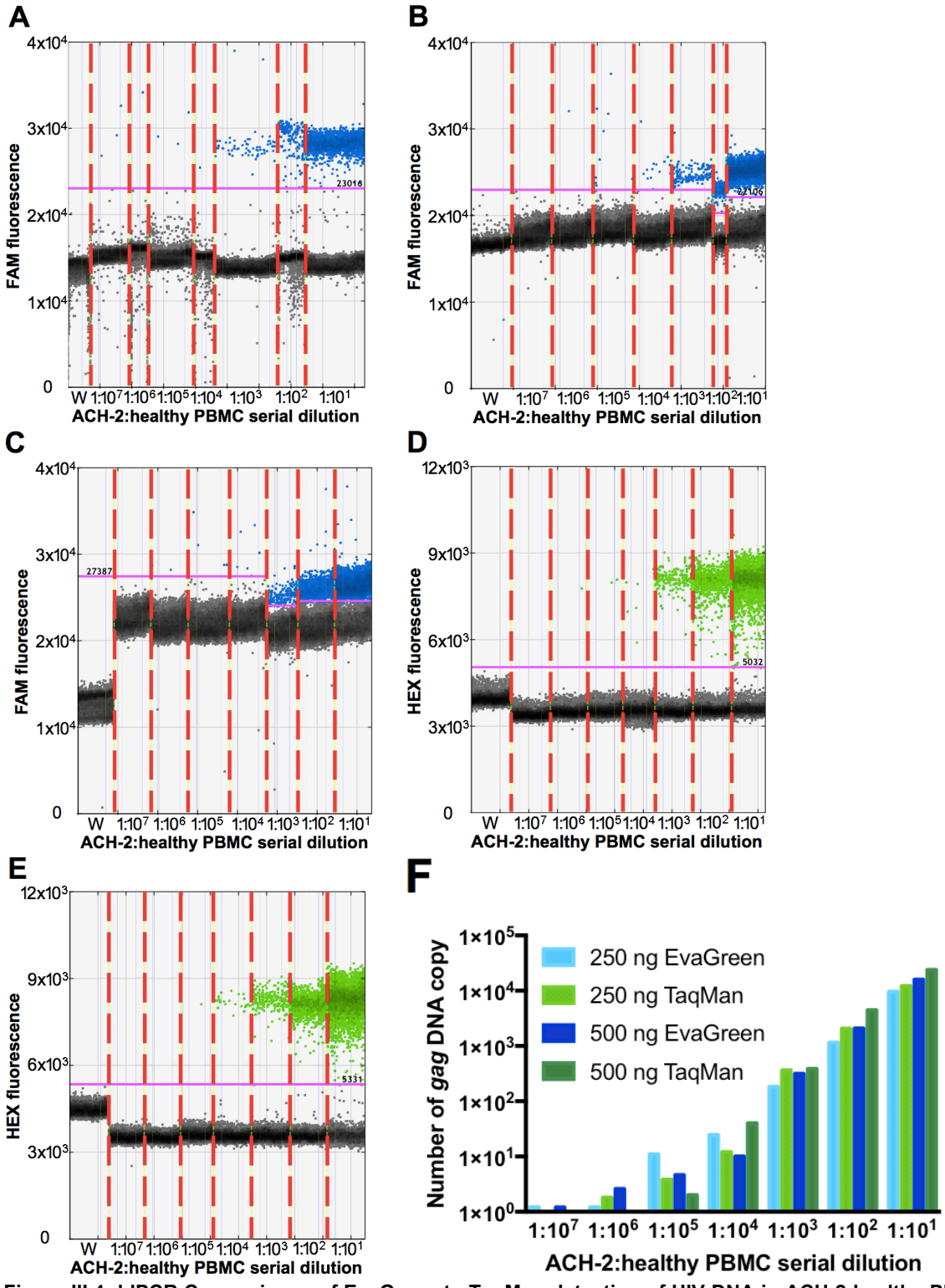

Figure III.4 ddPCR Comparisons of EvaGreen to TaqMan detection of HIV DNA in ACH-2:healthy PBMC serial dilutions. A – **C**: EvaGreen primers detection of HIV *gag* in 125 ng (**A**), 250 ng (**B**), and 500 ng (**C**). (**D**) and (**E**): TaqMan probes detection of HIV *gag* in 250 ng (**D**), and 500 ng (**E**). (**F**): Quantitation of amplified gag products detected in (**B**) – (**E**). Blue or dark gray dots: droplets containing (positive) or lacking (negative) amplified HIV gag gene segment, respectively. Vertical red dash lines separate individual ddPCR wells. Horizontal purple lines mark threshold separating positive droplets from negative droplets. FAM, 6-carboxyfluorescein; HEX, hexachlorofluorescein; W, Water.

As a result the ideal maximum amount of DNA that should be used for EvaGreen-based ddPCR is 125ng in order to avoid overloading the assay; any amount over 125ng should be split into multiple wells so as to achieve good positive-to-negative droplet separation. These findings also indicate that ddPCR can detect a rare target amidst a very large, irrelevant background, making it an optimal platform for detecting HIV latent reservoirs that are small in size.

HIV DNA is present in latently infected $CD4^+$ T cells from HIV^+ subjects

To quantify HIV DNA from 5 HIV^+ subjects (**Table III.1**), the ddPCR technique described above was repeated with *gag* TaqMan assay.

Subject ID	Sex	Race	Infection (years)	$CD4^+$ T cell count/µl blood	HIV load (RNA copies/ml plasma)	ART regimen	Time on ART (months)
HIV^+ subjects							
10031	F	B	15	591	27,800	n/a	n/a
10042	M	W	24	599	<48	TDF, FTC, ATV, RTV	30
10074	M	W	6	210	<50	3TC, ZDV, EFV	18
10092	M	W	1	1147	248	n/a	n/a
20052	M	W	<1	673	24,700	n/a	n/a
HIV^- controls							
30047	M	W	n/a	n/a	n/a	n/a	n/a
30049	F	W	n/a	n/a	n/a	n/a	n/a

Table III.1 Subject characteristics for ddPCR HIV DNA quantitation. HIV, Human Immunodeficiency Virus; ddPCR, droplet digital polymerase chain reaction; ART, antiretroviral therapy; F, female; M, male; B, black; W, white; TDF, tenofovir; FTC, emtricitabine; ATV, atazanavir; RTV, ritonavir; 3TC, lamivudine; ZDV, zidovudine; EFV, efavirenz; n/a, not applicable.

$CD4^+$ T cells from all subjects were first positively selected using beads and a minimum of 92% enriched CD4s within the lymphocyte population was achieved. HIV DNA was successfully detected and quantified from these cells in all 5 subjects with amounts ranging from 12 to 549 HIV DNA copies per million $CD4^+$ T cells (**Figure III.5**). Healthy volunteers and ACH-2 HIV cell-line were used for negative and positive controls, respectively. Since positive selection is rarely 100% efficient and some $CD4^+$ T cells remained within the non-$CD4^+$ T cell populations, an attempt was made to quantify HIV DNA within the latter as well. HIV DNA was detected in 3 out of the 5 non-CD4 samples (**Figure III.5**). However, the small difference compared to $CD4^+$ T cell counterparts suggests that HIV DNA from monocytes might be detected in the non-CD4 fractions. Collectively, these findings confirm that ddPCR can detect rare targets within actual patient cells.

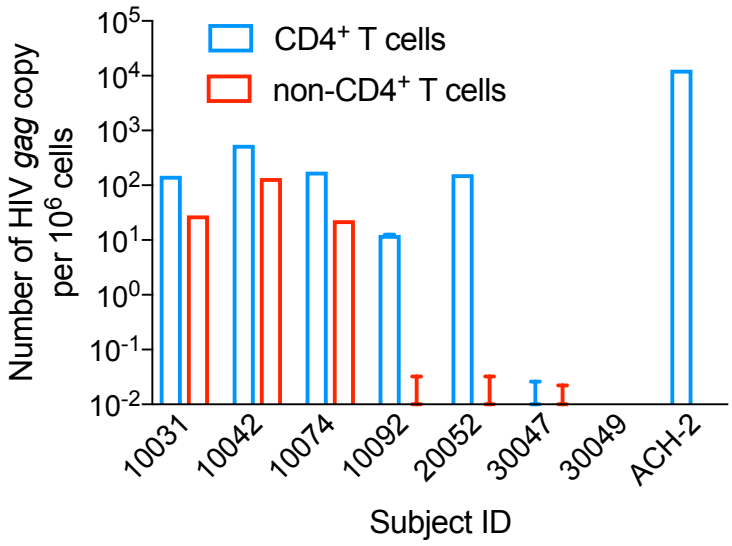

Figure III.5 ddPCR Quantitation of HIV DNA. 1 µg of each of $CD4^+$ and non-$CD4^+$ T cells from HIV^+ (10031, 10042, 10074, 10092, and 20052) and HIV-seronegative (30047 and 30049) subjects were assessed for HIV DNA content using *gag* TaqMan probes. ACH-2: latently-infected HIV cell line positive control. 95% CI are shown for each sample and the values were determined from the ratio of the concentration of HIV *gag* to *RNaseP*.± 1.96 times the standard error ratio of HIV *gag* to *RNaseP* as described in more detail in the materials and methods.

HIV DNA is not enriched in inflated DYS $CD4^+$ T cells

After identifying DR7 as the most common allele in HIV^+ subjects and optimizing the TaqMan-based ddPCR assay for HIV DNA quantitation in $CD4^+$ T cells obtained from HIV^+ subjects, the contribution of $DR7^+$ DYS^+ $CD4^+$ T cells to the HIV latent reservoir was determined. As discussed in **Chapter II**, with the exception of DYS epitope, most DR7-restricted epitopes were recognized by relatively few $CD4^+$ T cells compared to the inflated DYS^+ $CD4^+$ T cells. The inflated magnitude of DYS^+ $CD4^+$ T cells allowed easier quantitation of their HIV DNA content from bulk-cell sorting compared to the low-frequency $CD4^+$ T cells against these other epitopes. Paramagnetic bead-based enrichment of EPD^+ $CD4^+$ T cells from Subject 10027 from 0.021% to 1.071% (**Figure III.6**) did not attain sufficient cells for accurate HIV DNA quantitation. The limited number of cryopreserved samples and unavailability of most subjects for new blood draws, including leukapharesis, restricted latent HIV DNA quantitation to only DR7-restricted DYS^+ $CD4^+$ T cells from Subject 10027. The results in (**Figure III.7**) show that DYS^+ $CD4^+$ T cells in Subject 10027 are not enriched latent reservoirs of HIV DNA despite their clonal expansion compared to their DYS^- counterparts.

Some latent HIV DNA from aviremic HIV^+ subjects with inflated $CD4^+$ T cell responses are replication-competent

Since most of the latent reservoir harbors defective HIV-1 (Ho et al., 2013; Wong et al., 1997), a previously described viral outgrowth assay (VOA; (Laird et al., 2013)) was modified to determine the replication-competence of HIV-1 DNA detected by ddPCR.

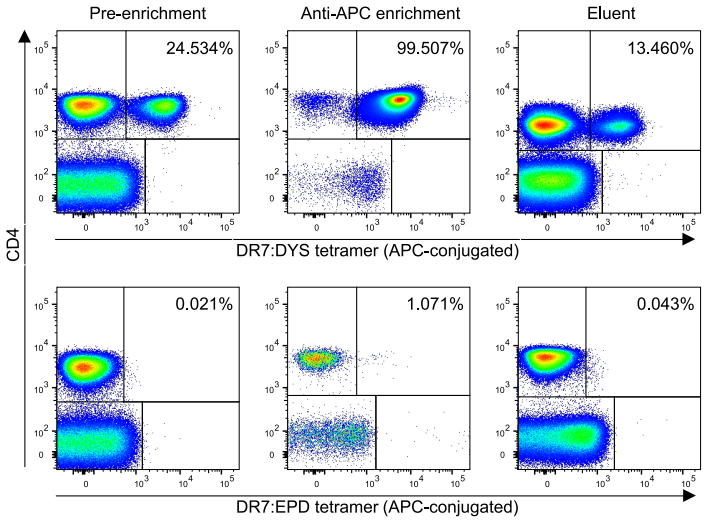

Figure III.6 Anti-APC beads enrichment of APC tetramer-labeled DR7-restricted EPD$^+$ CD4$^+$ T cells. PBMCs from Subject 10027 were stained separately with either DR7:DYS APC tetramer or DR7:EPD APC tetramer. Each sample was divided into the pre-enrichment fraction and the enrichment fraction. The enrichment fractions were ran through an APC beads column where the APC-labeled tetramer-positive cells were retained and the non-APC-labeled remainder were collected and stained as the eluent above. The anti-APC fractions were eventually plunged and stained similarly.

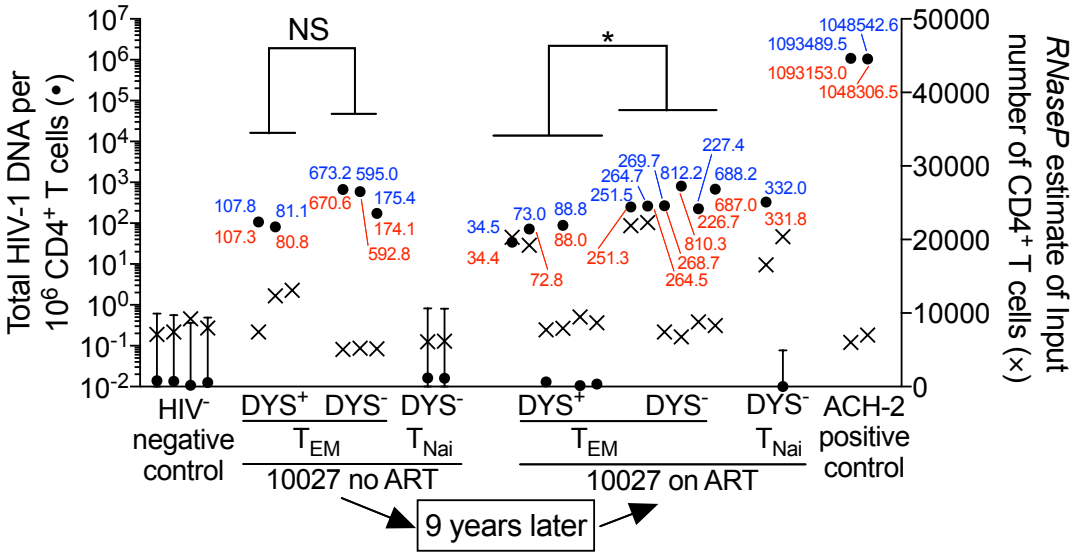

Figure III.7 Inflated DYS$^+$ CD4$^+$ T cells from Subject 10027 are not enriched for latent HIV DNA. ddPCR HIV DNA quantitation comparison between DYS$^+$ and DYS$^-$ CD4$^+$ T_{EM} from Subject 10027's tp1 (no ART) and tp2 (on ART). Left y-axis indicates HIV genome copy number after normalization with *RNaseP* housekeeping gene. Right y-axis indicates the number of cells, which was determined by dividing the *RNaseP* concentration (in g/µl) in the PCR reaction volume by 2 (because there are two copies of *RNaseP* per cell) and multiplying by the total ddPCR reaction volume (20 µl). Finally, this product is divided by the standard number of DNA per cell (6 pg/cell) to determine the number of cells in the reaction. The "no ART" time-point represents 3 technical replicates, while the "on ART" time-point shows two biological replicates containing 3 technical replicates each. Data points at 10^{-1} indicate undetected HIV DNA. Blue and red numbers: upper and lower 95% CI, respectively. 95% CI were determined from the ratio of the concentration of HIV *gag* to *RNaseP*.± 1.96 times the standard error ratio of HIV *gag* to *RNaseP* as described in more details in the materials and methods in **Equation VI.1**.

The assay was optimized to sensitively and specifically detect replication-competent HIV-1 from the ACH-2 HIV cell line as well as patients with both high and undetectable plasma viral loads. After CD8 depletion by positive selection, 1 x 10^6 non-$CD8^+$ PBMCs from Subject 10031 (due to the higher HIV viral load) and 11 x 10^6 non-$CD8^+$ PBMCs from Subject 10042 (due to the undetectable HIV viral load) were used to set-up the viral outgrowth assay. These cells were stimulated *in vitro* using anti-CD3 and anti-CD28 in the presence of CXCR4 and CCR5-expressing MOLT-4 cell line that allowed the expansion of reactivated HIV. At day 5, reactivated, replication-competent HIV was detected from the culture of Subject 10031 due to the higher viral load (**Figure III.8**). On the other hand, reactivated, replication-competent HIV DNA was not detected in Subject 10042's culture until day 9, and this is likely due to the HIV aviremia (**Figure III.8**). Together, these findings demonstrate that HIV^+ subjects with undetectable HIV load can develop viremia upon reactivation of HIV in the absence of robust $CD8^+$ T cells or ART.

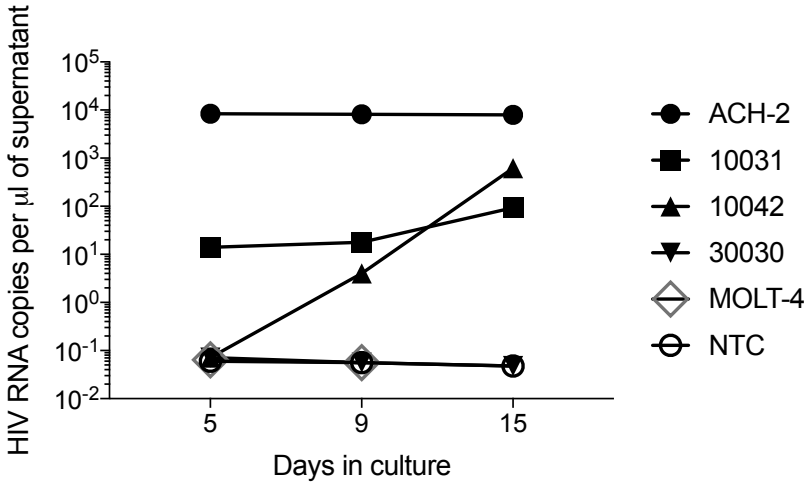

Figure III.8 Viral Outgrowth detection of replication-competent HIV from non-$CD8^+$ PBMCs from an aviremic HIV^+ subject. Non-$CD8^+$ PBMCs were stimulated overnight using 1µg/ml of anti-CD3 and 1µl/ml of anti-CD28 at 37°C for 18 hours to induce the reactivation of latent HIV DNA before the addition of MOLT-4 that expanded any produced virion. RNA is extracted from mature virions in the supernatant for reverse transcription and HIV DNA detected using ddPCR and *LTR* primers. ACH-2 = T cell clone latently-infected with HIV; its levels shown are saturated. Subject 30030 = HIV^- control. MOLT-4 = Feeder cell line with high CXCR4 and CCR5 dual expressions. NTC = No Template Control.

Discussion

In this chapter, I have shown that for one HIV subject, HIV DNA is present but not enriched in $CD4^+$ T cells that are specific for the HLA-DR7-restricted DYS epitope. This was determined by initially optimizing ddPCR as a sensitive assay to detect low frequency targets. It was shown that TaqMan ddPCR yielded better positive-negative droplet separation than EvaGreen when >125 ng of DNA are loaded in ddPCR reaction to detect rare targets such as HIV DNA in ACH-2 cell line. The poor separation with EvaGreen stemmed from its intercalation of both the amplicon and the loaded, background dsDNA. To our knowledge, this observation is the first documentation of the potential poor droplet separation that occurs when more than 125 ng of DNA is added to an EvaGreen ddPCR well. In addition to being able to handle much larger amounts of genome, TaqMan assay allows the interrogation of two different genomic segments. This multiplexing compatibility is important for the accurate quantitation and comparison of HIV latent reservoir because one set of primers can target HIV *LTR* gene while a second set can be designed to be specific for the *RNaseP* housekeeping gene.

Using the same TaqMan ddPCR, the assay to measure HIV DNA in enriched $CD4^+$ and non-$CD4^+$ cell samples was optimized from five HIV seropositive subjects in a specific manner as no HIV DNA was detected in healthy controls. The HIV DNA detected in the non-$CD4^+$ cells are most likely from either $CD4^+$ T cells lost during positive selection, or monocytes, as have been previously demonstrated (Gartner et al., 1986; Ho et al., 1986; McElrath et al., 1991).

The presence of latent HIV DNA in inflated, DR7-restricted DYS^+ T cells from an ART-treated subject indicates a potential to form significant HIV latent reservoirs during ART. This presumption is based on their higher contributions to and/or persistence among the total CD4 memory T cell pool. Such significant expansion would require the intermittent stimulation of the TCR of these inflated cells by their cognate DR7-DYS ligand. The stimulation could be just sufficient to cause cellular proliferation without inducing HIV reactivation to allow the expansion and maintenance of the latent HIV reservoir. It is important to note again that the persistent HIV latent reservoir is comprised of very few replication-competent HIV proviral genomes, which are the source of rebound viremia upon ART cessation. However, one of the caveats of this work is that sufficient numbers of inflated DYS^+ $CD4^+$ T cells were unable to be sorted for the serial dilutions needed in the VOA to determine whether they harbored any replication-competent HIV genome.

Latently and persistently infected $CD4^+$ memory T cells during ART sometimes harbor identical HIV-1 sequences (Bailey et al., 2006; Evering et al., 2012; Kearney et al., 2014; Kieffer et al., 2004; Mens et al., 2007; Persaud et al., 2007; Persaud et al., 2004; Ruff et al., 2002), and this may be linked to recent observations that HIV-1 preferentially integrates within genes or promoters associated with growth-, mitosis- or cancer (Maldarelli et al., 2014; Wagner et al., 2014). Some expanded HIV-1 sequences in effector memory T cells are replication-incompetent, suggesting that, in general, HIV-1 may persist in some cells by cellular proliferation (Josefsson et al., 2013). Although the specific epitopes recognized by those cells remain unknown, it is known that T cells respond to persistent HLA-restricted epitopes by clonal proliferation as observed in

oligoclonal α:β TCR sequences for CMV (Sester et al., 2002). Therefore, it is possible that HIV-1 within persistent epitope-specific $CD4^+$ T cells during ART are maintained by cell proliferation triggered by HLA-restricted epitope stimulation of their TCR. Although the clonality of the HIV genome within the DYS^+ $CD4^+$ T cells could not be determined, the observation of the nearly monoclonal nature of these cells at the TCR sequence level suggests it is possible that HIV genome in these cells will also contain oligoclonal HIV sequences and this warrants further investigation.

It is important to note that oligoclonal HIV sequences are often replication-incompetent (Ho et al., 2013). These defective sequences are characterized by APOBEC3G-induced hypermutations, insertions, deletions or large internal deletions that affect critical genes for viral replication such as rev and tat ORFs (Ho et al., 2013). Therefore, it was critical to determine the replication-competence of the HIV DNA in the DR7-restricted DYS-specific $CD4^+$ T cells. Although it was impossible to determine this using the VOA due to the large number of cells required, I was able to demonstrate that $CD4^+$ T cells from aviremic subjects contained replication-competent viruses. One of the future directions of this work is to develop a method for the detection of single cells that are latently infected with HIV. This will facilitate the efficient evaluation of the replication-competence of HIV within such cells.

The anatomy, trafficking and features of inflated CD4 responses to CMV are highly atypical (especially with the high magnitudes of T_{EMRA} subset). It is therefore not surprising that HIV is not well adapted for these types of cells. Nevertheless, it is important to determine whether the low frequency HIV DNA in these cells are replication-competent. If replication-competent HIV DNA is detected in inflated HLA-

restricted epitope-specific $CD4^+$ T cells, stimulation of the cells with their epitopes using the "shock-and-kill" approach might provide a more focused reactivation of the quiescent $CD4^+$ T cells theoretically to drive HIV out of hiding and allow its epitopes to be expressed and detected by cytotoxic $CD8^+$ T cells.

Contributions

The coordination of HIV^+ DNA samples for HLA-typing was done by Dr. Simon Mallal, Dr. Spyros Kalams, Dr. David Haas, and me. Dr. Mark Watson and Dr. Abha Chopra both conducted the PCR amplification to determine the six-digit HLA alleles. Primers and probes specific for the following genes were made by the following contributors: HIV *env*-V_3 designed by Dr. Chopra; HIV *gag* (Douek et al., 2002) modified by me; and HIV *LTR* designed by Dr. Mark Pilkinton. Dr. Ian James wrote the equations for calculating 95% confidence intervals. Viral outgrowth assay (VOA) was developed by Rama Gangula who later assisted me in conducting the main experiments; I set-up the VOA and harvested the supernatants at the different time-points for Ms. Gangula to test for reactivated HIV DNA using ddPCR.

CHAPTER IV

TRANSCRIPTOMIC ANALYSIS OF HLA-RESTRICTED EPITOPE-SPECIFIC $CD4^+$ T CELLS

Introduction

In the preceding chapters, I described the observation of inflated DR7-restricted DYS^+ $CD4^+$ T cells that appear to be amplified by HIV seropositive status. The mechanism driving the inflation is not known. We hypothesize that there would be distinctive transcriptional signatures in inflated DYS^+ $CD4^+$ T_{EM} with upregulations of mRNA transcripts of genes that mediate T cell homing to and interaction with endothelial cells such *CX_3CR1*; T cell activation such as *CD38* and *CD74* (HLA-DR), and polyfunctionality with cytotoxicity such as *granzyme B*, *IFN-γ*, and *TNF-α* as compared to conventional EPD^+ $CD4^+$ T cells. The alternate hypothesis is that genes of other undetected proteins in **Chapter II** that are involved in T cell-endothelial cell interaction, TCR-mediated T cell activation, and/or T cell polyfunctionality will have upregulated mRNA transcripts in inflated DYS^+ $CD4^+$ T cells compared to conventional EPD^+ $CD4^+$ T cells. Although the single cell RNA sequencing (scRNA-seq) results in this chapter require confirmation in more subjects and with more DYS^+ $CD4^+$ T cells, they seem to suggest that other gene expressions patterns mediating endothelial cell interaction by activated and functional T cells might govern memory inflation of DYS^+ $CD4^+$ T cells.

Inflated $CD8^+$ T cells upregulate a unique set of proteins that have become associated with memory inflation. These proteins are expressed during both acute and chronic HCMV infections and they include T-bet and eomesodermin (EOMES) transcription factors (Hertoghs et al., 2010). T-bet is encoded by the *TBX21* gene (Lazarevic et al., 2013). The primary role of T-bet is to induce the differentiation of $CD4^+$ T helper cells to Th1 lineage (Szabo et al., 2000). However, T-bet also plays an important role in $CD8^+$ T cells where it is expressed upon TCR stimulation or IL-12-induced signaling (Cruz-Guilloty et al., 2009; Takemoto et al., 2006). In these cells, early T-bet transcription directly facilitates the production of IFN-γ, CD122 (which supports homeostatic cell proliferation), and granzyme B. Late T-bet transcription indirectly drives the expression of EOMES and perforin in addition to IFN-γ and granzyme B via the Runx3 pathway (Lazarevic et al., 2013). The combined expression of T-bet and EOMES transcription factors is essential for the maturation and differentiation of $CD8^+$ T cells from naïve to effector memory phenotypes where they become cytotoxic (Intlekofer et al., 2008; Pearce et al., 2003; Sullivan et al., 2003). These transcription factors are believed to act in a concerted manner in order for $CD8^+$ T cells to effectively attain their cytotoxic potential (Intlekofer et al., 2008; Pearce et al., 2003). Other upregulated genes that have been reported among HCMV-specific $CD8^+$ T cells are *CX_3CR1* (fractalkine receptor) (Klenerman and Oxenius, 2016), which is believed to facilitate the interaction of the cells with the vascular endothelium that express fractalkine ligand; and *PRDM1* (Blimp-1 transcription factor), which drives CD8 differentiation to an effector phenotype instead of a memory phenotype (Hertoghs et al., 2010). Blimp-1 also modulates T cell proliferation and differentiation (Martins and

Calame, 2008). These observations are important in explaining the potential mechanisms governing $CD8^+$ T cell memory inflation (Klenerman and Oxenius, 2016; O'Hara et al., 2012). Additional studies have shown that inflated $CD8^+$ T cells express low levels of CD27, CD28, and CCR7; and express high levels of granzyme B, 4-1BB (TNF-α receptor) (Bolinger et al., 2015). Similar patterns of gene expression have been documented in DYS^+ $CD4^+$ T cells with high-magnitudes of response. These cells contained high transcript levels of granzyme B, granzyme A, granzyme H, perforin, beta-2 adrenergic receptor (ADRB2), fibroblast growth factor binding protein 2 (FGFBP2), and G protein-coupled receptor 56 (GPR56) (Pachnio et al., 2016). Despite the additional understanding gained from these studies, no mechanistic master gene modulations that might maintain DYS^+ $CD4^+$ T cells memory inflation have been discovered. Based on the reports of high magnitude T cell responses, we hypothesized that inflated DYS^+ $CD4^+$ T cells contain higher mRNA transcript levels of *granzyme B*, *IFN-γ*, *TNF-α*, *CX_3CR1*, *CD38*, and *CD74* (HLA-DR) compared to the same transcripts in non-inflated $CD4^+$ T cells specific for EPD epitope of pp65 protein.

To test this hypothesis, we used single-cell RNA-sequencing (scRNA-seq) to determine the transcriptional profiles of single $CD4^+$ T cells that are specific for either DYS or EPD epitope for comparison. scRNA-seq is a more reliable and robust approach for determining transcriptomes compared to microarray analysis, which was used in the latest report on DYS^+ $CD4^+$ T cells (Pachnio et al., 2016). Microarray has lower breadth and depth of coverage, sensitivity and specificity, absolute gene quantification, signal-to-noise ratio and is restricted to only previously identified probes for specific segments of the genome (Zhao et al., 2014). Additionally, microarray analyses of gene expression

were computed from bulk cell analyses (Pachnio et al., 2016). This has its own drawback because results from **Chapter II** showed that any given phenotype shared by a group of cells is not necessarily homogeneous among the cells individually; there were some TCR differences as well as protein level differences among bulk DYS^+ $CD4^+$ T cells in each individual. scRNA-seq is not affected by any of these limitations associated with microarray approaches. Instead, scRNA-seq is more sensitive at detecting rare transcripts, variations in the genome, and is able to detect a wider range of differential gene expressions (Zhao et al., 2014). Additionally, the ability to interrogate the transcriptomes of a group of cells on a cell-by-cell basis would provide a wealth of information on all possible differential transcriptional networks that might be causing the nearly monoclonal inflation observed against DYS epitope. This is evident in the application of scRNA-seq in characterizing glioblastoma primary tumor cells where the authors discovered heterogenous gene regulation among single cells (Patel et al., 2014). Some disadvantages of scRNA-seq include the cost of sequencing and data analysis (Zhao et al., 2014).

As scRNA-seq is a complex assay requiring extensive wet lab optimization and computational and statistical support, I worked with a team of senior staff scientists and a graduate student with expertise in bioinformatics to assess the sequencing data arising from these experiments. In comparison to traditional RNA-seq, scRNA-seq data is often rich in “zero-inflated” data—a phenomenon so called as many genes within a single cell may not be detected either due to lack of transcript presence or drop-out (type II error). Consequently, typical normalization and differential expression approaches developed in bulk RNA-seq do not translate well to scRNA-seq and data

must frequently be examined using several different sets of tools in order to establish internal validity at a minimum. Furthermore, transcript distributions in scRNA-seq data are often multimodal. To address these issues, our laboratory established a collaboration with Dr. Nir Yosef, a single-cell transcriptome expert at University of California Berkeley. Dr. Yosef trained our team members in both the design of our single-cell analytical pipeline and in the analysis of single-cell data. For detailed statistical and analytical methods, please see **Chapter VI** (Materials and Methods).

Results

EPD^+ $CD4^+$ T cells were sufficiently enriched for single-cell sorting into two 96-well plates

To address test our hypothesis, I focused on Subject 10027 as the most ideal candidate due to the inflated DYS^+ (26.3%) and conventional EPD^+ (0.04%) magnitudes of $CD4^+$ T cell responses. I used paramagnetic beads to enrich the extremely low frequency of EPD^+ $CD4^+$ T cells in freshly thawed PBMCs from the subject as shown in (**Figure III.6**) of **Chapter III**. DYS^+ $CD4^+$ T cells were similarly enriched as a control. The caveat of enrichment of tetramer-positive T cells is the propensity for mRNA transcripts or expressed proteins to be altered. The exact reason for this effect remains unknown, but it might involve triggering of the TCR by tetramer binding. I observed this change when I stained the $tetramer^+$ cells with the anti-PD-1 antibody. Compared to 22.22% of the extremely few EPD^+ $CD4^+$ T cells that expressed PD-1 in the pre-enrichment tube,

about 96% of the DR7:EPD tetramer-enriched EPD$^+$ CD4$^+$ T cells were PD-1$^+$ (**Figure IV.1**).

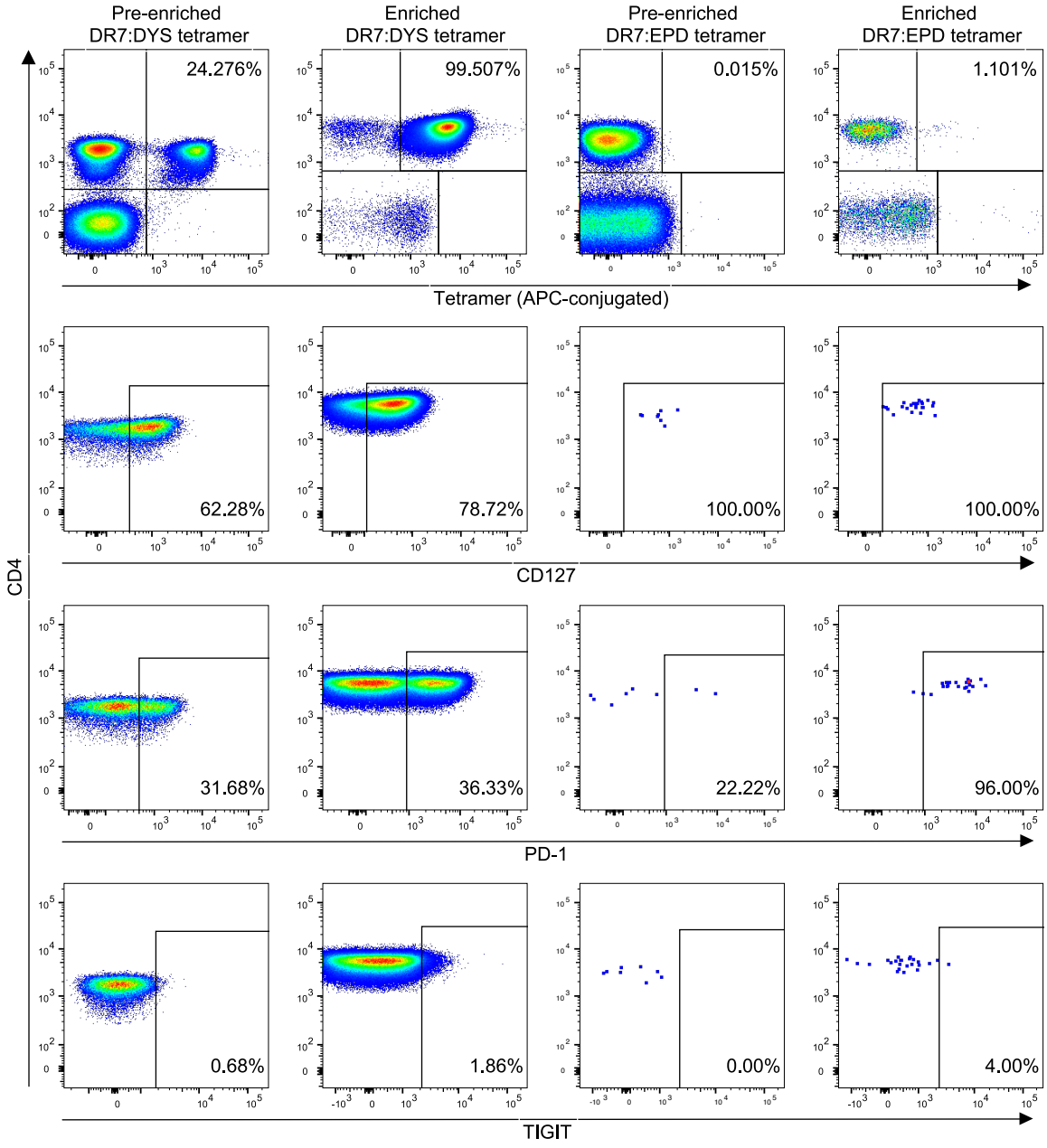

Figure IV.1 PD-1 protein expression on EPD$^+$ CD4$^+$ T cells is increased after bead enrichment. Subject 10027's PBMCs were split in two after live-dead staining for separate APC-conjugated tetramer staining with either DR7:DYS or DR7:EPD. A pre-enrichment portion was removed before bead enrichment of both tubes. All four the pre-enriched and the enriched tubes were subsequently stained with a surface staining panel of antibodies against the following proteins: CD3, CD4, CD8, CD127, PD-1 and TIGIT.

Single-cell sorting of DYS$^+$ and EPD$^+$ CD4$^+$ T cells into 96-well plates

Single cells of the enriched DYS- or EPD-specific CD4$^+$ T cell subsets were sorted into Smart-seq buffer containing Triton, dNTP, RNase Out at 0.125 µl/well, and no OligoDT. We were able to obtain one 96-well plate of DYS$^+$ CD4$^+$ T cells and two 96-well plates of EPD$^+$ CD4$^+$ T cells. After specific PCR amplifications, PCR products were used to generate Smart-seq2 libraries for Illumina Hi-Seq sequencing. Smart-seq2 generates improved yields of cDNA libraries by its combined use of locked nucleic acid (LNA)-containing template-switching oligonucleotides (TSOs) that stabilizes the DNA; betaine (methyl group donor) that "isostabilizes" the DNA during melting transitions; and increased $MgCl_2$ concentration during the reverse transcription reaction (Picelli et al., 2013; Picelli et al., 2014; Rees et al., 1993). In a single step, the cDNA was tagmented and ligated with adapters at both ends, making it ready for sequencing after a final amplification step with index primers that complement the adapters (Picelli et al., 2014).

The consensus transcriptome of a majority of DYS$^+$ CD4$^+$ T single cells is different from that of EPD$^+$ CD4$^+$ T single cells

After trimming the sequences for poor quality bases and sequencing adapters using Trimmomatic, running quality checks, and aligning against the human transcriptome with Bowtie2/RSEM, we normalized the data using SCONE (Wagner et al., 2016). We analyzed our normalized data for cell-cell similarity, differential gene expression and co-variance using Seurat (Satija et al., 2015), SC3 (Kiselev et al., 2017), single-cell differential expression analysis (SCDE) (Kharchenko et al., 2014) and Monocle 2.0 (Qiu et al., 2017) (see **Chapter VI**, Materials and Methods). With a 10,000 read count

threshold, we recovered 18 DYS^+ $CD4^+$ single T cells and 149 EPD^+ $CD4^+$ single T cells. One proposed reason for the huge loss of DYS^+ $CD4^+$ T cells could be the higher avidity of their TCRs for the DR7:DYS tetramer that could cause their apoptosis compared to the TCR and DR7:EPD tetramer interaction (Alexander-Miller et al., 1996). However, this does not explain the fact that apoptotic cells should still contain RNA, albeit RNA likely enriched in apoptotic, cell stress, and cell death transcripts. We performed an unsupervised clustering of the entire transcriptome for both epitope-specific groups of cells to generate a consensus transcriptome profile using the published SC3 platform (Kiselev et al., 2017). With a few exceptions, we observed more homogeneity amongst DYS^+ $CD4^+$ single T cells than between DYS^+ and EPD^+ $CD4^+$ T cells that clustered with other EPD^+ $CD4^+$ T cells (**Figure IV.2**). Despite the relatively few number of interrogated DYS^+ $CD4^+$ single T cells, this observation supports the hypothesis that inflated $CD4^+$ T cells appear to be fundamentally different at the transcriptomic level from the non-inflated $CD4^+$ T cells.

Inflated DYS^+ $CD4^+$ T cells upregulated gene expression of proteins associated with endothelial interaction and TCR stimulation-mediated cell proliferation compared to non-inflated EPD^+ $CD4^+$ T cells

Overall, 25 upregulated and 25 downregulated genes were identified using SC3 in DYS^+ $CD4^+$ T cells compared to EPD^+ $CD4^+$ T cells (**Figure IV.3**). It is important to emphasize that these observations were made from a single subject and there was a significant loss of DYS^+ $CD4^+$ T cells. These experiments would have to be repeated in order to validate these observations.

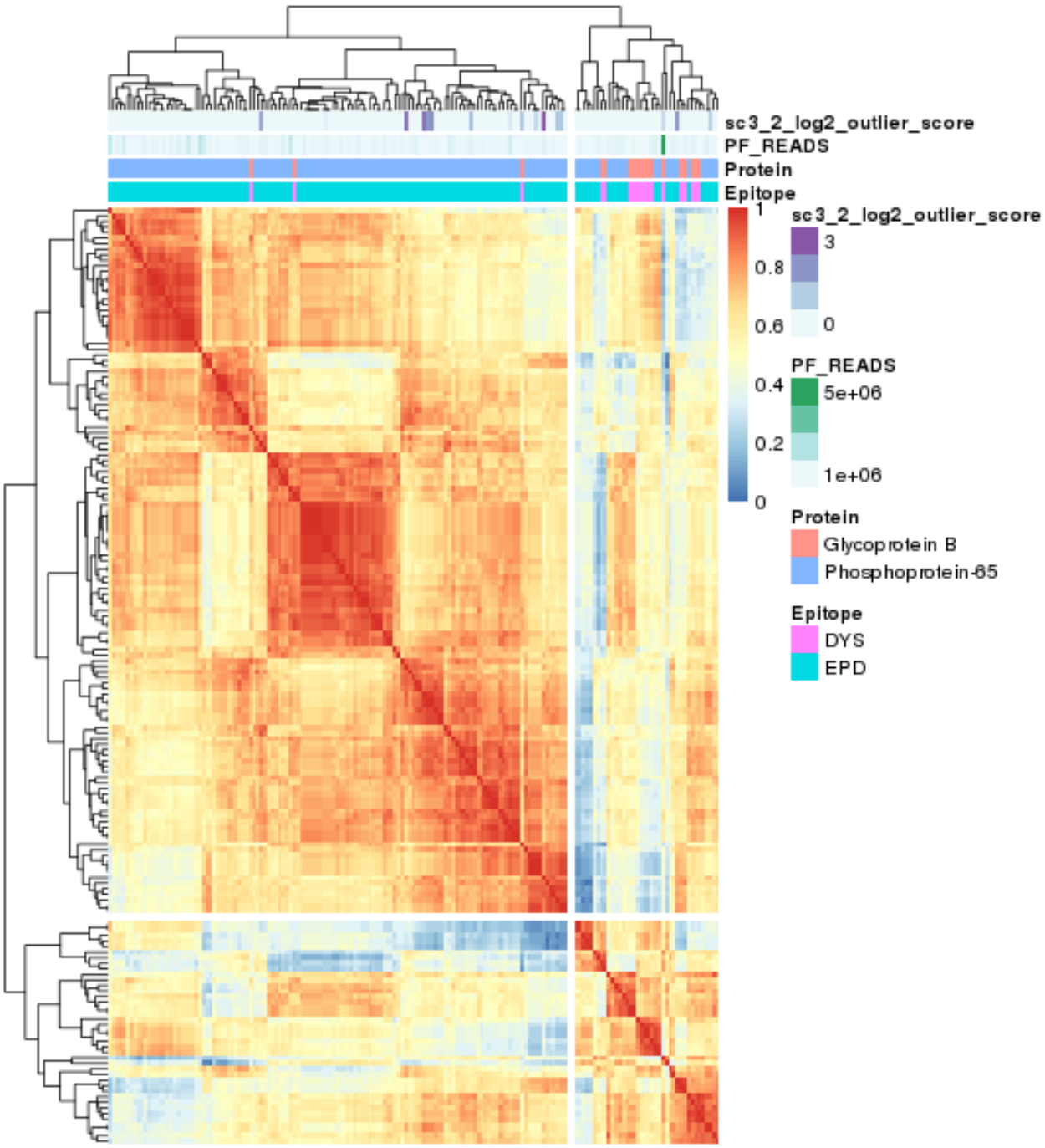

Figure IV.2 DYS^{+} and EPD^{+} CD4^{+} T single cells possess different, consensus transcriptome matrices. After single-cell sorting, cells were amplified and sequenced on Illumina Hi-Seq as described in **Chapter VI** Materials and Methods. Single-cell RNA sequences were trimmed, quality-checked, aligned and analyzed. A consensus clustering plot was generated using unsupervised single-cell consensus clustering (SC3). Signal threshold was set at 10,000 read counts. Each column represents a single T cell. The white vertical and horizontal lines separate single cell clusters of transcriptome. PF_READS: read count.

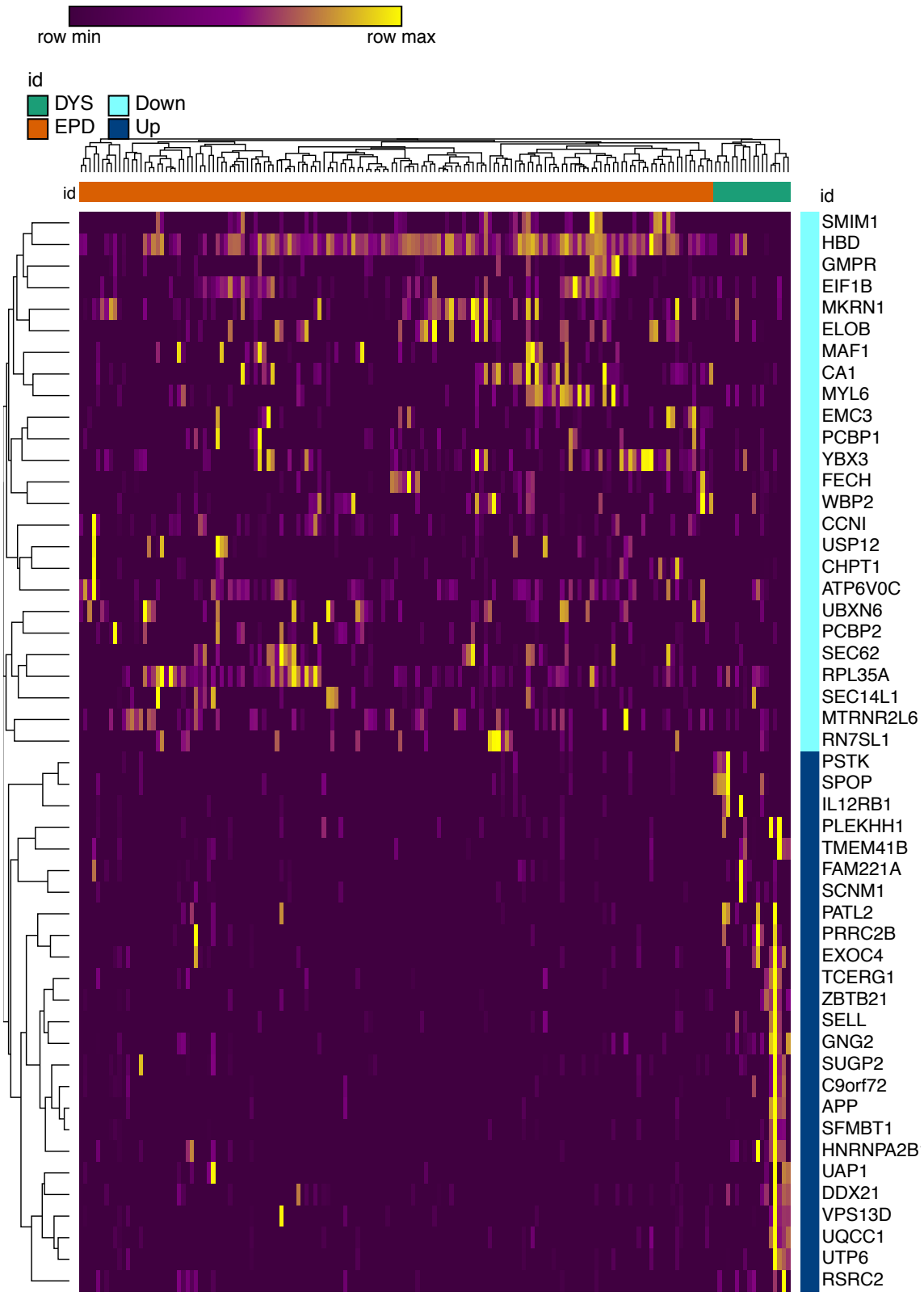

Figure IV.3 Single-cell transcriptomic comparison of differential gene expression between inflated DYS$^+$ CD4$^+$ T cells and non-inflated EPD$^+$ CD4$^+$ T cells. Upper 25 genes in cyan and lower 25 genes in blue indicate downregulated and upregulated genes in DYS$^+$ compared to EPD$^+$ CD4$^+$ T cells, respectively.

Most of these transcripts are translated into proteins with a wide range of functions such as spermatogenesis (*SFMBT1*) and neuronal growth (*APP* and *TMEM41B*), which are not currently known to be directly relevant to understanding the mechanism of memory inflation of DYS^+ $CD4^+$ T cells. Therefore, I highlighted potentially relevant transcripts (due to the need to repeat these experiments and analyze a larger number of DYS^+ $CD4^+$ T cells for proper confirmation of findings) based on known protein functions. A upregulated gene was *SELL*, whose gene product is L-selectin (CD62L), a lymphocyte surface adhesion molecule for high endothelial venules (HEV) in secondary lymphoid tissues like LNs (Gallatin et al., 1983). This finding contrasted the observation in **Chapter II** as well as other reports on memory inflated CMV-specific T cells have described these cells to bear a T_{EM} or T_{EMRA} phenotype that lacks CD62L surface protein expression (Klenerman and Oxenius, 2016; O'Hara et al., 2012).

Phosphoseryl-TRNA kinase (*PSTK*) was also upregulated and its protein product is involved in the initial biosynthesis pathway for the selenoprotein, selenocysteinyl-tRNA(Sec), that plays a role in the efficient induction of TCRs (Carlson et al., 2010). Additionally, the presence of higher levels of vacuolar protein sorting-associated protein 13D (*VPS13D*) that aids trafficking of membrane protein to cell surfaces, and exocyst complex component 4 (*EXOC4*) that targets exocytic vesicles to cell membranes indicate high levels of ongoing secretory activities within inflated DYS^+ $CD4^+$ T cells. Other upregulated mRNA transcripts generate proteins that mediate cell proliferation in general, and they include guanine nucleotide-binding protein G(I)/G(S)/G(O) subunit gamma-2 (*GNG2*), a component of G protein signal transducer (van Corven et al., 1989); nucleolar RNA helicase 2 (*DDX21*), which facilitates RNA polymerase I and II

activities (Calo et al., 2015); and sodium channel modifier 1 (*SCNM1*), which helps with RNA splicing (Buchner et al., 2003). Although it does not directly present a potential mechanism driving memory inflation of DYS^+ $CD4^+$ T cells, another important observation is the upregulation of IL-12 receptor beta 1 subunit (*IL12RB1*) that binds IL12 and facilitates the differentiation of $CD4^+$ naïve T_h0 T cells into $CD4^+$ Type 1 helper T cells (T_h1). This finding is noteworthy because it complements reports of the upregulation of T-bet transcription factor, which primarily drives T_h0 to T_h1 differentiation, in inflated T cells (Bolinger et al., 2015; Hertoghs et al., 2010).

Analysis of relatively downregulated mRNA transcripts in inflated DYS^+ $CD4^+$ T cells compared to non-inflated EPD^+ $CD4^+$ T cells revealed the repressor of RNA polymerase III transcription MAF1 homolog protein (*MAF1* gene) that is involved in the suppression of ribosomal RNA transcription. The remaining differential gene expressions could not further elucidate either why DYS^+ $CD4^+$ T cells were inflated or why EPD^+ $CD4^+$ T cells were non-inflated. This includes the hemoglobin subunit delta (*HBD*) protein that was higher in most EPD^+ $CD4^+$ T cells, but which simply helps distribute oxygen from the lungs to various tissues.

Discussion

In this chapter, I discussed one approach in identifying potential mechanisms driving the inflation of DYS^+ compared to EPD^+ $CD4^+$ T cells. This involves the use of scRNA-seq in analyzing single-sorted tetramer-positive T cells after enrichment. Based on the hypothesis, we expected to observe elevated gene expressions of *granzyme B*, *IFN-γ*,

TNF-α, *CX_3CR1*, *CD38*, and *CD74* (HLA-DR) among the single cells of the inflated DYS^+ $CD4^+$ T cells compared to EPD^+ $CD4^+$ T cells. We did not detect differential expression of these transcripts in DYS^+ v.s. EPD^+ $CD4^+$ T cells because few to none of them were detected even prior to data normalization, and the few transcripts detected were uniformly expressed, and therefore removed during normalization. However, we uncovered other relevant mRNA messages that, after confirmation, might further inform our understanding of drivers of memory inflation. There have been reports of potential disparity between proteomes and transcriptomes, even for cells that are treated under similar conditions (Chen et al., 2002; Fesenko et al., 2017; Ghazalpour et al., 2011; Yeung, 2011). Various reasons have been postulated for this lack of correlation including differences in the half-lives of mRNA transcripts compared to proteins (10–20 h for transcribed mRNA vs. 48–72 h for expressed proteins) (Hargrove and Schmidt, 1989), and post-transcription/pre-translational modifications such as alternative splicing (Fesenko et al., 2017). The lack of correlation between transcriptomic expression and protein expression in our case could be due to the differences in lengths of protocol from PBMC thawing either to fixation for protein staining analysis with antibody and flow cytometry (~6 h) or to cell lysis for transcriptome analysis (~12 h). It could also be due to post-translational modifications. Another reason could also be that the high functional TCR-avidity DYS^+ T cells that were lost during this single cell analysis expressed most of the proteins detected in flow cytometry with bulk cells.

Although the scRNA-seq findings need to be validated in more subjects and with more DYS^+ $CD4^+$ T cells, it is important to discuss the implications of potentially relevant, differentially-expressed genes. Among the relatively upregulated genes in

DYS^+ $CD4^+$ T cells compared to EPD^+ $CD4^+$ T cells, we detected *SELL* transcripts that are precursors of L-selectin protein (i.e. CD62L), which helps lymphocytes adhere to HEVs in LNs (Gallatin et al., 1983). Although bulk phenotypic analysis of DYS^+ T cells in **Chapter II** indicates these cells are T_{EM} or T_{EMRA} that do not express CCR7 and are thus incapable of homing to LNs, it is interesting to observe that some DYS^+ $CD4^+$ T single cells expressed SELL transcripts. A plausible explanation for this finding is that these cells were recently re-stimulated by DYS epitope as have been reported for CCR7 and CD62L re-expression on CMV-specific $CD8^+$ T cells after re-stimulation (van Leeuwen et al., 2005). Therefore, the detection of *SELL* transcripts in inflated DYS^+ but not EPD^+ $CD4^+$ T cells suggests that the former may have been recently re-stimulated by their cognate DR7:DYS ligand, leading to the expression of CD62L gene precursor. The re-expression of CD62L by re-stimulated, inflated DYS^+ $CD4^+$ T cells might further maintain their inflation because of their ability to re-enter LNs, via diapedetic movement across HEV, where they could be re-stimulated by HCMV latently infected LN stromal cells. Based on reports of HCMV DNA in endothelial cells from various other organs such as lungs, liver, kidney and gastrointestinal tract obtained from HIV^+ subjects (Keh and Gerber, 1988), it is also possible that the HEV are latently infected with HCMV and, thus, are directly re-stimulating DYS^+ $CD4^+$ T cells.

The selenoprotein product of the PSTK-catalyzed selenoamino acid metabolism reaction has been reported to play a role in the proliferation of T cells upon stimulation of their TCR: IL-2 receptor induction by IL-2 on T cells lacking selenoproteins is less efficient than on T cells with selenoproteins (Carlson et al., 2010). Again, this observation suggests that DYS^+ $CD4^+$ T cell inflation might be driven by the re-

stimulation and subsequent IL-2-mediated proliferation of these cells by DYS epitope that are presented by HCMV-infected reservoirs such as VECs that can endogenously process and present gB epitopes (Hegde et al., 2005; Pachnio et al., 2015). On the other hand, the EPD epitope is derived from pp65 protein for which there has been no documentation of endogenous processing and presentation by VECs (Walker et al., 2009), and *PSTK* levels in EPD^+ $CD4^+$ T cells were low. I had previously hypothesized that this polyfunctionality and targeting of VECs played a significant role in the immunopathogenesis of HCMV-related cardiovascular comorbidities in HIV^+ subjects. The findings that DYS^+ $CD4^+$ T cells expressed higher transcript levels of surrogate markers of TCR stimulation and cell proliferation such as SELL and PSTK, and of cytokine or protein secretion such as VPS13D membrane protein trafficker and EXOC4 exocytic vesicle driver to cell membranes suggest that the hypothesis might be true. Although we did not detect high transcript levels of CD38 and HLA-DR, two activation markers of T cells that are associated with increased likelihood of the development of non-AIDS comorbidities in HIV^+ subjects (Kaplan et al., 2011), it is possible that these markers were upregulated in the high avidity DYS^+ $CD4^+$ T cells that were lost. Future directions for this work include: (i) repeating the scRNA-seq and RNA-seq for both single-cell and bulk cells, respectively, using identical protocols on both DYS^+ and EPD^+ $CD4^+$ T cells at the same time to avoid a batch effect while sorting significantly larger number of DYS^+ $CD4^+$ T cells in case the preferential cell loss of this population occurs again, and (ii) determining the expression levels of protein products of upregulated and downregulated mRNA transcripts of DYS^+ $CD4^+$ T cells in relation to EPD^+ $CD4^+$ T cells using available antibodies with flow cytometry.

Despite the importance of these findings, there are several limitations that need to be considered. First, the number of interrogated DYS^+ $CD4^+$ T single cells was much fewer than the number of analyzed EPD^+ $CD4^+$ T cells, which could elevate type I error in differential expression. Another limitation is that these observations were made using cells from a single subject. Although the magnitudes of DYS^+ vs. EPD^+ $CD4^+$ T cells were remarkably different (26.34% v.s. 0.04%) to highlight any critical gene modulation involved in inflation, it is still necessary to confirm the findings in multiple other subjects to achieve appropriate statistical power and confidence. Additionally, as the DYS^+ and EPD^+ $CD4^+$ T cells were sorted on different days, there may be batch effects; however, these batch effects were accounted for during data analysis as described in **Chapter VI**. Finally, the transcriptomic profile of EPD^+ $CD4^+$ T cells might have been slightly modified by triggering of the TCR by the tetramer. Therefore, the observations should be interpreted with a level of caution.

Overall, single cell RNA-seq analysis enables a broader and in-depth characterization of gene expression patterns of inflated DYS^+ $CD4^+$ T cells. The contrasting observations to transcriptome profile of the non-inflated EPD^+ $CD4^+$ T cells from the same subject might help determine potential host-intrinsic and cell-based mechanisms that are maintaining the inflation.

Contributions

I stained the cells with the tetramers after enrichment of tetramer-positive cells, and sorted them as single cells with the help of Ms. Louise Barnett. The single-cell sorting,

lysis, cDNA generation, tagmentation and indexing for sequencing, all using Smart-Seq2, were developed and optimized by Dr. Abha Chopra, Dr. Mark Pilkinton, and Ms. Rama Gangula. As for the DYS^+ and EPD^+ sorted single cells, Ms. Gangula extracted . During the drafting of a manuscript in preparation, I developed language describing the computational pipeline, computational and statistical analyses, analytical and experimental challenges, and preliminary results of single-cell RNA sequencing in consultation with Wyatt J. McDonnell, who has contributed heavily to the development of these tools and analyses in the wet and dry laboratories. We have included this language to enable reproducibility of our analyses and for the benefit of the reader in understanding the complexity and requisite analytical considerations of scRNA-seq as an emerging technology. I also consulted with Dr. Matthew Scholz who helped with sequence data normalization, and Dr. Ramesh Ram who helped generate the consensus and differential gene expression transcriptomic plots.

CHAPTER V

SUMMARY AND FUTURE DIRECTIONS

Summary

The correlation of HCMV seroprevalence with increasing age suggests that most individuals will get infected by HCMV over the course of their lives (Staras et al., 2006). CMV establishes life-long asymptomatic latent infection in various cells and tissues of immune-competent hosts, and vascular endothelial cells (VECs) have been proposed as a CMV reservoir (Klenerman and Oxenius, 2016). CMV-specific T cell responses play an important role in the suppression of productive latent HCMV reactivation in humans, and the magnitudes of these responses are the largest reported for any pathogen (Sylwester et al., 2005). These cells are known to be critical in HIV^+ subjects or transplant recipients as these individuals are more prone to developing CMV disease the greater their degree of immune-deficiency or immunosuppression. Interestingly, all HLA-restricted CMV epitope-specific T cells do not contribute evenly to achieve a robust response. While most epitope-specific T cells respond with the conventional low magnitude response during latency, other cells specific for certain epitopes undergo "memory inflation," which is characterized by chronically elevated magnitudes of response to HLA-restricted epitopes. $CD8^+$ T cells have been well documented to undergo inflation. However, CD4 memory inflation has not been adequately studied, including in immune-deficient hosts such as HIV^+ subjects.

Identifying and characterizing inflated CMV-specific $CD4^+$ T cells in HIV^+ individuals expands the knowledge base regarding one of the critical cellular populations in HIV^+ subjects. The dedication of a significant proportion of the CD4 repertoire in HIV^+ subjects to a single epitope of a pathogen may influence the quality and quantity of the CD4 response available to help contain other pathogens either as part of natural immunity or a vaccine response. HIV^+ subjects with elevated magnitudes of activated T cells are associated with increased risks of developing CMV-related non-AIDS cardiovascular comorbidities in spite of effective ART. Therefore, it is important to determine the contributions of CMV-specific T cells, especially memory inflated responses, to the overall T cell activation in these subjects. The findings could also raise safety implications for CMV vaccines that contain inflation-inducing epitopes that should be considered in trials being planned in both HIV^+ and HIV^- subjects. Additionally, the clinical applications of CMV vectors in combatting other pathogens or even malignancies are believed to harness the abundance and cytotoxic potential of memory-inflated $CD8^+$ T cells (Hansen et al., 2013b; Hansen et al., 2016). As a result, the identification of memory-inflated $CD4^+$ T cells could reveal another means by which CMV vectors might induce effective and prolonged immune response. The overall observations and potential mechanisms are discussed below.

Memory inflation only occurs in response to CMV

The exact reason why memory inflation only occurs in response to CMV is not known. One possibility is that, as the most ubiquitous virus that infects more species of animals including humans (Klarenbeek et al., 2012; Waller et al., 2008), mouse (Bolinger et al.,

2015; Dekhtiarenko et al., 2016; Karrer et al., 2003; Munks et al., 2006; Sierro et al., 2005), monkey (Cicin-Sain et al., 2011), guinea pig (Choi and Hsiung, 1978), and chimpanzee (Swinkels et al., 1984) than any other pathogen, CMV has likely evolved over the years to co-adapt to and exploit these hosts while also providing some degree of protective immunity against other infections such as influenza, probably via inflated T cell responses (Furman et al., 2015). Furthermore, although there is no direct evidence for this, it has been shown that CMV seropositivity is associated with diminished EBV-specific $CD8^+$ T cell responses in the same otherwise healthy individuals compared to $HCMV^-$ subjects (Khan et al., 2004). The exact mechanism behind this has not been determined. However, it is possible that these subjects have reduced EBV infection and burden due to memory inflated CMV-specific responses that might help the host to curb EBV infection. Therefore, one potential explanation for why memory inflation only occurs in response to CMV is that it protects the host from other pathogen infections.

Only some CMV proteins and some epitopes within those proteins can induce memory inflation

Not all proteins and epitopes induce memory inflation because the few that do already occupy substantial proportions of $CD4^+$ and $CD8^+$ T cell immune repertoire. There is no report of cross-reactivity between inflated T cells and epitopes of other pathogens. As a result, the smaller, remaining proportion of the $CD4^+$ and $CD8^+$ T cell repertoire would be needed to combat all other pathogens an individual encounters over their lifetime. A more detailed assessment of CMV epitopes in (**Table I.2**) and (**Table I.3**) that display features of inflated T cell responses is shown in (**Table V.1**).

The evidence described for inflated DYS^+ $CD4^+$ T cells in this dissertation as shown in the table presents a holistic set of criteria for determining whether epitopes are truly inflated. In other words, we believe that an epitope would have to fulfill all five criteria under the “inflationary” column in the table to be considered inflated. However, as the table shows, there are so many gaps in the knowledge on whether most of these epitopes that induce T cell responses with some features of inflation are truly inflationary. This applies to NLVPMVATV, the most studied of all these epitopes that typically elicits conventional response (Gamadia et al., 2003; Wills et al., 1996), but also happens to induce a high magnitude and clonal response in three subjects (Khan et al., 2002b). Therefore, at this point, it remains an open question on whether a conventional epitope such as NLVPMVATV can transition into an inflationary epitope.

We do not know what drives the inflated response to an epitope in one individual and conventional response to the same epitope in another individual. One possible pathway is that all epitopes initially elicit conventional, polyclonal T cell responses during acute CMV infection as a first signal, after which T cells with specific receptors that avidly recognize the inflationary epitope become inflated as a result of an unknown second signal. Another pathway is that inflationary epitopes induce the inflation and clonal expansions of their specific T cells early during acute CMV infection and those cells remain elevated for the lifetime of the individual. However, it is important to emphasize that the exact pathway is not known. An ideal method to thoroughly evaluate how inflated $CD4^+$ T cells are formed is to longitudinally analyze the magnitudes, phenotypes, TCR sequences, and transcriptomic profile of known inflated T cells in mice, starting with acute MCMV infection and following the responses into latency.

HLA restriction	Epitope	Conventional properties					Inflationary properties					Reference
		Mag-L	Phe-c	TCR-p	Lon	Tra	Mag-H	Phe-i	TCR-o/m	Lon	Tra	
A2	NLVPMVATV	NT	NT	NT	NT	NT	+	+	+	NT	NT	(Khan et al., 2002b)
		+	+	NT	NT	NT	NT	NT	NT	NT	NT	(Gamadia et al., 2003)
B7	(T)PRVTGGGAM	NT	NT	NT	NT	NT	+	+	+	NT	NT	(Khan et al., 2002b)
A2	VLEETSVML	NT	NT	NT	NT	NT	+	+	+	NT	NT	(Khan et al., 2002a)
DR7	DYSNTHSTRYV	NT	NT	NT	NT	NT	+	+	+	+	+	This dissertation
		NT	NT	NT	NT	NT	+	+	NT	NT	+	(Pachnio et al., 2016)
		NT	NT	NT	NT	NT	+	+	+	NT	NT	(Crompton et al., 2008)
		NT	NT	NT	NT	NT	+	NT	NT	NT	NT	(Elkington et al., 2004)
DQ6	LLQTGIHVRVSQPSLILVSQ	NT	NT	NT	NT	NT	+	+	NT	NT	+	(Pachnio et al., 2016)
		NT	NT	NT	NT	NT	+	+	+	NT	NT	(Weekes et al., 2004)
DR3 DR11	AGILARNLVPMVATV	NT	NT	NT	NT	NT	+	+	NT	NT	NT	(Pachnio et al., 2016)
DR13	QPFMRPHERNGFTVL	NT	NT	NT	NT	NT	+	+	+	+	NT	(Weekes et al., 2004)
DR1 DR3	KYQEFFWDANDIYRI	NT	NT	NT	NT	NT	+	NT	+	NT	NT	(Bitmansour et al., 2002)

Table V.1 Detailed classification of HLA class I and II HCMV epitopes. Mag-L: low high magnitude CMV-specific T cell response after contraction of acute phase expansion; and Mag-H: high magnitude T cell response during chronic CMV infection, respectively; Phe-c and Phe-i, phenotypes of conventional (predominantly $CD45RO^+$ $CCR7^+$ [T_{CM}] and $CD45RO^+$ $CCR7^-$ [T_{EM}] during acute CMV infection) and inflationary (predominantly $CD45RO^+$ $CCR7^-$ [T_{EM}] and $CD45RA^+$ $CCR7^-$[T_{EMRA}] during chronic CMV infection) T cells, respectively; TCR-p and TCR-o/m: polyclonal and oligoclonal/monoclonal TCR repertoire, respectively; Lon, longitudinal detection of T cell response; and Tra: transcriptomic profile. “NT”: observation was not tested in the cited literature; “+”: evidence supporting the observation is documented in the cited literature.

Applying this same approach in humans would require the use of HCMV-acutely infected solid organ-, or hematopoietic stem cell-, transplant recipients with the HLA alleles of the epitope that induce inflation.

Other various mechanisms have been proposed regarding differential abilities of CMV proteins and/or epitopes to induce either inflated or non-inflated memory T cell responses. One proposed mechanism is that different proteins are processed differently into epitopes in proposed HCMV non-hematopoietic cell latent reservoirs. Memory inflation-inducing epitopes are processed by proteasomes that are constitutively active in acute and chronic/latent infection, while conventional epitopes are dependent on IFN-γ-induced immunoproteasomes that are active mostly during acute inflammatory infection (Hutchinson et al., 2011; Torti et al., 2011). In the case of inflated DYS^+ vs. non-inflated EPD^+ CD4 responses, it is possible that gB protein of DYS is processed into its epitopes by endosomes within VECs (Hegde et al., 2005; Pachnio et al., 2015) that are latently infected with HCMV, while pp65 protein of EPD depends on endosomes in professional APCs for processing. Although most class II epitopes that are recognized by $CD4^+$ T cells are presented via an exogenous pathway that involves uptake of exogenous antigens, some class II epitopes of CMV proteins such as glycoprotein B (which contains the inflation-inducing epitope, DYS) have been postulated to be presented endogenously (Hegde et al., 2005; Pachnio et al., 2015) like inflated $CD8^+$ T cell class I epitopes (Dekhtiarenko et al., 2016; Hutchinson et al., 2011). With VECs being potential HCMV reservoirs and able to express MHC II upon IFN-γ induction (Kambayashi and Laufer, 2014), this might provide some explanation regarding why both $CD4^+$ and $CD8^+$ T cells can experience memory inflation. This

model is shown in (**Figure V.1**; left panel). One drawback of this model is that it does not explain how pp65 epitopes in (**Table I.2**) induce high magnitude $CD4^+$ T cell response; the mechanism for those observations remains an open question.

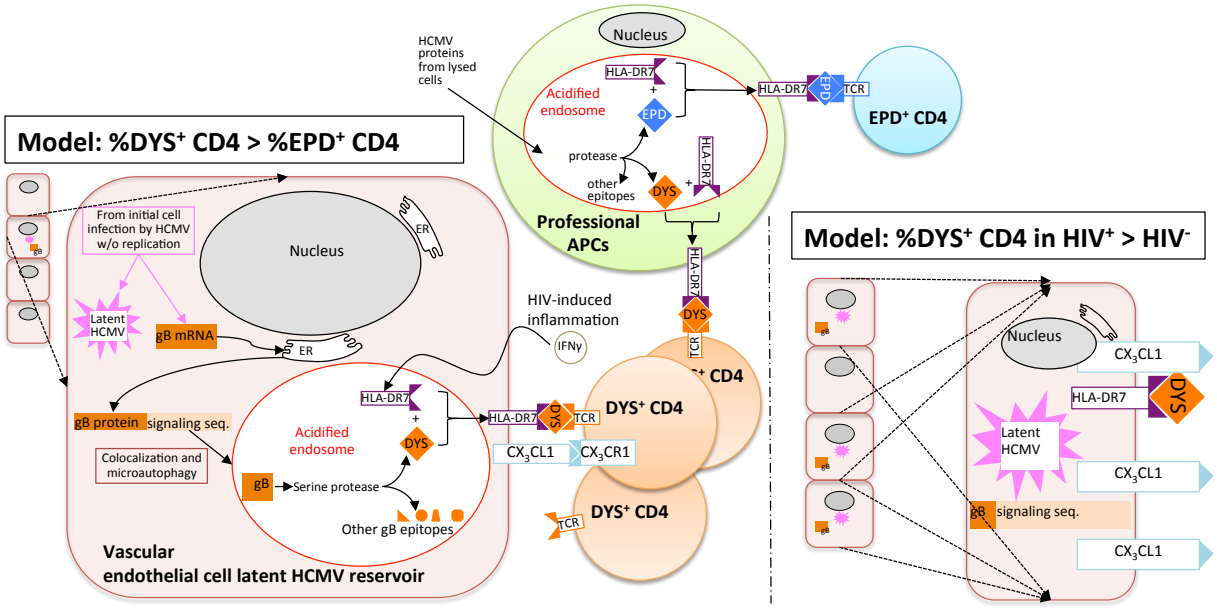

Figure V.1 One of many potential mechanisms driving DYS^+ $CD4^+$ T cell memory inflation in HIV^+ subjects. Left panel: HCMV-infected vascular endothelial cells (VECs) contain glycoprotein B (gB) transcripts that are introduced during cell infection. Each of these transcripts contains a signal sequence that directs the gB polyprotein to acidified endosomes where they are processed into DYS and loaded unto HLA-DR7 upon IFN-γ induction for presentation to DYS^+ $CD4^+$ T cells. The VECs express CX_3CL1 (fractalkine) that is bound by their CX_3CR1 receptors, which are expressed on DYS^+ $CD4^+$ T cells. On the other hand, VECs might be unable to process and present pp65 epitopes, including EPD. Instead, these cells might be re-stimulated by professional APCs, which also re-stimulate DYS^+ $CD4^+$ T cells. Therefore, the combined re-stimulation of DYS^+ $CD4^+$ T cells by VECs and professional APCs could be driving their inflation. **Right panel:** HCMV latent reservoirs might be expanded in HCMV and HIV co-infected subjects. As a result, there could be increased expression of CX_3CL1 by the VECs in HIV^+ subjects that attracts larger magnitudes of DYS^+ $CD4^+$ T cells for DYS re-stimulation compared to CX_3CL1 expression in HIV^- subjects.

Another potential mechanism is that genes of inflation-inducing epitopes might be more accessible to promoters or transcribed at a high rate during latency or nonproductive reactivation to support inflation. A final possibility is that epitopes with higher functional avidity TCRs might be more likely to induce inflation compared to epitopes with lower functional avidity TCRs.

Memory inflation is more likely to occur in HLA-DR7$^+$ HCMV$^+$ subjects with HIV co-infection (i.e. HIV$^+$ HCMV$^+$ subjects) but can also occur in HLA-DR7$^+$ HIV$^-$ HCMV$^+$ subjects

One reason why memory inflation occurred in DR7$^+$ HCMV$^+$ HIV$^+$ subjects more than in DR7$^+$ HCMV$^+$ HIV$^-$ subjects could be that the HIV$^+$ subjects probably need a larger proportion of CMV-specific T cells to contain their increased productive and nonproductive HCMV reactivations. These higher frequency HCMV reactivation events could be due to expansion in HCMV latent reservoir that occurred following the depletion of CMV-specific T cells during acute HIV infection. Therefore, HIV$^+$ subjects are more likely to experience higher prevalence of memory inflation compared to HIV$^-$ subjects. Furthermore, T_{EMRA} T cells that make-up inflated T cell responses along with T_{EM} T cells are rare in HIV$^-$ subjects as shown in **Chapter II**, and their decreased permissiveness for HIV replication (Casazza et al., 2009; Oswald-Richter et al., 2007) might indirectly enhance their memory inflation. In either case, it is important to note that many analyses are confounded by the problem of proportions (i.e. absolute count is needed for definitive conclusions).

The magnitude of memory inflation is higher in HCMV$^+$ subjects that are HIV$^+$ than subjects that are HIV$^-$

The more immunodeficient state of HIV$^+$ compared to HIV$^-$ subjects could mean that they are likely experiencing more sub-clinical HCMV reactivation events (Gianella et al., 2013), which, in turn, could be the source of the antigenic re-stimulation of CMV epitope-specific CD4$^+$ T cells in the HIV$^+$ subjects. The re-stimulation of CMV epitope-

specific T cells has been proposed as a potential mechanism driving memory inflation (Torti et al., 2011). Additionally, most memory inflated T cells are comprised of T_{EMRA} subsets, which are refractory to HIV entry (Casazza et al., 2009) or productive HIV infection (Oswald-Richter et al., 2007). Therefore, the infection and destruction of permissive cells by HIV in HIV^+ subjects might indirectly allow the expansion of non-permissive inflated T_{EMRA} cells. This could further enhance the inflation of CMV epitope-specific $CD4^+$ T cell magnitude in HIV^+ compared to HIV^- subjects. Another possible mechanism responsible for the higher magnitude of inflation in HIV^+ compared to HIV^- subjects is that HIV^+ subjects might have a larger HCMV latent reservoir and thus be more likely to re-stimulate T cells and cause their inflation. These larger reservoirs could express more CX_3CL1 as a chemoattractant for inflated CMV-specific T cells for re-stimulation. This model is depicted in (**Figure V.1**; right panel).

Memory-inflated cells are polyfunctional, non-exhausted T_{EM} or T_{EMRA} with preformed granzyme B granules, and noticeably absent from T_{CM}

If the hypothesis that inflated CMV specific T cells function to curb CMV reactivation is true, then it is logical that most inflated T cells are polyfunctional and cytotoxic with differentiated phenotypes of T_{EM} ($CD45RO^+$) and T_{EMRA} ($CD45RA^+$). This polyfunctionality also explains why these cells are not exhausted; a finding that has been previously documented for polyfunctional CMV-specific T cells (Chanouzas et al., 2015; Chanouzas et al., 2017; Khan et al., 2002b). It is important to note that even conventional CMV-specific T cells are mostly T_{EM} or T_{EMRA}, with mainly CD8s possessing cytotoxic capabilities (Appay et al., 2002a; Appay et al., 2002b; Khan et al.,

2002b; Komatsu et al., 2006; Wills et al., 1999). The T_{EM} and T_{EMRA} phenotypes are proposed to be due to the re-stimulation of these cells by cognate MHC-epitope ligands in the periphery by latently infected VECs unlike T_{CM} that are proposed to be stimulated primarily by LN stromal cells. Differences in the phenotypes of inflated DYS^+ $CD4^+$ T_{EM}, conventional $CD4^+$ T_{EM} and conventional $CD4^+$ T_{CM} are shown in (**Table V.2**).

It is not quite clear how these cells develop polyfunctionality and cytotoxicity. Cytotoxicity might be a feature of all memory-inflated $CD4^+$ T cell responses based on the observation of DYS^+ $CD4^+$ T_{EM} cytotoxicity in **Chapter II** and reports of cytotoxicity of other inflationary CMV class II epitopes (Pachnio et al., 2016). Furthermore, the DYS^- $CD4^+$ T_{EM} counterparts in **Chapter II**, which were speculated to be specific for inflationary CMV class II epitopes other than DYS due to their oligoclonality (**Figure II.8**, right column), also contain preformed granzyme B granules (**Figure II.11D**).

Memory-inflated DYS^+ $CD4^+$ T cells are near monoclonal with novel conserved residues in CDR3

The near monoclonality of the CDR3 repertoire of inflated DYS^+ $CD4^+$ T cells is likely important for the efficient recognition of the DR7-DYS ligand in order to maintain the inflation. This reason is further supported by the presence of conserved amino acid residues within the diversity (D)-segment of the CDR3. Similar observations of clonal CDR3 repertoire with conserved amino acids have been made both for DYS by other groups (Crompton et al., 2008) and for other CMV epitope- or protein-specific CD4 responses such as pp65 (Bitmansour et al., 2002; Weekes et al., 2004). The near monoclonality was present in both T_{EM} and T_{EMRA} due to the dynamic, reversible

Proteins	Inflated DYS^+ $CD4^+$ T cells	Conventional $CD4^+$ effector memory (T_{EM})	Conventional $CD4^+$ central memory (T_{CM})
CCR7	-/+	-	+
CD62L	low/high	high/low	high
CD45 isoform	$CD45RO^+$/$CD45RA^+$	$CD45RO^+$ $CD45RA^-$	$CD45RO^+$ $CD45RA^-$
CD27	-	-	++
CD28	-	-	++
CD127	+	-	++
IFN-γ	+++	++	+
IL-2	+/-	-	+++
TNF-α	++	+	-
Granzyme B	+++	-	-
Perforin	+++	-	-
CX_3CR1	high	medium	low

Table V.2 Comparison of phenotypes of inflated $CD4^+$ T cells to conventional effector and central memory $CD4^+$ T cells. Additional information for inflated DYS^+ $CD4^+$ T cells as well as conventional T_{EM} and T_{CM} cells were obtained from (Foussat et al., 2000; O'Hara et al., 2012; Pachnio et al., 2016; Pepper and Jenkins, 2011; Sallusto et al., 1999).

expression of CD45RO (T_{EM}) and CD45RA (T_{EMRA}) isoforms, and it also confirmed previous reports that these two subsets share the same dominant TCR clone (Wills et al., 1999). It is important to note that we cannot exclude the possibility that DYS^+ $CD4^+$ T cells were initially polyclonal during acute HCMV infection; TCR sequencing of bulk DYS^+ $CD4^+$ T cells in newly HCMV-seroconverted HLA-$DR7^+$ solid-organ or hematopoietic stem-cell transplant recipients could help rule this out.

CMV likely plays a significant role in the clonal expansion of DYS^+ $CD4^+$ T cells because comparison of $CD8^+$ T cell repertoire between $HCMV^+$ and $HCMV^-$ healthy individuals revealed the presence of more clonally expanded CD8s with HCMV seropositivity (Khan et al., 2002b). Another potential explanation could be that the monoclonality of these inflated $CD4^+$ T cells have been driven by HIV integration into cell proliferation and/or cancer genes that ultimately result in clonal expansion (Maldarelli et al., 2014; Wagner et al., 2014). However, that is less likely as we did not observe an enrichment of HIV DNA within these cells as shown in (**Figure III.7**), which would have been a consequence of such integration.

Memory-inflated DYS^+ $CD4^+$ T cells express CX_3CR1

Inflated DYS^+ $CD4^+$ T cells express CX_3CR1 fractalkine receptor most likely because it facilitates the trafficking and interaction of these cells with VECs that express CX_3CL1 fractalkine ligand. VECs serve as HCMV latent reservoirs and therefore might express fractalkine to induce CMV-specific T cell recruitment for restimulation as depicted in the model in (**Figure V.1**). This interaction may play a significant role in the immunopathogenesis of CMV-related cardiovascular morbidities because disrupting this interaction can prevent CMV-specific T cell-mediated vascular endothelial destruction (Bolovan-Fritts and Spector, 2008). Additional evidence for the possible role of this interaction in cardiovascular disease is the presence of high levels of fractalkine on VECs of atherosclerotic coronary artery tissues obtained posthumously from individuals diagnosed with atherosclerosis with over 25% narrowing of their lumina observed at autopsy (Wong et al., 2002). A final important role for CX_3CR1 expression by inflated

cells could be that CX_3CR1 engagement with fractalkine mediates the induction of anti-apoptotic Bcl-xL (Boehme et al., 2000) that might help maintain inflation. The high levels of CX_3CR1 on these inflated CMV-specific T cells could be as a result of the increased expression of fractalkine on CMV-infected VECs as observed in rat CMV (RCMV) and rat heart transplant models, where RCMV-infected allografts upregulated fractalkine expression (Streblow et al., 2003).

There is no evidence of apoptosis suppression or elevated active proliferation among memory-inflated DYS^+ $CD4^+$ T cells

It is not quite clear why apoptosis would not be suppressed in inflated DYS^+ $CD4^+$ T cells. Neither is it clear why these cells are not undergoing increased proliferation. Both observations suggest that there are other inflation-inducing mechanisms at play. Nevertheless, any inflation inducing mechanism would ultimately lead to the proliferation of these cells and the upregulation of the associated Ki67 protein. Another group documented the absence of increased proliferation among inflated cells, although in MCMV models of memory inflation (Bolinger et al., 2015; Sierro et al., 2005). One of the drawbacks of the analysis of increased proliferation using Ki67 expression is that I only sampled one time-point from the subjects. The disadvantage here is that the cells might have undergone proliferation already during stochastic HCMV reactivation events, for example, that occurred before the analyzed time point. Therefore, longitudinal analysis of Ki67 expression by inflated DYS^+ T cells from multiple subjects is warranted.

Memory-inflated DYS$^+$ CD4$^+$ T cells express CD38 or HLA-DR but rarely both

Although DYS$^+$ CD4$^+$ T cells did not mostly co-express CD38 and HLA-DR, the increased magnitudes of CD38 and HLA-DR individual expression could ultimately result in increased co-expression of both activation proteins, which elevates the risk of CMV-related non-AIDS cardiovascular comorbidities in HIV$^+$ HCMV$^+$ subjects (Kaplan et al., 2011). The cause of the upregulation of CD38 and HLA-DR activation proteins could be due to downstream signaling effects that occur after the TCR of these cells are stimulated by their cognate HLA-DR7-DYS ligand. Evidence for this assumption includes reports that CD38 intracellular signaling activity depends on the induction of the CD3-TCR complex (Morra et al., 1998) and that HLA-DR expression depends on CD3 and CD4 internalization after antigenic stimulation (Diepolder et al., 2001).

HIV DNA is not enriched in inflated DYS CD4$^+$ T cells

The primary hypothesis in **Chapter III** was that DYS$^+$ CD4$^+$ T cells were enriched HIV latent reservoirs because of their high magnitudes of response and clonality. However, the results confirmed the alternate hypothesis, which was that these cells were not enriched with HIV DNA, although the finding was obtained from one subject and needs confirmation. Enrichment of these cells with HIV could have reduced their magnitude of inflation due to destruction of infected cells upon HIV egress or by the host's immune system. One of the basic reasons why HIV is not enriched in inflated DYS$^+$ CD4$^+$ T cells is that inflated CD4$^+$ T cells are fundamentally different from conventional CD4$^+$ T cells that are the primary targets of HIV infection. Although noting that these inflated cells are not enriched for HIV DNA is important, it would have been more significant to determine

whether the detected HIV DNA content was replication-competent or defective. This is because replication-competent HIV poses the main threat of rebound viremia that occurs when ART is interrupted in HIV^+ subjects.

The mechanistic explanation for the lack of HIV enrichment in inflated $CD4^+$ T cells is not known. One potential mechanism is that some of these cells are T_{EMRA}, which are less supportive of productive HIV replication (Casazza et al., 2009; Meyer-Olson et al., 2010; Oswald-Richter et al., 2007). Another possible hypothesis is that inflated $CD4^+$ T cells are primed and stimulated by LN stromal cells in the paracortical T cell enriched region and not by follicular DCs (fDCs) in germinal centers of B cell follicles. This means that these inflated cells could be less likely to get infected by HIV that are transferred onto the surfaces of the LN fDCs by Langerhan cells from the submucosa and skin where infection first occurred. fDCs typically present HIV to $CD4^+$ T cells in the germinal centers, which are inaccessible by cytotoxic $CD8^+$ T cells.

Inflated DYS^+ $CD4^+$ single T cells might possess differential transcriptomic signatures and upregulated surrogate markers of TCR stimulation compared to non-inflated EPD^+ $CD4^+$ single T cells

Although the scRNA-seq findings warrant confirmation in more subjects and with more cells, it is possible that there is different transcript clustering between inflated DYS^+ and non-inflated EPD^+ $CD4^+$ T cells. It is unlikely that these cells were pre-programmed with each transcriptomic profile before developing memory against DYS epitope. Observations discussed in **Chapter II** show that being $HCMV^+$ HIV^+ and $HLA\text{-}DR7^+$ are all necessary, but not sufficient alone for DYS^+ $CD4^+$ T cell memory inflation to occur.

For instance, two subjects with DYS^+ $CD4^+$ T cell magnitudes of 0.42% and 0.014% did not undergo memory inflation based on our arbitrary cut-off of ≥1%. Several other variables could have led to this non-inflation: (i) both subjects might have been infected with HCMV for a shorter period of time. However, it is highly challenging to estimate when the infection occurred especially if it happened when the subjects were immunocompetent; (ii) though unlikely due to the lack of HIV DNA enrichment in inflated DYS^+ $CD4^+$ T cells, it is possible that HIV within the inflated DYS^+ $CD4^+$ T cells integrated into cell proliferation and/or cancer gene hotspots that mediate cell expansion, while HIV DNA in the non-inflated DYS^+ $CD4^+$ T cells might have integrated in other regions that do not drive proliferation; and (iii) although less likely as well, it is possible that DYS^+ $CD4^+$ T cell inflation in HIV^+ subjects is driven by cross-reactive HIV epitopes and these two non-inflated subjects were infected with HIV strains that have mutations in their HIV gene segments that produce the cross-reactive HIV epitopes.

Based on the findings in this dissertation and in published literature, a potential multi-omic definition for effectively identifying inflated CMV-specific $CD4^+$ T cells in future is any group of cells with:

1. Upregulated mRNA transcripts for the following genes: *TBX21* (T-bet), *EOMES*, *PRDM1* (Blimp-1), *ADRB2* (beta-2 adrenergic receptor), *FGFBP2* (fibroblast growth factor binding protein 2) and *GPR56* (G protein-coupled receptor 56), and after validation of the scRNA-seq findings, *SELL* (CD62L protein), *PSTK* (phosphoseryl-TRNA kinase), *VPS13D* (vacuolar protein sorting-associated protein 13D), *EXOC4* (exocyst complex component 4 protein), and *IL12RB1* (IL-12 receptor beta 1 subunit);

2. Downregulated *MAF1* gene transcript (repressor of RNA polymerase III transcription MAF1 homolog protein) after validation of the scRNA-seq findings;
3. Upregulated expression of the following proteins: CX_3CR1, granzymes A, B and H, perforin, IFN-γ and TNF-α; and
4. Downregulated expression of the following proteins: CD28, CD27, CD127 (IL-7R), TIGIT, and for most of the cells, and CCR7.

My dissertation documents the observation of circulating memory-inflated $CD4^+$ T cells that are specific for HCMV's glycoprotein B DYS epitope within HIV^+ subjects with undetectable CMV plasma viremia. The nearly monoclonal CDR3 repertoire of these inflated cells and their high expression of CX_3CR1 suggest that potential mechanism(s) of their inflation likely involves clonal expansion upon re-stimulation by latent HCMV reservoirs. Importantly, these highly abundant and extremely long-lived cells serve as latent HIV DNA reservoirs. Some of these findings are summarized in (**Figure V.2**), and overall, they inform the field on the inflationary impact on CMV-specific $CD4^+$ T cell responses by HIV co-infection, the possible immunopathogenic role for inflated CD4 responses in cardiovascular morbidities, the contributions of these cells to latent HIV reservoir, the potential mechanisms that cause chronic memory inflation of T cells, and the safety concerns that might be considered in CMV vaccine design for HIV^+ and HIV^- subjects.

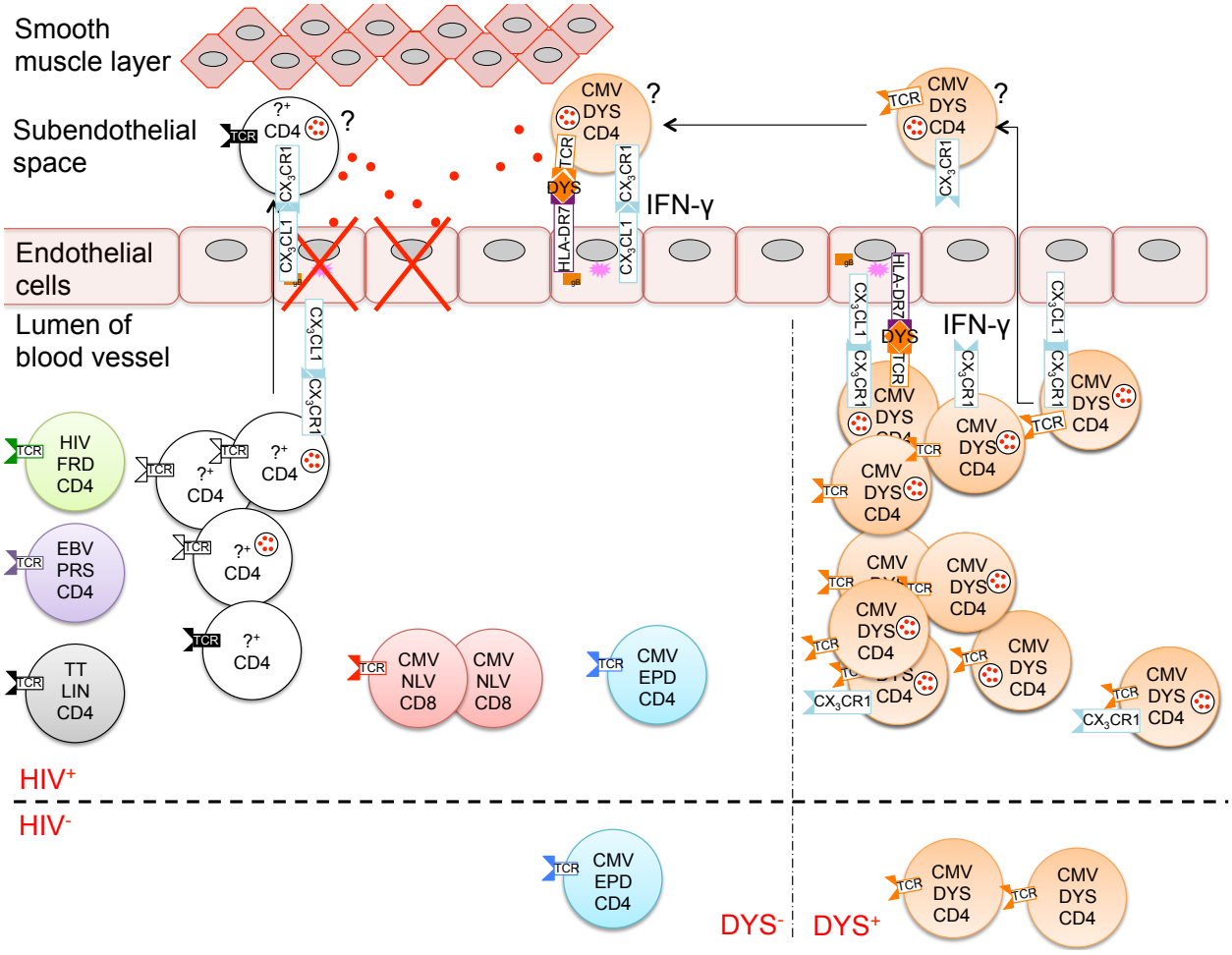

Figure V.2 Representative summary of findings as observed in Subject 10027. Blood vessel depicts peripheral circulation where observations were made, and the number of cells shown for each epitope (epitopes are written inside the cells) is proportional to the magnitude of response detected *ex vivo* with tetramers folded with the given epitope. Inflated, HLA-DR7-restricted DYS-specific (DYS^+) $CD4^+$ T cells were detected in HIV^+ (above horizontal dash line) compared to HIV^- (below horizontal dash line) subjects, all of whom were $HCMV^+$ and $DR7^+$. Within the same HIV^+ subjects, DYS^+ $CD4^+$ T cells were also inflated (right of vertical dash line) compared to $CD4^+$ T cells specific for other DR7-restricted epitopes (left of vertical dash line) that include CMV pp65 EPD, HIV gag FRD, EBV EBNA2 PRS, and tetanus toxoid precursor protein LIN epitopes. Also, DYS^+ $CD4^+$ T cells were inflated compared to $CD8^+$ T cells specific for the well-characterized A2-restricted NLV epitope. TCR CDR3 analyses revealed inflated DYS^+ $CD4^+$ T cell near monoclonality (identical orange-colored TCRs) and oligoclonal expansion of DYS^- $CD4^+$ T cells specific for unknown epitopes (white cells with "?"). One future direction is to determine these epitopes. *Ex vivo*, inflated DYS^+ $CD4^+$ T cells expressed high levels of CX_3CR1 that binds to CX_3CL1 expressed on endothelial cells latently infected with HCMV (purple dot in cells) and HCMV protein exosomes (orange square in cells). HCMV-infected endothelial cell expression of CX_3CL1 and IFN-γ-induced expression of HLA class II molecules (like DR7) that present class II epitopes (like DYS) are believed to facilitate DYS^+ $CD4^+$ T cell memory inflation. Inflated DYS^+ $CD4^+$ T cells also contain elevated levels of granzyme B (red dots) *ex vivo*. CX_3CR1-CX_3CL1 interaction might facilitate inflated DYS^+ $CD4^+$ T cell diapedesis into subendothelial space where, based on their phenotypic similarities to proposed CD4 mediators of endothelial dysfunction, they might mediate vascular damage (shown as red "Xs" over cells) via secretion of cytotoxic granules like granzyme B upon CX_3CL1-mediated recruitment by-, and stimulation by DYS-presenting HCMV-infected endothelial cells. Therefore, another future direction is to evaluate the roles of inflated DYS^+ $CD4^+$ T cells as well as other oligoclonally-expanded, potentially inflated $CD4^+$ T cells in the DYS^- compartment in the damage of vascular endothelium and immunopathogenesis of cardiovascular comorbidities, especially in HIV^+ subjects.

Future Directions

Mechanisms driving HLA-DR7-restricted DYS^+ $CD4^+$ T cell memory inflation

Memory inflation likely requires multifactorial processes to occur. In the case of DYS^+ $CD4^+$ T cell inflation in HIV^+ $HCMV^+$ subjects, various factors associated with HCMV, HIV, the inflated cells, the latent HCMV reservoirs or some combination of these elements might be responsible for the observation. CMV infection is necessary but not sufficient alone to cause memory inflation. As for the DYS epitope that is studied in this dissertation, the HLA-DR7 allele is similarly necessary but not sufficient to detect the observed phenotype. Understanding the mechanisms of memory inflation is a daunting task because of the lack of shared characteristics between different memory-inflated T cells. For instance, findings described in **Chapter II** show that memory inflation occurs in the $CD4^+$ T cells even though most of the literature documents it among $CD8^+$ T cells (Bolinger et al., 2013; Bolinger et al., 2015; Dekhtiarenko et al., 2016; Karrer et al., 2003; Khan et al., 2002a; Khan et al., 2002b; Klarenbeek et al., 2012; Munks et al., 2006; Sierro et al., 2005). Furthermore, some proteins of CMV induce inflation while others do not. Even within a given protein, only certain epitopes can induce inflation.

Focusing on potential roles of latent HCMV reservoirs such as VECs in causing inflation, one of the underlying reasons for these discordant responses to different epitopes of the same protein has been demonstrated in mice studies (Dekhtiarenko et al., 2016; Hutchinson et al., 2011). Both groups reported that inflation-inducing epitopes are more dependent on constitutively active proteosomal processing compared to conventional response-inducing epitopes that depend on immunoproteasomal

processing, which are regulated by inflammatory cytokines present mainly during acute infection. Hence, it will be of great importance to characterize and compare epitope-processing mechanisms of gB to pp65 proteins. Using Jurkat cell transfection systems that express either DYS or EPD-specific α:β TCRs, this can be tested by comparing the production and presentation of DYS (gB) to EPD (pp65) epitope by HCMV-infected, HLA-DR7^{+} permissive human cells modified with gene knockouts that inhibit the function of proteasomes, immunoproteasomes and/or endosomes. Additionally, modified MCMV strains containing gene knockouts for DYS or other interrogated gB epitopes could be designed and tested *in vivo* in mice to isolate essential epitopes of gB that are necessary to induce either memory inflation or conventional response of T cells.

In addition to genomic changes, epigenetic modifications of transcription factors or genes governing cell differentiation, proliferation or maintenance might contribute to the phenomenon of "memory inflation." One of the most current and advanced methods for epigenetic analysis is the use of Assay for Transposase-Accessible Chromatin using Sequencing (ATAC-seq). ATAC-seq facilitates the in-depth characterization of ongoing or potential gene expressions based on how the regions of the chromatin containing the genes are tightly packaged around histones as nucleosomes. ATAC-seq replaces the older methodologies that separately determined accessibility of DNA chromatin (Boyle et al., 2008; Thurman et al., 2012), the position of nucleosomes in relation to the packaged DNA (Barski et al., 2007; Schones et al., 2008; Valouev et al., 2011), and the binding (occupancy) of transcription factors to target sequences (Gerstein et al., 2012). ATAC-seq helps with the simultaneous detection of open chromatin segments in addition to the positions of nucleosomes and DNA-binding proteins (Buenrostro et al.,

2013). The working principle of ATAC-seq is a transposition reaction where the hyperactive Tn5 transposase (Adey et al., 2010; Goryshin and Reznikoff, 1998) is inserted into accessible chromatin segments that encompasses genomic regions with active gene expression (Buenrostro et al., 2013). This reaction can be conducted using as few as 500 cells, which is comparatively fewer than the input required for other tools used in epigenetic analysis (Buenrostro et al., 2013). Another merit of ATAC-seq is the novel single-cell application to obtain high-resolution epigenomic information regarding where cells fall on the homogeneity-heterogeneity spectrum (Buenrostro et al., 2015).

The application of ATAC-seq in understanding the epigenetic underpinnings of inflated DYS^+ $CD4^+$ T cell responses is an important future addition to the information obtained from the scRNA-seq in **Chapter IV**. We began this experiment by comparing the inflated, bulk-sorted DYS^+ $CD4^+$ T_{EM} and T_{EMRA} cells (26.34% response magnitude) from Subject 10027 to the non-inflated, bulk-sorted A2-restricted NLV^+ $CD8^+$ T cells (0.75% response magnitude) from the same subject for differences in the accessibility of chromatin sites involved in the proliferation or maintenance of long-lived epitope-specific memory T cells. $CD4^+$ naïve T cells from the same individual were also sorted as another internal control. All samples were amplified and sequenced, and our bioinformaticians are currently designing the coding platform for analysis.

Overall, CD3 chromatin in all four samples should be similarly accessible in the ATAC-seq results because all four samples are either $CD4^+$ or $CD8^+$ T cells. We expect to find more accessible chromatin for all gene segments of interest (*granzyme B*, *IFN-γ*, *TNF-α*, *CX_3CR1*, *CD38*, *CD74* (HLA-DR), *TBX21* (T-bet), *EOMES*, *PRDM1* (Blimp-1), *SELL*, *PSTK*, *VPS13D* and *EXOC4*) in DYS^+ $CD4^+$ T_{EM}, DYS^+ $CD4^+$ T_{EMRA} and NLV^+

$CD8^+$ T cells compared to the $CD4^+$ naïve T cells. This expectation is due to the lack of differentiation of, or antigen recognition by naïve T cells. Compared to the epigenetic findings from NLV^+ $CD8^+$ T cells, we expect to find similar degrees of accessibility to chromatin gene segments for *granzyme B*, *IFN-γ* and *TNF-α* in both DYS^+ $CD4^+$ T cell T_{EM} and T_{EMRA} subsets because these 3 sets of cells are polyfunctional and cytotoxic.

Focusing on inflation, we expect to see more accessible chromatins around *SELL*, *PSTK*, *VPS13D*, *EXOC4*, *CX_3CR1*, *CD38*, *CD74*, *TBX21*, *EOMES*, and *PRDM1* in both DYS^+ $CD4^+$ T_{EM} and T_{EMRA} subsets compared to the NLV^+ $CD8^+$ T cells. These findings would corroborate the scRNA-seq findings and protein expression of these genes in this dissertation and in published literature on inflated T cells, which suggest that inflation is partly and likely driven by re-stimulation of the T cells at latently infected vascular endothelial cells that present the epitopes endogenously. The CD45RO isoform chromatin is expected to be more accessible in the DYS^+ $CD4^+$ T_{EM} compared to the DYS^+ $CD4^+$ T_{EMRA} cells, although there might be a dynamic range between both subsets due to the reversibility of CD45RO protein expression. We expect the CD4 chromatin to be constitutively accessible by transcription factors and other DNA-binding proteins essential for transcription among the DYS^+ $CD4^+$ T cells, and the CD8 chromatin to be similarly accessible by relevant factors necessary for CD8 TCR expression in the NLV^+ $CD8^+$ T cells.

Other attributes of the inflated DYS^+ $CD4^+$ T cell might modulate inflation. A common factor among all inflated DYS^+ $CD4^+$ T cell responses in multiple subjects that is described in **Chapter II** is the conservation of glutamine, serine or threonine amino acids with polar, neutral side chains among the highest-magnitude DYS^+ CDR3

clonotype. This indicates that the presence of certain TCR might cause memory inflation to occur. The absence of these residues might explain why low-magnitude DYS^+ $CD4^+$ T cells were observed in HIV^+ $HCMV^+$ $DR7^+$ subjects, although we were unable to determine the CDR3 of the cells from bulk sorts due to their low response magnitudes. Using single cell sorting and sequencing, one approach to test this involves the alignment and comparison of the dominant CDR3s of a collection of low magnitude DYS^+ $CD4^+$ T cell responses. If the single cell sorting and sequencing of low magnitude DYS^+ $CD4^+$ T cells reveal diverse CDR3 clonotypes that lack the conserved amino acids, an alternate hypothesis could be that TCR avidity and not amino acid conservation determines whether a known inflationary epitope (such as DYS) induces memory inflation in subjects bearing the HLA allele. Therefore, a different future direction could then be to evaluate and compare the efficiency of stimulation of these low magnitude and polyclonal TCRs by DYS to that of inflated TCRs from Subject 10027 using the Jurkat cell transfection system.

The ability of HCMV to initiate the expression of certain transcripts during latency could also explain differential magnitudes of $CD4^+$ T cell response to DYS and EPD epitopes. An in-depth characterization of the entire CMV latency-associated transcripts and selective knockdowns of some of them would provide a wealth of knowledge, not only on potential CMV-intrinsic drivers of life-long memory inflation of DYS^+ $CD4^+$ T cells, but also on the features that support ordinary transcript expression over productive CMV reactivation.

The effects of HIV co-infection should be investigated as well. A study comparing the sizes of all known latent HCMV reservoirs in tissues obtained posthumously from

HIV^+ subjects to HIV^- subjects could explain the higher prevalence and response magnitude of memory inflation that occurs with HIV co-infection. Additionally, it is important to evaluate the roles of cross-reactive response against DYS-specific TCR in HIV^+ subjects. These experiments were conducted using nineteen high DR7-affinity HIV gag epitopes in Jurkat cell transfection system but no cross-reactivity was observed. There is a plethora of other unidentified HIV gag epitopes in addition to the rest of the HIV proteome that ought to be combed through thoroughly to confidently exclude cross-reactive HIV epitopes as contributors to the enhancement of DYS^+ $CD4^+$ T cell response with HIV co-infection. Another potential mechanism causing this inflation could be that the T_{EMRA} subsets of DYS^+ $CD4^+$ T cells do not support productive HIV replication (Casazza et al., 2009; Meyer-Olson et al., 2010; Oswald-Richter et al., 2007). The sparing of these less permissive cells by HIV while the virus infects and destroys other permissive cells could have allowed the expansion of these cells in HIV^+ subjects. With low CCR5 expression being partly responsible for the reduced infectivity of T_{EMRA} by HIV, it is important to determine the CCR5 expression of DYS^+ $CD4^+$ T cells and, more importantly, the ability to infect their enriched populations with HIV *in vitro*. A final potential but unlikely mechanism of inflation involving HIV directly could be the integration of HIV DNA in genes associated with cell growth, proliferation or cancer within DYS^+ $CD4^+$ T cells (Maldarelli et al., 2014; Wagner et al., 2014). Such integration events could lead to unchecked proliferation and eventual memory inflation. As discussed already, this hypothesis is not likely due to the lack of HIV DNA enrichment in these cells. Nevertheless, it will be of great importance to use a combination of HIV integration site sequencing and ATAC-seq to determine whether the HIV integration

sites make the surrounding genes more accessible to transcription factors and other protein machineries needed for cell proliferation. This experiment will involve epigenetic comparison of HIV integration sites in inflated DYS^+ $CD4^+$ T cells from HIV^+ $HCMV^+$ subjects to similar gene segments in the same cells from HIV^- $HCMV^+$ subjects.

Contributions of CMV-specific inflated T cell responses to the development of CMV-related non-AIDS cardiovascular comorbidities

An extremely important future direction from these findings is to determine the relative contributions of inflated and conventional responses to the elevated CD38 and HLA-DR protein co-expression, CX_3CR1 and granzyme B protein upregulation as well as CD28 protein downregulation on $CD4^+$ T cells in HIV^+ subjects. The advent of suppressive ART has reduced the incidence of AIDS in HIV^+ subjects. However, this has unmasked the emerging CMV-related non-AIDS cardiovascular comorbidities among these subjects (Barbaro et al., 2001; Cheng et al., 2009; Hsue et al., 2004; Lichtner et al., 2015; Slot et al., 2017; Wall et al., 2013). This is critical because the presence of T cells with increased CD38 and HLA-DR co-expression increases the risk of these comorbidities (Kaplan et al., 2011). Additionally, cytotoxic CMV-specific $CD4^+$ T cells that express high levels of the fractalkine receptor, CX_3CR1, for homing to endothelial cells, and low levels of CD28, which has been detected on clonally expanded CD4s isolated from plaques obtained posthumously from unstable angina patients (Liuzzo et al., 2000) have been proposed to cause endothelial damage and dysfunction that initiates the process of vascular disease (Broadley et al., 2017; van de Berg et al., 2012). In **Chapter II**, I showed that although DYS^+ $CD4^+$ T cells did not have

significantly higher levels of $CD38^+HLA\text{-}DR^+$ co-expression compared to controls, the collection of DYS^- $CD4^+$ T cells within the same HIV^+ subjects displayed statistically higher $CD38^+HLA\text{-}DR^+$ co-expression. Other results in that same chapter suggest that inflated DYS^+ $CD4^+$ T cells possess a CX_3CR1^{hi}, granzyme B^{hi}, and $CD28^{lo}$ phenotype. Therefore, the first step would be to map the epitopes recognized by the high-magnitude oligoclonal CDR3s of the DYS^- $CD4^+$ T_{EM} and T_{EMRA} cells. The HLA class II restriction molecules of the epitopes could be predicted (Erup Larsen et al., 2011) in order to design tetramers to be used to effectively isolate and characterize the contributions of the oligoclonal $CD4^+$ T cell responses to the activated T cell phenotype. Of interest would be determining and comparing the specific contributions of the $CD4^+$ $CD28^-$ T_{EMRA} subsets from HIV^+ and HIV^- subjects to the T cell activation, as well as CX_3CR1 and granzyme B expression. This is important because expansion of $CD4^+$ $CD28^-$ T_{EMRA} subsets is strongly associated with HCMV seropositivity of the host and might be linked to the incidence of HCMV-related comorbidities (Broadley et al., 2017; Escarra-Senmarti et al., 2017; Murakami and Riella, 2016; Shabir et al., 2016).

Mechanisms of HIV persistence in HLA-restricted epitope-specific $CD4^+$ T cells

Latent, replication-competent HIV in long-lived, resting $CD4^+$ T cells continues to pose a barrier to eradicating this virus. The persistence mechanism of HIV in this CD4 reservoir has been an area of active investigation over the last decade. The finding that the life-long inflated DYS^+ $CD4^+$ T cells in HIV^+ subjects serve as persistent HIV reservoirs presents a unique opportunity to investigate the role of cognate HLA-restricted epitope stimulation of $CD4^+$ TCR in the maintenance of latent HIV genome. The ideal and most

informative approach to solve this problem is the use of single-cell sorting and sequencing. This would first require a method for the identification of HIV-infected cells. A recently published technique involves the use of anti-CD32 antibody to label HIV-infected cells (Descours et al., 2017); however, we and others have been unable to reproduce this study. The discovery of a more reliable method for finding HIV latently infected T cells can be used to sort such cells as single cells for α:β TCR sequencing combined with single-cell whole genome amplification. The whole genome amplification will provide information on the integration site as well replication-competence of the latent HIV DNA based on the presence of critical gene segments such as *rev* and *tat* that are essential in HIV replication (Ho et al., 2013). Analyses of the degrees of clonality among the TCRs, replication-competent HIV sequences, and their integration sites in the host genome would effectively define the mechanism of HIV persistence in HLA-restricted epitope-specific $CD4^+$ T cells such as DYS^+ $CD4^+$ T cells. Findings from the RNA-seq of the transcriptome and ATAC-seq of the genome could supplement the conclusions deduced from these experiments.

The identification of these latent, replication-competent HIV DNA-harboring $CD4^+$ T cell reservoirs could provide a focused approach on eliminating persistent HIV reservoirs using “shock-and-kill” therapy. Elucidating HIV’s mechanism of persistence in $CD4^+$ T cells that recognize persistent epitopes of antigens like CMV will provide opportunities to interrupt viral persistence. Proving that HIV exploits physiologic TCR stimulation-dependent clonal expansion of HLA class II-restricted, epitope-specific $CD4^+$ T cells would also inform the broader fields of virology and immunology.

CHAPTER VI

MATERIALS AND METHODS

Contributions

Experimental design: Simon Mallal, Spyros Kalams, Elizabeth Philips, Mark Pilkinton, David Koelle, Paul Klenerman, and Chike Abana

Subject recruitment and blood draw: Simon Mallal, Spyros Kalams, Chike Abana, Mark Pilkinton, Kristina Williams, Alec Redwood, Madan Jagasia, Brian Engelhardt, the Vanderbilt Comprehensive Care Center, the Vanderbilt Stem-Cell Clinic, and the Institute for Immunology and Infectious Diseases

PBMC processing: Chike Abana, Cindy Hager, Rita Smith, Louise Barnett, Rama Gangula, Wannakuwatte Fernando, and Dae Jung

Research-and-development for all assays: Chike Abana, Simon Mallal, Spyros Kalams, Abha Chopra, Rama Gangula, Mark Pilkinton, Katie Nicholas, Silvana Gaudieri, Heather Long, Celestine Wanjalla, and Jessica Thomas

HLA-typing coordination and execution: Chike Abana, Simon Mallal, Elizabeth Philips, Mark Watson, Abha Chopra, and David Haas

Fluorescence-activated cell sorting: Chike Abana and Louise Barnett

Bulk-cell TCR sequencing: Chike Abana, Rama Gangula, and Abha Chopra

Jurkat cell transfection system: Chike Abana, Silvana Gaudieri, Abha Chopra, and Rama Gangula

Viral Outgrowth Assay: Chike Abana and Rama Gangula

Single-cell RNA sequencing: Chike Abana, Rama Gangula, Abha Chopra, and Mark Pilkinton

Assay for Transposase-Accessible Chromatin using Sequencing (ATAC-seq): Chike Abana, Rama Gangula, and Abha Chopra

Bioinformatic analyses of sequences: Wyatt McDonnell, Ramesh Ram, Matthew Scholz, and Shay Leary

Statistical analysis: Chike Abana, Ian James and Wyatt McDonnell

Ethics Statement

All studies were approved by the Vanderbilt Comprehensive Care Clinic (Institutional Review Board [IRB] 030005), Vanderbilt Stem-Cell Clinic (IRB 061215), and the Australian Red Cross (IRB 2011/02). All subjects signed informed consent forms authorized by the respective IRBs.

Selection of Subjects

HIV^+ and HIV^- subjects were randomly recruited through the Vanderbilt Comprehensive Care Clinic, the Vanderbilt Stem-Cell Clinic and the Australian Red Cross. $HCMV^+$ or $HCMV^-$ status was determined by CMV IgG serology.

Isolations and Cryopreservations of Peripheral Blood Mononuclear Cells (PBMCs) and Plasma

120ml or leukopharesed volumes of whole blood were obtained from at least 40 chronically infected $DR7^+$ subjects who sign an informed consent, and are on cART with ≤50 HIV-1 RNA copies per ml plasma (below clinical limit of detection) and >200 $CD4^+$ T-cell count per µl of blood. Blood samples from subjects lacking either alleles were obtained to validate the specificity of the class II-restricted tetramers to bind only DR7-restricted $CD4^+$ T-cells. Plasma and lymphocytes were separated by ficcoll-based density gradient centrifugation, and plasma samples for future HIV-1 RNA analysis were stored at -80°C. PBMCs were counted using an automated BECKMAN COULTER® cell counter and 10^6 cell aliquots were frozen in 1% dimethyl sulfoxide at -180°C for future use.

DNA Extraction

All DNA extractions were performed using the appropriate Qiagen® DNA extraction kits for ≥4 x 10^5 cells or Promega DNA IQ™ System (catalog # DC6701) for <4 x10^5 cells following the manufacturer's respective protocols.

Automated Determination of High Resolution (six-digit) HLA Haplotype of HIV^+ and HIV^- Cohorts

To identify $DR7^+$ HIV^+ subjects, a research proposal to the Vanderbilt HIV Epi-Outcomes group was submitted to perform full HLA-typing of 865 consented HIV seropositive subjects seen at the Vanderbilt Comprehensive Care Center (VCCC) in accordance with Institutional Review Board approved protocols. The VCCC is the largest clinic dedicated to HIV care in middle Tennessee that cares for a diverse cohort of HIV-infected individuals. Upon approval of the research proposal, I worked with the Vanderbilt Technologies for Advanced Genomics (VANTAGE) where the subjects' previously extracted genomic DNA samples were banked to identify, plate, dilute and ship the samples to the DCI Tissue Typing Laboratory (Nashville, TN) or to our collaborators at the Institute for Immunology and Infectious Diseases (IIID, Perth, Western Australia) for high-resolution six-digit HLA-typing. The American Society for Histocompatibility and Immunogenetics, and the National Association of Testing Authorities accredit the HLA testing lab at IIID. The procedure involves PCR amplification of specific HLA loci using sample specific molecular identifier, MID-tagged primers that amplify polymorphic exons from Class I (A, B, C) and Class II (DPB1, DQ, and DRB) MHC genes. MID-tagged primers have been optimized to minimize allele dropouts and primer bias. We pooled the amplified DNA products for library preparation, quantitation and emulsion PCR for 454 FLX sequencing of clonally enriched beads. Alleles are called using an in-house accredited HLA allele caller software with minimal systematic sequencing errors and using the latest IMGT (international ImMunoGeneTics

information system) HLA allele database as reference (http://www.imgt.org/). Finally, the integrity of the HLA assignments were internally validated using accredited Laboratory Information and Management Systems and HLA analysis reporting software.

Tetramers and Peptides

The NIH Tetramer Core Facility (contract HHSN272201300006C) synthesized DRB1*07:01-restricted PE-, APC-, and BV421-conjugated HCMV $gB_{217-227}$ | DYSNTHSTRYV; HCMV $pp65_{177-191}$ | EPDVYYTSAFVFPTK (EPD) (Li Pira et al., 2004); Human $CLIP_{87-101}$ | PVSKMRMATPLLMQA; tetanus toxoid (TT) $precursor_{586-605}$ | LINSTKIYSYFPSVISKVNQ (LIN) (James et al., 2007) and HIV $gag_{293-312}$ | FRDYVDRFYKTLRAEQASQE (FRD) (Vingert et al., 2010) tetramers. DRB1*07:01:PRSPTVFYNIPPMPLPPSQL (DR7:PRS, EBV $EBNA2_{276-295}$) tetramer was synthesized by Beranoya Research Institute (Seattle, WA) (Long et al., 2013). A2:NLVPMVATV (A2:NLV, CMV $pp65_{495-503}$) tetramer was synthesized in the lab as described (Leisner et al., 2008) using peptides manufactured by Schafer-N, and reagents obtained from Dr. Søren Buus and ImmunAware. The NIH AIDS Reagent Program, Division of AIDS, NIAID, provided HCMV pp65 Peptide Pool (overlapping 15-mers; #11549), HIV-1 PTE Gag Peptide Pool (overlapping 15-mers; #12437), and CMV AD169 strain (#1910). Lyophilized DYS, EPD, FRD, PRS and LIN peptides, and 19 overlapping, high DR7-affinity HIV gag peptides from the HIV-1 PTE Gag Peptide Pool (predicted by NetMHCII 2.2 Server) were synthesized at ≥98% purity (GenScript).

Tetramer, Surface and Intracellular Antibody Staining and Sorting Using Flow Cytometry

1–2 x 10^7 cryopreserved PBMCs were thawed, washed them in PBS (Corning), and disentangled using Nuclease S7 (Roche). Depending on assay, PBMCs were left untouched or negatively enriched for $CD4^+$ T cells (Miltenyi Biotec). Using our modified version of a class II tetramer stain protocol (Long et al., 2013), cells were first stained to highlight dead cells (Life Technologies), and washed with human Ab serum (Corning). Next, cells were stained with pre-titrated tetramer volumes at 37°C (1 h), anti-CCR7 Ab at 37°C (20 m), and room temperature surface protein stain (20 m) and, if necessary, intracellular Ab stain (20 m) at room temperature after fixation and permeabilization (BD). mAbs included CCR7-BV421 (150503), CD3-BV711 (UCHT1), CD4-PerCP-Cy5.5 (RPA-T4), CD45RO-PE-CF594 (UCHL1), CD27-PE-Cy7 (M-T271), CD14-V500 (M5E2), CD19-V500 (HIB19), IFN-γ-FITC (B27), TNF-α-PE-Cy7 (MAb11), CD4-FITC (SK3), Bcl-2-PE (Bcl-2/100), Granzyme-B-FITC (GB11), CX_3CR1-PE (2A9-1), Ki-67-PE-Cy7 (B56), CD57-FITC (NK-1), CD45RA-PE-Cy7 (L48), CD38-PE-Cy7 (HIT2), and HLA-DR-FITC (G46-6) that were ordered from BD; CD8-APC-AF750 (3B5) from Invitrogen; PD-1-PE (EH12.2H7) from BioLegend; TIGIT-PE-Cy7 (MBSA43) and CD28-PE-Cy7 (CD28.2) from eBiosciences; and custom CD127-PE-Cy5.5 (R34.34) from Beckman Coulter. Cells were sorted as bulk or single cells where stated with FACSAria-IIIu (BD) or collected on LSR Fortessa (BD).

For most downstream assays in this dissertation that involved tetramer staining and sorting, the starting amount of PBMCs was ≥1 x 10^8 cells due to the extremely low

frequency of epitope-specific $CD4^+$ T-cells. Furthermore, the samples were not fixed with PFA after staining, and they were sorted using a BD FACSAria IIIu directly into appropriate reagents for total HIV-1 DNA quantitation, viral outgrowth assay, deep sequencing of single cell and/or bulk α:β TCR, single cell RNA sequencing or bulk-cell Assay for Transposase-Accessible Chromatin using Sequencing (ATAC-sequencing).

FlowJo (v10.1r5; Tree Star) was used for gating analysis. Only background-subtracted, $tetramer^+$ response magnitudes 3x > the respective CLIP tetramer response magnitudes were considered positive. Median fluorescence intensity (MFI) analyses were done only on samples stained and collected the same day.

Interferon-Gamma (IFN- γ) ELISpot

IFN-γ ELISpot on a BioMek FX^P high-throughput platform (Beckman Coulter) was conducted using the Human IFN-γ $ELISpot^{BASIC}$ (HRP) kit (Mabtech). On day 1, cryopreserved PBMCs were thawed and rested overnight in nutrient media and the Millipore® Multiscreen-IP Filter Plate (MAIPS4510) was also coated with the IFN-γ capture antibody. On day 2, triplicates of 150,000-250,000 cells per well were stimulated in MultiScreen-IP Filter Plates (Millipore) with no peptide, or with 0.001 μg/μl final concentrations of DYS, EPD, FRD, PRS or LIN epitope, or HCMV pp65 peptide pool, HIV-1 PTE Gag peptide pool, or anti-human CD3 (Mabtech) in the coated wells for 18 h at 37°C. On day 3, the plate(s) were incubated at room temperature with biotinylated IFN-γ detection antibody for 2 h, followed by streptavidin-horseradish peroxidase for 30 m to bind the biotin, and finally, with tetramethylbenzidine substrate

for 10 m to develop the spots. The plate(s) were dried overnight and the number of spot forming units (SFU) was determined using an automated ELISpot reader (Autoimmun Diagnostika). Positive spot responses were accepted when they were greater than the sum of the background mean and three times background SEM (Elkington et al., 2004).

Bulk-Cell TCR Sequencing

TCRβ gene sequencing of extracted DNA from bulk-sorted T_{EM} or T_{EMRA} DYS^+ and DYS^- $CD4^+$ T cells were completed, and the data was bioinformatically analyzed by Adaptive Biotechnologies. CDR3 proportions, productive template fractions and clonalities, and V(D)J segments were analyzed on ImmunoSEQ Analyzer v3.0. Circos plots were generated using VDJtools and *circlize* (Gu et al., 2014; Shugay et al., 2015). The TCR CDR3 data have been deposited in the NCBI Sequence Read Archive repository under accession number SRP113337 (https://trace.ncbi.nlm.nih.gov/Traces/study/?acc=SRP113337&go=go) and the VDJdb database (https://vdjdb.cdr3.net).

TCR Artificial Expression and Stimulation By LCL-Pulsed Epitopes Using a Jurkat Cell Transfection System

TCRα and TCRβ CDR3 sequences of Subject 10027's DYS^+ sorted single-cells were determined using a previously published technique (Han et al., 2014). Briefly, single cells were sorted into separate wells in a 96-well plate containing RT-PCR buffer using

FACSAria-IIIu cell sorter (BD) for three rounds of PCR amplification using nested, barcoded, TCR-specific and Illumina Paired-End primers (Han et al., 2014). Purified PCR products were sequenced on Illumina MiSeq platform. After sequence analyses, TCRα and TCRβ products with identical barcodes were selected for full TCR gene completion using the international ImMunoGeneTics database. Following published methods (Anmole et al., 2015), the DYS-specific TCRα and TCRβ genes were cloned into pSELECT-GFPzeo plasmids (InvivoGen) and expressed in Jurkat cells (clone E6-1, TIB-152; American Type Culture Collection) along with pNFAT-Luciferase (Affymetrix). These cells and lymphoblastoid cell lines (LCLs) were maintained in R10 media (Nicholas et al., 2017). DYS or control epitopes were pulsed with the LCLs to stimulate the DYS-specific TCRs expressed on the Jurkat cells. Luciferase absolute light units were measured using a FilterMax F5 Multi-Mode Microplate Reader (Molecular Devices). The TCRα and TCRβ CDR3 data have been deposited in the NCBI Sequence Read Archive repository under accession number SRP113337 (https://trace.ncbi.nlm.nih.gov/Traces/study/?acc=SRP113337&go=go) and the VDJdb database (https://vdjdb.cdr3.net).

Droplet Digital PCR (ddPCR)

ddPCRs were performed entirely using a QX200 AutoDG Droplet Digital PCR System (Bio-Rad). For both HIV and CMV DNA quantitation assays, plates of oil droplets of PCR mixtures automatically were generated with an Auto-droplet generator/AutoDG and TaqMan oil for probes in ddPCR Twin-Tec 96-well plates. The plates were heat-

sealed with a foil lid and amplified with C1000 Touch thermal cycler. Droplets were read using a Droplet Reader. The magnitude of false-positive responses in no-template controls was 15%. DNA concentrations were determined from only wells with >12,000 droplets using QuantaSoft v1.7.4.0917 after manually setting the positive droplet threshold above the negative droplet signal of the no template controls in the same plate. Primers and probes concentrations: 900nM and 250nM, respectively. All PCRs were multiplexed with *RNaseP RPP30* housekeeping gene.

HCMV DNA quantitation

20µl PCR mixture was prepared using DNA, ddPCR SuperMix for Probes, water and these CMV primers and probes: *IE1*-specific forward primer 5'-TGAAGCGCCGCATTGA, *IE2*-specific reverse primer 5'-TGGCCCGTAGGTCATCCA, and *IE1*-specific probe 5'-6FAM-TCTGCATGAAGGTCTTTGCCCAGTACATCC-TAMRA. Thermocycling conditions: 50°C (2 m), 95°C (10 m), 40 cycles of 95°C (15 s) with 60°C (1 m) (2°C/s ramp rate).

HIV DNA quantitation

A modification of a published method (Strain et al., 2013) was used. Various in-house and previously published HIV primers and probes were screened for their conservation by comparison to the HxB2 (HIV) reference full-length sequence on the Los Alamos National Laboratory database. New and previously described probe and primer pairs were generated that targeted conserved sequences within the *LTR* (forward: 5'-TGTACTGGGTCTCTCTGGTTAG, reverse: 5'-AGCACTCAAGGCAAGCTTTA, and

probe: 5'-FAM/GCAGTGGGTTCCCTAGTTAGCCAGAGAGAG) and *gag* (forward: 5'-GGTGCGAGAGCGTCARTATTAAG, reverse: 5'-AGCTCCCTGCTTGCCCATA, and probe: 5'-VIC/TTCTTTCCCCCTGGCCTTAACCGAATTTT/MGBNFQ; (Douek et al., 2002)) genes, respectively. To optimize the precision and accuracy of ddPCR to detect the extremely rare HIV-1 DNA amidst very high background, 1.1 x 10^6 ACH-2 cells were serially diluted by ten-folds to 11 cells and each dilution was mixed with about 11 x 10^6 healthy PBMCs to generate ACH-2:healthy PBMC cell dilution ratios from 1-to-10 to 1-to-10M (i.e. 1-to-10 x 10^6). The 1-to-10 x 10^6 ratio represented ≤1 ACH-2 cell among the healthy PBMCs. After gDNA extraction, the DNA was digested with NEW ENGLAND BioLabs® EcoRI-HF® restriction endonuclease that cuts outside the HIV *gag* and *LTR*, and housekeeping *RNaseP* genes. 20µl PCR volumes were prepared using 500ng of gDNA of each ratio and Bio-Rad® Supermix for Probes on the BECKMAN COULTER® Biomek FX^P Laboratory Automation Workstation. Thermocycling conditions: 95°C (10 m), 40 cycles of 94°C (30 s) with 60°C (1 m), and 98°C (10 m) (2°C/s ramp rate).

Equation VI. 1

$$\text{Upper or lower 95\% CI limit} = \frac{[gag]}{[RNaseP]} \times \left(\pm 1.96 \times \text{standard error} \left(\frac{[gag]}{[RNaseP]} \right) \right)$$

$$\text{Standard error} \left(\frac{[gag]}{[RNaseP]} \right) = \left(\frac{[gag]}{[RNaseP]} \right) \times \text{standard error} \left(\log \left(\frac{[gag]}{[RNaseP]} \right) \right)$$

$$\text{Standard error} \left(\log \left(\frac{[gag]}{[RNaseP]} \right) \right) = \sqrt{\left(\left(\frac{\text{variance}[gag]}{[gag]^2} \right) + \left(\frac{\text{variance}[RNaseP]}{[RNaseP]^2} \right) \right)}$$

HIV Viral Outgrowth Assay (VOA)

To determine the replication-competence of the HIV DNA in DR7-restricted DYS^+ $CD4^+$ T-cells, a qualitative viral outgrowth assay (VOA; (Laird et al., 2013)) that uses MOLT-4 cell line (expresses the CD4 TCR, and CCR5 and CXCR4 HIV co-receptors) was modified to expand reactivated HIV. A quantitative VOA was not performed because it was impractical to obtain sufficient numbers of tetramer-positive cells for the assay. The VOA was optimized to detect replication-competent HIV-1 in aviremic subjects on ART by first depleting $CD8^+$ T-cells from a minimum of 1 x 10^6 PBMCs using STEM CELL™ EasySep™ Human CD8 Positive Selection Kit to ensure that $CD4^+$ T-cells that produce replicating viruses are not destroyed. Next, the non-CD8 PBMCs were stimulated with 1µg/ml anti-CD3 and 1µl/ml anti-CD28 at 37°C for 18 hours to induce reactivation of all resting $CD4^+$ T-cells in the presence of IL-2-enriched nutrient media to facilitate $CD4^+$ T-cell proliferation. For negative controls, unstimulated aviremic PBMCs, stimulated and unstimulated healthy PBMCs, and the MOLT-4 cells alone were all used. ACH-2 was used as a positive control. On day 2, MOLT-4 cells (ten-fold > cultured non-CD8 PBMCs) were added, and the media was replaced periodically when oxidized. 1.5ml of supernatant were collected on days 5, 9, 14 and 21 for HIV-1 RNA detection. This procedure involves (i) RNA extraction with DNase treatment to ensure that any detected HIV-1 sequence is only from its released RNA virion, and (ii) a one-step reverse transcription and ddPCR amplification to generate and detect complimentary DNA (cDNA) using ddPCR and HIV's *LTR* primers. A positive signal meant the virus could

replicate since this is a qualitative assay. A minimum of two biological replicates was conducted to confirm the observations.

HIV RNA extraction

Using ZR Viral RNA Kit™ (Zymo Research), 300 µl viral RNA buffer (ZyMo Research) were added to 100 µl of the supernatant obtained from VOA. Supernatants must be spun at 2,000 revolutions per minute (rpm) for 2 m to pellet any residual cells without pelleting any virus. The mixture should be spun briefly at 4,000 rpm for 30 s and transferred to RNA extraction column (Zymo-Spin™ IC Column). After spinning the column at 12,000 rpm for 1-2 m, the flow-through is discarded. The mixture is washed with 500 µl wash buffer at 12,000 rpm for 1 - 2 m, followed by a 2 m incubation. Finally, the RNA was eluted with about 9 µl of DNase-free, RNase-free water at 12,000 rpm for 1 - 2 m.

Complementary DNA generation from HIV RNA

The SuperScript™ III First-Strand Synthesis System (Invitrogen catalog #18080051) was used in these experiments. Working with a senior research associate, I incubated a 10 µl cocktail comprising of 7 µl of each subject's HIV RNA, 2 µl of 25 µM oligo$(dT)_{20}$, 1 µl of 10mM dNTP mix, and if necessary, UltraPure™ diethylpyrocarbonate (DEPC)-treated water at 65°C for 5 m followed by 1 m cooling on ice to denature the genome. Each of this cocktail is added to a 10 µl cDNA synthesis mix comprised of 2 µl of 10X RT buffer, 4 µl of 25 mM of $MgCl_2$, 2 µl of 0.1 M DTT, 1 µl of 40U/µl RNaseOUT, and 1 µl of 200U/µl SuperScript III RT. These mixtures were incubated at 50°C for 50 m to

synthesize the cDNA, followed by the 85°C termination at 5 m. Residual RNA were removed using 1 µl of RNase H at 37°C for 20 m. The cDNA were analyzed for potential HIV DNA content using ddPCR as described above.

Single-Cell RNA Sequencing

All procedures described below except for the sorting were conducted on a BioMek FX^P high-throughput platform (Beckman Coulter).

Fluorescence-activated cell sorting (FACS) of single cells

Working with a FACS expert, we sorted single cell into a lysis buffer that is comprised of 2 µl of 0.2% Triton X 100 (in nuclease-free water), 0.125 µl of RNase Out, 1 µl of 10 mM deoxynucleotide phosphate (dNTP), 1 µl of barcoded 10 µM oligo deoxy-thymidine (oligo dT) and nuclease-free water in each well of a 96-well plate. The plates were stored at -80°C before and after sorting, except during the sorting where it was stored on dry ice.

cDNA generation, amplification and clean-up

cDNA were generated by initially incubating the plates at 72°C followed by cooling to 4°C. 5 µl of cDNA reaction that consisted of 0.25 µl of SuperScript IV reverse transcriptase kit (Invitrogen), 0.125 µl of RNase inhibitor, 2 µl of 5x SuperScript IV reverse transcriptase buffer, 0.5 µl of 100 mM dithiothreitol (DTT), 2 µl Betaine (5M), 0.06 µl of $MgCl_2$ (1 M), and nuclease-free water (0.065 µl) was added to each well. 1 µl

of 10 µM template-switching oligonucleotide (TSO) was also added to each well. Cycling conditions involved a first cycle at 50°C (30 m) and a second cycle at 80°C (10 m), followed by a hold at 4°C. Next, 10.25 µl of kappa reaction PCR pre-amplification mixture was prepared using 10 µl of 2X KAPA HiFi HotStart Ready mix (Kapa Biosystems) and 0.25 µl of IS PCR primers, and added to each well. The PCR cycling conditions for pre-amplification include cycle 1 at 95°C (3 m); cycles 2 – 22 at 98°C (20 s), 67°C (15 s) and 72°C (6 m); cycle 23 at 72°C (5 m) and hold cycle 24 at 4°C.

Next, the cDNA was cleaned up using 20 µl of 10 mM Tris buffer (pH 8) and 1.2–1.4x of in-house beads. The samples were eluted in 20 µl of 10 mM Tris buffer (pH 8). Before proceeding with the RNA sequencing protocol, the concentrations of the cDNA were verified using Qubit fluorometer.

RNA sequencing

The RNA sequencing protocol begins with the tagmentation of 0.5 µl of the cDNA using the mixture from the Nextera XT Index Kit for 96 Indexes (catalog # FC-131-1002). The mixture is prepared adding 1 µl of Nextera XT Tagment buffer and 0.5 µl of Nextera XT Tagment mix for each well. The 2 µl final volume is amplified for the tagmentation cycle: 55°C (5 m), followed by cooling to 10°C. We stopped the reaction using 0.5 µl of Neutralize Tagment stop solution.

Tagmentation

2 µl of the RNA PCR mix were added to the tagmented well, followed by the addition of 1 µl of a 1-to-10 diluted index primers for 96-well plates. The plates were then cycled at

72°C (3 m); 95°C (30 s); 15 cycles of 95°C (30 s), 55°C (30 s), and 72°C (30 s); 72°C (5 m) and a final hold at 4°C. The PCR products are cleaned using the same homemade beads followed by an elution using 20 µl of 10 mM Tris (pH 8). After determining the concentrations using an AccuBlue High Sensitivity dsDNA quantitation kit, we pooled normalized libraries and cleaned the products for a third time using similar techniques as above. The samples were examined using BioAnalyzer to determine the library size, before pooling of multiple plates containing unique index primers for sequencing on Illumina Hi-Seq.

Automated sequence quality assurance, analysis and visualization

Following sequencing, the FASTQ data were transferred to an in-house automated pipeline that involves the trimming of adapter and/or low-quality sequences using Trimmomatic software (Bolger et al., 2014), after which they are checked for quality control before alignment against the human transcriptome and transcript quantification using Bowtie2 (Langmead and Salzberg, 2012) and RSEM (Li and Dewey, 2011), respectively. The data matrices was then fed into Single-Cell Overview of Normalized Expression (SCONE) for normalization (Wagner et al., 2016), before they are transferred to single-cell consensus clustering (SC3) software (Kiselev et al., 2017), single-cell differential expression (SCDE) (Kharchenko et al., 2014), Seurat or Monocle 2.0 (Qiu et al., 2017; Satija et al., 2015) for analysis of differential expression, co-variance and visualization.

The single-cell pipeline that we used to analyze the data I collected consists of four major steps, built around standards developed by the Broad Institute: (i) sequence

quality control and processing, (ii) transcript alignment and quantification, (iii) data normalization and filtering, and (iv) differential expression, multidimensional reduction, and classification modeling (among other advanced downstream analyses). Each of these steps is computationally intensive, and our group recommends that several experts examine the output from each step in order to identify potential confounding factors and analytical problems. In step (i), poor quality bases and sequencing adapter sequences are removed using Trimmomatic (Bolger et al., 2014). Reads that are of overall poor quality or that contain less than 50 bases after adapter removal are discarded and excluded from further analysis. In step (ii), we use Bowtie2 (Langmead and Salzberg, 2012) to align read pairs to the human genome (GRCh38); once all reads have been aligned, RSEM (Li and Dewey, 2011) is used to quantify how many reads are aligned to each gene, and to the various isoforms of each gene. For downstream analysis, the large BED and BAM files are condensed into a simple matrix with cells as columns and genes as rows.

Once the condensed cells x genes matrix has been generated, (iii) data normalization proceeds using the Single-Cell Overview of Normalized Expression (SCONE) R package developed by the Yosef laboratory (Wagner et al., 2016). SCONE is designed to handle the two major informatics challenges of scRNA-seq data: analysis of highly heterogeneous biological data and modeling of per-cell transcript drop-out and zero-inflated data. In a fashion similar to modeling a binary clinical outcome, SCONE fits a logistic regression model against mean expression of each transcript using a curated set of transcripts believed to be uniformly expressed among all cell types. For these analyses, we also used gene symbols corresponding to our flow cytometry panel as a

set of housekeeping genes. After fitting these logistic drop-out models, SCONE was used to filter out poor-quality libraries (identified using QC metrics such as percent ribosomal RNA content, total number of reads, and alignment ratio) and to automatically compare 50 methods of data normalization. Because different normalization schemes are required for meta-analysis and also for different experimental models of scRNA-seq, SCONE also enables transparent and computationally appropriate comparison of scRNA-seq data from different experiments and different laboratories. SCONE automatically selects the normalization method that best balances between removal of cell-cell variation (noise) and preservation of biological heterogeneity.

After normalization and quality filtering, 18 DYS^+ $CD4^+$ single-cell libraries were preserved alongside 149 EPD^+ $CD4^+$ single-cell libraries. At this point, (iv) the normalized cells x genes matrix was imported into the Seurat, SC3, and Monocle R packages for clustering analysis, differential expression, and multidimensional reduction (Kiselev et al., 2017; Qiu et al., 2017; Satija et al., 2015). These steps are further expanded below.

Single-cell RNA-seq quality filtering, transcriptomic alignment and quantification

FASTQ sequences that passed internal quality assurance and control at the VANTAGE core laboratory were first processed using Trimmomatic (Bolger et al., 2014) to remove low-quality bases and sequencing adapters from reads. Reads with less than 50 bases remaining after quality and adapter trimming were discarded and excluded from further analysis. Retained reads were aligned to the human genome using Bowtie2 (Langmead and Salzberg, 2012). Reference segments of the human and mitochondrial genomes

containing ribosomal RNA or mitochondrial genes were used to quantify the contribution of ribosomal and other contaminating nucleotide sequences to each single-cell library. These reads were excluded from downstream analysis, along with reads that did not map to a known region of the human genome.

RSEM was used to simultaneously quantify the number of transcripts corresponding to each gene and its isoforms during alignment with Bowtie2. Once quantitation was complete, the transcript counts from each cell were concatenated into a single cells x genes matrix with cells as columns and genes as rows. This raw data matrix was used for differential expression in SCDE (Kharchenko et al., 2014) and carried forward for normalization using SCONE and further differential expression and advanced analysis after normalization.

Single-cell RNA-seq analysis and differential expression

As stated above, raw data matrices were first imported into the SCDE package for differential expression. SCDE fits a Poisson component to zero-inflated genes, and a negative binomial component to non-zero genes in the raw data matrix. SCONE was used to import the raw data matrix and to automatically normalize the data. Libraries with less than 10,000 reads were discarded, and genes that were uniformly not detected (i.e. 0 transcripts detected in all cells) were removed prior to further analysis. The log-normalized data matrix was then exported as a tab-separated text file. We used a curated housekeeping gene list to account for cell cycle variation between cells from MSigDB and the gene symbols corresponding to the major flow cytometry markers as controls.

The SCEset R object is the computational object accepted for analysis in Seurat and SC3; the normalized data matrix was imported as an SCEset object, and metadata including date of sort, index flow cytometry values, epitope specificity, read count, alignment ratio, and coverage were imported and included for each cell that passed quality control in SCONE. Seurat was used to examine the multidimensional orientation of all cells relative to each other using t-stochastic neighbor embedding (t-SNE), principal component analysis (PCA), and to determine which principal components were statistically reliable to distinguish between cells using the jackstraw procedure as previously described (Satija et al., 2015). Seurat was also used to estimate gene dispersion and highly variant genes, which were then assessed for differential expression between DYS^+ and EPD^+ cells using a negative binomial model and regression against highly variant genes to identify genes enriched in each cluster. SC3 was used to perform consensus clustering of all cells using several clustering methods as previously described (Kiselev et al., 2017), and to perform differential expression using a non-parametric Kruskal-Wallis test as previously described to detect genes in one cluster that dominate another cluster at $\alpha = 0.01$. Clustering stability was assessed using silhouette plots to ensure that the specific permutation of the data in the normalized matrix was responsible for the multidimensional structure seen in consensus clustering visualization. The top 25 upregulated and top 25 downregulated genes between EPD^+ and DYS^+ cells were used to visualize differential expression using hierarchical clustering in SC3. It should be noted that it is inappropriate to perform this particular visualization prior to differential expression as failure to do so leads to unacceptable levels of both type I and type II error. Seurat was also used to perform

differential expression between EPD^+ and DYS^+ cells using a modified likelihood ratio test previously optimized and tested on single T cell data that tests for both differences in mean expression and proportional expression (McDavid et al., 2013).

Monocle 2.0 was used for and differential expression as well. Monocle begins by performing multidimensional reduction using PCA. The distance between cells is then estimated based on the centroids of variant genes selected using k-means clustering. This distance is then used to update the position of each cell along a trajectory in multidimensional space. This process is repeated until a clear minimum distance spanning tree is produced with a single or multiple root cells. This process is known as reverse graph embedding, and is allowed to iterate until both the tree's location in multidimensional space and the position of each cell in multidimensional space reach convergence. The distance of each cell from the root cell(s) determines its place in pseudotime, and branches of the tree represent distinctive fates (i.e. epitope specificities). Each branch of the minimum distance tree was analyzed using branch expression analysis modeling (BEAM) controlled at a false discovery rate of 1% to assess which genes were enriched in a given set of epitope-specific cells. BEAM is implemented as part of the Monocle 2.0 R package (Qiu et al., 2017).

In addition to the analytical workflow described above, scRNA-seq data can be visualized using the Qlucore Omics Explorer platform. Qlucore allows users with minimal expertise or experience in bioinformatics to readily examine their data using standard bioinformatics techniques such as multidimensional reduction, hierarchical clustering, gene filtering, pathway analysis, and differential expression. All of these steps are logged and language describing each step is exported alongside figures from

the program. The ability to use permutation and randomization to validate the structure observed in Qlucore Omics Explorer is also helpful for visualizing whether or not the structure observed is likely by chance alone. The import process into Qlucore is highly user friendly and readily compatible with the tab-separated text of the cells x genes matrix that is produced as both raw data and normalized data after processing in SCONE.

Assay for Transposase-Accessible Chromatin using Sequencing (ATAC-seq)

Nucleus isolation and transposition reaction

A modified version of a previously published protocol (Buenrostro et al., 2013) was used. After working with a FACS expert to sort bulk cells into 1X PBS buffer, cells were pelleted for nuclei isolation that begins with the resuspension of 10,000 - 50,000 cells in 50 µl cold lysis buffer (10mM Tris-HCl pH 7.4, 10mM NaCl, 3mM $MgCl_2$, and 0.1% IGEPAL CA-630). After pelleting again, the transposase reaction was performed at 37°C (30 m) next, using 22.5 µl of nuclease-free water and 2.5 µl of transposase. The product was cleaned with 32.5 µl of Ampure Beads before eluting with 10 µl of Qiagen EB elution buffer.

Library preparation and purification

The library was prepared using Nextera multiplexing primers by adding 7.5 µl NPM buffer, 2.5 µl PCR mix and 2.5 µl of each index primer (N7XX and N5XX). The PCR cycle involved 72°C (5 m); 98°C (30 s); followed by 5 cycles of 98°C (10 s), 63°C (30 s),

and 72°C (60 s). The PCR is temporarily paused to determine the number of additional cycles needed to amplify the samples to mid-exponential phase without reaching saturation. This is predicted by transferring 2.5 µl of the amplified library to a separate plate with wells each containing 7.5 µl of SYBR Green real-time master mix and 5 µl of water for real-time qPCR amplification using the sample cycling conditions but for 20 cycles instead of 5. We restarted the conventional PCR with the estimated number of cycles.

Finally, the library is purified using 20 µl of Ampure Beads and eluted in 30 µl of Qiagen EB elution buffer. We quantified the samples with Qubit and Agilent Bioanalyzer before pooling the samples for sequencing.

Statistics

GraphPad Prism v7.0a was used for non-parametric, two-tailed analyses of *Wilcoxon matched-pairs signed rank test* (paired), *Mann-Whitney U test* (non-paired), and *Spearman's rank correlation (ρ)* (linear regression). *$P \leq 0.05$, **$P \leq 0.01$, ***$P \leq 0.001$. For scRNA-seq, several statistical models were used: (i) a logistic regression model against mean expression to account for false negative rate in single-cell expression data (SCONE); (ii) a Bayesian two-component Poisson and negative binomial model for differential expression of non-zero and zero-inflated transcripts via posterior likelihood comparison; and (iii) BEAM analysis along minimum distance trees connecting cells in pseudotemporal space using Monocle 2.0 controlling for a false discovery rate of 1% or less.

REFERENCES

Abate, D.A., Watanabe, S., and Mocarski, E.S. (2004). Major human cytomegalovirus structural protein pp65 (ppUL83) prevents interferon response factor 3 activation in the interferon response. J Virol *78*, 10995-11006.

Acierno, P.M., Newton, D.A., Brown, E.A., Maes, L.A., Baatz, J.E., and Gattoni-Celli, S. (2003). Cross-reactivity between HLA-A2-restricted FLU-M1:58-66 and HIV p17 GAG:77-85 epitopes in HIV-infected and uninfected individuals. J Transl Med *1*, 3.

Adey, A., Morrison, H.G., Asan, Xun, X., Kitzman, J.O., Turner, E.H., Stackhouse, B., MacKenzie, A.P., Caruccio, N.C., Zhang, X.*, et al.* (2010). Rapid, low-input, low-bias construction of shotgun fragment libraries by high-density in vitro transposition. Genome Biol *11*, R119.

Alexander-Miller, M.A., Leggatt, G.R., Sarin, A., and Berzofsky, J.A. (1996). Role of antigen, CD8, and cytotoxic T lymphocyte (CTL) avidity in high dose antigen induction of apoptosis of effector CTL. J Exp Med *184*, 485-492.

Almeida, C.A., Roberts, S.G., Laird, R., McKinnon, E., Ahmed, I., Pfafferott, K., Turley, J., Keane, N.M., Lucas, A., Rushton, B.*, et al.* (2009). Automation of the ELISpot assay for high-throughput detection of antigen-specific T-cell responses. J Immunol Methods *344*, 1-5.

Amir, A.L., D'Orsogna, L.J., Roelen, D.L., van Loenen, M.M., Hagedoorn, R.S., de Boer, R., van der Hoorn, M.A., Kester, M.G., Doxiadis, II, Falkenburg, J.H.*, et al.* (2010). Allo-HLA reactivity of virus-specific memory T cells is common. Blood *115*, 3146-3157.

Andersen, H.K., and Spencer, E.S. (1969). Cytomegalovirus infection among renal allograft recipients. Acta Med Scand *186*, 7-19.

Anmole, G., Kuang, X.T., Toyoda, M., Martin, E., Shahid, A., Le, A.Q., Markle, T., Baraki, B., Jones, R.B., Ostrowski, M.A.*, et al.* (2015). A robust and scalable TCR-based reporter cell assay to measure HIV-1 Nef-mediated T cell immune evasion. J Immunol Methods *426*, 104-113.

Appay, V., Dunbar, P.R., Callan, M., Klenerman, P., Gillespie, G.M., Papagno, L., Ogg, G.S., King, A., Lechner, F., Spina, C.A.*, et al.* (2002a). Memory CD8+ T cells vary in differentiation phenotype in different persistent virus infections. Nat Med *8*, 379-385.

Appay, V., Zaunders, J.J., Papagno, L., Sutton, J., Jaramillo, A., Waters, A., Easterbrook, P., Grey, P., Smith, D., McMichael, A.J.*, et al.* (2002b). Characterization of CD4(+) CTLs ex vivo. J Immunol *168*, 5954-5958.

Archin, N.M., Sung, J.M., Garrido, C., Soriano-Sarabia, N., and Margolis, D.M. (2014). Eradicating HIV-1 infection: seeking to clear a persistent pathogen. Nat Rev Microbiol *12*, 750-764.

Arens, R., Wang, P., Sidney, J., Loewendorf, A., Sette, A., Schoenberger, S.P., Peters, B., and Benedict, C.A. (2008). Cutting edge: murine cytomegalovirus induces a polyfunctional CD4 T cell response. J Immunol *180*, 6472-6476.

Arthurs, S.K., Eid, A.J., Pedersen, R.A., Kremers, W.K., Cosio, F.G., Patel, R., and Razonable, R.R. (2008). Delayed-onset primary cytomegalovirus disease and the risk of allograft failure and mortality after kidney transplantation. Clin Infect Dis *46*, 840-846.

Audard, V., Matignon, M., Hemery, F., Snanoudj, R., Desgranges, P., Anglade, M.C., Kobeiter, H., Durrbach, A., Charpentier, B., Lang, P.*, et al.* (2006). Risk factors and long-term outcome of transplant renal artery stenosis in adult recipients after treatment by percutaneous transluminal angioplasty. Am J Transplant *6*, 95-99.

Bailey, J.R., Sedaghat, A.R., Kieffer, T., Brennan, T., Lee, P.K., Wind-Rotolo, M., Haggerty, C.M., Kamireddi, A.R., Liu, Y., Lee, J.*, et al.* (2006). Residual human immunodeficiency virus type 1 viremia in some patients on antiretroviral therapy is dominated by a small number of invariant clones rarely found in circulating CD4+ T cells. J Virol *80*, 6441-6457.

Baldick, C.J., Jr., Marchini, A., Patterson, C.E., and Shenk, T. (1997). Human cytomegalovirus tegument protein pp71 (ppUL82) enhances the infectivity of viral DNA and accelerates the infectious cycle. J Virol *71*, 4400-4408.

Baldick, C.J., Jr., and Shenk, T. (1996). Proteins associated with purified human cytomegalovirus particles. J Virol *70*, 6097-6105.

Balthesen, M., Dreher, L., Lucin, P., and Reddehase, M.J. (1994). The establishment of cytomegalovirus latency in organs is not linked to local virus production during primary infection. J Gen Virol *75 (Pt 9)*, 2329-2336.

Barbaro, G., Fisher, S.D., and Lipshultz, S.E. (2001). Pathogenesis of HIV-associated cardiovascular complications. Lancet Infect Dis *1*, 115-124.

Barski, A., Cuddapah, S., Cui, K., Roh, T.Y., Schones, D.E., Wang, Z., Wei, G., Chepelev, I., and Zhao, K. (2007). High-resolution profiling of histone methylations in the human genome. Cell *129*, 823-837.

Bassing, C.H., Alt, F.W., Hughes, M.M., D'Auteuil, M., Wehrly, T.D., Woodman, B.B., Gartner, F., White, J.M., Davidson, L., and Sleckman, B.P. (2000). Recombination signal sequences restrict chromosomal V(D)J recombination beyond the 12/23 rule. Nature *405*, 583-586.

Beninga, J., Kropff, B., and Mach, M. (1995). Comparative analysis of fourteen individual human cytomegalovirus proteins for helper T cell response. J Gen Virol *76 (Pt 1)*, 153-160.

Best, N.G., Trull, A.K., Tan, K.K., Spiegelhalter, D.J., Wreghitt, T.G., and Wallwork, J. (1995). Blood cyclosporine concentrations and cytomegalovirus infection following heart transplantation. Transplantation *60*, 689-694.

Biberfeld, P., Porwit, A., Biberfeld, G., Harper, M., Bodner, A., and Gallo, R. (1988). Lymphadenopathy in HIV (HTLV-III/LAV) infected subjects: the role of virus and follicular dendritic cells. Cancer Detect Prev *12*, 217-224.

Bitmansour, A.D., Douek, D.C., Maino, V.C., and Picker, L.J. (2002). Direct ex vivo analysis of human CD4(+) memory T cell activation requirements at the single clonotype level. J Immunol *169*, 1207-1218.

Boeckh, M., Nichols, W.G., Papanicolaou, G., Rubin, R., Wingard, J.R., and Zaia, J. (2003). Cytomegalovirus in hematopoietic stem cell transplant recipients: Current status, known challenges, and future strategies. Biol Blood Marrow Transplant *9*, 543-558.

Boehme, S.A., Lio, F.M., Maciejewski-Lenoir, D., Bacon, K.B., and Conlon, P.J. (2000). The chemokine fractalkine inhibits Fas-mediated cell death of brain microglia. J Immunol *165*, 397-403.

Bolger, A.M., Lohse, M., and Usadel, B. (2014). Trimmomatic: a flexible trimmer for Illumina sequence data. Bioinformatics *30*, 2114-2120.

Bolinger, B., Sims, S., O'Hara, G., de Lara, C., Tchilian, E., Firner, S., Engeler, D., Ludewig, B., and Klenerman, P. (2013). A new model for CD8+ T cell memory inflation based upon a recombinant adenoviral vector. J Immunol *190*, 4162-4174.

Bolinger, B., Sims, S., Swadling, L., O'Hara, G., de Lara, C., Baban, D., Saghal, N., Lee, L.N., Marchi, E., Davis, M.*, et al.* (2015). Adenoviral Vector Vaccination Induces a

Conserved Program of CD8(+) T Cell Memory Differentiation in Mouse and Man. Cell Rep *13*, 1578-1588.

Bolovan-Fritts, C.A., and Spector, S.A. (2008). Endothelial damage from cytomegalovirus-specific host immune response can be prevented by targeted disruption of fractalkine-CX3CR1 interaction. Blood *111*, 175-182.

Boppana, S.B., Pass, R.F., Britt, W.J., Stagno, S., and Alford, C.A. (1992). Symptomatic congenital cytomegalovirus infection: neonatal morbidity and mortality. Pediatr Infect Dis J *11*, 93-99.

Boudreault, A.A., Xie, H., Rakita, R.M., Scott, J.D., Davis, C.L., Boeckh, M., and Limaye, A.P. (2011). Risk factors for late-onset cytomegalovirus disease in donor seropositive/recipient seronegative kidney transplant recipients who receive antiviral prophylaxis. Transpl Infect Dis *13*, 244-249.

Bowen, E.F., Griffiths, P.D., Davey, C.C., Emery, V.C., and Johnson, M.A. (1996). Lessons from the natural history of cytomegalovirus. AIDS *10 Suppl 1*, S37-41.

Boyle, A.P., Davis, S., Shulha, H.P., Meltzer, P., Margulies, E.H., Weng, Z., Furey, T.S., and Crawford, G.E. (2008). High-resolution mapping and characterization of open chromatin across the genome. Cell *132*, 311-322.

Braendstrup, P., Mortensen, B.K., Justesen, S., Osterby, T., Rasmussen, M., Hansen, A.M., Christiansen, C.B., Hansen, M.B., Nielsen, M., Vindelov, L.*, et al.* (2014). Identification and HLA-tetramer-validation of human CD4+ and CD8+ T cell responses against HCMV proteins IE1 and IE2. PLoS One *9*, e94892.

Brenchley, J.M., Karandikar, N.J., Betts, M.R., Ambrozak, D.R., Hill, B.J., Crotty, L.E., Casazza, J.P., Kuruppu, J., Migueles, S.A., Connors, M.*, et al.* (2003). Expression of CD57 defines replicative senescence and antigen-induced apoptotic death of CD8+ T cells. Blood *101*, 2711-2720.

Brenchley, J.M., Ruff, L.E., Casazza, J.P., Koup, R.A., Price, D.A., and Douek, D.C. (2006). Preferential infection shortens the life span of human immunodeficiency virus-specific CD4+ T cells in vivo. J Virol *80*, 6801-6809.

Britt, W.J., Vugler, L., Butfiloski, E.J., and Stephens, E.B. (1990). Cell surface expression of human cytomegalovirus (HCMV) gp55-116 (gB): use of HCMV-recombinant vaccinia virus-infected cells in analysis of the human neutralizing antibody response. J Virol *64*, 1079-1085.

Broadley, I., Pera, A., Morrow, G., Davies, K.A., and Kern, F. (2017). Expansions of Cytotoxic CD4+CD28- T Cells Drive Excess Cardiovascular Mortality in Rheumatoid Arthritis and Other Chronic Inflammatory Conditions and Are Triggered by CMV Infection. Front Immunol *8*, 195.

Broers, A.E., van Der Holt, R., van Esser, J.W., Gratama, J.W., Henzen-Logmans, S., Kuenen-Boumeester, V., Lowenberg, B., and Cornelissen, J.J. (2000). Increased transplant-related morbidity and mortality in CMV-seropositive patients despite highly effective prevention of CMV disease after allogeneic T-cell-depleted stem cell transplantation. Blood *95*, 2240-2245.

Buchner, D.A., Trudeau, M., and Meisler, M.H. (2003). SCNM1, a putative RNA splicing factor that modifies disease severity in mice. Science *301*, 967-969.

Buenrostro, J.D., Giresi, P.G., Zaba, L.C., Chang, H.Y., and Greenleaf, W.J. (2013). Transposition of native chromatin for fast and sensitive epigenomic profiling of open chromatin, DNA-binding proteins and nucleosome position. Nat Methods *10*, 1213-1218.

Buenrostro, J.D., Wu, B., Litzenburger, U.M., Ruff, D., Gonzales, M.L., Snyder, M.P., Chang, H.Y., and Greenleaf, W.J. (2015). Single-cell chromatin accessibility reveals principles of regulatory variation. Nature *523*, 486-490.

Burgers, W.A., Riou, C., Mlotshwa, M., Maenetje, P., de Assis Rosa, D., Brenchley, J., Mlisana, K., Douek, D.C., Koup, R., Roederer, M.*, et al.* (2009). Association of HIV-specific and total CD8+ T memory phenotypes in subtype C HIV-1 infection with viral set point. J Immunol *182*, 4751-4761.

Burrows, J.M., Bell, M.J., Brennan, R., Miles, J.J., Khanna, R., and Burrows, S.R. (2008). Preferential binding of unusually long peptides to MHC class I and its influence on the selection of target peptides for T cell recognition. Mol Immunol *45*, 1818-1824.

Buzon, M.J., Sun, H., Li, C., Shaw, A., Seiss, K., Ouyang, Z., Martin-Gayo, E., Leng, J., Henrich, T.J., Li, J.Z.*, et al.* (2014). HIV-1 persistence in CD4+ T cells with stem cell-like properties. Nat Med *20*, 139-142.

Calo, E., Flynn, R.A., Martin, L., Spitale, R.C., Chang, H.Y., and Wysocka, J. (2015). RNA helicase DDX21 coordinates transcription and ribosomal RNA processing. Nature *518*, 249-253.

Cameron, P., Pope, M., Granelli-Piperno, A., and Steinman, R.M. (1996). Dendritic cells and the replication of HIV-1. J Leukoc Biol *59*, 158-171.

Cameron, P.U., Freudenthal, P.S., Barker, J.M., Gezelter, S., Inaba, K., and Steinman, R.M. (1992). Dendritic cells exposed to human immunodeficiency virus type-1 transmit a vigorous cytopathic infection to CD4+ T cells. Science *257*, 383-387.

Caposio, P., Streblow, D.N., and Nelson, J.A. (2013). Cytomegalovirus Proteomics. In Cytomegalovirus From Molecular Pathogenesis to Intervention, M.J.L. Reddehase, N. A. W., ed. (Norfolk, UK: Caister Academic Press), pp. 86-87.

Carlson, B.A., Yoo, M.H., Shrimali, R.K., Irons, R., Gladyshev, V.N., Hatfield, D.L., and Park, J.M. (2010). Role of selenium-containing proteins in T-cell and macrophage function. Proc Nutr Soc *69*, 300-310.

Carter, C.C., McNamara, L.A., Onafuwa-Nuga, A., Shackleton, M., Riddell, J.t., Bixby, D., Savona, M.R., Morrison, S.J., and Collins, K.L. (2011). HIV-1 utilizes the CXCR4 chemokine receptor to infect multipotent hematopoietic stem and progenitor cells. Cell Host Microbe *9*, 223-234.

Carter, C.C., Onafuwa-Nuga, A., McNamara, L.A., Riddell, J.t., Bixby, D., Savona, M.R., and Collins, K.L. (2010). HIV-1 infects multipotent progenitor cells causing cell death and establishing latent cellular reservoirs. Nat Med *16*, 446-451.

Casazza, J.P., Brenchley, J.M., Hill, B.J., Ayana, R., Ambrozak, D., Roederer, M., Douek, D.C., Betts, M.R., and Koup, R.A. (2009). Autocrine production of beta-chemokines protects CMV-Specific CD4 T cells from HIV infection. PLoS Pathog *5*, e1000646.

Cellerai, C., Harari, A., Vallelian, F., Boyman, O., and Pantaleo, G. (2007). Functional and phenotypic characterization of tetanus toxoid-specific human CD4+ T cells following re-immunization. European journal of immunology *37*, 1129-1138.

Chang, C.P., Malone, C.L., and Stinski, M.F. (1989). A human cytomegalovirus early gene has three inducible promoters that are regulated differentially at various times after infection. J Virol *63*, 281-290.

Chanouzas, D., Dyall, L., Dale, J., Moss, P., Morgan, M., and Harper, L. (2015). CD4+CD28- T-cell expansions in ANCA-associated vasculitis and association with arterial stiffness: baseline data from a randomised controlled trial. Lancet *385 Suppl 1*, S30.

Chanouzas, D., Sagmeister, M., Dyall, L., Nightingale, P., Ferro, C., Moss, P., Morgan, M., and Harper, L. (2017). Role of cytomegalovirus in the expansion of CD4+CD28– T cells in patients with ANCA-associated vasculitis: a proof-of-concept, randomised controlled trial. The Lancet *389*, S17.

Chattopadhyay, P.K., and Roederer, M. (2010). Good cell, bad cell: flow cytometry reveals T-cell subsets important in HIV disease. Cytometry A *77*, 614-622.

Chen, G., Gharib, T.G., Huang, C.C., Taylor, J.M., Misek, D.E., Kardia, S.L., Giordano, T.J., Iannettoni, M.D., Orringer, M.B., Hanash, S.M.*, et al.* (2002). Discordant protein and mRNA expression in lung adenocarcinomas. Mol Cell Proteomics *1*, 304-313.

Chen, T., and Hudnall, S.D. (2006). Anatomical mapping of human herpesvirus reservoirs of infection. Mod Pathol *19*, 726-737.

Cheng, J., Ke, Q., Jin, Z., Wang, H., Kocher, O., Morgan, J.P., Zhang, J., and Crumpacker, C.S. (2009). Cytomegalovirus infection causes an increase of arterial blood pressure. PLoS Pathog *5*, e1000427.

Choi, Y.C., and Hsiung, G.D. (1978). Cytomegalovirus infection in guinea pigs. II. Transplacental and horizontal transmission. J Infect Dis *138*, 197-202.

Chomont, N., El-Far, M., Ancuta, P., Trautmann, L., Procopio, F.A., Yassine-Diab, B., Boucher, G., Boulassel, M.-R., Ghattas, G., Brenchley, J.M.*, et al.* (2009). HIV reservoir size and persistence are driven by T cell survival and homeostatic proliferation. Nature Medicine *15*, 893-900.

Chun, T.W., Carruth, L., Finzi, D., Shen, X., DiGiuseppe, J.A., Taylor, H., Hermankova, M., Chadwick, K., Margolick, J., Quinn, T.C.*, et al.* (1997). Quantification of latent tissue reservoirs and total body viral load in HIV-1 infection. Nature *387*, 183-188.

Chun, T.W., Engel, D., Berrey, M.M., Shea, T., Corey, L., and Fauci, A.S. (1998). Early establishment of a pool of latently infected, resting CD4(+) T cells during primary HIV-1 infection. Proc Natl Acad Sci U S A *95*, 8869-8873.

Chun, T.W., Finzi, D., Margolick, J., Chadwick, K., Schwartz, D., and Siliciano, R.F. (1995). In vivo fate of HIV-1-infected T cells: quantitative analysis of the transition to stable latency. Nat Med *1*, 1284-1290.

Cicin-Sain, L., Sylwester, A.W., Hagen, S.I., Siess, D.C., Currier, N., Legasse, A.W., Fischer, M.B., Koudelka, C.W., Axthelm, M.K., Nikolich-Zugich, J.*, et al.* (2011). Cytomegalovirus-specific T cell immunity is maintained in immunosenescent rhesus macaques. J Immunol *187*, 1722-1732.

Cohn, L.B., Silva, I.T., Oliveira, T.Y., Rosales, R.A., Parrish, E.H., Learn, G.H., Hahn, B.H., Czartoski, J.L., McElrath, M.J., Lehmann, C.*, et al.* (2015). HIV-1 integration landscape during latent and active infection. Cell *160*, 420-432.

Compton, T., Nowlin, D.M., and Cooper, N.R. (1993). Initiation of human cytomegalovirus infection requires initial interaction with cell surface heparan sulfate. Virology *193*, 834-841.

Conrad, J.A., Ramalingam, R.K., Smith, R.M., Barnett, L., Lorey, S.L., Wei, J., Simons, B.C., Sadagopal, S., Meyer-Olson, D., and Kalams, S.A. (2011). Dominant clonotypes within HIV-specific T cell responses are programmed death-1high and CD127low and display reduced variant cross-reactivity. J Immunol *186*, 6871-6885.

Craig, J.M., Macauley, J.C., Weller, T.H., and Wirth, P. (1957). Isolation of intranuclear inclusion producing agents from infants with illnesses resembling cytomegalic inclusion disease. Proc Soc Exp Biol Med *94*, 4-12.

Cranage, M.P., Smith, G.L., Bell, S.E., Hart, H., Brown, C., Bankier, A.T., Tomlinson, P., Barrell, B.G., and Minson, T.C. (1988). Identification and expression of a human cytomegalovirus glycoprotein with homology to the Epstein-Barr virus BXLF2 product, varicella-zoster virus gpIII, and herpes simplex virus type 1 glycoprotein H. J Virol *62*, 1416-1422.

Cristea, I.M., Moorman, N.J., Terhune, S.S., Cuevas, C.D., O'Keefe, E.S., Rout, M.P., Chait, B.T., and Shenk, T. (2010). Human cytomegalovirus pUL83 stimulates activity of the viral immediate-early promoter through its interaction with the cellular IFI16 protein. J Virol *84*, 7803-7814.

Crompton, L., Khan, N., Khanna, R., Nayak, L., and Moss, P.A. (2008). CD4+ T cells specific for glycoprotein B from cytomegalovirus exhibit extreme conservation of T-cell receptor usage between different individuals. Blood *111*, 2053-2061.

Crough, T., Burrows, J.M., Fazou, C., Walker, S., Davenport, M.P., and Khanna, R. (2005). Contemporaneous fluctuations in T cell responses to persistent herpes virus infections. Eur J Immunol *35*, 139-149.

Cruz-Guilloty, F., Pipkin, M.E., Djuretic, I.M., Levanon, D., Lotem, J., Lichtenheld, M.G., Groner, Y., and Rao, A. (2009). Runx3 and T-box proteins cooperate to establish the transcriptional program of effector CTLs. J Exp Med *206*, 51-59.

D'Orsogna, L.J., van Besouw, N.M., van der Meer-Prins, E.M., van der Pol, P., Franke-van Dijk, M., Zoet, Y.M., van der Slik, A., Weimar, W., van Kooten, C., Mulder, A.*, et al.* (2011). Vaccine-induced allo-HLA-reactive memory T cells in a kidney transplantation candidate. Transplantation *91*, 645-651.

Dag, F., Dolken, L., Holzki, J., Drabig, A., Weingartner, A., Schwerk, J., Lienenklaus, S., Conte, I., Geffers, R., Davenport, C.*, et al.* (2014). Reversible silencing of

cytomegalovirus genomes by type I interferon governs virus latency. PLoS Pathog *10*, e1003962.

Davey, R.T., Jr., Bhat, N., Yoder, C., Chun, T.W., Metcalf, J.A., Dewar, R., Natarajan, V., Lempicki, R.A., Adelsberger, J.W., Miller, K.D.*, et al.* (1999). HIV-1 and T cell dynamics after interruption of highly active antiretroviral therapy (HAART) in patients with a history of sustained viral suppression. Proc Natl Acad Sci U S A *96*, 15109-15114.

Davignon, J.L., Castanie, P., Yorke, J.A., Gautier, N., Clement, D., and Davrinche, C. (1996). Anti-human cytomegalovirus activity of cytokines produced by CD4+ T-cell clones specifically activated by IE1 peptides in vitro. J Virol *70*, 2162-2169.

Davignon, J.L., Clement, D., Alriquet, J., Michelson, S., and Davrinche, C. (1995). Analysis of the proliferative T cell response to human cytomegalovirus major immediate-early protein (IE1): phenotype, frequency and variability. Scand J Immunol *41*, 247-255.

Davison, A.J., Dolan, A., Akter, P., Addison, C., Dargan, D.J., Alcendor, D.J., McGeoch, D.J., and Hayward, G.S. (2003). The human cytomegalovirus genome revisited: comparison with the chimpanzee cytomegalovirus genome. J Gen Virol *84*, 17-28.

Davison, A.J., Holton, M., Dolan, A., Dargan, D.J., Gatherer, D., and Hayward, G.S. (2013). Comparative Genomics of Primate Cytomegaloviruses. In Cytomegalovirus From Molecular Pathogenesis to Intervention, M.J.L. Reddehase, N. A. W., ed. (Norfolk, UK: Caister Academic Press), pp. 1-22.

Dekhtiarenko, I., Jarvis, M.A., Ruzsics, Z., and Cicin-Sain, L. (2013). The context of gene expression defines the immunodominance hierarchy of cytomegalovirus antigens. J Immunol *190*, 3399-3409.

Dekhtiarenko, I., Ratts, R.B., Blatnik, R., Lee, L.N., Fischer, S., Borkner, L., Oduro, J.D., Marandu, T.F., Hoppe, S., Ruzsics, Z.*, et al.* (2016). Peptide Processing Is Critical for T-Cell Memory Inflation and May Be Optimized to Improve Immune Protection by CMV-Based Vaccine Vectors. PLoS Pathog *12*, e1006072.

Deng, H., Liu, R., Ellmeier, W., Choe, S., Unutmaz, D., Burkhart, M., Di Marzio, P., Marmon, S., Sutton, R.E., Hill, C.M.*, et al.* (1996). Identification of a major co-receptor for primary isolates of HIV-1. Nature *381*, 661-666.

Descours, B., Petitjean, G., Lopez-Zaragoza, J.L., Bruel, T., Raffel, R., Psomas, C., Reynes, J., Lacabaratz, C., Levy, Y., Schwartz, O.*, et al.* (2017). CD32a is a marker of a CD4 T-cell HIV reservoir harbouring replication-competent proviruses. Nature *543*, 564-567.

Diepolder, H.M., Gruener, N.H., Gerlach, J.T., Jung, M.C., Wierenga, E.A., and Pape, G.R. (2001). Different levels of T-cell receptor triggering induce distinct functions in hepatitis B and hepatitis C virus-specific human CD4(+) T-cell clones. J Virol *75*, 7803-7810.

Dockrell, D.H., Prada, J., Jones, M.F., Patel, R., Badley, A.D., Harmsen, W.S., Ilstrup, D.M., Wiesner, R.H., Krom, R.A., Smith, T.F.*, et al.* (1997). Seroconversion to human herpesvirus 6 following liver transplantation is a marker of cytomegalovirus disease. J Infect Dis *176*, 1135-1140.

Dolan, A., Cunningham, C., Hector, R.D., Hassan-Walker, A.F., Lee, L., Addison, C., Dargan, D.J., McGeoch, D.J., Gatherer, D., Emery, V.C.*, et al.* (2004). Genetic content of wild-type human cytomegalovirus. J Gen Virol *85*, 1301-1312.

Douek, D.C., Brenchley, J.M., Betts, M.R., Ambrozak, D.R., Hill, B.J., Okamoto, Y., Casazza, J.P., Kuruppu, J., Kunstman, K., Wolinsky, S.*, et al.* (2002). HIV preferentially infects HIV-specific CD4+ T cells. Nature *417*, 95-98.

Drew, W.L., Mintz, L., Miner, R.C., Sands, M., and Ketterer, B. (1981). Prevalence of cytomegalovirus infection in homosexual men. J Infect Dis *143*, 188-192.

Dunn, H.S., Haney, D.J., Ghanekar, S.A., Stepick-Biek, P., Lewis, D.B., and Maecker, H.T. (2002). Dynamics of CD4 and CD8 T cell responses to cytomegalovirus in healthy human donors. J Infect Dis *186*, 15-22.

Edwards, J.N., and Morris, H.B. (1985). Langerhans' cells and lymphocyte subsets in the female genital tract. Br J Obstet Gynaecol *92*, 974-982.

Einsele, H., Roosnek, E., Rufer, N., Sinzger, C., Riegler, S., Loffler, J., Grigoleit, U., Moris, A., Rammensee, H.G., Kanz, L.*, et al.* (2002). Infusion of cytomegalovirus (CMV)-specific T cells for the treatment of CMV infection not responding to antiviral chemotherapy. Blood *99*, 3916-3922.

Elkington, R., Shoukry, N.H., Walker, S., Crough, T., Fazou, C., Kaur, A., Walker, C.M., and Khanna, R. (2004). Cross-reactive recognition of human and primate cytomegalovirus sequences by human CD4 cytotoxic T lymphocytes specific for glycoprotein B and H. Eur J Immunol *34*, 3216-3226.

Elkington, R., Walker, S., Crough, T., Menzies, M., Tellam, J., Bharadwaj, M., and Khanna, R. (2003). Ex vivo profiling of CD8+-T-cell responses to human cytomegalovirus reveals broad and multispecific reactivities in healthy virus carriers. J Virol *77*, 5226-5240.

Embretson, J., Zupancic, M., Ribas, J.L., Burke, A., Racz, P., Tenner-Racz, K., and Haase, A.T. (1993). Massive covert infection of helper T lymphocytes and macrophages by HIV during the incubation period of AIDS. Nature *362*, 359-362.

Ertelt, J.M., Johanns, T.M., Mysz, M.A., Nanton, M.R., Rowe, J.H., Aguilera, M.N., and Way, S.S. (2011). Selective culling of high avidity antigen-specific CD4+ T cells after virulent Salmonella infection. Immunology *134*, 487-497.

Erup Larsen, M., Kloverpris, H., Stryhn, A., Koofhethile, C.K., Sims, S., Ndung'u, T., Goulder, P., Buus, S., and Nielsen, M. (2011). HLArestrictor--a tool for patient-specific predictions of HLA restriction elements and optimal epitopes within peptides. Immunogenetics *63*, 43-55.

Escarra-Senmarti, M., Bueno-Topete, M.R., Jave-Suarez, L.F., Gomez-Banuelos, E., Gutierrez-Franco, J., Vega-Magana, N., Aguilar-Lemarroy, A., Pereira-Suarez, A.L., Haramati, J., and Del Toro-Arreola, S. (2017). Loss of CD28 within CD4+ T cell subsets from cervical cancer patients is accompanied by the acquisition of intracellular perforin, and is further enhanced by NKG2D expression. Immunol Lett *182*, 30-38.

Evering, T.H., Mehandru, S., Racz, P., Tenner-Racz, K., Poles, M.A., Figueroa, A., Mohri, H., and Markowitz, M. (2012). Absence of HIV-1 evolution in the gut-associated lymphoid tissue from patients on combination antiviral therapy initiated during primary infection. PLoS Pathog *8*, e1002506.

Falk, C.S., Mach, M., Schendel, D.J., Weiss, E.H., Hilgert, I., and Hahn, G. (2002). NK cell activity during human cytomegalovirus infection is dominated by US2-11-mediated HLA class I down-regulation. J Immunol *169*, 3257-3266.

Falta, M.T., Fontenot, A.P., Rosloniec, E.F., Crawford, F., Roark, C.L., Bill, J., Marrack, P., Kappler, J., and Kotzin, B.L. (2005). Class II major histocompatibility complex-peptide tetramer staining in relation to functional avidity and T cell receptor diversity in the mouse CD4(+) T cell response to a rheumatoid arthritis-associated antigen. Arthritis Rheum *52*, 1885-1896.

Farrington, L.A., Smith, T.A., Grey, F., Hill, A.B., and Snyder, C.M. (2013). Competition for antigen at the level of the APC is a major determinant of immunodominance during memory inflation in murine cytomegalovirus infection. J Immunol *190*, 3410-3416.

Feire, A.L., Compton, T. (2013). Virus Entry and Activation of Innate Defence. In Cytomegalovirus From Molecular Pathogenesis to Intervention, M.J.L. Reddehase, N. A. W., ed. (Norfolk, UK: Caister Academic Press), pp. 125-140.

Fesenko, I., Khazigaleeva, R., Kirov, I., Kniazev, A., Glushenko, O., Babalyan, K., Arapidi, G., Shashkova, T., Butenko, I., Zgoda, V.*, et al.* (2017). Alternative splicing

shapes transcriptome but not proteome diversity in Physcomitrella patens. Sci Rep *7*, 2698.

Fiala, M., Cone, L.A., Chang, C.M., and Mocarski, E.S. (1986). Cytomegalovirus viremia increases with progressive immune deficiency in patients infected with HTLV-III. AIDS Res *2*, 175-181.

Fietze, E., Prosch, S., Reinke, P., Stein, J., Docke, W.D., Staffa, G., Loning, S., Devaux, S., Emmrich, F., von Baehr, R.*, et al.* (1994). Cytomegalovirus infection in transplant recipients. The role of tumor necrosis factor. Transplantation *58*, 675-680.

Finzi, D., Blankson, J., Siliciano, J.D., Margolick, J.B., Chadwick, K., Pierson, T., Smith, K., Lisziewicz, J., Lori, F., Flexner, C.*, et al.* (1999). Latent infection of CD4+ T cells provides a mechanism for lifelong persistence of HIV-1, even in patients on effective combination therapy. Nat Med *5*, 512-517.

Finzi, D., Hermankova, M., Pierson, T., Carruth, L.M., Buck, C., Chaisson, R.E., Quinn, T.C., Chadwick, K., Margolick, J., Brookmeyer, R.*, et al.* (1997). Identification of a reservoir for HIV-1 in patients on highly active antiretroviral therapy. Science *278*, 1295-1300.

Fiorentini, S., Luganini, A., Dell'Oste, V., Lorusso, B., Cervi, E., Caccuri, F., Bonardelli, S., Landolfo, S., Caruso, A., and Gribaudo, G. (2011). Human cytomegalovirus productively infects lymphatic endothelial cells and induces a secretome that promotes angiogenesis and lymphangiogenesis through interleukin-6 and granulocyte-macrophage colony-stimulating factor. J Gen Virol *92*, 650-660.

Fischer, M., Hafner, R., Schneider, C., Trkola, A., Joos, B., Joller, H., Hirschel, B., Weber, R., and Gunthard, H.F. (2003). HIV RNA in plasma rebounds within days during structured treatment interruptions. Aids *17*, 195-199.

Foussat, A., Coulomb-L'Hermine, A., Gosling, J., Krzysiek, R., Durand-Gasselin, I., Schall, T., Balian, A., Richard, Y., Galanaud, P., and Emilie, D. (2000). Fractalkine receptor expression by T lymphocyte subpopulations and in vivo production of fractalkine in human. Eur J Immunol *30*, 87-97.

Fowler, K.B., and Boppana, S.B. (2006). Congenital cytomegalovirus (CMV) infection and hearing deficit. J Clin Virol *35*, 226-231.

Fowler, K.B., Stagno, S., Pass, R.F., Britt, W.J., Boll, T.J., and Alford, C.A. (1992). The outcome of congenital cytomegalovirus infection in relation to maternal antibody status. N Engl J Med *326*, 663-667.

Frankenberg, N., Pepperl-Klindworth, S., Meyer, R.G., and Plachter, B. (2002). Identification of a conserved HLA-A2-restricted decapeptide from the IE1 protein (pUL123) of human cytomegalovirus. Virology *295*, 208-216.

Fuhrmann, S., Streitz, M., Reinke, P., Volk, H.D., and Kern, F. (2008). T cell response to the cytomegalovirus major capsid protein (UL86) is dominated by helper cells with a large polyfunctional component and diverse epitope recognition. J Infect Dis *197*, 1455-1458.

Fukazawa, Y., Lum, R., Okoye, A.A., Park, H., Matsuda, K., Bae, J.Y., Hagen, S.I., Shoemaker, R., Deleage, C., Lucero, C*., et al.* (2015). B cell follicle sanctuary permits persistent productive simian immunodeficiency virus infection in elite controllers. Nat Med *21*, 132-139.

Furman, D., Jojic, V., Sharma, S., Shen-Orr, S.S., Angel, C.J., Onengut-Gumuscu, S., Kidd, B.A., Maecker, H.T., Concannon, P., Dekker, C.L*., et al.* (2015). Cytomegalovirus infection enhances the immune response to influenza. Sci Transl Med *7*, 281ra243.

Gallant, J.E., Moore, R.D., Richman, D.D., Keruly, J., and Chaisson, R.E. (1992). Incidence and natural history of cytomegalovirus disease in patients with advanced human immunodeficiency virus disease treated with zidovudine. The Zidovudine Epidemiology Study Group. J Infect Dis *166*, 1223-1227.

Gallatin, W.M., Weissman, I.L., and Butcher, E.C. (1983). A cell-surface molecule involved in organ-specific homing of lymphocytes. Nature *304*, 30-34.

Gamadia, L.E., Remmerswaal, E.B., Weel, J.F., Bemelman, F., van Lier, R.A., and Ten Berge, I.J. (2003). Primary immune responses to human CMV: a critical role for IFN-gamma-producing CD4+ T cells in protection against CMV disease. Blood *101*, 2686-2692.

Gamadia, L.E., van Leeuwen, E.M., Remmerswaal, E.B., Yong, S.L., Surachno, S., Wertheim-van Dillen, P.M., Ten Berge, I.J., and Van Lier, R.A. (2004). The size and phenotype of virus-specific T cell populations is determined by repetitive antigenic stimulation and environmental cytokines. J Immunol *172*, 6107-6114.

Garg, A., Trout, R., and Spector, S.A. (2017). Human Immunodeficiency Virus Type-1 Myeloid Derived Suppressor Cells Inhibit Cytomegalovirus Inflammation through Interleukin-27 and B7-H4. Sci Rep *7*, 44485.

Gartner, S., Markovits, P., Markovitz, D.M., Kaplan, M.H., Gallo, R.C., and Popovic, M. (1986). The role of mononuclear phagocytes in HTLV-III/LAV infection. Science *233*, 215-219.

Gautier, N., Chavant, E., Prieur, E., Monsarrat, B., Mazarguil, H., Davrinche, C., Gairin, J.E., and Davignon, J.L. (1996). Characterization of an epitope of the human cytomegalovirus protein IE1 recognized by a CD4+ T cell clone. Eur J Immunol *26*, 1110-1117.

Geldmacher, C., Ngwenyama, N., Schuetz, A., Petrovas, C., Reither, K., Heeregrave, E.J., Casazza, J.P., Ambrozak, D.R., Louder, M., Ampofo, W.*, et al.* (2010). Preferential infection and depletion of Mycobacterium tuberculosis-specific CD4 T cells after HIV-1 infection. J Exp Med *207*, 2869-2881.

Gerli, R., Schillaci, G., Giordano, A., Bocci, E.B., Bistoni, O., Vaudo, G., Marchesi, S., Pirro, M., Ragni, F., Shoenfeld, Y.*, et al.* (2004). CD4+CD28- T lymphocytes contribute to early atherosclerotic damage in rheumatoid arthritis patients. Circulation *109*, 2744-2748.

Gerstein, M.B., Kundaje, A., Hariharan, M., Landt, S.G., Yan, K.K., Cheng, C., Mu, X.J., Khurana, E., Rozowsky, J., Alexander, R.*, et al.* (2012). Architecture of the human regulatory network derived from ENCODE data. Nature *489*, 91-100.

Gertler, S.L., Pressman, J., Price, P., Brozinsky, S., and Miyai, K. (1983). Gastrointestinal cytomegalovirus infection in a homosexual man with severe acquired immunodeficiency syndrome. Gastroenterology *85*, 1403-1406.

Ghazal, P., Mazein, A., Watterson, S., Angulo, A., and Kropp, K.A. (2013). A Systems Pathway View of Cytomegalovirus Infection. In Cytomegalovirus From Molecular Pathogenesis to Intervention, M.J.L. Reddehase, N. A. W., ed. (Norfolk, UK: Caister Academic Press), pp. 109-124.

Ghazalpour, A., Bennett, B., Petyuk, V.A., Orozco, L., Hagopian, R., Mungrue, I.N., Farber, C.R., Sinsheimer, J., Kang, H.M., Furlotte, N.*, et al.* (2011). Comparative analysis of proteome and transcriptome variation in mouse. PLoS Genet *7*, e1001393.

Gianella, S., Anderson, C.M., Vargas, M.V., Richman, D.D., Little, S.J., Morris, S.R., and Smith, D.M. (2013). Cytomegalovirus DNA in semen and blood is associated with higher levels of proviral HIV DNA. J Infect Dis *207*, 898-902.

Glanville, J., Huang, H., Nau, A., Hatton, O., Wagar, L.E., Rubelt, F., Ji, X., Han, A., Krams, S.M., Pettus, C.*, et al.* (2017). Identifying specificity groups in the T cell receptor repertoire. Nature *547*, 94-98.

Gordon, C.L., Miron, M., Thome, J.J., Matsuoka, N., Weiner, J., Rak, M.A., Igarashi, S., Granot, T., Lerner, H., Goodrum, F.*, et al.* (2017). Tissue reservoirs of antiviral T cell immunity in persistent human CMV infection. J Exp Med *214*, 651-667.

Gorry, P.R., Howard, J.L., Churchill, M.J., Anderson, J.L., Cunningham, A., Adrian, D., McPhee, D.A., and Purcell, D.F. (1999). Diminished production of human immunodeficiency virus type 1 in astrocytes results from inefficient translation of gag, env, and nef mRNAs despite efficient expression of Tat and Rev. J Virol *73*, 352-361.

Goryshin, I.Y., and Reznikoff, W.S. (1998). Tn5 in vitro transposition. J Biol Chem *273*, 7367-7374.

Gorzer, I., Guelly, C., Trajanoski, S., and Puchhammer-Stockl, E. (2010). Deep sequencing reveals highly complex dynamics of human cytomegalovirus genotypes in transplant patients over time. J Virol *84*, 7195-7203.

Grattan, M.T., Moreno-Cabral, C.E., Starnes, V.A., Oyer, P.E., Stinson, E.B., and Shumway, N.E. (1989). Cytomegalovirus infection is associated with cardiac allograft rejection and atherosclerosis. JAMA *261*, 3561-3566.

Grefte, A., van der Giessen, M., van Son, W., and The, T.H. (1993). Circulating cytomegalovirus (CMV)-infected endothelial cells in patients with an active CMV infection. J Infect Dis *167*, 270-277.

Gu, Z., Gu, L., Eils, R., Schlesner, M., and Brors, B. (2014). circlize Implements and enhances circular visualization in R. Bioinformatics *30*, 2811-2812.

Gulick, R.M., Mellors, J.W., Havlir, D., Eron, J.J., Gonzalez, C., McMahon, D., Richman, D.D., Valentine, F.T., Jonas, L., Meibohm, A.*, et al.* (1997). Treatment with indinavir, zidovudine, and lamivudine in adults with human immunodeficiency virus infection and prior antiretroviral therapy. N Engl J Med *337*, 734-739.

Hagemeier, C., Walker, S.M., Sissons, P.J., and Sinclair, J.H. (1992). The 72K IE1 and 80K IE2 proteins of human cytomegalovirus independently trans-activate the c-fos, c-myc and hsp70 promoters via basal promoter elements. J Gen Virol *73 (Pt 9)*, 2385-2393.

Han, A., Glanville, J., Hansmann, L., and Davis, M.M. (2014). Linking T-cell receptor sequence to functional phenotype at the single-cell level. Nat Biotechnol *32*, 684-692.

Hansen, S.G., Ford, J.C., Lewis, M.S., Ventura, A.B., Hughes, C.M., Coyne-Johnson, L., Whizin, N., Oswald, K., Shoemaker, R., Swanson, T.*, et al.* (2011). Profound early control of highly pathogenic SIV by an effector memory T-cell vaccine. Nature *473*, 523-527.

Hansen, S.G., Piatak, M., Jr., Ventura, A.B., Hughes, C.M., Gilbride, R.M., Ford, J.C., Oswald, K., Shoemaker, R., Li, Y., Lewis, M.S.*, et al.* (2013a). Immune clearance of highly pathogenic SIV infection. Nature *502*, 100-104.

Hansen, S.G., Sacha, J.B., Hughes, C.M., Ford, J.C., Burwitz, B.J., Scholz, I., Gilbride, R.M., Lewis, M.S., Gilliam, A.N., Ventura, A.B.*, et al.* (2013b). Cytomegalovirus vectors violate CD8+ T cell epitope recognition paradigms. Science *340*, 1237874.

Hansen, S.G., Wu, H.L., Burwitz, B.J., Hughes, C.M., Hammond, K.B., Ventura, A.B., Reed, J.S., Gilbride, R.M., Ainslie, E., Morrow, D.W.*, et al.* (2016). Broadly targeted CD8(+) T cell responses restricted by major histocompatibility complex E. Science *351*, 714-720.

Harada, N., Shimada, M., Suehiro, T., Soejima, Y., Ninomiya, M., Shiotani, S., and Sugimachi, K. (2005). Unusual endoscopic findings of CMV esophagitis after liver transplantation. Hepatogastroenterology *52*, 1236-1239.

Hargrove, J.L., and Schmidt, F.H. (1989). The role of mRNA and protein stability in gene expression. FASEB J *3*, 2360-2370.

Harrigan, P.R., Whaley, M., and Montaner, J.S. (1999). Rate of HIV-1 RNA rebound upon stopping antiretroviral therapy. Aids *13*, F59-62.

Hassan-Walker, A.F., Vargas Cuero, A.L., Mattes, F.M., Klenerman, P., Lechner, F., Burroughs, A.K., Griffiths, P.D., Phillips, R.E., and Emery, V.C. (2001). CD8+ cytotoxic lymphocyte responses against cytomegalovirus after liver transplantation: correlation with time from transplant to receipt of tacrolimus. J Infect Dis *183*, 835-843.

Hattori, N., Kawamoto, H., Fujimoto, S., Kuno, K., and Katsura, Y. (1996). Involvement of transcription factors TCF-1 and GATA-3 in the initiation of the earliest step of T cell development in the thymus. J Exp Med *184*, 1137-1147.

Heath, S.L., Tew, J.G., Tew, J.G., Szakal, A.K., and Burton, G.F. (1995). Follicular dendritic cells and human immunodeficiency virus infectivity. Nature *377*, 740-744.

Hebart, H., and Einsele, H. (2004). Clinical aspects of CMV infection after stem cell transplantation. Hum Immunol *65*, 432-436.

Hegde, N.R., Dunn, C., Lewinsohn, D.M., Jarvis, M.A., Nelson, J.A., and Johnson, D.C. (2005). Endogenous human cytomegalovirus gB is presented efficiently by MHC class II molecules to CD4+ CTL. J Exp Med *202*, 1109-1119.

Hegde, N.R., Tomazin, R.A., Wisner, T.W., Dunn, C., Boname, J.M., Lewinsohn, D.M., and Johnson, D.C. (2002). Inhibition of HLA-DR assembly, transport, and loading by human cytomegalovirus glycoprotein US3: a novel mechanism for evading major histocompatibility complex class II antigen presentation. J Virol *76*, 10929-10941.

Hermiston, T.W., Malone, C.L., and Stinski, M.F. (1990). Human cytomegalovirus immediate-early two protein region involved in negative regulation of the major immediate-early promoter. J Virol *64*, 3532-3536.

Hertoghs, K.M., Moerland, P.D., van Stijn, A., Remmerswaal, E.B., Yong, S.L., van de Berg, P.J., van Ham, S.M., Baas, F., ten Berge, I.J., and van Lier, R.A. (2010). Molecular profiling of cytomegalovirus-induced human CD8+ T cell differentiation. J Clin Invest *120*, 4077-4090.

Ho, D.D., Neumann, A.U., Perelson, A.S., Chen, W., Leonard, J.M., and Markowitz, M. (1995). Rapid turnover of plasma virions and CD4 lymphocytes in HIV-1 infection. Nature *373*, 123-126.

Ho, D.D., Rota, T.R., and Hirsch, M.S. (1986). Infection of monocyte/macrophages by human T lymphotropic virus type III. J Clin Invest *77*, 1712-1715.

Ho, M. (2008). The history of cytomegalovirus and its diseases. Med Microbiol Immunol *197*, 65-73.

Ho, Y.C., Shan, L., Hosmane, N.N., Wang, J., Laskey, S.B., Rosenbloom, D.I., Lai, J., Blankson, J.N., Siliciano, J.D., and Siliciano, R.F. (2013). Replication-competent noninduced proviruses in the latent reservoir increase barrier to HIV-1 cure. Cell *155*, 540-551.

Holtappels, R., Pahl-Seibert, M.F., Thomas, D., and Reddehase, M.J. (2000). Enrichment of immediate-early 1 (m123/pp89) peptide-specific CD8 T cells in a pulmonary CD62L(lo) memory-effector cell pool during latent murine cytomegalovirus infection of the lungs. J Virol *74*, 11495-11503.

Homman-Loudiyi, M., Hultenby, K., Britt, W., and Soderberg-Naucler, C. (2003). Envelopment of human cytomegalovirus occurs by budding into Golgi-derived vacuole compartments positive for gB, Rab 3, trans-golgi network 46, and mannosidase II. J Virol *77*, 3191-3203.

Hsue, P.Y., Lo, J.C., Franklin, A., Bolger, A.F., Martin, J.N., Deeks, S.G., and Waters, D.D. (2004). Progression of atherosclerosis as assessed by carotid intima-media thickness in patients with HIV infection. Circulation *109*, 1603-1608.

Hui, E., Cheung, J., Zhu, J., Su, X., Taylor, M.J., Wallweber, H.A., Sasmal, D.K., Huang, J., Kim, J.M., Mellman, I.*, et al.* (2017). T cell costimulatory receptor CD28 is a primary target for PD-1-mediated inhibition. Science *355*, 1428-1433.

Hunt, P.W., Martin, J.N., Sinclair, E., Epling, L., Teague, J., Jacobson, M.A., Tracy, R.P., Corey, L., and Deeks, S.G. (2011). Valganciclovir reduces T cell activation in HIV-infected individuals with incomplete CD4+ T cell recovery on antiretroviral therapy. J Infect Dis *203*, 1474-1483.

Hutchinson, S., Sims, S., O'Hara, G., Silk, J., Gileadi, U., Cerundolo, V., and Klenerman, P. (2011). A dominant role for the immunoproteasome in CD8+ T cell responses to murine cytomegalovirus. PLoS One *6*, e14646.

Ibanez, C.E., Schrier, R., Ghazal, P., Wiley, C., and Nelson, J.A. (1991). Human cytomegalovirus productively infects primary differentiated macrophages. J Virol *65*, 6581-6588.

Igarashi, T., Brown, C.R., Endo, Y., Buckler-White, A., Plishka, R., Bischofberger, N., Hirsch, V., and Martin, M.A. (2001). Macrophage are the principal reservoir and sustain high virus loads in rhesus macaques after the depletion of CD4+ T cells by a highly pathogenic simian immunodeficiency virus/HIV type 1 chimera (SHIV): Implications for HIV-1 infections of humans. Proc Natl Acad Sci U S A *98*, 658-663.

Intlekofer, A.M., Banerjee, A., Takemoto, N., Gordon, S.M., Dejong, C.S., Shin, H., Hunter, C.A., Wherry, E.J., Lindsten, T., and Reiner, S.L. (2008). Anomalous type 17 response to viral infection by CD8+ T cells lacking T-bet and eomesodermin. Science *321*, 408-411.

Irmiere, A., and Gibson, W. (1983). Isolation and characterization of a noninfectious virion-like particle released from cells infected with human strains of cytomegalovirus. Virology *130*, 118-133.

Iskenderian, A.C., Huang, L., Reilly, A., Stenberg, R.M., and Anders, D.G. (1996). Four of eleven loci required for transient complementation of human cytomegalovirus DNA replication cooperate to activate expression of replication genes. J Virol *70*, 383-392.

Jackson, S.E., Mason, G.M., Okecha, G., Sissons, J.G., and Wills, M.R. (2014). Diverse specificities, phenotypes, and antiviral activities of cytomegalovirus-specific CD8+ T cells. J Virol *88*, 10894-10908.

Jacobson, M.A., Maecker, H.T., Orr, P.L., D'Amico, R., Van Natta, M., Li, X.D., Pollard, R.B., Bredt, B.M., Adult, A.C.T.G., and the Studies of Ocular Complications of, A.R.G. (2004). Results of a cytomegalovirus (CMV)-specific CD8+/interferon- gamma+ cytokine

flow cytometry assay correlate with clinical evidence of protective immunity in patients with AIDS with CMV retinitis. J Infect Dis *189*, 1362-1373.

Jahn, G., Scholl, B.C., Traupe, B., and Fleckenstein, B. (1987). The two major structural phosphoproteins (pp65 and pp150) of human cytomegalovirus and their antigenic properties. J Gen Virol *68 (Pt 5)*, 1327-1337.

James, E.A., Bui, J., Berger, D., Huston, L., Roti, M., and Kwok, W.W. (2007). Tetramer-guided epitope mapping reveals broad, individualized repertoires of tetanus toxin-specific CD4+ T cells and suggests HLA-based differences in epitope recognition. Int Immunol *19*, 1291-1301.

Johnston, R.J., Comps-Agrar, L., Hackney, J., Yu, X., Huseni, M., Yang, Y., Park, S., Javinal, V., Chiu, H., Irving, B.*, et al.* (2014). The immunoreceptor TIGIT regulates antitumor and antiviral CD8(+) T cell effector function. Cancer Cell *26*, 923-937.

Jones, R.B., Kovacs, C., Chun, T.W., and Ostrowski, M.A. (2012). Short communication: HIV type 1 accumulates in influenza-specific T cells in subjects receiving seasonal vaccination in the context of effective antiretroviral therapy. AIDS Res Hum Retroviruses *28*, 1687-1692.

Jones, T.R., Hanson, L.K., Sun, L., Slater, J.S., Stenberg, R.M., and Campbell, A.E. (1995). Multiple independent loci within the human cytomegalovirus unique short region down-regulate expression of major histocompatibility complex class I heavy chains. J Virol *69*, 4830-4841.

Josefsson, L., von Stockenstrom, S., Faria, N.R., Sinclair, E., Bacchetti, P., Killian, M., Epling, L., Tan, A., Ho, T., Lemey, P.*, et al.* (2013). The HIV-1 reservoir in eight patients on long-term suppressive antiretroviral therapy is stable with few genetic changes over time. Proc Natl Acad Sci U S A *110*, E4987-4996.

Kagele, D., Rossetto, C.C., Tarrant, M.T., and Pari, G.S. (2012). Analysis of the interactions of viral and cellular factors with human cytomegalovirus lytic origin of replication, oriLyt. Virology *424*, 106-114.

Kaleebu, P., Nankya, I.L., Yirrell, D.L., Shafer, L.A., Kyosiimire-Lugemwa, J., Lule, D.B., Morgan, D., Beddows, S., Weber, J., and Whitworth, J.A. (2007). Relation between chemokine receptor use, disease stage, and HIV-1 subtypes A and D: results from a rural Ugandan cohort. J Acquir Immune Defic Syndr *45*, 28-33.

Kalejta, R.F. (2008). Tegument proteins of human cytomegalovirus. Microbiol Mol Biol Rev *72*, 249-265, table of contents.

Kalejta, R.F. (2013). Pre-Immediate Early Tegument Protein Functions. In Cytomegalovirus From Molecular Pathogenesis to Intervention, M.J.L. Reddehase, N. A. W., ed. (Norfolk, UK: Caister Academic Press), pp. 141-151.

Kambayashi, T., and Laufer, T.M. (2014). Atypical MHC class II-expressing antigen-presenting cells: can anything replace a dendritic cell? Nat Rev Immunol *14*, 719-730.

Kamphorst, A.O., Wieland, A., Nasti, T., Yang, S., Zhang, R., Barber, D.L., Konieczny, B.T., Daugherty, C.Z., Koenig, L., Yu, K.*, et al.* (2017). Rescue of exhausted CD8 T cells by PD-1-targeted therapies is CD28-dependent. Science *355*, 1423-1427.

Kaplan, R.C., Sinclair, E., Landay, A.L., Lurain, N., Sharrett, A.R., Gange, S.J., Xue, X., Hunt, P., Karim, R., Kern, D.M.*, et al.* (2011). T cell activation and senescence predict subclinical carotid artery disease in HIV-infected women. J Infect Dis *203*, 452-463.

Karrer, U., Sierro, S., Wagner, M., Oxenius, A., Hengel, H., Koszinowski, U.H., Phillips, R.E., and Klenerman, P. (2003). Memory inflation: continuous accumulation of antiviral CD8+ T cells over time. J Immunol *170*, 2022-2029.

Karrer, U., Wagner, M., Sierro, S., Oxenius, A., Hengel, H., Dumrese, T., Freigang, S., Koszinowski, U.H., Phillips, R.E., and Klenerman, P. (2004). Expansion of protective CD8+ T-cell responses driven by recombinant cytomegaloviruses. J Virol *78*, 2255-2264.

Kearney, M.F., Spindler, J., Shao, W., Yu, S., Anderson, E.M., O'Shea, A., Rehm, C., Poethke, C., Kovacs, N., Mellors, J.W.*, et al.* (2014). Lack of detectable HIV-1 molecular evolution during suppressive antiretroviral therapy. PLoS Pathog *10*, e1004010.

Keele, B.F., Giorgi, E.E., Salazar-Gonzalez, J.F., Decker, J.M., Pham, K.T., Salazar, M.G., Sun, C., Grayson, T., Wang, S., Li, H.*, et al.* (2008). Identification and characterization of transmitted and early founder virus envelopes in primary HIV-1 infection. Proc Natl Acad Sci U S A *105*, 7552-7557.

Keh, W.C., and Gerber, M.A. (1988). In situ hybridization for cytomegalovirus DNA in AIDS patients. Am J Pathol *131*, 490-496.

Kenneson, A., and Cannon, M.J. (2007). Review and meta-analysis of the epidemiology of congenital cytomegalovirus (CMV) infection. Rev Med Virol *17*, 253-276.

Kern, F., Bunde, T., Faulhaber, N., Kiecker, F., Khatamzas, E., Rudawski, I.M., Pruss, A., Gratama, J.W., Volkmer-Engert, R., Ewert, R.*, et al.* (2002). Cytomegalovirus (CMV) phosphoprotein 65 makes a large contribution to shaping the T cell repertoire in CMV-exposed individuals. J Infect Dis *185*, 1709-1716.

Kern, F., Khatamzas, E., Surel, I., Frommel, C., Reinke, P., Waldrop, S.L., Picker, L.J., and Volk, H.D. (1999). Distribution of human CMV-specific memory T cells among the CD8pos. subsets defined by CD57, CD27, and CD45 isoforms. Eur J Immunol *29*, 2908-2915.

Keunen, J.E., and Rothova, A. (1995). Images in clinical medicine. Cytomegalovirus retinitis in AIDS. N Engl J Med *333*, 637.

Khan, N., Cobbold, M., Keenan, R., and Moss, P.A. (2002a). Comparative analysis of CD8+ T cell responses against human cytomegalovirus proteins pp65 and immediate early 1 shows similarities in precursor frequency, oligoclonality, and phenotype. J Infect Dis *185*, 1025-1034.

Khan, N., Hislop, A., Gudgeon, N., Cobbold, M., Khanna, R., Nayak, L., Rickinson, A.B., and Moss, P.A. (2004). Herpesvirus-specific CD8 T cell immunity in old age: cytomegalovirus impairs the response to a coresident EBV infection. J Immunol *173*, 7481-7489.

Khan, N., Shariff, N., Cobbold, M., Bruton, R., Ainsworth, J.A., Sinclair, A.J., Nayak, L., and Moss, P.A. (2002b). Cytomegalovirus seropositivity drives the CD8 T cell repertoire toward greater clonality in healthy elderly individuals. J Immunol *169*, 1984-1992.

Kharchenko, P.V., Silberstein, L., and Scadden, D.T. (2014). Bayesian approach to single-cell differential expression analysis. Nat Methods *11*, 740-742.

Kieffer, T.L., Finucane, M.M., Nettles, R.E., Quinn, T.C., Broman, K.W., Ray, S.C., Persaud, D., and Siliciano, R.F. (2004). Genotypic analysis of HIV-1 drug resistance at the limit of detection: virus production without evolution in treated adults with undetectable HIV loads. J Infect Dis *189*, 1452-1465.

Kim, C., Wilson, T., Fischer, K.F., and Williams, M.A. (2013). Sustained interactions between T cell receptors and antigens promote the differentiation of CD4(+) memory T cells. Immunity *39*, 508-520.

Kimata, M., Cullins, D.L., Brown, M.L., Brand, D.D., Rosloniec, E.F., Myers, L.K., Stuart, J.M., and Kang, A.H. (2012). Characterization of inhibitory T cells induced by an analog of type II collagen in an HLA-DR1 humanized mouse model of autoimmune arthritis. Arthritis Res Ther *14*, R107.

Kiselev, V.Y., Kirschner, K., Schaub, M.T., Andrews, T., Yiu, A., Chandra, T., Natarajan, K.N., Reik, W., Barahona, M., Green, A.R.*, et al.* (2017). SC3: consensus clustering of single-cell RNA-seq data. Nat Methods *14*, 483-486.

Klarenbeek, P.L., Remmerswaal, E.B., ten Berge, I.J., Doorenspleet, M.E., van Schaik, B.D., Esveldt, R.E., Koch, S.D., ten Brinke, A., van Kampen, A.H., Bemelman, F.J., *et al.* (2012). Deep sequencing of antiviral T-cell responses to HCMV and EBV in humans reveals a stable repertoire that is maintained for many years. PLoS Pathog *8*, e1002889.

Klassen, D.K., Drachenberg, C.B., Papadimitriou, J.C., Cangro, C.B., Fink, J.C., Bartlett, S.T., and Weir, M.R. (2000). CMV allograft pancreatitis: diagnosis, treatment, and histological features. Transplantation *69*, 1968-1971.

Klatzmann, D., Champagne, E., Chamaret, S., Gruest, J., Guetard, D., Hercend, T., Gluckman, J.C., and Montagnier, L. (1984). T-lymphocyte T4 molecule behaves as the receptor for human retrovirus LAV. Nature *312*, 767-768.

Klenerman, P., Cerundolo, V., and Dunbar, P.R. (2002). Tracking T cells with tetramers: new tales from new tools. Nat Rev Immunol *2*, 263-272.

Klenerman, P., and Hill, A. (2005). T cells and viral persistence: lessons from diverse infections. Nat Immunol *6*, 873-879.

Klenerman, P., and Oxenius, A. (2016). T cell responses to cytomegalovirus. Nat Rev Immunol *16*, 367-377.

Kline, J.N., Hunninghake, G.M., He, B., Monick, M.M., and Hunninghake, G.W. (1998). Synergistic activation of the human cytomegalovirus major immediate early promoter by prostaglandin E2 and cytokines. Exp Lung Res *24*, 3-14.

Knapp, A.B., Horst, D.A., Eliopoulos, G., Gramm, H.F., Gaber, L.W., Falchuk, K.R., Falchuk, Z.M., and Trey, C. (1983). Widespread cytomegalovirus gastroenterocolitis in a patient with acquired immunodeficiency syndrome. Gastroenterology *85*, 1399-1402.

Koehne, G., Hasan, A., Doubrovina, E., Prockop, S., Tyler, E., Wasilewski, G., and O'Reilly, R.J. (2015). Immunotherapy with Donor T Cells Sensitized with Overlapping Pentadecapeptides for Treatment of Persistent Cytomegalovirus Infection or Viremia. Biol Blood Marrow Transplant *21*, 1663-1678.

Koenig, S., Gendelman, H.E., Orenstein, J.M., Dal Canto, M.C., Pezeshkpour, G.H., Yungbluth, M., Janotta, F., Aksamit, A., Martin, M.A., and Fauci, A.S. (1986). Detection of AIDS virus in macrophages in brain tissue from AIDS patients with encephalopathy. Science *233*, 1089-1093.

Komanduri, K.V., Donahoe, S.M., Moretto, W.J., Schmidt, D.K., Gillespie, G., Ogg, G.S., Roederer, M., Nixon, D.F., and McCune, J.M. (2001). Direct measurement of CD4+ and CD8+ T-cell responses to CMV in HIV-1-infected subjects. Virology *279*, 459-470.

Komatsu, H., Inui, A., Sogo, T., Fujisawa, T., Nagasaka, H., Nonoyama, S., Sierro, S., Northfield, J., Lucas, M., Vargas, A.*, et al.* (2006). Large scale analysis of pediatric antiviral CD8+ T cell populations reveals sustained, functional and mature responses. Immun Ageing *3*, 11.

Komatsu, H., Sierro, S., A, V.C., and Klenerman, P. (2003). Population analysis of antiviral T cell responses using MHC class I-peptide tetramers. Clin Exp Immunol *134*, 9-12.

Kondo, E., Akatsuka, Y., Kuzushima, K., Tsujimura, K., Asakura, S., Tajima, K., Kagami, Y., Kodera, Y., Tanimoto, M., Morishima, Y.*, et al.* (2004). Identification of novel CTL epitopes of CMV-pp65 presented by a variety of HLA alleles. Blood *103*, 630-638.

Kondrack, R.M., Harbertson, J., Tan, J.T., McBreen, M.E., Surh, C.D., and Bradley, L.M. (2003). Interleukin 7 regulates the survival and generation of memory CD4 cells. J Exp Med *198*, 1797-1806.

Koskinen, P.K., Nieminen, M.S., Krogerus, L.A., Lemstrom, K.B., Mattila, S.P., Hayry, P.J., and Lautenschlager, I.T. (1993). Cytomegalovirus infection accelerates cardiac allograft vasculopathy: correlation between angiographic and endomyocardial biopsy findings in heart transplant patients. Transpl Int *6*, 341-347.

Kurz, S.K., Rapp, M., Steffens, H.P., Grzimek, N.K., Schmalz, S., and Reddehase, M.J. (1999). Focal transcriptional activity of murine cytomegalovirus during latency in the lungs. J Virol *73*, 482-494.

Kutza, A.S., Muhl, E., Hackstein, H., Kirchner, H., and Bein, G. (1998). High incidence of active cytomegalovirus infection among septic patients. Clin Infect Dis *26*, 1076-1082.

Kuzushima, K., Hayashi, N., Kimura, H., and Tsurumi, T. (2001). Efficient identification of HLA-A*2402-restricted cytomegalovirus-specific CD8(+) T-cell epitopes by a computer algorithm and an enzyme-linked immunospot assay. Blood *98*, 1872-1881.

LaFemina, R.L., Hayward, G. S. (1980). Structural Organization of the DNA Molecules From Human Cytomegalovirus. In Animal Virus Genetics, R.F. Jaenisch, B.; Fox, C. F., ed. (New York, NY: Academic Press), pp. 39-55.

Laird, G.M., Eisele, E.E., Rabi, S.A., Lai, J., Chioma, S., Blankson, J.N., Siliciano, J.D., and Siliciano, R.F. (2013). Rapid Quantification of the Latent Reservoir for HIV-1 Using a Viral Outgrowth Assay. PLoS Pathogens *9*, e1003398.

Lambotte, O., Taoufik, Y., de Goer, M.G., Wallon, C., Goujard, C., and Delfraissy, J.F. (2000). Detection of infectious HIV in circulating monocytes from patients on prolonged highly active antiretroviral therapy. J Acquir Immune Defic Syndr *23*, 114-119.

Lang, A., Brien, J.D., and Nikolich-Zugich, J. (2009). Inflation and long-term maintenance of CD8 T cells responding to a latent herpesvirus depend upon establishment of latency and presence of viral antigens. J Immunol *183*, 8077-8087.

Langmead, B., and Salzberg, S.L. (2012). Fast gapped-read alignment with Bowtie 2. Nat Methods *9*, 357-359.

Lanzer, K.G., Johnson, L.L., Woodland, D.L., and Blackman, M.A. (2014). Impact of ageing on the response and repertoire of influenza virus-specific CD4 T cells. Immun Ageing *11*, 9.

Lazarevic, V., Glimcher, L.H., and Lord, G.M. (2013). T-bet: a bridge between innate and adaptive immunity. Nat Rev Immunol *13*, 777-789.

Leach, C.T., Cherry, J.D., English, P.A., Hennessey, K., Giorgi, J.V., Visscher, B.R., Dudley, J.P., and Detels, R. (1993). The relationship between T-cell levels and CMV infection in asymptomatic HIV-1 antibody-positive homosexual men. J Acquir Immune Defic Syndr *6*, 407-413.

Legoux, F., Gautreau, L., Hesnard, L., Leger, A., Moyon, M., Devilder, M.C., Bonneville, M., and Saulquin, X. (2013). Characterization of the human CD4(+) T-cell repertoire specific for major histocompatibility class I-restricted antigens. Eur J Immunol *43*, 3244-3253.

Leisner, C., Loeth, N., Lamberth, K., Justesen, S., Sylvester-Hvid, C., Schmidt, E.G., Claesson, M., Buus, S., and Stryhn, A. (2008). One-pot, mix-and-read peptide-MHC tetramers. PLoS One *3*, e1678.

Li, B., and Dewey, C.N. (2011). RSEM: accurate transcript quantification from RNA-Seq data with or without a reference genome. BMC Bioinformatics *12*, 323.

Li, C.R., Greenberg, P.D., Gilbert, M.J., Goodrich, J.M., and Riddell, S.R. (1994). Recovery of HLA-restricted cytomegalovirus (CMV)-specific T-cell responses after allogeneic bone marrow transplant: correlation with CMV disease and effect of ganciclovir prophylaxis. Blood *83*, 1971-1979.

Li, J., Huston, G., and Swain, S.L. (2003). IL-7 promotes the transition of CD4 effectors to persistent memory cells. J Exp Med *198*, 1807-1815.

Li Pira, G., Bottone, L., Ivaldi, F., Pelizzoli, R., Del Galdo, F., Lozzi, L., Bracci, L., Loregian, A., Palu, G., De Palma, R.*, et al.* (2004). Identification of new Th peptides from the cytomegalovirus protein pp65 to design a peptide library for generation of CD4 T cell lines for cellular immunoreconstitution. Int Immunol *16*, 635-642.

Li, S., Juarez, J., Alali, M., Dwyer, D., Collman, R., Cunningham, A., and Naif, H.M. (1999). Persistent CCR5 utilization and enhanced macrophage tropism by primary blood human immunodeficiency virus type 1 isolates from advanced stages of disease and comparison to tissue-derived isolates. J Virol *73*, 9741-9755.

Lichtner, M., Cicconi, P., Vita, S., Cozzi-Lepri, A., Galli, M., Lo Caputo, S., Saracino, A., De Luca, A., Moioli, M., Maggiolo, F.*, et al.* (2015). Cytomegalovirus coinfection is associated with an increased risk of severe non-AIDS-defining events in a large cohort of HIV-infected patients. J Infect Dis *211*, 178-186.

Limaye, A.P., Bakthavatsalam, R., Kim, H.W., Kuhr, C.S., Halldorson, J.B., Healey, P.J., and Boeckh, M. (2004). Late-onset cytomegalovirus disease in liver transplant recipients despite antiviral prophylaxis. Transplantation *78*, 1390-1396.

Liuzzo, G., Goronzy, J.J., Yang, H., Kopecky, S.L., Holmes, D.R., Frye, R.L., and Weyand, C.M. (2000). Monoclonal T-cell proliferation and plaque instability in acute coronary syndromes. Circulation *101*, 2883-2888.

Ljungman, P., Boeckh, M., Hirsch, H.H., Josephson, F., Lundgren, J., Nichols, G., Pikis, A., Razonable, R.R., Miller, V., Griffiths, P.D.*, et al.* (2017). Definitions of Cytomegalovirus Infection and Disease in Transplant Patients for Use in Clinical Trials. Clin Infect Dis *64*, 87-91.

Llado, L., Castellote, J., Fabregat, J., Carratala, J., Serrano, T., Ramos, E., Torras, J., and Rafecas, A. (2008). Antral mass due to cytomegalovirus infection requiring gastrectomy in a liver transplant recipient. Transpl Infect Dis *10*, 354-357.

Llano, M., Guma, M., Ortega, M., Angulo, A., and Lopez-Botet, M. (2003). Differential effects of US2, US6 and US11 human cytomegalovirus proteins on HLA class Ia and HLA-E expression: impact on target susceptibility to NK cell subsets. Eur J Immunol *33*, 2744-2754.

Long, H.M., Chagoury, O.L., Leese, A.M., Ryan, G.B., James, E., Morton, L.T., Abbott, R.J., Sabbah, S., Kwok, W., and Rickinson, A.B. (2013). MHC II tetramers visualize human CD4+ T cell responses to Epstein-Barr virus infection and demonstrate atypical kinetics of the nuclear antigen EBNA1 response. J Exp Med *210*, 933-949.

Longmate, J., York, J., La Rosa, C., Krishnan, R., Zhang, M., Senitzer, D., and Diamond, D.J. (2001). Population coverage by HLA class-I restricted cytotoxic T-lymphocyte epitopes. Immunogenetics *52*, 165-173.

Lorenzo-Redondo, R., Fryer, H.R., Bedford, T., Kim, E.Y., Archer, J., Pond, S.L.K., Chung, Y.S., Penugonda, S., Chipman, J., Fletcher, C.V.*, et al.* (2016). Persistent HIV-1 replication maintains the tissue reservoir during therapy. Nature *530*, 51-56.

Macagno, A., Bernasconi, N.L., Vanzetta, F., Dander, E., Sarasini, A., Revello, M.G., Gerna, G., Sallusto, F., and Lanzavecchia, A. (2010). Isolation of human monoclonal antibodies that potently neutralize human cytomegalovirus infection by targeting different epitopes on the gH/gL/UL128-131A complex. J Virol *84*, 1005-1013.

Mach, M., Osinski, K., Kropff, B., Schloetzer-Schrehardt, U., Krzyzaniak, M., and Britt, W. (2007). The carboxy-terminal domain of glycoprotein N of human cytomegalovirus is required for virion morphogenesis. J Virol *81*, 5212-5224.

Maidji, E., Somsouk, M., Rivera, J.M., Hunt, P.W., and Stoddart, C.A. (2017). Replication of CMV in the gut of HIV-infected individuals and epithelial barrier dysfunction. PLoS Pathog *13*, e1006202.

Maldarelli, F., Wu, X., Su, L., Simonetti, F.R., Shao, W., Hill, S., Spindler, J., Ferris, A.L., Mellors, J.W., Kearney, M.F.*, et al.* (2014). HIV latency. Specific HIV integration sites are linked to clonal expansion and persistence of infected cells. Science *345*, 179-183.

Malone, C.L., Vesole, D.H., and Stinski, M.F. (1990). Transactivation of a human cytomegalovirus early promoter by gene products from the immediate-early gene IE2 and augmentation by IE1: mutational analysis of the viral proteins. J Virol *64*, 1498-1506.

Marker, S.C., Howard, R.J., Simmons, R.L., Kalis, J.M., Connelly, D.P., Najarian, J.S., and Balfour, H.H., Jr. (1981). Cytomegalovirus infection: a quantitative prospective study of three hundred twenty consecutive renal transplants. Surgery *89*, 660-671.

Martins, G., and Calame, K. (2008). Regulation and functions of Blimp-1 in T and B lymphocytes. Annu Rev Immunol *26*, 133-169.

Marvel, J., Lightstone, E., Samberg, N.L., Ettinghausen, D., and Stauss, H.J. (1991). The CD45RA molecule is expressed in naive murine CTL precursors but absent in memory and effector CTL. Int Immunol *3*, 21-28.

Mason, G.M., Jackson, S., Okecha, G., Poole, E., Sissons, J.G., Sinclair, J., and Wills, M.R. (2013). Human cytomegalovirus latency-associated proteins elicit immune-suppressive IL-10 producing CD4(+) T cells. PLoS Pathog *9*, e1003635.

Masopust, D., Vezys, V., Marzo, A.L., and Lefrancois, L. (2001). Preferential localization of effector memory cells in nonlymphoid tissue. Science *291*, 2413-2417.

Masuoka, M., Yoshimuta, T., Hamada, M., Okamoto, M., Fumimori, T., Honda, J., Oizumi, K., and Itoh, K. (2001). Identification of the HLA-A24 peptide epitope within cytomegalovirus protein pp65 recognized by CMV-specific cytotoxic T lymphocytes. Viral Immunol *14*, 369-377.

McDavid, A., Finak, G., Chattopadyay, P.K., Dominguez, M., Lamoreaux, L., Ma, S.S., Roederer, M., and Gottardo, R. (2013). Data exploration, quality control and testing in single-cell qPCR-based gene expression experiments. Bioinformatics *29*, 461-467.

McDonald, K., Rector, T.S., Braulin, E.A., Kubo, S.H., and Olivari, M.T. (1989). Association of coronary artery disease in cardiac transplant recipients with cytomegalovirus infection. Am J Cardiol *64*, 359-362.

McElrath, M.J., Steinman, R.M., and Cohn, Z.A. (1991). Latent HIV-1 infection in enriched populations of blood monocytes and T cells from seropositive patients. J Clin Invest *87*, 27-30.

Meijer, E., Dekker, A.W., Rozenberg-Arska, M., Weersink, A.J., and Verdonck, L.F. (2002). Influence of cytomegalovirus seropositivity on outcome after T cell-depleted bone marrow transplantation: contrasting results between recipients of grafts from related and unrelated donors. Clin Infect Dis *35*, 703-712.

Mendelson, M., Monard, S., Sissons, P., and Sinclair, J. (1996). Detection of endogenous human cytomegalovirus in CD34+ bone marrow progenitors. J Gen Virol *77 (Pt 12)*, 3099-3102.

Mens, H., Pedersen, A.G., Jorgensen, L.B., Hue, S., Yang, Y., Gerstoft, J., and Katzenstein, T.L. (2007). Investigating signs of recent evolution in the pool of proviral HIV type 1 DNA during years of successful HAART. AIDS Res Hum Retroviruses *23*, 107-115.

Meyer, H., Bankier, A.T., Landini, M.P., Brown, C.M., Barrell, B.G., Ruger, B., and Mach, M. (1988). Identification and procaryotic expression of the gene coding for the highly immunogenic 28-kilodalton structural phosphoprotein (pp28) of human cytomegalovirus. J Virol *62*, 2243-2250.

Meyer-Olson, D., Simons, B.C., Conrad, J.A., Smith, R.M., Barnett, L., Lorey, S.L., Duncan, C.B., Ramalingam, R., and Kalams, S.A. (2010). Clonal expansion and TCR-independent differentiation shape the HIV-specific CD8+ effector-memory T-cell repertoire in vivo. Blood *116*, 396-405.

Miller, C.J., McChesney, M., and Moore, P.F. (1992). Langerhans cells, macrophages and lymphocyte subsets in the cervix and vagina of rhesus macaques. Lab Invest *67*, 628-634.

Mocarski, E.S., Shenk, T., Griffiths, P.D., and Pass, R.F. (2013). Cytomegaloviruses. In Fields Virology, D.M. Knipe, and P.M. Howley, eds. (Philadelphia, PA: Lippincott Williams & Wilkins), pp. 1960-2014.

Monack, D.M., Mueller, A., and Falkow, S. (2004). Persistent bacterial infections: the interface of the pathogen and the host immune system. Nat Rev Microbiol *2*, 747-765.

Morra, M., Zubiaur, M., Terhorst, C., Sancho, J., and Malavasi, F. (1998). CD38 is functionally dependent on the TCR/CD3 complex in human T cells. FASEB J *12*, 581-592.

Muhlemann, K., Miller, R.K., Metlay, L., and Menegus, M.A. (1992). Cytomegalovirus infection of the human placenta: an immunocytochemical study. Hum Pathol *23*, 1234-1237.

Munks, M.W., Cho, K.S., Pinto, A.K., Sierro, S., Klenerman, P., and Hill, A.B. (2006). Four distinct patterns of memory CD8 T cell responses to chronic murine cytomegalovirus infection. J Immunol *177*, 450-458.

Murakami, N., and Riella, L.V. (2016). CD4+ CD28-Negative Cells: Armed and Dangerous. Am J Transplant *16*, 1045-1046.

Murphy, K., and Weaver, C. (2017). Janeway's Immunobiology, 9 edn (New York, NY: Garland Science, Taylor & Francis Group).

Mutimer, D.J., Shaw, J., O'Donnell, K., and Elias, E. (1997). Enhanced (cytomegalovirus) viral replication after transplantation for fulminant hepatic failure. Liver Transpl Surg *3*, 506-512.

Myerson, D., Hackman, R.C., Nelson, J.A., Ward, D.C., and McDougall, J.K. (1984). Widespread presence of histologically occult cytomegalovirus. Hum Pathol *15*, 430-439.

Naeger, D.M., Martin, J.N., Sinclair, E., Hunt, P.W., Bangsberg, D.R., Hecht, F., Hsue, P., McCune, J.M., and Deeks, S.G. (2010). Cytomegalovirus-specific T cells persist at

very high levels during long-term antiretroviral treatment of HIV disease. PLoS One *5*, e8886.

Nastke, M.D., Herrgen, L., Walter, S., Wernet, D., Rammensee, H.G., and Stevanovic, S. (2005). Major contribution of codominant CD8 and CD4 T cell epitopes to the human cytomegalovirus-specific T cell repertoire. Cell Mol Life Sci *62*, 77-86.

Nebbia, G., Mattes, F.M., Smith, C., Hainsworth, E., Kopycinski, J., Burroughs, A., Griffiths, P.D., Klenerman, P., and Emery, V.C. (2008). Polyfunctional cytomegalovirus-specific CD4+ and pp65 CD8+ T cells protect against high-level replication after liver transplantation. Am J Transplant *8*, 2590-2599.

Neiman, P.E., Reeves, W., Ray, G., Flournoy, N., Lerner, K.G., Sale, G.E., and Thomas, E.D. (1977). A prospective analysis interstitial pneumonia and opportunistic viral infection among recipients of allogeneic bone marrow grafts. J Infect Dis *136*, 754-767.

Ng-Bautista, C.L., and Sedmak, D.D. (1995). Cytomegalovirus infection is associated with absence of alveolar epithelial cell HLA class II antigen expression. J Infect Dis *171*, 39-44.

Nicholas, K.J., Flaherty, D.K., Smith, R.M., Sather, D.N., and Kalams, S.A. (2017). Chronic HIV-1 Infection Impairs Superantigen-Induced Activation of Peripheral CD4+CXCR5+PD-1+ Cells, With Relative Preservation of Recall Antigen-Specific Responses. J Acquir Immune Defic Syndr *74*, 72-80.

Nose, H., Kubota, R., Seth, N.P., Goon, P.K., Tanaka, Y., Izumo, S., Usuku, K., Ohara, Y., Wucherpfennig, K.W., Bangham, C.R.*, et al.* (2007). Ex vivo analysis of human T lymphotropic virus type 1-specific CD4+ cells by use of a major histocompatibility complex class II tetramer composed of a neurological disease-susceptibility allele and its immunodominant peptide. J Infect Dis *196*, 1761-1772.

O'Bryan, J.M., Woda, M., Co, M., Mathew, A., and Rothman, A.L. (2013). Telomere length dynamics in human memory T cells specific for viruses causing acute or latent infections. Immun Ageing *10*, 37.

O'Hara, G.A., Welten, S.P., Klenerman, P., and Arens, R. (2012). Memory T cell inflation: understanding cause and effect. Trends Immunol *33*, 84-90.

Ogawa-Goto, K., Tanaka, K., Gibson, W., Moriishi, E., Miura, Y., Kurata, T., Irie, S., and Sata, T. (2003). Microtubule network facilitates nuclear targeting of human cytomegalovirus capsid. J Virol *77*, 8541-8547.

Okoye, A.A., Rohankhedkar, M., Abana, C., Pattenn, A., Reyes, M., Pexton, C., Lum, R., Sylwester, A., Planer, S.L., Legasse, A.*, et al.* (2012). Naive T cells are dispensable for memory CD4+ T cell homeostasis in progressive simian immunodeficiency virus infection. J Exp Med *209*, 641-651.

Okoye, A.A., Rohankhedkar, M., Konfe, A.L., Abana, C.O., Reyes, M.D., Clock, J.A., Duell, D.M., Sylwester, A.W., Sammader, P., Legasse, A.W.*, et al.* (2015). Effect of IL-7 Therapy on Naive and Memory T Cell Homeostasis in Aged Rhesus Macaques. J Immunol *195*, 4292-4305.

Oswald-Richter, K., Grill, S.M., Leelawong, M., Tseng, M., Kalams, S.A., Hulgan, T., Haas, D.W., and Unutmaz, D. (2007). Identification of a CCR5-expressing T cell subset that is resistant to R5-tropic HIV infection. PLoS Pathog *3*, e58.

Pachnio, A., Ciaurriz, M., Begum, J., Lal, N., Zuo, J., Beggs, A., and Moss, P. (2016). Cytomegalovirus Infection Leads to Development of High Frequencies of Cytotoxic Virus-Specific CD4+ T Cells Targeted to Vascular Endothelium. PLoS Pathog *12*, e1005832.

Pachnio, A., Zuo, J., Ryan, G.B., Begum, J., and Moss, P.A. (2015). The Cellular Localization of Human Cytomegalovirus Glycoprotein Expression Greatly Influences the Frequency and Functional Phenotype of Specific CD4+ T Cell Responses. J Immunol *195*, 3803-3815.

Palella, F.J., Jr., Delaney, K.M., Moorman, A.C., Loveless, M.O., Fuhrer, J., Satten, G.A., Aschman, D.J., and Holmberg, S.D. (1998). Declining morbidity and mortality among patients with advanced human immunodeficiency virus infection. HIV Outpatient Study Investigators. N Engl J Med *338*, 853-860.

Pari, G.S., and Anders, D.G. (1993). Eleven loci encoding trans-acting factors are required for transient complementation of human cytomegalovirus oriLyt-dependent DNA replication. J Virol *67*, 6979-6988.

Pari, G.S., Kacica, M.A., and Anders, D.G. (1993). Open reading frames UL44, IRS1/TRS1, and UL36-38 are required for transient complementation of human cytomegalovirus oriLyt-dependent DNA synthesis. J Virol *67*, 2575-2582.

Pass, R.F., Fowler, K.B., Boppana, S.B., Britt, W.J., and Stagno, S. (2006). Congenital cytomegalovirus infection following first trimester maternal infection: symptoms at birth and outcome. J Clin Virol *35*, 216-220.

Patel, A.P., Tirosh, I., Trombetta, J.J., Shalek, A.K., Gillespie, S.M., Wakimoto, H., Cahill, D.P., Nahed, B.V., Curry, W.T., Martuza, R.L.*, et al.* (2014). Single-cell RNA-seq highlights intratumoral heterogeneity in primary glioblastoma. Science *344*, 1396-1401.

Pearce, E.L., Mullen, A.C., Martins, G.A., Krawczyk, C.M., Hutchins, A.S., Zediak, V.P., Banica, M., DiCioccio, C.B., Gross, D.A., Mao, C.A.*, et al.* (2003). Control of effector CD8+ T cell function by the transcription factor Eomesodermin. Science *302*, 1041-1043.

Pepper, M., and Jenkins, M.K. (2011). Origins of CD4(+) effector and central memory T cells. Nat Immunol *12*, 467-471.

Persaud, D., Ray, S.C., Kajdas, J., Ahonkhai, A., Siberry, G.K., Ferguson, K., Ziemniak, C., Quinn, T.C., Casazza, J.P., Zeichner, S.*, et al.* (2007). Slow human immunodeficiency virus type 1 evolution in viral reservoirs in infants treated with effective antiretroviral therapy. AIDS Res Hum Retroviruses *23*, 381-390.

Persaud, D., Siberry, G.K., Ahonkhai, A., Kajdas, J., Monie, D., Hutton, N., Watson, D.C., Quinn, T.C., Ray, S.C., and Siliciano, R.F. (2004). Continued production of drug-sensitive human immunodeficiency virus type 1 in children on combination antiretroviral therapy who have undetectable viral loads. J Virol *78*, 968-979.

Petersen, J., van Bergen, J., Loh, K.L., Kooy-Winkelaar, Y., Beringer, D.X., Thompson, A., Bakker, S.F., Mulder, C.J., Ladell, K., McLaren, J.E.*, et al.* (2015). Determinants of gliadin-specific T cell selection in celiac disease. J Immunol *194*, 6112-6122.

Picelli, S., Bjorklund, A.K., Faridani, O.R., Sagasser, S., Winberg, G., and Sandberg, R. (2013). Smart-seq2 for sensitive full-length transcriptome profiling in single cells. Nat Methods *10*, 1096-1098.

Picelli, S., Faridani, O.R., Bjorklund, A.K., Winberg, G., Sagasser, S., and Sandberg, R. (2014). Full-length RNA-seq from single cells using Smart-seq2. Nat Protoc *9*, 171-181.

Pido-Lopez, J., Wang, Y., Seidl, T., Babaahmady, K., Vaughan, R., and Lehner, T. (2009). The effect of allogeneic in vitro stimulation and in vivo immunization on memory CD4(+) T-cell APOBEC3G expression and HIV-1 infectivity. Eur J Immunol *39*, 1956-1965.

Pierson, T., McArthur, J., and Siliciano, R.F. (2000). Reservoirs for HIV-1: mechanisms for viral persistence in the presence of antiviral immune responses and antiretroviral therapy. Annual review of immunology *18*, 665-708.

Podlech, J., Holtappels, R., Wirtz, N., Steffens, H.P., and Reddehase, M.J. (1998). Reconstitution of CD8 T cells is essential for the prevention of multiple-organ cytomegalovirus histopathology after bone marrow transplantation. J Gen Virol *79 (Pt 9)*, 2099-2104.

Poli, C., Raffin, C., Dojcinovic, D., Luescher, I., Ayyoub, M., and Valmori, D. (2013). MHC class II/ESO tetramer-based generation of in vitro primed anti-tumor T-helper lines for adoptive cell therapy of cancer. Haematologica *98*, 316-322.

Portela, D., Patel, R., Larson-Keller, J.J., Ilstrup, D.M., Wiesner, R.H., Steers, J.L., Krom, R.A., and Paya, C.V. (1995). OKT3 treatment for allograft rejection is a risk factor for cytomegalovirus disease in liver transplantation. J Infect Dis *171*, 1014-1018.

Pouria, S., State, O.I., Wong, W., and Hendry, B.M. (1998). CMV infection is associated with transplant renal artery stenosis. QJM *91*, 185-189.

Price, D.A., Brenchley, J.M., Ruff, L.E., Betts, M.R., Hill, B.J., Roederer, M., Koup, R.A., Migueles, S.A., Gostick, E., Wooldridge, L.*, et al.* (2005). Avidity for antigen shapes clonal dominance in CD8+ T cell populations specific for persistent DNA viruses. J Exp Med *202*, 1349-1361.

Price, R.W., Brew, B., Sidtis, J., Rosenblum, M., Scheck, A.C., and Cleary, P. (1988). The brain in AIDS: central nervous system HIV-1 infection and AIDS dementia complex. Science *239*, 586-592.

Prichard, M.N., Jairath, S., Penfold, M.E., St Jeor, S., Bohlman, M.C., and Pari, G.S. (1998). Identification of persistent RNA-DNA hybrid structures within the origin of replication of human cytomegalovirus. J Virol *72*, 6997-7004.

Prosch, S., Staak, K., Stein, J., Liebenthal, C., Stamminger, T., Volk, H.D., and Kruger, D.H. (1995). Stimulation of the human cytomegalovirus IE enhancer/promoter in HL-60 cells by TNFalpha is mediated via induction of NF-kappaB. Virology *208*, 197-206.

Prosch, S., Wendt, C.E., Reinke, P., Priemer, C., Oppert, M., Kruger, D.H., Volk, H.D., and Docke, W.D. (2000). A novel link between stress and human cytomegalovirus (HCMV) infection: sympathetic hyperactivity stimulates HCMV activation. Virology *272*, 357-365.

Puchtler, E., and Stamminger, T. (1991). An inducible promoter mediates abundant expression from the immediate-early 2 gene region of human cytomegalovirus at late times after infection. J Virol *65*, 6301-6306.

Qiu, X., Mao, Q., Tang, Y., Wang, L., Chawla, R., Pliner, H.A., and Trapnell, C. (2017). Reversed graph embedding resolves complex single-cell trajectories. Nat Methods.

Quayle, A.J., Xu, C., Mayer, K.H., and Anderson, D.J. (1997). T lymphocytes and macrophages, but not motile spermatozoa, are a significant source of human immunodeficiency virus in semen. J Infect Dis *176*, 960-968.

Quinnan, G.V., Jr., Kirmani, N., Rook, A.H., Manischewitz, J.F., Jackson, L., Moreschi, G., Santos, G.W., Saral, R., and Burns, W.H. (1982). Cytotoxic t cells in cytomegalovirus infection: HLA-restricted T-lymphocyte and non-T-lymphocyte cytotoxic responses correlate with recovery from cytomegalovirus infection in bone-marrow-transplant recipients. N Engl J Med *307*, 7-13.

Rabenau, H.F., Lennemann, T., Kircher, C., Gurtler, L., Staszewski, S., Preiser, W., McPherson, P., Allwinn, R., and Doerr, H.W. (2010). Prevalence- and gender-specific immune response to opportunistic infections in HIV-infected patients in Lesotho. Sex Transm Dis *37*, 454-459.

Ranasinghe, S., Lamothe, P.A., Soghoian, D.Z., Kazer, S.W., Cole, M.B., Shalek, A.K., Yosef, N., Jones, R.B., Donaghey, F., Nwonu, C.*, et al.* (2016). Antiviral CD8+ T Cells Restricted by Human Leukocyte Antigen Class II Exist during Natural HIV Infection and Exhibit Clonal Expansion. Immunity *45*, 917-930.

Redeker, A., Welten, S.P., and Arens, R. (2014). Viral inoculum dose impacts memory T-cell inflation. Eur J Immunol *44*, 1046-1057.

Rees, W.A., Yager, T.D., Korte, J., and von Hippel, P.H. (1993). Betaine can eliminate the base pair composition dependence of DNA melting. Biochemistry *32*, 137-144.

Reeves, M.B., MacAry, P.A., Lehner, P.J., Sissons, J.G., and Sinclair, J.H. (2005). Latency, chromatin remodeling, and reactivation of human cytomegalovirus in the dendritic cells of healthy carriers. Proc Natl Acad Sci U S A *102*, 4140-4145.

Remmerswaal, E.B., Klarenbeek, P.L., Alves, N.L., Doorenspleet, M.E., van Schaik, B.D., Esveldt, R.E., Idu, M.M., van Leeuwen, E.M., van der Bom-Baylon, N., van Kampen, A.H.*, et al.* (2015). Clonal evolution of CD8+ T cell responses against latent viruses: relationship among phenotype, localization, and function. J Virol *89*, 568-580.

Rentenaar, R.J., Gamadia, L.E., van DerHoek, N., van Diepen, F.N., Boom, R., Weel, J.F., Wertheim-van Dillen, P.M., van Lier, R.A., and ten Berge, I.J. (2000). Development of virus-specific CD4(+) T cells during primary cytomegalovirus infection. J Clin Invest *105*, 541-548.

Renzette, N., Bhattacharjee, B., Jensen, J.D., Gibson, L., and Kowalik, T.F. (2011). Extensive genome-wide variability of human cytomegalovirus in congenitally infected infants. PLoS Pathog *7*, e1001344.

Retiere, C., Prod'homme, V., Imbert-Marcille, B.M., Bonneville, M., Vie, H., and Hallet, M.M. (2000). Generation of cytomegalovirus-specific human T-lymphocyte clones by using autologous B-lymphoblastoid cells with stable expression of pp65 or IE1 proteins: a tool to study the fine specificity of the antiviral response. J Virol *74*, 3948-3952.

Reusser, P., Cathomas, G., Attenhofer, R., Tamm, M., and Thiel, G. (1999). Cytomegalovirus (CMV)-specific T cell immunity after renal transplantation mediates protection from CMV disease by limiting the systemic virus load. J Infect Dis *180*, 247-253.

Reusser, P., Riddell, S.R., Meyers, J.D., and Greenberg, P.D. (1991). Cytotoxic T-lymphocyte response to cytomegalovirus after human allogeneic bone marrow transplantation: pattern of recovery and correlation with cytomegalovirus infection and disease. Blood *78*, 1373-1380.

Rist, M., Cooper, L., Elkington, R., Walker, S., Fazou, C., Tellam, J., Crough, T., and Khanna, R. (2005). Ex vivo expansion of human cytomegalovirus-specific cytotoxic T cells by recombinant polyepitope: implications for HCMV immunotherapy. Eur J Immunol *35*, 996-1007.

Robain, M., Carre, N., Dussaix, E., Salmon-Ceron, D., and Meyer, L. (1998). Incidence and sexual risk factors of cytomegalovirus seroconversion in HIV-infected subjects. The SEROCO Study Group. Sex Transm Dis *25*, 476-480.

Roberts, W.H., Sneddon, J.M., Waldman, J., and Stephens, R.E. (1989). Cytomegalovirus infection of gastrointestinal endothelium demonstrated by simultaneous nucleic acid hybridization and immunohistochemistry. Arch Pathol Lab Med *113*, 461-464.

Roizmann, B., Desrosiers, R.C., Fleckenstein, B., Lopez, C., Minson, A.C., and Studdert, M.J. (1992). The family Herpesviridae: an update. The Herpesvirus Study Group of the International Committee on Taxonomy of Viruses. Arch Virol *123*, 425-449.

Ross, S.A., and Boppana, S.B. (2005). Congenital cytomegalovirus infection: outcome and diagnosis. Semin Pediatr Infect Dis *16*, 44-49.

Rowe, W.P., Hartley, J.W., Cramblett, H.G., and Mastrota, F.M. (1958). Detection of human salivary gland virus in the mouth and urine of children. Am J Hyg *67*, 57-65.

Rowe, W.P., Hartley, J.W., Waterman, S., Turner, H.C., and Huebner, R.J. (1956). Cytopathogenic agent resembling human salivary gland virus recovered from tissue cultures of human adenoids. Proc Soc Exp Biol Med *92*, 418-424.

Ruff, C.T., Ray, S.C., Kwon, P., Zinn, R., Pendleton, A., Hutton, N., Ashworth, R., Gange, S., Quinn, T.C., Siliciano, R.F.*, et al.* (2002). Persistence of wild-type virus and lack of temporal structure in the latent reservoir for human immunodeficiency virus type 1 in pediatric patients with extensive antiretroviral exposure. J Virol *76*, 9481-9492.

Ruger, B., Klages, S., Walla, B., Albrecht, J., Fleckenstein, B., Tomlinson, P., and Barrell, B. (1987). Primary structure and transcription of the genes coding for the two virion phosphoproteins pp65 and pp71 of human cytomegalovirus. J Virol *61*, 446-453.

Ruiz, L., Martinez-Picado, J., Romeu, J., Paredes, R., Zayat, M.K., Marfil, S., Negredo, E., Sirera, G., Tural, C., and Clotet, B. (2000). Structured treatment interruption in chronically HIV-1 infected patients after long-term viral suppression. AIDS *14*, 397-403.

Sabatino, J.J., Jr., Huang, J., Zhu, C., and Evavold, B.D. (2011). High prevalence of low affinity peptide-MHC II tetramer-negative effectors during polyclonal CD4+ T cell responses. J Exp Med *208*, 81-90.

Sacre, K., Hunt, P.W., Hsue, P.Y., Maidji, E., Martin, J.N., Deeks, S.G., Autran, B., and McCune, J.M. (2012). A role for cytomegalovirus-specific CD4+CX3CR1+ T cells and cytomegalovirus-induced T-cell immunopathology in HIV-associated atherosclerosis. AIDS *26*, 805-814.

Sagedal, S., Nordal, K.P., Hartmann, A., Sund, S., Scott, H., Degre, M., Foss, A., Leivestad, T., Osnes, K., Fauchald, P*., et al.* (2002). The impact of cytomegalovirus infection and disease on rejection episodes in renal allograft recipients. Am J Transplant *2*, 850-856.

Sallusto, F., Lenig, D., Forster, R., Lipp, M., and Lanzavecchia, A. (1999). Two subsets of memory T lymphocytes with distinct homing potentials and effector functions. Nature *401*, 708-712.

Salmon-Ceron, D., Mazeron, M.C., Chaput, S., Boukli, N., Senechal, B., Houhou, N., Katlama, C., Matheron, S., Fillet, A.M., Gozlan, J*., et al.* (2000). Plasma cytomegalovirus DNA, pp65 antigenaemia and a low CD4 cell count remain risk factors for cytomegalovirus disease in patients receiving highly active antiretroviral therapy. AIDS *14*, 1041-1049.

Satija, R., Farrell, J.A., Gennert, D., Schier, A.F., and Regev, A. (2015). Spatial reconstruction of single-cell gene expression data. Nat Biotechnol *33*, 495-502.

Scalzo, A.A., Forbes, C.A., Smith, L.M., and Loh, L.C. (2009). Transcriptional analysis of human cytomegalovirus and rat cytomegalovirus homologues of the M73/M73.5 spliced gene family. Arch Virol *154*, 65-75.

Schones, D.E., Cui, K., Cuddapah, S., Roh, T.Y., Barski, A., Wang, Z., Wei, G., and Zhao, K. (2008). Dynamic regulation of nucleosome positioning in the human genome. Cell *132*, 887-898.

Schrier, R.D., Nelson, J.A., and Oldstone, M.B. (1985). Detection of human cytomegalovirus in peripheral blood lymphocytes in a natural infection. Science *230*, 1048-1051.

Seckert, C.K., Griessl, M., Buttner, J.K., Scheller, S., Simon, C.O., Kropp, K.A., Renzaho, A., Kuhnapfel, B., Grzimek, N.K., and Reddehase, M.J. (2012). Viral latency drives 'memory inflation': a unifying hypothesis linking two hallmarks of cytomegalovirus infection. Med Microbiol Immunol *201*, 551-566.

Seckert, C.K., Renzaho, A., Tervo, H.M., Krause, C., Deegen, P., Kuhnapfel, B., Reddehase, M.J., and Grzimek, N.K. (2009). Liver sinusoidal endothelial cells are a site of murine cytomegalovirus latency and reactivation. J Virol *83*, 8869-8884.

Seckert, C.K., Schader, S.I., Ebert, S., Thomas, D., Freitag, K., Renzaho, A., Podlech, J., Reddehase, M.J., and Holtappels, R. (2011). Antigen-presenting cells of haematopoietic origin prime cytomegalovirus-specific CD8 T-cells but are not sufficient for driving memory inflation during viral latency. J Gen Virol *92*, 1994-2005.

Senechal, B., Boruchov, A.M., Reagan, J.L., Hart, D.N., and Young, J.W. (2004). Infection of mature monocyte-derived dendritic cells with human cytomegalovirus inhibits stimulation of T-cell proliferation via the release of soluble CD83. Blood *103*, 4207-4215.

Sester, M., Sester, U., Gartner, B., Heine, G., Girndt, M., Mueller-Lantzsch, N., Meyerhans, A., and Kohler, H. (2001). Levels of virus-specific CD4 T cells correlate with cytomegalovirus control and predict virus-induced disease after renal transplantation. Transplantation *71*, 1287-1294.

Sester, M., Sester, U., Gartner, B., Kubuschok, B., Girndt, M., Meyerhans, A., and Kohler, H. (2002). Sustained high frequencies of specific CD4 T cells restricted to a single persistent virus. J Virol *76*, 3748-3755.

Shabir, S., Smith, H., Kaul, B., Pachnio, A., Jham, S., Kuravi, S., Ball, S., Chand, S., Moss, P., Harper, L.*, et al.* (2016). Cytomegalovirus-Associated CD4(+) CD28(null) Cells in NKG2D-Dependent Glomerular Endothelial Injury and Kidney Allograft Dysfunction. Am J Transplant *16*, 1113-1128.

Shimamura, M., Mach, M., and Britt, W.J. (2006). Human cytomegalovirus infection elicits a glycoprotein M (gM)/gN-specific virus-neutralizing antibody response. J Virol *80*, 4591-4600.

Shugay, M., Bagaev, D.V., Turchaninova, M.A., Bolotin, D.A., Britanova, O.V., Putintseva, E.V., Pogorelyy, M.V., Nazarov, V.I., Zvyagin, I.V., Kirgizova, V.I.*, et al.*

(2015). VDJtools: Unifying Post-analysis of T Cell Receptor Repertoires. PLoS Comput Biol *11*, e1004503.

Sia, I.G., and Patel, R. (2000). New strategies for prevention and therapy of cytomegalovirus infection and disease in solid-organ transplant recipients. Clin Microbiol Rev *13*, 83-121, table of contents.

Sierro, S., Rothkopf, R., and Klenerman, P. (2005). Evolution of diverse antiviral CD8+ T cell populations after murine cytomegalovirus infection. Eur J Immunol *35*, 1113-1123.

Silva, M.C., Yu, Q.C., Enquist, L., and Shenk, T. (2003). Human cytomegalovirus UL99-encoded pp28 is required for the cytoplasmic envelopment of tegument-associated capsids. J Virol *77*, 10594-10605.

Simon, C.O., Holtappels, R., Tervo, H.M., Bohm, V., Daubner, T., Oehrlein-Karpi, S.A., Kuhnapfel, B., Renzaho, A., Strand, D., Podlech, J.*, et al.* (2006). CD8 T cells control cytomegalovirus latency by epitope-specific sensing of transcriptional reactivation. J Virol *80*, 10436-10456.

Sinclair, J., and Sissons, P. (2006). Latency and reactivation of human cytomegalovirus. J Gen Virol *87*, 1763-1779.

Sinzger, C., Grefte, A., Plachter, B., Gouw, A.S., The, T.H., and Jahn, G. (1995). Fibroblasts, epithelial cells, endothelial cells and smooth muscle cells are major targets of human cytomegalovirus infection in lung and gastrointestinal tissues. J Gen Virol *76 (Pt 4)*, 741-750.

Sinzger, C., Kahl, M., Laib, K., Klingel, K., Rieger, P., Plachter, B., and Jahn, G. (2000). Tropism of human cytomegalovirus for endothelial cells is determined by a post-entry step dependent on efficient translocation to the nucleus. J Gen Virol *81*, 3021-3035.

Sinzger, C., Muntefering, H., Loning, T., Stoss, H., Plachter, B., and Jahn, G. (1993). Cell types infected in human cytomegalovirus placentitis identified by immunohistochemical double staining. Virchows Arch A Pathol Anat Histopathol *423*, 249-256.

Sissons, J.G., Bain, M., and Wills, M.R. (2002). Latency and reactivation of human cytomegalovirus. J Infect *44*, 73-77.

Slobedman, B., and Mocarski, E.S. (1999). Quantitative analysis of latent human cytomegalovirus. J Virol *73*, 4806-4812.

Slot, M.C., Kroon, A.A., Damoiseaux, J.G., Theunissen, R., Houben, A.J., de Leeuw, P.W., and Tervaert, J.W. (2017). CD4+CD28null T Cells are related to previous cytomegalovirus infection but not to accelerated atherosclerosis in ANCA-associated vasculitis. Rheumatol Int.

Smith, C.J., Turula, H., and Snyder, C.M. (2014). Systemic hematogenous maintenance of memory inflation by MCMV infection. PLoS Pathog *10*, e1004233.

Smith, M.G. (1956). Propagation in tissue cultures of a cytopathogenic virus from human salivary gland virus (SGV) disease. Proc Soc Exp Biol Med *92*, 424-430.

Smith, M.Z., Bastidas, S., Karrer, U., and Oxenius, A. (2013). Impact of antigen specificity on CD4+ T cell activation in chronic HIV-1 infection. BMC Infect Dis *13*, 100.

Smuda, C., Bogner, E., and Radsak, K. (1997). The human cytomegalovirus glycoprotein B gene (ORF UL55) is expressed early in the infectious cycle. J Gen Virol *78 (Pt 8)*, 1981-1992.

Snyder, C.M., Cho, K.S., Bonnett, E.L., van Dommelen, S., Shellam, G.R., and Hill, A.B. (2008). Memory inflation during chronic viral infection is maintained by continuous production of short-lived, functional T cells. Immunity *29*, 650-659.

Soderberg, C., Larsson, S., Bergstedt-Lindqvist, S., and Moller, E. (1993). Definition of a subset of human peripheral blood mononuclear cells that are permissive to human cytomegalovirus infection. J Virol *67*, 3166-3175.

Solache, A., Morgan, C.L., Dodi, A.I., Morte, C., Scott, I., Baboonian, C., Zal, B., Goldman, J., Grundy, J.E., and Madrigal, J.A. (1999). Identification of three HLA-A*0201-restricted cytotoxic T cell epitopes in the cytomegalovirus protein pp65 that are conserved between eight strains of the virus. J Immunol *163*, 5512-5518.

Spaete, R.R., and Mocarski, E.S. (1985). Regulation of cytomegalovirus gene expression: alpha and beta promoters are trans activated by viral functions in permissive human fibroblasts. J Virol *56*, 135-143.

Spira, A.I., Marx, P.A., Patterson, B.K., Mahoney, J., Koup, R.A., Wolinsky, S.M., and Ho, D.D. (1996). Cellular targets of infection and route of viral dissemination after an intravaginal inoculation of simian immunodeficiency virus into rhesus macaques. J Exp Med *183*, 215-225.

Stagno, S., Pass, R.F., Cloud, G., Britt, W.J., Henderson, R.E., Walton, P.D., Veren, D.A., Page, F., and Alford, C.A. (1986). Primary cytomegalovirus infection in pregnancy. Incidence, transmission to fetus, and clinical outcome. JAMA *256*, 1904-1908.

Stagno, S., Pass, R.F., Dworsky, M.E., Henderson, R.E., Moore, E.G., Walton, P.D., and Alford, C.A. (1982). Congenital cytomegalovirus infection: The relative importance of primary and recurrent maternal infection. N Engl J Med *306*, 945-949.

Staras, S.A., Dollard, S.C., Radford, K.W., Flanders, W.D., Pass, R.F., and Cannon, M.J. (2006). Seroprevalence of cytomegalovirus infection in the United States, 1988-1994. Clin Infect Dis *43*, 1143-1151.

Stein, J., Volk, H.D., Liebenthal, C., Kruger, D.H., and Prosch, S. (1993). Tumour necrosis factor alpha stimulates the activity of the human cytomegalovirus major immediate early enhancer/promoter in immature monocytic cells. J Gen Virol *74 (Pt 11)*, 2333-2338.

Steininger, C., Puchhammer-Stockl, E., and Popow-Kraupp, T. (2006). Cytomegalovirus disease in the era of highly active antiretroviral therapy (HAART). J Clin Virol *37*, 1-9.

Stenberg, R.M., Depto, A.S., Fortney, J., and Nelson, J.A. (1989). Regulated expression of early and late RNAs and proteins from the human cytomegalovirus immediate-early gene region. J Virol *63*, 2699-2708.

Stinski, M.F. (1978). Sequence of protein synthesis in cells infected by human cytomegalovirus: early and late virus-induced polypeptides. J Virol *26*, 686-701.

Strain, M.C., Lada, S.M., Luong, T., Rought, S.E., Gianella, S., Terry, V.H., Spina, C.A., Woelk, C.H., and Richman, D.D. (2013). Highly precise measurement of HIV DNA by droplet digital PCR. PLoS One *8*, e55943.

Streblow, D.N., Kreklywich, C., Yin, Q., De La Melena, V.T., Corless, C.L., Smith, P.A., Brakebill, C., Cook, J.W., Vink, C., Bruggeman, C.A.*, et al.* (2003). Cytomegalovirus-mediated upregulation of chemokine expression correlates with the acceleration of chronic rejection in rat heart transplants. J Virol *77*, 2182-2194.

Sullivan, B.M., Juedes, A., Szabo, S.J., von Herrath, M., and Glimcher, L.H. (2003). Antigen-driven effector CD8 T cell function regulated by T-bet. Proc Natl Acad Sci U S A *100*, 15818-15823.

Swinkels, B.W., Geelen, J.L., Wertheim-van Dillen, P., van Es, A.A., and van der Noordaa, J. (1984). Initial characterization of four cytomegalovirus strains isolated from chimpanzees. Brief report. Arch Virol *82*, 125-128.

Sylwester, A.W., Mitchell, B.L., Edgar, J.B., Taormina, C., Pelte, C., Ruchti, F., Sleath, P.R., Grabstein, K.H., Hosken, N.A., Kern, F.*, et al.* (2005). Broadly targeted human

cytomegalovirus-specific CD4+ and CD8+ T cells dominate the memory compartments of exposed subjects. J Exp Med *202*, 673-685.

Szabo, S.J., Kim, S.T., Costa, G.L., Zhang, X., Fathman, C.G., and Glimcher, L.H. (2000). A novel transcription factor, T-bet, directs Th1 lineage commitment. Cell *100*, 655-669.

Takemoto, N., Intlekofer, A.M., Northrup, J.T., Wherry, E.J., and Reiner, S.L. (2006). Cutting Edge: IL-12 inversely regulates T-bet and eomesodermin expression during pathogen-induced CD8+ T cell differentiation. J Immunol *177*, 7515-7519.

Taylor-Wiedeman, J., Sissons, J.G., Borysiewicz, L.K., and Sinclair, J.H. (1991). Monocytes are a major site of persistence of human cytomegalovirus in peripheral blood mononuclear cells. J Gen Virol *72 (Pt 9)*, 2059-2064.

Thurman, R.E., Rynes, E., Humbert, R., Vierstra, J., Maurano, M.T., Haugen, E., Sheffield, N.C., Stergachis, A.B., Wang, H., Vernot, B.*, et al.* (2012). The accessible chromatin landscape of the human genome. Nature *489*, 75-82.

Ting, C.N., Olson, M.C., Barton, K.P., and Leiden, J.M. (1996). Transcription factor GATA-3 is required for development of the T-cell lineage. Nature *384*, 474-478.

Tomazin, R., Boname, J., Hegde, N.R., Lewinsohn, D.M., Altschuler, Y., Jones, T.R., Cresswell, P., Nelson, J.A., Riddell, S.R., and Johnson, D.C. (1999). Cytomegalovirus US2 destroys two components of the MHC class II pathway, preventing recognition by CD4+ T cells. Nat Med *5*, 1039-1043.

Tornatore, C., Chandra, R., Berger, J.R., and Major, E.O. (1994). HIV-1 infection of subcortical astrocytes in the pediatric central nervous system. Neurology *44*, 481-487.

Torti, N., Walton, S.M., Brocker, T., Rulicke, T., and Oxenius, A. (2011). Non-hematopoietic cells in lymph nodes drive memory CD8 T cell inflation during murine cytomegalovirus infection. PLoS Pathog *7*, e1002313.

Trivedi, D., Williams, R.Y., O'Reilly, R.J., and Koehne, G. (2005). Generation of CMV-specific T lymphocytes using protein-spanning pools of pp65-derived overlapping pentadecapeptides for adoptive immunotherapy. Blood *105*, 2793-2801.

Tu, W., Chen, S., Sharp, M., Dekker, C., Manganello, A.M., Tongson, E.C., Maecker, H.T., Holmes, T.H., Wang, Z., Kemble, G.*, et al.* (2004). Persistent and selective deficiency of CD4+ T cell immunity to cytomegalovirus in immunocompetent young children. J Immunol *172*, 3260-3267.

UNAIDS (2017). Fact sheet - Latest statistics on the status of the AIDS epidemic.

Utz, U., Koenig, S., Coligan, J.E., and Biddison, W.E. (1992). Presentation of three different viral peptides, HTLV-1 Tax, HCMV gB, and influenza virus M1, is determined by common structural features of the HLA-A2.1 molecule. J Immunol *149*, 214-221.

Valouev, A., Johnson, S.M., Boyd, S.D., Smith, C.L., Fire, A.Z., and Sidow, A. (2011). Determinants of nucleosome organization in primary human cells. Nature *474*, 516-520.

van Corven, E.J., Groenink, A., Jalink, K., Eichholtz, T., and Moolenaar, W.H. (1989). Lysophosphatidate-induced cell proliferation: identification and dissection of signaling pathways mediated by G proteins. Cell *59*, 45-54.

van de Berg, P.J., Yong, S.L., Remmerswaal, E.B., van Lier, R.A., and ten Berge, I.J. (2012). Cytomegalovirus-induced effector T cells cause endothelial cell damage. Clin Vaccine Immunol *19*, 772-779.

van der Bij, W., Torensma, R., van Son, W.J., Anema, J., Schirm, J., Tegzess, A.M., and The, T.H. (1988). Rapid immunodiagnosis of active cytomegalovirus infection by monoclonal antibody staining of blood leucocytes. J Med Virol *25*, 179-188.

van Leeuwen, E.M., van Buul, J.D., Remmerswaal, E.B., Hordijk, P.L., ten Berge, I.J., and van Lier, R.A. (2005). Functional re-expression of CCR7 on CMV-specific CD8+ T cells upon antigenic stimulation. Int Immunol *17*, 713-719.

Varnum, S.M., Streblow, D.N., Monroe, M.E., Smith, P., Auberry, K.J., Pasa-Tolic, L., Wang, D., Camp, D.G., 2nd, Rodland, K., Wiley, S.*, et al.* (2004). Identification of proteins in human cytomegalovirus (HCMV) particles: the HCMV proteome. J Virol *78*, 10960-10966.

Ventura, C., Bisceglia, H., Girerd-Chambaz, Y., Burdin, N., and Chaux, P. (2012). HLA-DR and HLA-DP restricted epitopes from human cytomegalovirus glycoprotein B recognized by CD4+ T-cell clones from chronically infected individuals. J Clin Immunol *32*, 1305-1316.

Veroux, M., Puzzo, L., Corona, D., Buffone, A., Tallarita, T., Murabito, P., and Veroux, P. (2007). Cytomegalovirus and Clostridium difficile ischemic colitis in a renal transplant recipient: a lethal complication of anti-rejection therapy? Urol Int *79*, 177-179; discussion 180.

Vescovini, R., Biasini, C., Fagnoni, F.F., Telera, A.R., Zanlari, L., Pedrazzoni, M., Bucci, L., Monti, D., Medici, M.C., Chezzi, C.*, et al.* (2007). Massive load of functional effector

CD4+ and CD8+ T cells against cytomegalovirus in very old subjects. J Immunol *179*, 4283-4291.

Vingert, B., Perez-Patrigeon, S., Jeannin, P., Lambotte, O., Boufassa, F., Lemaitre, F., Kwok, W.W., Theodorou, I., Delfraissy, J.F., Theze, J.*, et al.* (2010). HIV controller CD4+ T cells respond to minimal amounts of Gag antigen due to high TCR avidity. PLoS Pathog *6*, e1000780.

Wagner, A., Regev, A., and Yosef, N. (2016). Revealing the vectors of cellular identity with single-cell genomics. Nat Biotechnol *34*, 1145-1160.

Wagner, T.A., McLaughlin, S., Garg, K., Cheung, C.Y., Larsen, B.B., Styrchak, S., Huang, H.C., Edlefsen, P.T., Mullins, J.I., and Frenkel, L.M. (2014). HIV latency. Proliferation of cells with HIV integrated into cancer genes contributes to persistent infection. Science *345*, 570-573.

Walker, J.D., Maier, C.L., and Pober, J.S. (2009). Cytomegalovirus-infected human endothelial cells can stimulate allogeneic CD4+ memory T cells by releasing antigenic exosomes. J Immunol *182*, 1548-1559.

Wall, N.A., Chue, C.D., Edwards, N.C., Pankhurst, T., Harper, L., Steeds, R.P., Lauder, S., Townend, J.N., Moss, P., and Ferro, C.J. (2013). Cytomegalovirus seropositivity is associated with increased arterial stiffness in patients with chronic kidney disease. PLoS One *8*, e55686.

Waller, E.C., Day, E., Sissons, J.G., and Wills, M.R. (2008). Dynamics of T cell memory in human cytomegalovirus infection. Med Microbiol Immunol *197*, 83-96.

Walton, S.M., Torti, N., Mandaric, S., and Oxenius, A. (2011). T-cell help permits memory CD8(+) T-cell inflation during cytomegalovirus latency. Eur J Immunol *41*, 2248-2259.

Weekes, M.P., Wills, M.R., Mynard, K., Carmichael, A.J., and Sissons, J.G. (1999). The memory cytotoxic T-lymphocyte (CTL) response to human cytomegalovirus infection contains individual peptide-specific CTL clones that have undergone extensive expansion in vivo. J Virol *73*, 2099-2108.

Weekes, M.P., Wills, M.R., Sissons, J.G., and Carmichael, A.J. (2004). Long-term stable expanded human CD4+ T cell clones specific for human cytomegalovirus are distributed in both CD45RAhigh and CD45ROhigh populations. J Immunol *173*, 5843-5851.

Weststrate, M.W., Geelen, J.L., and van der Noordaa, J. (1980). Human cytomegalovirus DNA: physical maps for restriction endonucleases BglII, hindIII and XbaI. J Gen Virol *49*, 1-21.

Williams, M.A., Ravkov, E.V., and Bevan, M.J. (2008). Rapid culling of the CD4+ T cell repertoire in the transition from effector to memory. Immunity *28*, 533-545.

Wills, M.R., Carmichael, A.J., Mynard, K., Jin, X., Weekes, M.P., Plachter, B., and Sissons, J.G. (1996). The human cytotoxic T-lymphocyte (CTL) response to cytomegalovirus is dominated by structural protein pp65: frequency, specificity, and T-cell receptor usage of pp65-specific CTL. J Virol *70*, 7569-7579.

Wills, M.R., Carmichael, A.J., Weekes, M.P., Mynard, K., Okecha, G., Hicks, R., and Sissons, J.G. (1999). Human virus-specific CD8+ CTL clones revert from CD45ROhigh to CD45RAhigh in vivo: CD45RAhighCD8+ T cells comprise both naive and memory cells. J Immunol *162*, 7080-7087.

Wills, M.R., Mason, G.M., and Sissons, J.G.P. (2013). Adaptive Cellular Immunity to Human Cytomegalovirus. In Cytomegalovirus From Molecular Pathogenesis to Intervention, M.J.L. Reddehase, N. A. W., ed. (Norfolk, UK: Caister Academic Press), pp. 142-172.

Wills, M.R., Okecha, G., Weekes, M.P., Gandhi, M.K., Sissons, P.J., and Carmichael, A.J. (2002). Identification of naive or antigen-experienced human CD8(+) T cells by expression of costimulation and chemokine receptors: analysis of the human cytomegalovirus-specific CD8(+) T cell response. J Immunol *168*, 5455-5464.

Wong, B.W., Wong, D., and McManus, B.M. (2002). Characterization of fractalkine (CX3CL1) and CX3CR1 in human coronary arteries with native atherosclerosis, diabetes mellitus, and transplant vascular disease. Cardiovasc Pathol *11*, 332-338.

Wong, J.K., Hezareh, M., Gunthard, H.F., Havlir, D.V., Ignacio, C.C., Spina, C.A., and Richman, D.D. (1997). Recovery of replication-competent HIV despite prolonged suppression of plasma viremia. Science *278*, 1291-1295.

Wynn, K.K., Fulton, Z., Cooper, L., Silins, S.L., Gras, S., Archbold, J.K., Tynan, F.E., Miles, J.J., McCluskey, J., Burrows, S.R.*, et al.* (2008). Impact of clonal competition for peptide-MHC complexes on the CD8+ T-cell repertoire selection in a persistent viral infection. Blood *111*, 4283-4292.

Yeung, E.S. (2011). Genome-wide correlation between mRNA and protein in a single cell. Angew Chem Int Ed Engl *50*, 583-585.

Yu, X., Shah, S., Lee, M., Dai, W., Lo, P., Britt, W., Zhu, H., Liu, F., and Zhou, Z.H. (2011). Biochemical and structural characterization of the capsid-bound tegument proteins of human cytomegalovirus. J Struct Biol *174*, 451-460.

Zaitseva, M., Blauvelt, A., Lee, S., Lapham, C.K., Klaus-Kovtun, V., Mostowski, H., Manischewitz, J., and Golding, H. (1997). Expression and function of CCR5 and CXCR4 on human Langerhans cells and macrophages: implications for HIV primary infection. Nat Med *3*, 1369-1375.

Zhang, H., Dornadula, G., Beumont, M., Livornese, L., Jr., Van Uitert, B., Henning, K., and Pomerantz, R.J. (1998). Human immunodeficiency virus type 1 in the semen of men receiving highly active antiretroviral therapy. N Engl J Med *339*, 1803-1809.

Zhao, S., Fung-Leung, W.P., Bittner, A., Ngo, K., and Liu, X. (2014). Comparison of RNA-Seq and microarray in transcriptome profiling of activated T cells. PLoS One *9*, e78644.

Zhu, T., Mo, H., Wang, N., Nam, D.S., Cao, Y., Koup, R.A., and Ho, D.D. (1993). Genotypic and phenotypic characterization of HIV-1 patients with primary infection. Science *261*, 1179-1181.

Zhu, T., Wang, N., Carr, A., Nam, D.S., Moor-Jankowski, R., Cooper, D.A., and Ho, D.D. (1996). Genetic characterization of human immunodeficiency virus type 1 in blood and genital secretions: evidence for viral compartmentalization and selection during sexual transmission. J Virol *70*, 3098-3107.

Zhu, Y., Huang, L., and Anders, D.G. (1998). Human cytomegalovirus oriLyt sequence requirements. J Virol *72*, 4989-4996.